

Development and Characterization of some nanocomposites for Applications in various Electrical, Optical, Electro-magnetic and Fields pertaining to Electronic Industry

Thesis submitted to partial fulfillment of the degree of doctor of philosophy (Ph.D) in Science

of

Jadavpur University



by

Anandalal Gayen

Department of Physics

Jadavpur University

Kolkata-700032

Dedicated to

Parents


&

Family members and labmates.

Certificates from the Supervisors

This is to certify that the thesis entitled “**Development and Characterization of some nanocomposites for Applications in various Electrical, Optical, Electro-magnetic and Fields pertaining to Electronic Industry**” submitted by **Sri Anandalal Gayen** who got his name registered on 12/04/2021 for the award of Ph.D (Science) degree of Jadavpur University, is absolutely based upon his own work under the supervision of **Prof. Sukhen Das**, Department of Physics, Jadavpur University and Co-supervision of **Dr. Smarajit Manna**, Student Advisor, Jagadis Bose National Science Talent Search, Kolkata -700107 and that neither this thesis nor any part of it has been submitted for either degree/ diploma / or any other academic award anywhere before.


 **Prof. Sukhen Das**
Department of Physics,
Jadavpur University
Kolkata - 700 032


..... **24/08/2023**

Dr. Smarajit Manna
Student Advisor and Nodal Officer
Vidyasagar Science Olympiad
Jagadis Bose National Science Talent Search
1300, Rajdanga Main Road
Kolkata-700 107

(Signature of the supervisor(s) date with official seal)



CERTIFICATE OF SIMILARITY CHECK

This is to certify that the plagiarism checking for this thesis authored by Sri Anandalal Gayen has been performed using professional plagiarism prevention software *iThenticate* According to the report generated after plagiarism checking there is **13%** similarity in this thesis, which is in the category “Level 0” (minor similarities) as per the “Promotion of Academic Integrity and Prevention of Plagiarism in Higher Education Institutions Regulations, 2018” of the University Grand Commission (UGC) of India. The common knowledge or coincidental terms upto 10 (ten) consecutive words (as prescribed in the above said UGC Regulation upto 14 (fourteen) terms for such common knowledge or coincidental terms can be excluded) and own works of the candidate published in various peer-reviewed journals (those are attached in the thesis) are excluded from the similarity checking. It is certified that the present thesis submitted by **Anandalal Gayen** is plagiarism free and has been followed standard norms of academic integrity and scientific ethics.

Smarajit Manna
24/08/2023

Dr.Smarajit Manna

Student Advisor,

Jagadis Bose National Science Talent Search

Kolkata-700107, India

Dr. Smarajit Manna
Student Adviser and Nodal Officer
Vidyasagar Science Olympiad
Jagadis Bose National Science Talent Search
1500, Main Road
Kolkata-700107

Sukhen Das

Prof. Sukhen Das

Department of Physics,

Jadavpur University,

Kolkata- 700032, India



Prof. Sukhen Das
Department of Physics,
Jadavpur University
Kolkata - 700 032

ABSTRACT

Title of the Thesis: “Development and Characterization of some nanocomposites for Applications in various Electrical, Optical, Electro-magnetic and Fields pertaining to Electronic Industry”

(A) Proposed Area/Theme of Research:

In this study we have focused for the development and characterization of some nanocomposite materials with improved electrical properties. Nanocomposites are prepared by doping several nanometals in the polymer matrix. A series of characterization techniques have been employed to those nanocomposites for investigating the enhancements of various electrical properties in terms their extensive application in electronic industry to mitigate the global crisis of energy harvesting and storage devices.

(B) Statement of Purpose Regarding Research Objective:

In order to strengthen the future sustainability towards energy crunch, emphasis has been given to develop new materials having a superior capability of energy storage and have wide application in electronic industry.

In this work, we have made our exploration for preparing metal (Cu, Co, Cr, Mn, etc.) oxide based nanocomposites through cost effective, simple and modified chemical synthesis procedure. The characterization and measurements of these materials have been performed using various physical techniques to confirm their enhanced capability in terms of electrical properties with the objective for its wide range application in charge storage device, dielectric applications as separators, electromagnetic interference shielding and other applications pertaining to electronic industry.

Signature of the candidate

Smarajit Manna
24/08/2023

Dr. Smarajit Manna

Dr. Smarajit Manna
Student Adviser and Nodal Officer
Vidyasagar Science Olympiad
Jagadis Bose National Science Talent Search
1300, Rajdanga Main Road
Kolkata-700 107

Jagadis Bose National Science Talent Search

Kolkata-700107, India

Sukhen Das

Prof. Sukhen Das

Department of Physics,

Jadavpur University,

Kolkata- 700032, India



Prof. Sukhen Das
Department of Physics,
Jadavpur University
Kolkata - 700 032

DECLARATION

I, hereby, declare that the work included in the present thesis has been carried out by me under the supervision of Prof. Sukhen Das, Department of Physics, Jadavpur University, Kolkata-700032, India and Dr. Smarajit Manna, Student Advisor, Jagadis Bose National Science Talent Search, Kolkata-700107, India. Neither this thesis nor any part thereof has been submitted for any degree whatsoever.

Anandalal Gayen

Mr. Anandalal Gayen
Department of Physics
Jadavpur University
Kolkata-700032, India

24.08.23.

CONTENTS

Abbreviations	i
List of Publications	iii
List of Conferences/ Seminars Attended	iv
List of Figures	v
List of Tables	ix
Chapter-1: Literature Review	1
1.1 Introduction to Nanoparticle.....	1
1.1.1 Overview	1
1.1.2 Research Scope	2
1.2 Introduction to β phase crystallinity.....	3
1.2.1 Background	3
1.2.2 Why polyvinylidene fluoride Cohexafluoropropylene (PVDF-HFP)?.....	5
1.2.3 Why β phase Polymorphos of PVDF-HFP?	6
1.2.4 Bulk vs Micro vs Nanoparticle	6
1.2.5 Literature review	8
1.2.6 Synthesis Techniques	10
1.2.6.1 Sol-Gel Method	11
1.3 Introduction to Polymer	12
1.3.1 Classification of Polymers	12
1.3.2 Electro Active Polymer	14
1.3.2.1 Poly (Vinylidene Fluoride) and its Structure	15
1.3.2.2 Possible applications of PVDF and its Composites	17
1.4 Introduction to Electro Active Polymer Nano (EPNs) Composite	18
1.4.1 Synthesis	18
1.4.2 Fabrication Techniques	19
1.4.2.1 Solution Casting Method.....	20
1.4.3 Properties	20
1.5 Characterization Techniques	20
1.5.1 Structural Property	20
1.5.1.1 X-ray Diffraction (XRD)	21
1.5.1.2 Fourier Transform Infrared Spectroscopy (FTIR)	24
1.5.1.3 Differential Thermal Analysis (DTA)	26

1.5.2 Morphological Property	27
1.5.2.1 Field Emission Scanning Electron Microscope (FESEM)	28
1.5.2.2 Energy Dispersive X-ray (EDX) Analysis	29
1.5.3 Electrical Properties	29
1.5.3.1 Impedance Spectroscopy (LCR meter)	29
1.5.3.1.1 Dielectric Constant	31
1.5.3.1.2 Tangent Loss	32
1.5.3.1.3 AC Conductivity	32
1.6 Applications	33
1.6.1 High Dielectric Appliances	33
1.6.2 Non-Conventional Charge Storage Device	34
1.7 Objectives of the Thesis	35
References	36
Chapter-2 Enhancement of dielectric properties and conductivity of materials doped with different nanoparticles.....	42
2.1 Chapter Overview	43
2.2 Introduction	43
2.3 Materials and Methods	45
2.4 Instrumentation for Characterization of Samples	47
2.5 Results and Discussion	48
2.5.1 FTIR Analysis	48
2.5.2 Field Emission Scanning Electron Microscopy Analysis	49
2.6. Electrical Properties Measurement.....	50
2.6.1 Dielectric Constant Measurement	51
2.6.2 Frequency vs Dielectric Constant	51
2.6.3 Concentration vs Dielectric Constant	52
2.6.4 Frequency vs Tangent loss Analysis	54
2.6.5 Frequency vs ac Conductivity Analysis.....	55
2.7 Conclusions	56
References	57
Chapter-03 Further Improvisation of Electrical properties of PVDF-HFP: Investigation of various materials doped with nanoparticles with different sizes.....	61
3.1 Chapter Overview	62
3.2 Introduction	63

3.3 Materials and Methods	64
3.4 Sample Details	65
3.5 Instrumentation	66
3.5.1 Characterization	66
3.5.2 XRD Analysis.....	66
3.5.3 FTIR Analysis.....	68
3.5.4 DTA Analysis.....	69
3.5.5 Zeta Potential Analysis.....	71
3.5.6 Microstructure and Elemental Composition Analysis	73
3.5.6.1FESEM Analysis of Pristine and doped TCu & TCo.....	73
3.5.6.2 EDX Analysis.....	75
3.6 Electrical Properties Measurement.....	76
3.6.1 Frequency vs Dielectric Constant Measurement	76
3.6.2 Frequency vs Tangent loss Analysis	78
3.6.3 Frequency vs AC Conductivity Analysis.....	79
3.6.4 Concentration vs Dielectric Constant.....	80
3.7 Conclusions	82
References	83
Chapter-04 Effect of Homeopathic Dilutions of Cuprum Arsenicosum on the Electrical Properties of Poly (Vinylidene Fluoride-Cohexafluoropropylene).....	88
4.1 Overview.....	89
4.2 Introduction.....	90
4.3 Method.....	91
4.3.1 Solution Casting Method.....	91
4.3.2 Electrical Characteristics, Phase Change, Morphology, and Particle Size.....	93
4.3.3 Sample Details.....	93
4.4 Result & Discussion.....	93
4.4.1 FTIR Analysis.....	94
4.4.2 FESEM Analysis.....	95
4.4.3 EDX Analysis.....	96
4.5 Study of Electrical Properties of PVDF-HFP.....	98
4.5.1 Frequency vs Dielectric Constant.....	98
4.5.2 Tangent loss Analysis	99

4.5.3 Frequency vs Electrical Conductivity.....	100
4.6. Conclusion.....	102
Reference.....	103
Chapter-05 Effect of Cuprum metallicum potentized through both serial dilution and succussion in comparison to succussion alone on Escherichia coli bacterial system and electrical properties of poly (vinylidene fluoride-Cohexafluoropropylene) polymer.....	106
5.1 Overview.....	107
5.2 Introduction.....	108
5.3 Method.....	111
5.3.1 Preparation of the two Sets of Nanoparticle.....	111
5.3.2 Antibacterial Effect of Cuprum Metallicum.....	113
5.3.3 Cuprum Metallicum Poly (vinylidene fluoride-Cohexafluoropropylene) Composite film Preparation Technique	114
5.4 Result.....	115
5.4.1 FESEM of Set A and Set B.....	115
5.4.2 FESEM of Antibacterial Effect of Cuprum Metallicum	117
5.4.3 Measurement of Electrical Properties of Polymer Matrix: Effect of Potentized Cuprum Metallicum in Set A and Set B.....	120
5.4.4 Frequency vs Dielectric Constant.....	121
5.4.5 Frequency vs Tangent loss Analysis	122
5.4.6 Frequency vs Electrical Conductivity.....	123
5.5 Conclusion.....	124
Reference.....	125
Chapter 06 Summery	129
6.1. General Conclusion.....	130
6.2 Future Prospects.....	132
Thesis Publications.....	
Certificates of Seminar/Conference.....	

ABBREVIATIONS

Abbreviations

AO

ASS

CB

CNT

Cp

C_{sp}

DC

DI

DMF

DTA

DMSO

EAP

EDX

ϵ_r

EPN

Esp

FESEM

FTIR

HFP

HR

KeV

LED

MO

M.W.

NCs

Nm

NPs

PL

Expansion

Atomic Orbital

Asymmetric Solid State Super capacitor

Conduction Band

Carbon nanotubes

Parallel Capacitance

Specific Capacitance

Dielectric Constant

Deionized

Dimethyl formamide

Differential Thermal Analysis

Dimethyl Sulphoxide

Electro Active Polymer

Energy dispersive X-ray Spectroscopy

Dielectric Constant / Permittivity

Electro active Polymer Nano Composite

Specific energy density

Field Emission Scanning Electron Microscope

Fourier Transforms Infrared Spectroscopy

Hexafluoropropylene

High Resolution

Kilo electron Volt

Light Emitting Diode

Molecular Orbital

Molar Weight

Nano Crystals

Nanometer

Nanoparticles

Photoluminescence

PVDF	Poly (vinylidene Fluoride)
PVDF-HFP	Poly (vinylidene fluoride-Cohexafluoropropylene)
RF	Radio Frequency
RT	Room Temperature
ρ	Resistivity
σ_{ac}	AC Conductivity
SCPC	Self-Charging Power Cell
Tan δ	Tangent loss
TGA	Thermal Gravimetric Analysis
UV-Vis	Ultra Violet Visible Spectroscopy
VB	Valance Band
Vol%	Volume Percent
Wt%	Weight Percent
XRD	X-ray Diffraction

List of Publications

- (I) **A. L. Gayen**, B. K. Paul, D. Roy, S. Kar, P. Bandyopadhyay, R. Basu, S. Das, D. S. Bhar, R. K. Manchanda, A. K. Khurana, D. Nayak & P. Nandy (2016): “Enhanced dielectric properties and conductivity of triturated copper and cobalt nanoparticles doped PVDF-HFP film and their possible use in electronic industry”, Materials Research Innovations, DOI:10.1080/14328917.2016.1196563
- (II) **Gayen, A. L.**; Mondal D.; Roy, D.; Bandyopadhyay, P.; Manna, S.; Basu, R.; Das, S.; Bhar, D. S.; Paul, B. K.; Nandy, P. “Improvisation of Electrical Properties of PVDF-HFP: Use of Novel Metallic Nanoparticles”. J. Mater. Sci. Mater. Electron. 2017, 28 (19), 14798–14808.
- (III) **Gayen, A.L.**; Mondal D.; Bandyopadhyay, P.; Bera, D.; Bhar, D. S.; Das, S.; Manchanda, R. K.; Khurana, A. K.; Nayak, D.; Paul, B.K.; Nandy P. “Effect of Homeopathic Dilutions of Cuprum Arsenicosum on the Electrical Properties of Poly(Vinylidene Fluoride-Cohexafluoropropylene)”. Homeopathy, 2018, 107 (2), 130–136.
- (IV) **Gayen, A.L.**; Mondal D.; Bera, D.; Biswas, P.; Paul, B. K.; Bhar, D. S.; Das, S.; Narula, R.; Khurana, A. K.; Manchanda, R. K.; Nandy P.; “Effect of Cuprum metallicum potentized through both serial dilution and succussion in comparison to succussion alone on Escherichia coli bacterial system and electrical properties of poly(vinylidene fluoride cohexafluoropropylene) polymer”. IJRH, 2019, 13 (4), 209-218.
- (V) Mondal D.; **Gayen A. L.**; Paul B. K.; Bandyopadhyay P.; Bera D.; Bhar D. S.; Das K.; Nandy P.; Das S.; “Enhancement of β -phase crystallization and electrical properties of PVDF by impregnating ultra-high diluted novel metal derived nanoparticles: prospect of use as a charge storage device”. J. Matter. Sci. Mater. Electron. 2018, 29, 14535–14545.
- (VI) Mondal D.; Das S.; Paul B. K.; Bhattacharya D.; Ghoshal D.; **Gayen A. L.**; Das K.; Das S.; “Size Engineered Cu-Doped α -MnO₂ Nanoparticles for Exaggerated Photocatalytic Activity and Energy Storage Application”. Materials Research Bulletin, 2019, 115, 159–169.
- (VII) Mondal D.; **Gayen A. L.**; Paul B. K.; Bhar D. S.; Das K.; Nandy P.; Das S.; “Colossal Dielectric Response of PVDF-HFP Amalgamated Ultra-Low-Density Metal-Derived Nanoparticles: Frontier of an Excellent Charge Separator”. Journal of Electronic Materials. 2019, 48, 5570–5580.
- (VIII) Nandy P, Bandyopadhyay P, Paul BK, Bera D, **Gayen AL**, Das S, *et al.* “Technohomeopathy, the science of application of homeopathy in technology – A short review”. Int J Curr Res 2017; 9:51772-778.

List of Conferences/Seminars attended

International

(i) Two days international conference on “Emerging Trends in Chemical Science (ETCS-2018)”, Dept. of Chemistry, Dibrugarh University, Assam, India held on 26th-28th February 2018.

(ii) Two days International Conference on “Microscope & XXXIX Annual Meeting of Electron Microscope Society of India”, IOP, NISER, CSIR-IMMT, IITB BSR, ILS & CSIR-CGCRI held on 18th - 20th July 2018.

National

(i) One day seminar on “Recent Trend in Frontier Research in Physics” (SRTRP-6th March, 2018), Dept. of Physics, Jadavpur University, Kolkata, 2016.

(ii) One day national symposium on “Nanotechnology: From Materials to Medicine and Their Social Impact”, Centre for Interdisciplinary Research and Education (CIRE), Kolkata, on 25th March 2017.

List of Figures

Chapter 1

Figure 1.1 A schematic representation of Bulk to Nanoparticle distribution (adopted from webpage, www.google.com)

Figure 1.2 PVDF, electro active polymer (adopted from webpage, www.google.com)

Figure 1.3 PVDF-HFP (where $n > m$) electro active polymer (adopted from webpage, www.google.com)

Figure 1.4 β phase of PVDF-HFP electro active polymer (adopted from webpage)

Figure 1.5 Application of metal nano particle(adopted from webpage,www.google.com)

Figure 1.6 Flow chart of Sol-gel method

Figure 1.7 Classification of different types of Polymers.

Figure 1.8 Different types of Electro active Polymers.

Figure 1.9 (a) PVDF-HFP structure (C= Carbon; F= Fluorine; H= Hydrogen) and (b) Commercially available PVDF-HFP (adopted from webpage, www.google.com).

Figure 1.10 Application of PVDF-HFP metal nanocomposite film.

Figure 1.11 Photograph of X-ray Diffractometer and X-ray diffraction principle (adopted from webpage, www.google.com).

Figure 1.12 Photograph of FTIR and FTIR principle (adopted from webpage, www.google.com).

Figure 1.13 Photograph of DTA and DTA principle (adopted from webpage, www.google.com).

Figure 1.14 FESEM arrangement and Schematic diagram of FESE (adopted from webpage, www.google.com).

Figure 1.15 LCR meter setup (adopted from webpage, www.google.com).

Chapter 2

Figure 2.1 Flow chart of the sample preparation.

Figure 2.2(a) and 2.2(b) Fourier transform infrared spectra of CuPC and CoPC for all concentrations.

Figure 2.3 Field Emission Scanning Electron Micrograph of (a) 0.2CuPC, (b) 0.5CuPC, (c) 2CuPC, (d) 0.2CoPC, (e) 0.5CoPC and (f) 2.0CoPC films.

Figure 2.4(a) and 2.4(b) Frequency dependent dielectric constant (ϵ_r) of CuPC and CoPC for all concentrations.

Figure 2.5(a) and 2.5(b) Concentration dependent dielectric constant (ϵ_r) and tangent loss ($\tan\delta$) of CuPC and CoPC at various constant frequencies.

Figure 2.6(a) and 2.6(b) Frequency dependence of tangent loss ($\tan\delta$) of CuPC and CoPC at various concentrations.

Figure 2.7(a) and 2.7(b) Frequency dependence of AC conductivity (σ_{ac}) of CuPC and CoPC at various concentrations.

Chapter 3

Figure 3.1 XRD patterns of pure and all composite films doped with TCu and TCo of 6C, 30C and 200C potencies.

Figure 3.2(a) Fourier Transform Infrared Spectra of CuPC and CoPC for all potency. **(b)** Increase of $F(\beta)\%$ with increase in potency.

Figure 3.3 DTA patterns of pure and of composite films doped with TCu and TCo of 6C, 30C and 200C potencies.

Figure 3.4 Zeta Potential of Pristine TCu and TCo of 6C, 30C and 200C potencies.

Figure 3.5 Schematic diagram showing the growth mechanism for the formation of TCu or TCo/PVDF-HFP composites.

Figure 3.6 Field Emission Scanning Electron Micrograph (FESEM) of Pristine, (a) TCu and (b) TCo of 200C.

Figure 3.7 Field Emission Scanning Electron Micrograph (FESEM) of (a) CuPC-6, (b) CuPC-30, (c) CuPC-200, (d) CoPC-6, (e) CoPC-30 and (f) CoPC-200films.

Figure 3.8 High resolution elemental mapping images of (a) CuPC-200, (b) CoPC-200 and EDX spectra of (c) CuPC-200, (d) CoPC-200. (e) Elements obtained from EDX study with their normality weight percentages are shown in the inserted table.

Figure 3.9 Frequency dependent Dielectric Constant (ϵ_r) of (a) CuPC and (b) CoPC for all Potency.

Figure 3.10 Frequency dependent Tangent loss ($\tan\delta$) of (a) CuPC and (b) CoPC for all Potency.

Figure 3.11 Frequency dependent ac Conductivity (σ_{ac}) of a CuPC and b CoPC for all potency.

Figure 3.12 Potency dependent dielectric constant and tangent loss of (a) CuPC and (b) CoPC for all potency at a specific frequency (500 Hz).

Chapter 4

Figure 4.1 Flow chart to synthesize PVDF-HFP-CuAs nanoparticle composite films.

Figure 4.2 Phase identification and confirmation study by FTIR of all the samples.

Figure 4.3 Morphology and micro structural analysis of (a) 0(PVDF-HFP,) (b) 0.5(CuAsPC), (c) 2.0(CuAsPC) and (d) 5.0(CuAs PC) CuAs incorporated PVDF-HFP films by FESEM.

Figure 4.4. (a) Elemental confirmation of all elements present in the 2 ml CuAs incorporated PVDF film by EDX spectra (C, Carbon; Cu, Copper; F, Fluorine; As, Arsenic); (b) selected area for measurement; and (c–f) elemental mapping image (c) Carbon, (d) Fluorine, (e) Arsenic, and (f) Copper of 2 ml CuAs-doped PVDF-HFP film. K, L, and Ka1 refer respectively to the K-band, L-band, and K_{α} -band of the X-ray beam used for the EDX spectroscopy.

Figure 4.5 Variation of dielectric constant with frequency for all CuAs incorporated PVDF films.

Figure 4.6 Variation of tangent loss with frequency for all CuAs incorporated PVDF films. CuAs, Cuprum Arsenicosum; PVDF-HFP.

Figure 4.7 Variation of AC conductivity (Siemens/meter) with frequency for all CuAs incorporated PVDF films.

Chapter 5

Figure 5.1 The two sets of potentization: Set A and Set B.

Figure 5.2 The schematic diagram for the preparation of Cup. met. poly (vinylidene fluoride Cohexafluoropropylene) composite films.

Figure 5.3 Field emission scanning electron microscope images of poly (vinylidene fluoride Cohexafluoropropylene) doped 200C Cup. met. nanoparticle of (a) Set A and (b) Set B.

Figure 5.4 Anti-bacterial effect of Cup. met. for Set A (a) 6C, (b) 30C and (c) 200C and Set B (d) 6C, (e) 30C and (f) 200C.

Figure 5.5 Field emission scanning electron microscope micro structural overview for Set A of Poly (vinylidene fluoride Cohexafluoropropylene) doped Cuprum Metallicum (a) 6C, (b) 30C and (c) 200C.

Figure 5.6 Field emission scanning electron microscope micro structural overview for Set B of PVDF-HFP doped Cup. met. (a) 30C, (b) 200C and (c) microstructure of PVDF-HFP doped Cup. met. of 200C and the crystal structure of β -polymorph (inset graph) and (d) microstructure of Cup. met. of 200C embedded PVDF-HFP and the crystal structure of β -polymorph (inset graph).

Figure 5.7 The schematic representation for nucleation of β polymorph in poly (vinylidene fluoride Cohexafluoropropylene).

Figure 5.8. Frequency vs Dielectric Constant (a) of Set-A and (b) Set-B.

Figure 5.9. Frequency vs Tangent loss (a) of Set-A and (b) Set-B.

Figure 5.9. Frequency vs ac Conductivity (a) of Set-A and (b) Set-B.

List of Tables

Chapter1

Table 1.1 Different types of nanocomposites.

Table 1.2 Classification of polymers and their examples.

Chapter4

Table 4.1 Variation in dielectric constant and AC conductivity of polymer film due to incorporation of CuAs at 10 kHz frequency

1.1 Introduction to nanoparticle

1.1.1 Overview

A nanoparticle is a ultrafine particle of dimension ranges between 1 to 100 nanometers (nm) in diameter. The metal particles of dimension less than 1 nm are generally cluster of atoms. Nanoparticles are distinguishable through their size from other particles like micro particles (1 μm to 1000 μm), coarse particles (ranging from 2500 nm to 10,000 nm) and fine particles (100 nm to 2500 nm). Due to the smaller in size, nanoparticle creates more interaction area as a result of high surface to volume ratio with the other doping matrix which drives very exceptional physical, chemical, optical, electric, magnetic properties. There is a remarkable difference on above mentioned properties of nanoparticles than that of other relatively larger particles of the same material. Usually the typical atomic diameter lies between 0.15 and 0.60 nm, so a portion of the nanoparticle material is located in just a few atomic diameters of its surface. Therefore, in the nano dimension the surface layer's characteristics will prevail over those of the bulk material. Since the interactions between the two materials at their interface also become relevant, this dimensional impact is predominantly powerful for nanoparticles distributed in other medium of different composition. Recently, a fast growing area like nanotechnology has gained more importance and interest by spreading its wings over a wide range of research fields. A schematic representation is demonstrated in Figure 1.1 to visualize the transition from bulk to nano regime.

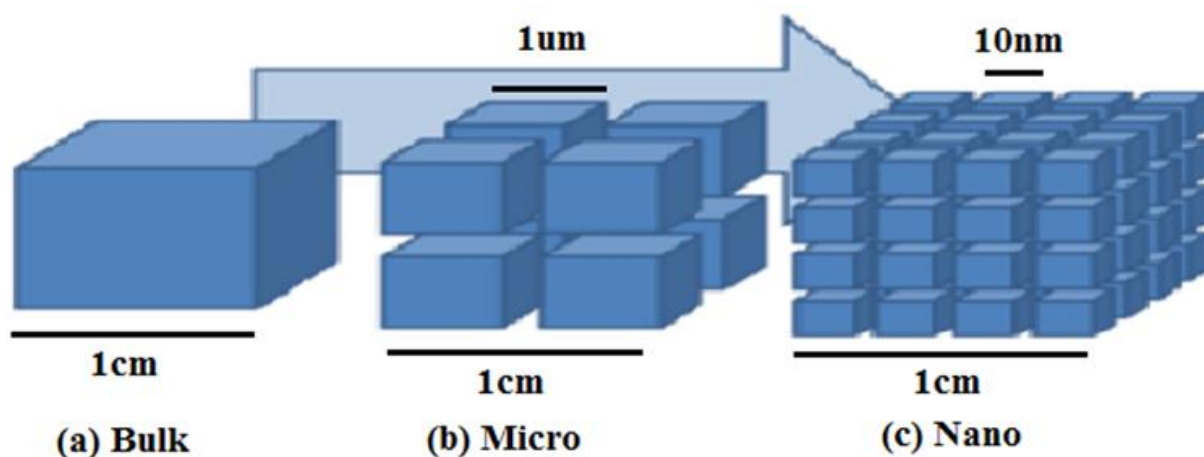


Figure 1.1 A schematic representation of Bulk to nanoparticle distribution (adopted from webpage, www.google.com)

A large difference in bandgap as well as electrical and optical properties are modified with the reduction of the size of the particle. Also the magnetic, mechanical, electrical, electrochemical properties alter with the specific surface area. For an instance different characteristics in physical and chemical behavior e.g., higher surface to volume ratio, lower melting points, specific optical properties, specific magnetic property, high energy density, high power density and mechanical strengths [1] are achieved in metals with the transformation from bulk to nano regime.

1.1.2. Research Scope

Electrical Properties of a material mostly depends on its electrical parameters like dipole moment, polarization, dielectric constant, ac conductivity, tangent loss and structural parameters like surface to volume ratio, porosity etc. nanoparticle is very beneficial for regulating the intrinsic properties of the materials. Also, the synthesis route, percentage of doping and sintering temperature can change the properties. Furthermore, the tunable properties like electrical, optical, structural, thermal, mechanical of the nanomaterial have drawn a great interest in a vast

area of technologies, ranging from modern electronics like semiconductor[1], sensor, energy storage[1-2], biomedical imaging[4], photovoltaic, optoelectronics to thermoelectric, and other electronic aspects. Therefore, engineering the various types of new nanomaterial and fabricating of new devices using their favorable properties have been playing a significant role to extend the diverse scope of research for future application [5].

1.2 Introduction to β phase Crystallinity

β Phase crystallinity of electro active polymer is the most electro active properties among several other crystallinity phases like α , γ , δ and ε . Electro active polymer has a good interaction between its negatively or positively charged dipole with positively or negatively charged zeta potential of any doped element to form electro active β phase. Electro active polymer and β phase crystallinity were discovered in 1960. Kawai demonstrated in 1969 that polyvinylidene fluoride (PVDF) shows a huge piezoelectric effect[3,7]. Among different well known electro active semi crystalline polymer with colossal dielectric properties, an electrical, optical, magnetic, physical property mostly depends on β phase.[6] This formation of β phase depends on the number and size of the doped materials. This β phase enhance the dielectric constant which is implemented in capacitive performance of polymer material. It can be used as dielectric material of super capacitor, multilayer capacitor, gas sensor, rail run, nonvolatile memory devices and very recently in the biomedical and electronic fields.[5]

1.2.1 Background

There are so many insulating medium is like wood, clay, plastic, polymer, quartz, mica, ceramic material, graphene, carbon nanotube, carbon nano fiber[40] etc. Out of them few are non-electro active and nonpolar, like wood, plastic etc and few are non-electro active and polar like polymer.

Polar polymers get easily polarized and take part in nucleation with other electro negative and electro active positive surface charge materials. Beside that polymer has good electrical, mechanical, thermal strength, long durability, easy to available, nontoxic, and some time low processing temperature.[7] Some of the polymers are electro active with different thermodynamically stable and unstable polymorphs.[8] The electro active polymer PVDF and its copolymer PVDF-HFP has five different crystalline polymorphs like α , β , γ , δ and ϵ . Among them, these α phase is nonpolar with the conformation as TGTG' (T-trans, G-gauche⁺, G'-gauche) dihedral. This nonpolar α phase is thermodynamically more stable than other polymorphs at normal temperature and standard pressure. Here the β phase is electrically polar and electro active with TTTT conformation.

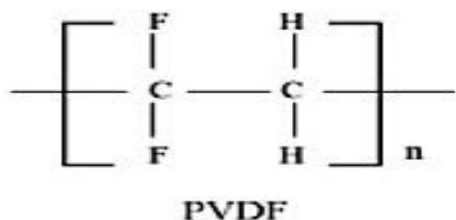


Figure 1.2 PVDF, electro active polymer (adopted from webpage, www.google.com)[9]



Figure 1.3 PVDF-HFP (where $n > m$) electro active polymer (adopted from webpage, www.google.com) [8]

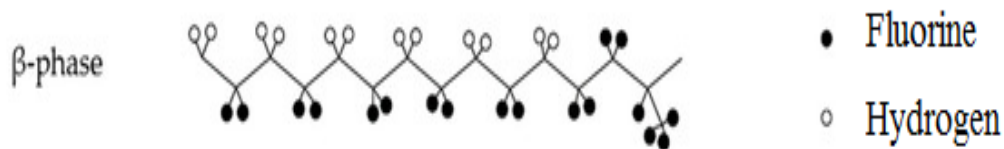


Figure 1.4. β phase of PVDF-HFP electro active polymer (adopted from webpage, www.google.com) [8]

In PVDF-HFP, compared to other phases, β phase shows highest dielectric, piezoelectric, pyroelectric and ferroelectric properties. In contrast, the γ phase is polar with conformation TTTGTTG' which exhibits [9] above properties moderately. And rest of the two phases δ and ϵ are nonpolar and thermodynamically unstable at room temperature and normal pressure and are easily converted to α , β and γ phases.

1.2.2. Why Polyvinylidene fluoride Co hexafluoropropylene (PVDF-HFP)?

Polyvinylidene fluoride Co hexafluoropropylene (PVDF-HFP) is a co polymer of Polyvinylidene fluoride (PVDF). Most of the substance of PVDF-HFP is the PVDF and small amount of molecule of hexafluoropropylene (HFP). It has so many tunable properties like electrical, mechanical, thermal, optical, magnetic, catalytic etc with doping by other nanomaterials. Also it has some unique properties like high power density, high energy density, high thermal strength, high mechanical strength, long durability, good interaction with doping material maintaining high surface to volume ratio, low processing temperature, low cost, nontoxic, low dielectric constant, large electro dielectric breakdown, high tangent loss, high ac conductivity etc. Its most of the phases are α , which is most stable, electro active in nature and another phase β is electro actively polar which makes dipole with doping materials for enhancing the tunable properties.

1.2.3. Why β Phase Polymorphos of PVDF-HFP?

PVDF-HFP has five semi crystalline polymorphos (phases). These are α , β , γ , δ and ϵ . Out of them α polymorphos is the most thermodynamically stable and β phase is polar and electro active. This β polymorphos makes covalent bond with electronegative and electro positive surface charges and gets polarized in electric field to enhance the capacitive performance of the capacitor. As others are unstable so α , γ , δ and ϵ can be easily convert to β polymorphos.

1.2.4 Bulk vs Micro vs metal nanoparticle

The basic difference among bulk, micro and nanoparticle lies in their size. Generally bulk materials are in centimeter in dimension, micro particles are in micro meter and nanoparticles have nanometer (1-100nm) dimensions. The bulk materials are those have at least one dimension is above $1000\mu\text{m}$ and micro materials are those have one dimensions is less than one micrometer ($1000\mu\text{m}$). The range of micro particle is 1- $1000\mu\text{m}$. We can see the bulk and micro particles in naked eye and nanoparticle cannot be visualize in naked eye. Bulk materials has low surface to volume ratios and have better performance in catalysis, gas sensors etc. In bulk materials there are low number of atoms or molecules on the surface which triggers to these properties. Bulk materials of metal have normal scattering properties and bulk semiconductor materials may not show confined energy state. In electronics, band structure of bulk materials, physical and chemical properties cannot be regulated, adsorption and absorptions of molecules are low and

slow. Physical properties are independent of size in bulk material. Examples of bulk materials are sand, any metallic salt, alumina, ore etc.

On the other hand the term micro particle is used to describe spherical particles of physical dimension between 1 and 1000 μm in diameter. In 1967, Peter Wolf first recognized micro-particles during his ongoing research in the field of blood coagulation. Micro particles are available commercially in wide variety of materials like ceramics, metal, glass, polymer etc. The small size of micro particles has an advantage over larger, macro scale particles due to the larger surface-to-volume ratio. Micro particles are formed by step down or step up approach from bulk or nanomaterials respectively and it is embedded or present at surface in the form of solid, liquid, or gas particles in the polymeric matrix or shell. Micro spheres provide moderately large surface area to volume ratio. In spite of the same composition of the corresponding bulk materials these nanoparticles display exceptional optical, electrical, thermal, and magnetic characteristics due to its size effects. Different metals like silver, iron, zinc, copper and cobalt platinum in their draw an utmost interest of researcher in diverse fields of science and technology including medicine. As it is established that a substance's size affects its physicochemical qualities, including it's chemical, electrical, mechanical, and optical properties, the significance of NMs have been increase profoundly. Thus, due to their unique properties, metal nanoparticles have drawn considerable interest in the scientific community (Gleiter, 2000). Metal nanoparticles (NPs) exhibits potential ability in several applications including electrical, electronics, petrochemical industries, water treatment industry, oil refineries, catalytic processes, industrial processes, building materials, medical diagnostics, and drug delivery industry, etc. Various protocols have been adopted to produce NPs, such as step down approach, attrition, pyrolysis, precipitation of chemicals, condensation, ion implantation, and synthesis of

hydrothermal (Pokropivny and Skorokhod, 2007) etc. Different application of metal nanoparticles has been schematically shown in figure 5.

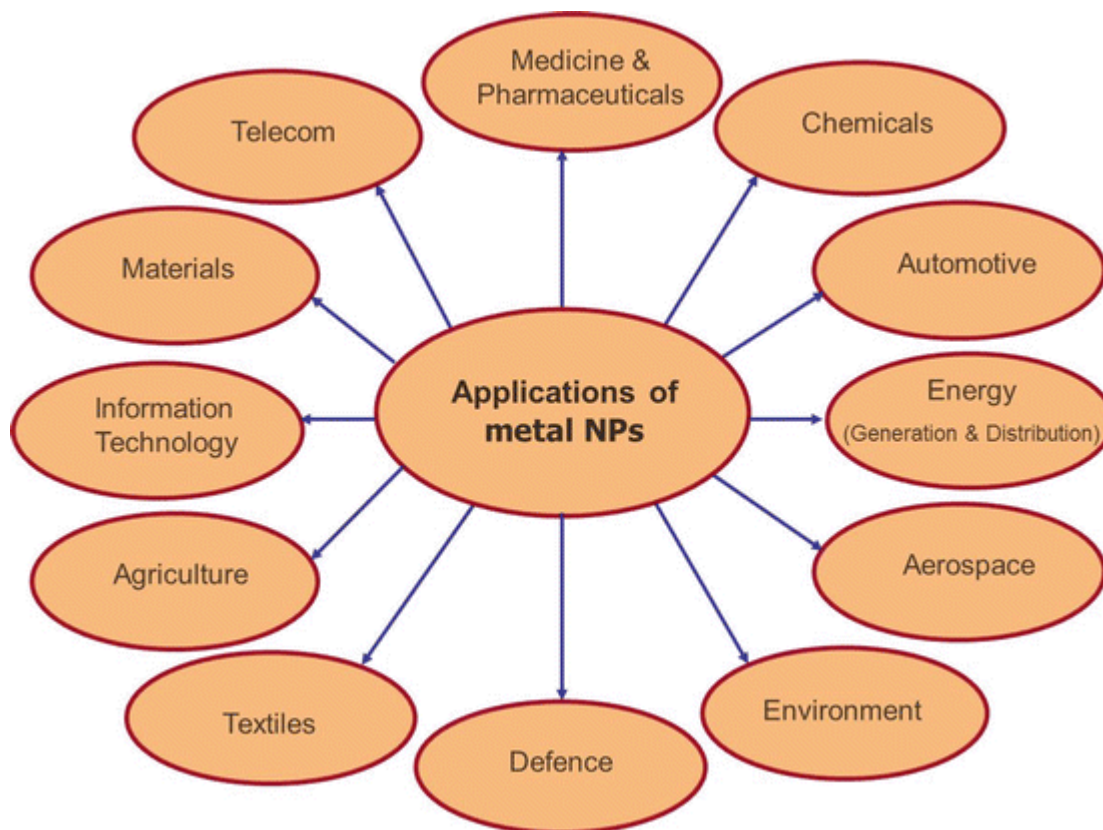


Figure 1.5. Application of metal nano particle(adopted from webpage,www.google.com)

1.2.5 Literature review

Storage of energy has now become a challenging job and a key focus of the worldwide scientific faculties. There has been a great attention for developing and proper tuning of more storage devices with higher efficiency. To fulfill the above requirement nanocomposite materials of dimensions less than 100nm consider as a key element in this respect. Over the last decade has been observed that super capacitor have significant energy storage capacity and have been drawn the attention of researcher for its further improvement by using nanocomposites. Super capacitor

[10], multilayer capacitors utilize electrode materials with high surface to volume ratio and thin electrolytic dielectrics to enhance the capacitances with magnitude in several orders than conventional capacitors. In this respect, super capacitors are able to achieve higher energy densities by maintaining the high power density characteristic of conventional capacitors [11]. Additionally, it has been noted that there are many promising uses for nanocomposite systems, including the creation of new materials and the improvement of the functionality of well-known products like fuel cells, sensors, and coatings.

Nanocomposites are composites in which at least one of the phases exhibits nano scale dimensions. While offering preparatory issues related to the regulation of elements composition and stoichiometry in the Nano cluster phase, nanocomposite materials have emerged as viable options to solve the shortcomings of micro composites and monolithic materials. Nanocomposite materials are generally classified in three different categories depending on their matrix materials, as shown in the table1.1.

Serial Number	Class	Examples
1	Polymer	Thermoplastic/ Thermoset polymer/layered silicates, Polyester/TiO ₂ , Polymer/CNT Polymer/layered double hydroxides.
2	Metal	Cu, Co, As, Fe, Ni, Cr/Al ₂ O ₃ , Ni/Al ₂ O ₃ , Co/Cr, Fe/MgO, Al/CNT, Mg/CNT
3	Ceramic	Al ₂ O ₃ /SiO ₂ , SiO ₂ /Ni, Al ₂ O ₃ /TiO ₃ , Al ₂ O ₃ /SiC, Al ₂ O ₃ /CNT

Table 1.1 Different types of nanocomposites

The objective of this review is to accumulate a comprehensive outline of various types of nanomaterials (NMs) and the protocol of preparation, which in turn would be helpful for developing modified nanofabrication techniques, to develop advanced nanomaterials for different functional applications. Furthermore, this review in various techniques used for the physical and chemical characterizations of NMs' properties and high-light their possible environmental toxicity will be understood. When the particles are transforming from bulk to micro then nano form the energy levels [12] become discretized. Based on various criteria, NMs are classified into different groups. Dimensionality, morphology, state, and chemical composition are the major factors by which NMs are categorized (Gleiter, 2000). This categorization is also dependent on their size ranges from 1–100 nm in at least one dimension.

1.2.6 Synthesis Technique

Initially, there are two mostly used approaches such as breakdown (top-down) and build-up (bottom-up) were mostly used. In first approach of an external force is required to break up a

solid into smaller particles and in other case atoms of gas or liquids based on molecular condensations or atomic transformations are assembled for preparing NMS. Here we have followed the step down approach which is similar to method of trituration or succussion [13-15] to prepare nanoparticles (nanomaterials). Following conditions have to consider during the synthesis of nanoparticles and fabrication of a device:

- control of particle size, size distribution, shape, crystal structure and composition distribution
- improvement of the purity of nanoparticles (lower impurities)
- control of aggregation
- stabilization of physical properties, structures and reactants
- higher reproducibility
- higher mass production, scale-up and lower costs

1.2.6.1 Sol-Gel Method

Based on their polarity polar solvent are the most useful solvent to synthesis the nonmaterial by Sol-gel method [16]. It is one of the most widely used preparation techniques for synthesis of very low dimensional nanoparticles. If a bulk solid is dispersed in a liquid medium, the colloidal system is called sol. Gel is referred to the uniformly distributed particles in the dispersed medium. By this technique we are able to make the highly pure and homogeneous powder sample even at comparatively very low temperature. Strong particle solvent interaction is a crucial phenomenon for gel formation and the repulsive force between particles make the sol stable. This force will prevent agglomeration. Here is the flow chart if figure 1.6 of preparation of nanocomposite by sol-gel method.

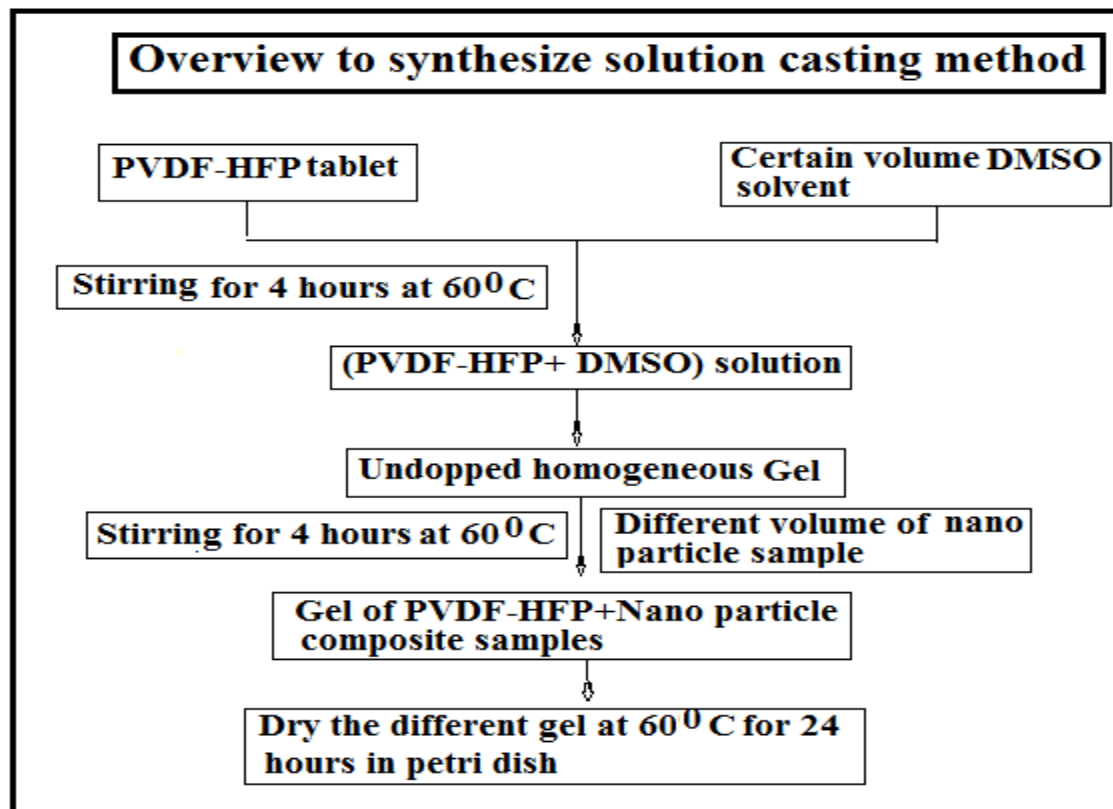


Figure 1.6 Flow chart of Sol-gel method [16]

1.3 Introduction to Polymer

1.3.1 Classification of Polymers

Polymer is one of the most important matrix elements to prepare nanocomposite material in nano dimension. Polymers are categorized depending upon their source, structure, molecular orientations and polymerization procedure. A flowchart has been shown in Figure 1.7 to illustrate intensely the classification of polymers. Also table 1.2 is presented here for denoting some examples of the classified polymers.

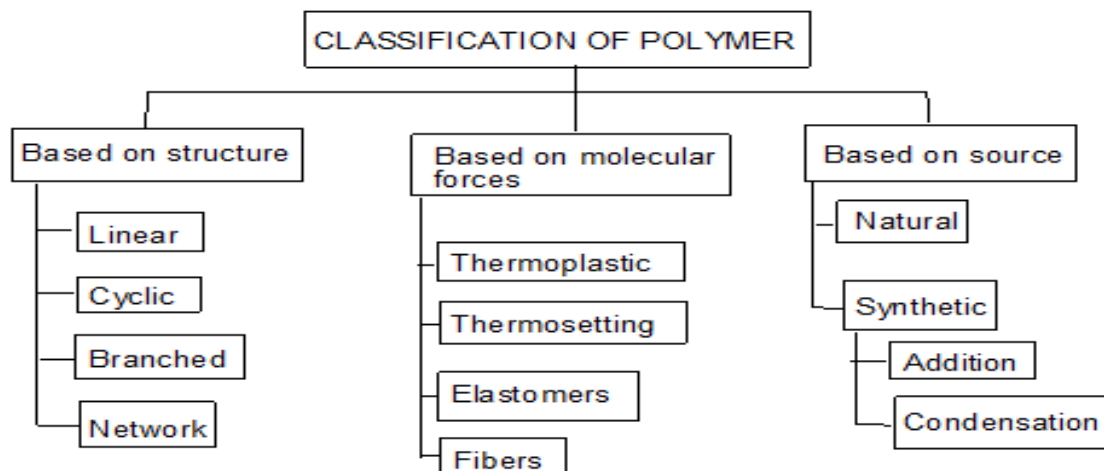


Figure 1.7 Classification of different types of Polymers

SL No	Polymer Type	Example
1	Natural Polymer	DNA, RNA, Proteins
2	Semi synthetic Polymer	Vulcanized rubber, Cellulose rubber
3	Synthetic Polymer	Polysterins, Polypropeline
4	Linear Polymer	Polyster, Nnylon
5	Branched chain Polymer	Low density polythene, Phenol formaldehyde.
6	Cross linked Polymer	Bakelite
7	Elastomers	Natural rubber, Fluoro elastomers
8	Fibers	Cotton, Jute etc.
9	Thermoplastics	Polyvinylidene Fluoride, Polyvinylidene Fluoride Co hexa fluoropropylene

10	Thermo setting Polymers	Epoxy resin, Melamine Formaldehyde
11	Addition Polymers	Polyvinyl Chloride, Teflon
12	Condensation Polymers	Poly (β hydroxyl butyric Acid.

Table 1.2 Classification of polymers and their examples.

1.3.2 Electro active Polymers (EAPs)

Electro active polymers are the most widely used matrix for the formation of nano composite materials. Electro active polymers (EAP) are a relatively new class of “smart material” that deformed in the presence of an applied electric field, like piezoelectric actuators. Unlike piezoelectric actuators the EAPs are fundamentally operated on different principles and produce force, stress, strain, deflections like biological muscles.[18]

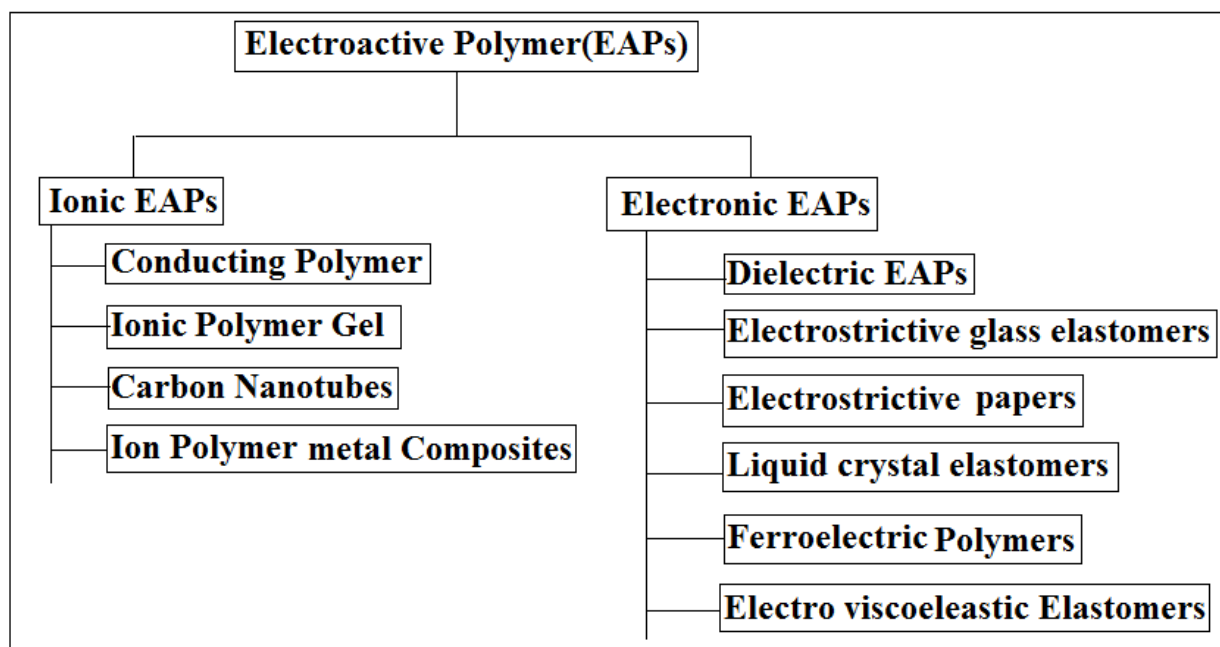


Fig.1.8. Different types of Electro active Polymers

Basically these EAPs are classified in two types: ionic and electric[17]. The ionic EAPs are operated by the process of ion movements inside the polymer. Although only a few volts are required for actuation, the ionic flow suggests that a higher electrical power is required for actuation and that more energy is required to maintain the actuator in a specific position. Conductive polymers, ionic polymer metal composites (IMPCs), responsive gels are various kinds of ionic EAPs. Electric EAPs are material in which actuation is caused by electrostatic forces between the two electrodes by squeezing the polymer. Dielectric elastomers are able to face very high strains and these are comparable with a capacitor that changes its capacitance in accordance with in applied voltage allowing the polymer to compress the thickness and expand in area due to electric field. Dielectric EAPs require no power to keep the actuator at a fixed position. Recently, Poly vinylidene fluoride (PVDF) and its copolymers like poly vinylidene fluoride trifluoroethylene [PVDF-TrFE], polyvinylidene fluoride hexafluoropropylene [(VDF-HFP)] & poly(vinylidene fluoride trifluoro ethylene chlorofluoro ethylene) [PVDF-TrFECFE] built nanocomposites with higher dielectric constants are evolving as potential material candidate and it has broad range of applications such as in grid leveling, rail runs, pulsed laser, electric or hybrid vehicles, communications devices, actuators, artificial muscles, charge storage capacitors systems, etc.

1.3.2.1 Polyvinylidene Fluoride Cohexafluoropropylene (PVDF-HFP) and its structure

PVDF-HFP is a highly insulating, chemically stable, non-reactive, semi formed from repetition of subunits of monomer vinylidene fluoride (VDF) ($\text{CH}_2\text{-CF}_2$) consisting of fluorine 59 wt% and hydrogen (3 wt%) and rest is carbon 38%. It has many attractive distinguishable characteristics like flexibility, light weight, thermal stability ($\sim 150^\circ\text{C}$), high dielectric break down, power density is high, energy density is high, processing temperature is low, dipole moment is high,

good interaction with doped materials, high thermal stability and non-toxicity in nature and it has drawn the attention to a researcher over the globe. A schematic structure of PVDF containing basic elements carbon (C), hydrogen (H) and fluorine (F) commercially available PVDF-HFP is shown in Fig.1.9

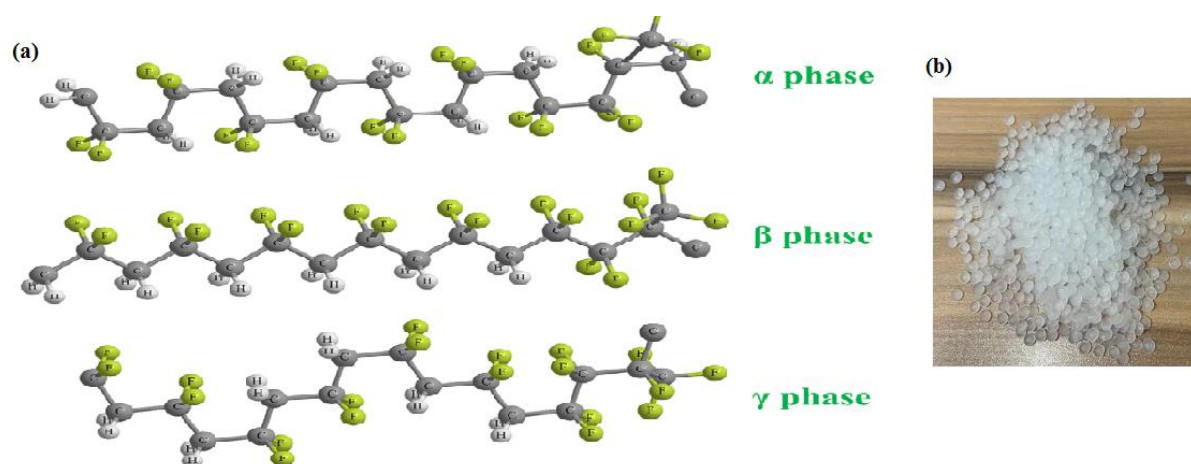


Figure1.9. (a) PVDF-HFP structure (C= Carbon; F= Fluorine; H= Hydrogen) and (b) Commercially available PVDF-HFP (adopted from web page, www.google.com).

PVDF-HFP structure has five polymorphic phases. They are α , β , γ , δ , and ϵ . The α -phase (conformation) has para electric property and it is thermodynamically stable. In PVDF-HFP the most interesting phase structure is found for the β polymorphs where all are in Trans (TTTT) conformation [17]. This type of regular electrically polar structure is not only more stable but also electro statically very active. It has largest polarization ability per unit cell (8×10^{-30} Cm) that makes its more superior amongst all its 5 phases. A schematic diagram is displayed in Figure 1.9(a) to understand the structure of α phase, β phase and γ phase of PVDF-HFP properly. β phase shows an attractive electro active behavior. It's all Trans structure attracts the fluorine atoms along with the carbon skeleton to bring them close together. As a result, their van der Waals radii overlap to each other. In this way, a head to tail organization or planar regular

structure is found to be formed. This structure makes it a very stable crystal. The total value of the van der Waals radii for hydrogen and fluorine is larger than the distance between the atoms. So a slight strain develops in between the atoms. The sum of the van der Waals radii can be greater than the space in between them, 2.7 \AA , when two fluorine atoms are adjacent along the carbon backbone. It creates strain between the two atoms. This β -structure is able to produce tighter packing density and also able to reduce the inter molecular strain allowing greater chain movement. Hence, to improve the β phase formation of PVDF-HFP draws a significant attention of researchers. Co polymer of this type can deliver a good response towards piezo, pyro and ferroelectric characteristics. If the PVDF-HFP chain experiences an electric field, dipole moments of fluoro carbons can switch frequently inside the matrix which gives rise to its ferroelectric response. A high dielectric constant and breakdown field is also notable features of this polymer.

1.3.2.2 Possible applications of PVDF-HFP and its composites

The properties like electrical, optical and magnetic of the high dielectric electro active polymer composites (EAPNCs) can be enhanced by doping several transition metals in the polymer PVDF-HFP. Incorporation of metal nanomaterial increases the capacitance as high surface to volume ratio becomes and matrix resistivity becomes low. These properties make the material highly efficient candidate for super capacitor application.

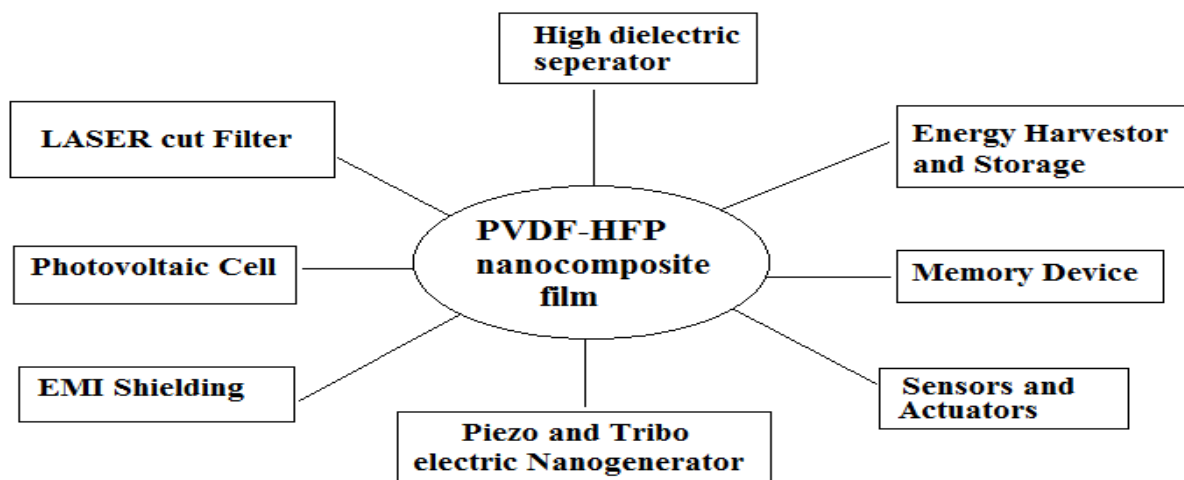


Figure1.10 Application of PVDF-HFP metal nanocomposite film

1.4 Introduction to Electro active Polymer Nano (EPNCs) Composite

1.4.1 Synthesis

PVDF, PVDF-HFP are highly non-reactive thermo plastic fluoro polymers they are produced by polymerization of vinylidene di fluoride. PVDF-HFP can be synthesized from the VDF monomer (gases) through a free radical polymerization process followed the process of melt casting or processing from a solution by solution casting, spin coating, and film casting. Typical solvents are used including Dimethyl sulfoxide (DMSO)[17], dimethyl formamide and more volatile butanone in solution based processing.

EAPNCs in material science one or multiple steps optimization of electrochemical process has been used for dissolve EAPNCs by directly manipulate polymers in the form of thin film or coating. Whereas in electrochemical synthesis the process is often limited for using of monomers which are to be oxidized for generating intermediates of reactive radicals for triggering polymerization process. In spite of various conducting polymers with selected monomer are

processable through chemical polymerization, only EAPs (i.e. PVDF, PVDF-HFP) may be polymerized through both chemical and electrochemical process. For fabricating polymer films having regulated thickness, there are several techniques. For the fabrication of polymer with ordered films of doped nanocomposites solutions cast and spin cast methods have been used depending on appropriate conducting polymers. In the solution cast thin films are produced by depositing drop wise monomer and oxidant solution on the surface of the substrate and then evaporating the solvent. This is a simple process and confirms the surface polymerization exclusively but in this case uniform layering of film cannot be assured. In spin coating method, the solution of the polymer is deposited on the rotating substrate, followed by solvent and evaporation a thin layer is formed. Here, synthesis of PVDF-HFP may be conducted through a controlled free radical. Polymerization process from the gaseous VDF monomer. In this fluoro surfactant acid (perfluoro nonanoic) is used as an anion in the aqueous emulsion polymerization process.

1.4.2 Fabrication Techniques

Thin polymer film or free standing polymer substrate are prepared using various techniques. Fabrication processes are solution casting,[33] stretching, annealing, electrode deposition, Spin coating, chemical deposition, chemical solution deposition (CSD),[19] atomic layer deposition (ALD),[21] chemical vapor deposition (CVD)[20] and plasma enhanced CVD (PECVD)[28] thermal evaporation, molecular beam epitaxy, electron beam evaporation, electro hydrodynamic deposition (electro spray deposition)[32] sputtering, cathodic arc deposition (arc-PVD),[22] pulsed laser deposition, thermal spray processing (gun), hot press technique, dip coating, painting etc. These different types of techniques are used for different application purposes. Among them, very simple and low cost technique is solution casting technique which is widely

used for fabrication of free standing polymer film. We have applied this process for better results.

1.4.2.1 Solution Casting

Out of so many sample preparations technique solution casting technique is an easy, cost effective and well known technique. The polymer content, dust or pellets are taken in proper amount and dissolved in the specific solvent. For example, PVDF-HFP is fully soluble in DMSO.[17-19] The solution is heated and stirred continuously at a critical temperature in which electrostatic interaction between polymer chains with the doping element or β -phase formation becomes maximum. Then the solution is cast over a substrate made of glass or Teflon and kept horizontally on the surface in an undisturbed condition. In this moment, a specific pressure and temperature is maintained. After a certain time, a thin film of polymer solution is formed in that specified environment. The film is taken out from the substrate with a controlled precession followed by the process of curing or drying. To maximize actuation strain, the polymer chains are aligned using a stretching process. Through this process, a thin film of thickness around a few nanometers is possible.

1.4.3 Properties

The electrical properties of doped PVDF-HFP have been extensively studied and it is found that doped PVDF-HFP evidenced a promising result [17-19]. So the material can be used for future application.

1.5 Characterization Techniques

1.5.1 Structural property

1.5.1.1 X-ray diffraction (XRD) techniques

X-ray crystallography is one of the structure characterization technique used to determine the atomic and molecular orientation of crystal structure and any impurities present in a crystal[19]. If crystalline atoms are imposed in ray beam diffraction occurs in many specific directions. Through measurement of the angles and intensities of these diffracted beams a three dimensional picture of the electrons density in the crystal is produced through array of the atoms. Then from this electron density distribution the array of the atoms in the crystal can be located, further more chemical bonds, their disorder can be identified.

X-ray diffraction is a fundamental technique to find out the structure of various crystallite materials such as salts, metals, minerals, semiconductors etc. This structure is also useful to depict the structure of organic and biological molecules.

In the X-ray diffraction an emission of electromagnetic radiation having energy of photon between 100eV–100keV. In this technique the hard X-rays of short wavelength like 0.1 angstrom is necessary where the energy of photon rays from 1keV-120keV are applicable. As the wavelength of X-rays is in the range of atoms size, they are able to penetrate inside the atomic and molecular arrangements of materials, and hence provide the information of parameters regarding the atomic orientation and structure. As a source of X-ray beams, X-ray tube or synchrotron radiation is used. X-ray beams are produced as the accelerating collimated electron beam with high energy strikes on the solid target at high electric field. When X-ray photon collides with electrons of the materials or target several photons get deflected away in various directions through the interaction with atoms in various lattice planes. If the scattered X-ray photons have the same wavelength than that of incident photons, this scattering is called elastic

scattering or Thomson Scattering. Through characterization of the scattered X-rays, the orientation of the atoms and all information about the crystal structure are explored which in turn gives us the detailed crystal structure. X-ray diffraction technique is helpful to explore stress and strain measurement, structural properties, chemical properties and substance of phase equilibrium study, estimation of crystallite and analysis of crystal structure. In our research works, Bruker X-ray diffractometer (D8, AXS, Advance) [17] has been employed. Germanium (022) monochromator has also been used to produce Cu K α (1.5406 Å) X-ray radiation using highly stabilized Bruker X-ray generator (K780) in our experiment the diffraction patterns are recorded in θ -2 θ mode. Collimated X-ray beams are incident on the target sample and the X-ray is diffracted in regular 3D lattice plane. From the diffraction pattern, the lattice spacing of the crystals are calculated using Bragg's equation-

$$2d \sin\theta = n\lambda \quad \dots\dots (1)$$

where, λ is the wavelength of incident X-rays, θ is equal to glancing angle and 'd' distance between planes. Then the intensity of the diffracted X-rays are plotted as a function of the angle. Shifting of peak position in the plot determines the change of d-spacing which indicates the variation of lattice constant under regular or uniform elastic strain. Inhomogeneous strain depends on crystal structure which results in peak broadening (FWHM variation). Peak broadening or FWHM variation can also alter the crystalline size. For a system with no inhomogeneous strain, the average crystallite size, D can be estimated from Scherrer's formula[23]:

$$\langle D \rangle = \frac{k\lambda}{\cos\theta \beta_{\frac{1}{2}}} \quad \dots\dots(2)$$

where, $\beta_{\frac{1}{2}}$ stands for the full width at half maximum (FWHM) of a diffraction peak, θ is the diffraction angle and K is the Scherrer's constant (~ 0.9). Optical focusing of the X-ray diffractometer is fabricated based on Bragg-Brentano para focusing geometry. A photograph of Bruker-D8 X-ray diffractometer and the schematic diagram of the X-ray interaction with material have been presented in Figure 1. 11.



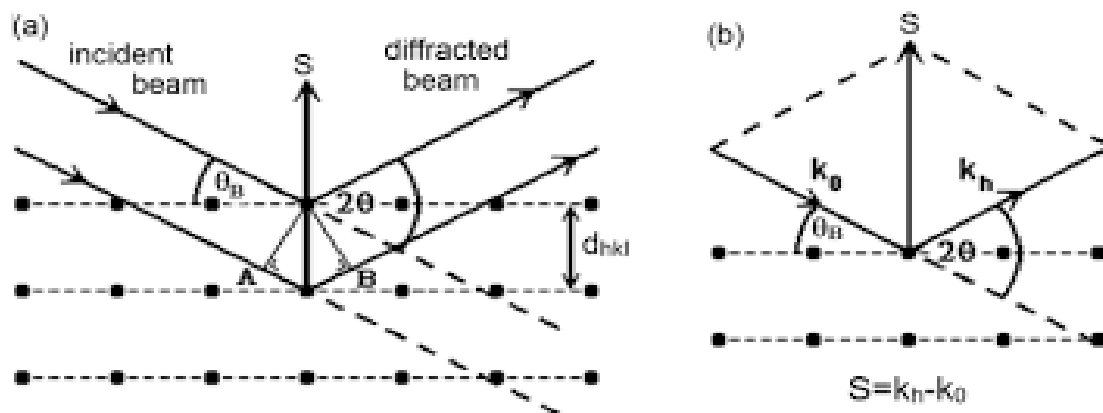


Figure 1.11. Photograph of X-ray Diffractometer and X-ray diffraction principle (adopted from webpage, www.google.com)

1.5.1.2 Fourier Transform Infrared Spectroscopy (FTIR)

To identify the molecular fingerprint of a sample, FTIR have been widely used as a characterization technique. In the process of FTIR the sample gets an exposure of IR radiation and some of the infrared radiation is absorbed by the sample and some of its passed through (transmitted). By modifying resulting spectrum, the molecular absorption and transmission curve calculated which in terms gives the information about molecular fingerprint [24] of the sample. Any specific finger print is unique i.e. there are no two molecular structure which have same infrared spectrum. This makes the technique of infrared spectroscopy is useful and widely used in various analysis.

It has diverse use such as-

- to identify unknown materials.
- to determine the quality or consistency of a sample.
- to determine the amount of components in a mixture.

Infrared absorption, transmission or emission spectrum of various solids or gases is obtained by the technique FTIR. Through the determination of frequencies of the absorbed energy, chemical bonding present in a molecular assembly are identified. In the FTIR arrangement, as the source of radiation, infrared light is used. In this electromagnetic spectrum, Infrared (IR) radiation consists of a region of wavelength lies between the visible and microwave range. But only under some consideration the interaction of IR radiation with the sample are measured. FTIR spectrometer is able to achieve information over a wide spectral range. The region of IR spectra can be classified into three sub categories known as $400\text{-}4000\text{ cm}^{-1}$ wavelength i.e., near-IR, $4000\text{-}400\text{ cm}^{-1}$ wavelength i.e., mid-IR and far-IR i.e., having wavelength of $400\text{-}20\text{ cm}^{-1}$. The infrared spectrometer employed an interferometer to collect interferogram of a sample signal. Fourier Transformation of the interferogram leads to achieve the actual spectrum. In the IR-spectrometer, the intensity of absorption is proportional to the number of molecules involved in IR-interactions. Using the principle of Lambert -Beer law, the infrared absorption signals are characterized. In modern FTIR system, Michelson Interferometer is used for better optical characterization where a beam splitter and two mirrors are employed. Two light beams from separate optical path produce interference. By using FTIR one can identify the sample, determine consistency and the number of components present in the sample. A photograph of FTIR instrument and a schematic ray-diagram of the principle of FTIR spectrometer is shown in Figure 1.12. In the present thesis all the FTIR spectra are recorded using the instrument, FTIR-8400S, Shimadzu.[18]

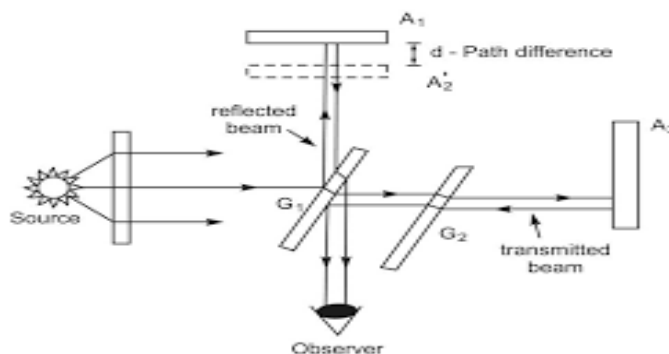


Figure1.12. Photograph of FTIR Instrument and FTIR principle (adopted from webpage, www.google.com)

1.5.1.3 Differential Thermal Analysis (DTA)

Differential Thermal Analysis (DTA) is a widely used thermo analytic characterization technique where, difference of temperature between sample and reference are recorded when both the sample material and an inert reference material are come across identical thermal cycles. Then differential temperature versus time graph is plotted. The sample undergoes through either exothermic or endothermic process[25] and the relative change between the sample and the inert reference is detected. A DTA curve thus offers information on the changes that have taken place, including glass transitions, crystallization, melting, and sublimation. The heat capacity of the sample has no impact on the area under a DTA peak, which represents the enthalpy change. In a DTA device there several parts such as a sample holder including sample containers, two thermocouples and a block made of ceramics or metal, a furnace, a temperature programming unit, and also a system for recording. One thermocouple is connected with an inert material (e.g., Al_2O_3), whereas another one is situated at the sight of the material sample. When the sample undertakes a phase transition due to the increase of temperature a deflection of the voltmeter is

noticed. A picture of DTA instrument and schematic diagram of its working principle are shown in figure.1.13

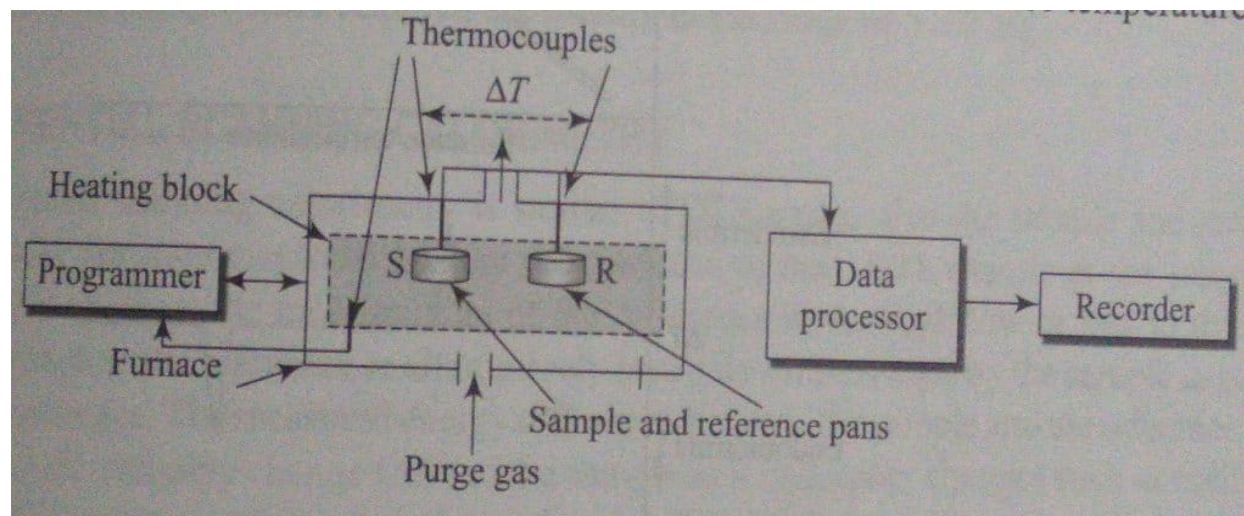


Figure1.13 Photograph of DTA and DTA principle (adopted from webpage, www.google.com)

1.5.2 Morphological Property

1.5.2.1 Field Emission Scanning Electron Microscope (FESEM)

It is a widely used characterization technique for depicting the surface morphology and microstructure of the materials of nano/micro dimension. In FESEM an electron gun made of filament of Lanthanum hexaboride or tungsten is used as field emitted electron source. A system of electromagnetic lenses is involved to keep electron focusing on the sample. Followed by, interaction between high energy electrons and the sample which leads to release of secondary and back scattered electrons. By using detectors these released electrons are firstly detected and then converted into electronic signals which further processed an imaging view. This technique is favorable for conducting surface of the sample. If the sample is insulating in nature, charges arise but cannot drift to the ground which results inferior images with poor contrast of the sample surface. To solve this problem, surface of non-conducting samples are coated with highly conducting gold or platinum film. In this thesis, FESEM images are taken with the help of FESEM, (INSPECT, F50, Netherlands)[18]. A photograph of the FESEM instrument and schematic diagram of FESEM mechanism are demonstrated in Figure 1.14

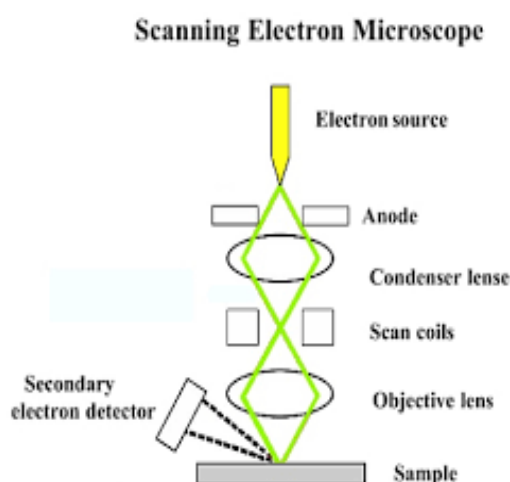


Figure 1.14 FESEM arrangement and Schematic diagram of FESEM (adopted from webpage, www.google.com)

1.5.2.2 Energy Dispersive X-ray (EDX) Analysis

The compositions of elements and stoichiometry of a material are determined by EDX technique [25]. The instrument is a modified part of an electron microscope such as FESEM or TEM. The basic principle is that the energy dispersive X-ray electrons interact with atoms present in materials in various ways and the scattering of electrons occurs in either elastic or inelastic manner. In case of inelastic scattering orbital electrons are displaced leading to a vacancy in that orbit, which is filled by the electron from a higher energy shell. Here, the electronic transition releases excess energy in the form of emitted X-ray photon. EDX detector evaluates the number of emitted photons of X-ray with respect to their corresponding energies which are specific for the element from which the X-ray is originated. The atoms undergo de-excitation by some energy releasing technique like cathodoluminescence (CL), Auger effect [26] etc.

1.5.3 Electrical properties

1.5.3.1 Impedance Spectroscopy with LCR meter

An Impedance analyzer is an electronic equipment which is widely used to measure the Inductance (L), Capacitance (C), and Resistance (R) of a sample [27]. Simply, the instrument measures the impedance internally and converts it to the corresponding capacitance or inductance value to display. If the capacitor or inductor that undergoes through the test does not have a significant resistive component of impedance it gives result in a very accurate manner. More advantage of this instrument is that it measures true inductance or capacitance accurately

and also the equivalent series resistance of capacitance and the Q factor of the inductive components.

LCR meter has the components of inductance (L), [28] capacitance (C), and resistance (R) and it is the electronic testing tool which can measure directly various electrical properties with a high degree of precision. In the most cases, the impedance is studied and transformed to the equivalent inductance or capacitance. Recently, more accurate values of inductance, capacitance and equivalent resistance (parallel/series) of the capacitive materials can be obtained through the advanced LCR meters; even in some variants the Q factor of inductive components can also be estimated. Usually, most of the hand held LCR meter works in the frequency range lying between 100Hz to 100 kHz but more high-end bench top LCR meters can work above the frequency range of 100 kHz and also some model works at lower than 100 Hz frequency region. In this thesis all data are collected from the digital LCR meter or impedance analyzer (Model: Agilent, E4980A) [18] which can provide a test frequency range from 40 Hz to 2 MHz. LCR meters frequently can overlay a DC electric constituent on the AC measuring signal. Some low cost variants of bench top LCR meters can provide these DC electrical components externally, while more sophisticated and expensive meters can internally supply the DC electrical components. [28] The electrical properties of dust material samples are measured by forming the dust material to a pellet or incorporating the material within the free standing polymer film. Figure 1.15. presents a schematic diagram of an LCR meter and its measuring setup.

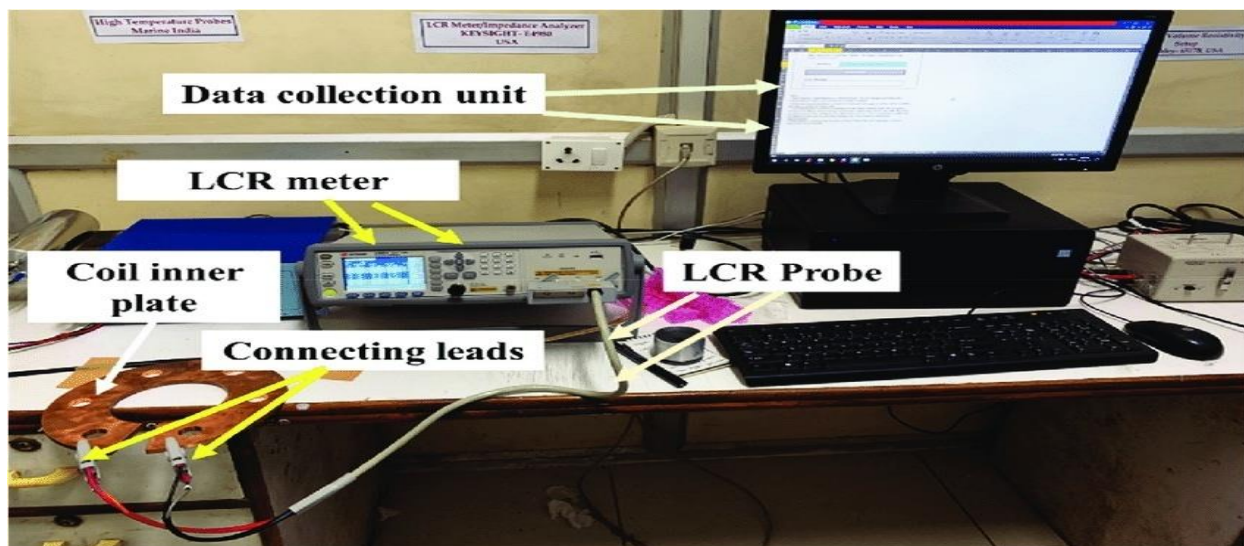


Figure 1.15 LCR meter setup (adopted from webpage, www.google.com)

1.5.3.1.1 Dielectric Constant

The dielectric property of a material is a fundamental molecular property which is to impend the movement of electrons, as a result of polarization within the material in presence of an external electric field. Dielectric material has very poor electrical conductivity and is widely used to build a capacitor as storage of electrical energy[29]. The Dielectric Constant (ϵ_r) is a factor which determines how much the capacitance of a capacitor increases by using a dielectric material relative to air. Dielectric material with a high dielectric constant is better than a dielectric material with a low dielectric constant for boosting capacitance in a capacitor. As dielectric constant is a ratio it is a dimensionless quantity. The dielectric constant (k) or relative permittivity (ϵ_r) of a sample is calculated by using the formula,[34-36]

$$\epsilon_r = \frac{dC_p}{A\epsilon_0}$$

Here ϵ_r , C_p , d , A and ϵ_0 are respectively the dielectric constant, capacitance, thickness of the dielectric material, cross-sectional area and permittivity of the free space.

1.5.3.1.2 Tangent Loss

The ratio of conduction current and displacement current of a material is known as tangent loss ($\tan \delta$) or dielectric damping loss or conductivity loss. This tangent loss is occurred due to the dissipation of heat energy as an electromagnetic energy or any type of leakage current. This is an intrinsic property and the loss factor varies with the applied field frequency. The tangent loss is determined by the formula [37-38]

$$\tan \delta = \frac{\epsilon''}{\epsilon'}$$

Here, ϵ'' is the imaginary part and ϵ' is the real part of permittivity.

1.5.3.1.3 AC Conductivity

Electrical conductivity(σ) is a measure of the ability of a material to conduct an electric current and it is the reciprocal of electrical resistivity. AC conductivity (σ_{ac}) is calculated by using the following formula,[39-40]

$$\sigma_{ac} = 2\pi f \tan \delta \epsilon_r \epsilon_0$$

Here, σ_{ac} and f are the AC conductivity, frequency(Hz) respectively, and $\tan \delta$, ϵ_r and ϵ_0 are respectively the tangent loss factor, dielectric constant and permittivity of free space.

1.6 Applications

1.6.1 High Dielectric Appliance

Dielectric material acts as an electrical insulator due to its non-conducting property of electricity but main difference to the insulator is the ability of highly polarizability in an electrical field (this is articulated as the material's dielectric constant). Dielectric substances in an electric field displace the charges from an equilibrium position towards the periphery. The charge may be aligned to the applied field rather than passing through the material. When the electric field is stopped, the material returns to its original state and the time taken in this process is called the relaxation period which is a characteristic of the dielectric. Material like CuPC, CoPC, AsPC inside the matrix enhance its dielectric performance to a greater extent. This type of high dielectric materials can be applied in various fields like -

1. In capacitors for energy storage.
2. In a semiconductor device.
3. In Liquid Crystal Displays.
4. In Dielectric Resonator Oscillator.
5. With high tune ability and low leakage current in microwave tunable devices.
6. For coating in electronic elements where it acts as a barrier between the substrate and the external environment.
7. In power transformers
8. In highly charge storage capacitors as a dielectric media to increase its capacitance value.

In my research work, dielectrics plays an important role in fabrication of a high dielectric separator for a charge storage system or other electronic applications. A better dielectric material must have a high dielectric constant and low tangent loss, storage stability, high temperature stability, high dielectric strength, strong frequency responsiveness, and be amenable to industrial processes. All these properties have been analyzed minutely in my research work. The measurements not only yield the dielectric properties of material but also informative about the electrical or magnetic properties of the material. We are also able to fabricate a charge storage device where high dielectric materials serve some crucial role such as:

1. To enhance the efficiency of capacitance by reducing the strength of the electric field, resulting equivalent charge even at lower voltage
2. To avoid the contact of conducting plates, followed by separation of smaller plate and thus the higher capacitances
3. To prevent the dielectric breakdown during operation by sparking at high voltage.

1.6.2 Non-conventional charge storage device

In the last decades, technological advancement and fast growing industrialization is a serious threat for the environment. This is the prime time for utilizing the stable renewable energy sources as the substitute of conventional fossil fuel. Supercapacitors are well recognized non-conventional charge storage devices which can mitigate the crisis of energy without any harm. Supercapacitors play a superior role than that of conventional batteries due to have several exceptional properties such as long durability, power density and short response etc. In my research work, nontoxic CuPC, CoPC, AsPC nanomaterial may be used in fabrication of a supercapacitor device.

1.7 Objectives of the Thesis

In order to optimize the future of sustainability and to save the mother nature, it is essential for us to move away from our traditional way of exploitation in terms of energy usage and storage and also search for superior energy storage materials. With the fast growing of energy consumption, the amount of fossil fuels i.e., gas, petroleum, and coal is shrinking day by day. It is the critical time to save and harvest our future energy supply since the conventional energy sources limit our usability. Additionally, the fossil fuels are one of the major pollutants for the environment. Subsequently, in order to fulfill the energy requirement of the expanding population, it is important for us to develop various strategies to explore different non-conventional energy storage sources, which are almost pollution-free.

In my work, I propose to investigate the electrical properties of some doped metal (transitional, rare earth) nanoparticles. The synthesis route of which involves both chemical sol-gel technique as well as direct heating of nanocomposites. Here, some transitional and rare earth elements will be impregnated into the polymer matrix. Since, specific surface area, adsorption capacities, reactivity mostly depend on the surface to volume ratio of the nanoparticles, my study will be focused to make the low dimensional non-toxic high temperature sustainable polymer composite nanoparticles. Present research works include enhancement of said properties of some electro active polymer by incorporating nano metal particles for industrial application. X-ray diffraction (XRD) technique will be employed to characterize the materials towards more crystallinity, purity and phase formation. Electron microscopy (FESEM) will be employed to understand the surface morphology and microstructure, surface to volume ratio, porosity, adsorption and desorption of the materials. EDX studies will be carried out to know about the stoichiometry ratio of the materials. Fourier transform infrared spectrometry (FTIR) will be conducted to

explore the purity, functional group present, better phase formation and phase transformation of the materials etc. Electrical properties (e.g. Dielectric measurements), of the materials will be studied in detail by L.C.R meter. A comparative study of electrical properties will be performed among different doped nanocomposites and also with their PVDF-HFP composites. Thus the whole work will have some impetus to submit new promising materials to mitigate the crisis in terms of energy harvesting and its storage.

References

- [1] C.M.Costa, J.L.Gomez Ribelles, S.Lanceros Méndez, G.B.Appetecchi, B.Scrosati, “Poly (vinylidene fluoride) based, co-polymer separator electrolyte membranes for lithium-ion battery systems”. J. Power Sources.245,779–786(2014).
- [2] T.Nestler, R.Schmid, W.Münchgesang, V.Bazhenov, J.Schilm, T.Leisegang, D.C.Meyer, “*Separators Technology Review: Ceramic Based Separators for Secondary Batteries*”, (2014), vol.1597.
- [3] A.Bruna, M.Arjmand, U. Sundararaj, R. Elida, S. Bretas, “Novel composites of copper nanowire/PVDF with superior dielectric properties”. Polymer55,226–234(2014).
- [4] L.Yang, J. Qiu, H. Ji, K. Zhu, J. Wang, Composites: “Enhanced dielectric and ferroelectric properties induced by TiO₂ of MWCNTs nanoparticles in flexible poly (vinylidene fluoride) composites”. Compos.PartA65,125–134(2014).
- [5] P.S. Chikramane, D. Kalita, A.K. Suresh, S.G. Kane, J.R. Bel-lare, “Why extreme dilutions reach non-zero asymptotes: a nano-particulate hypothesis based on froth flotation”. Langmuir, 28,15864–15875(2012)

- [6] P.Martins,C.M.Costa,M.Benelmekki,S.Lanceros-mendez,“On the origin of the electroactive poly (vinylidene fluoride) β -phase nucleation by ferrite nanoparticles via surface electrostatic inter-actions”. *Cryst Eng Comm*14,2807–2811(2012).
- [7] P.Martins,C.Caparros,R.Gonc,P.M.Martins,M.Benelmekki,G.Botelho, “Role of nanoparticle surface charge on the nucleationof the electroactive β -poly (vinylidene fluoride) nanocomposites for sensor and actuator applications”. *J. Phys. Chem. C* 116(29),15790–15794(2012).
- [8] Q. Chen, P. Y. Du, L. Jin, W. J. Weng and G. R. Han: ‘Percolative conductor/polymer composite films with significant dielectric properties’,*Appl. Phys. Lett.*, **2007**, **91**, 022912-1–022912-3.
- [9] X. Y. Huang, P. K. Jiang and L. Y. Xie: ‘Ferroelectric polymer/silver nanocomposites with high dielectric constant and high thermal conductivity’, *Appl. Phys. Lett.*, **2009**, **95**, 24290-1–24290-3.
- [10] I. Moreels, Y. Justo, B. De Geyter, K. Haustraete, J. C. Martins, and Z. Hens, “Quantum Dots: A Surface Chemistry Study,” *ACS Nano*, vol. 5, no. 3, pp. 2004–2012, 2012.
- [11] P. Nandy, S. Bhandary, S. Das, R. Basu and S. Bhattacharya: ‘Nanoparticles and membrane anisotropy’, *Homeopathy*, **2011**, **100**, 194.
- [12] X.Wei, L.I.Xin hai, G.U.O.Huajun, W.Zhi-xing, Y.Bo, W.U.Xian wen, M. Science, S.B. Heidelberg, “Preparation and properties of composite polymer electrolyte modified with nano-size rare earth oxide”.*J.CentralSouthUniv.*2,3378–3384(2012).
- [13] H.Chang,C.Chang,Y.Tsai, “Electro chemically synthesized graphene/polypyrrole composites and their use in supercapacitor”.*Carbon*N.Y.50,2331–2336(2012).
- [14] P. Nandy: ‘A review of basic research on homoeopathy from a physicist’spoint of view’, *Indian J. Res. Homeopath.*, **2015**, **9**, 141–151.

- [15] M. Jayalakshmi and K. Balasubramanian, “Simple capacitors to supercapacitors - An overview,” *Int. J. Electrochem. Sci.*, vol. 3, no. 11, pp. 1196–1217, 2008.
- [16] B. K. Paul, S. Kar, P. Bandyopadhyay, R. Basu, S. Das, D. S. Bhar, R.K. Manchanda, A. K. Khurana, D. Nayak and P. Nandy: ‘Significant enhancement of dielectric and conducting properties of electroactive polymer polyvinylidene fluoride films: an innovative use of *Ferrum metallicum* at different concentrations’, *Indian J. Res. Homeopath.*, **2016**, **10**, (1), 52–57.
- [17] B. K. Paul, S. Das, R. Basu, D. S. Bhar, R. K. Manchanda, A. K. Khurana, D. Nayak, P. Nandy: ‘Effect of dilution of *Ferrum metallicum* and zincum oxidatum, homeopathic nanomedicines on the dielectric properties of poly(PVDF-HFP) film’, *Int. J. High Dilution Res.*, **2016**, **15**, (1), 10–17
- [18] B. Kang and G. Ceder, “Battery materials for ultrafast charging and discharging,” *Nature*, vol. 458, no. 7235, pp. 190–193, 2009.
- [19] G. Wang, “Enhanced dielectric properties of three-phase-percolative composites based on thermoplastic-ceramic matrix (BaTiO₃ + PVDF) and ZnO radial nanostructures,” *ACS Appl. Mater. Interfaces*, vol. 2, no. 5, pp. 1290–1293, 2010.
- [20] A.Manivannan, P.N.Kumta, “Advancing the supercapacitor materials and technology frontier for improving power quality”. *Elec-tro chem.Soc.Interf.*19,57–62(2010)
- [21] H. Xu, Z. Dang, N. Bing, Y. Wu, D. Yang, H. Xu, Z. Dang, N.Bing, Y. Wu, D. Yang, Temperature dependence of electric and dielectric behaviors of Ni/polyvinylidene fluoride composites. *J.Appl.Phys.*(2010).<https://doi.org/10.1063/1.3289731>
- [22] P. Dvořák, “Overview of Non-Aqueous Electrolytes for Supercapacitors,” *Energy*, vol. 4, no. 3, pp. 2–6, 2010.

- [23] Y. Li, H. Xie, J. Wang, and L. Chen, “Preparation and electrochemical performances of MnO₂ nanorod for supercapacitor,” *Mater. Lett.*, vol. 65, no. 2, pp. 403–405, 2011.
- [24] G. Yu, L. Hu, N. Liu, H. Wang, M. Vosgueritchian, Y. Yang, Y. Cui, and Z. Bao, “Enhancing the supercapacitor performance of graphene/MnO₂ nanostructured electrodes by conductive wrapping,” *Nano Lett.*, vol. 11, no. 10, pp. 4438–4442, 2011.
- [25] D.-J. Kim, “Oxygen Position and Bond Lengths from Lattice Parameters in Tetragonal Zirconias,” *J. Am. Ceram. Soc.*, vol. 81, no. 191022, pp. 241–243, 1998.
- [26] B.E. Conway, “*Electrochemical Supercapacitors: Scientific Fundamentals and Technological Applications*” (Springer Science+Business Media, LLC, 1999). <https://doi.org/10.1007/978-1-4757-3058-6>
- [27] S. C. Pang, M. A. Anderson, and T. W. Chapman, “Novel electrode materials for thin film ultracapacitors: Comparison of electrochemical properties of sol-gel-derived and electrodeposited manganese dioxide,” *J. Electrochem. Soc.*, vol. 147, no. 2, pp. 444–450, 2000.
- [28] W. L. Barnes, A. Dereux, and T. W. Ebbesen, “Surface plasmon subwavelength optics,” *Nature*, vol. 424, no. 6950, pp. 824–830, 2003.
- [29] B. Horgan, “Investigating Grain Boundaries in BaCuS_{1-x}Se_xF Using Impedance Spectroscopy,” pp. 0–30, 2004.
- [30] J. Robertson, “High density plasma enhanced chemical vapor deposition of optical thin films,” *Eur. Phys. J. Appl. Phys.*, vol. 28, pp. 265–291, 2004.
- [31] S. Hassan, M. Suzuki, and A. A. El-Moneim, “Capacitive Behavior of Manganese Dioxide/Stainless Steel Electrodes at Different Deposition Currents,” *Am. J. Mater. Sci.*, vol. 2, no. 2, pp. 11–14, 2012.

- [32] A. V. Dobrynin and M. Rubinstein, “Theory of polyelectrolytes in solutions and at surfaces,” *Prog. Polym. Sci.*, vol. 30, no. 11, pp. 1049–1118, 2005.
- [33] K.F. Lin, H.-M. Cheng, H.-C. Hsu, L.-J. Lin, and W.-F. Hsieh, “Band gap variation of size-controlled ZnO quantum dots synthesized by sol–gel method,” *Chem. Phys. Lett.*, vol. 409, no. 4–6, pp. 208–211, 2005.
- [34] Z.Dang,J.Wu,H.Xu,S.Yao,M.Jiang,J.Bai,Z.Dang,J.Wu,H.Xu,S.Yao,M.Jiang, “Dielectric properties of upright carbon fiber filled poly (vinylidene fluoride) composite with low percolation threshold and weak temperature dependence”. *Appl. Phys. Lett.*(2007)
<https://doi.org/10.1063/1.2770664>
- [35] K. Gong, P. Yu, L. Su, S. Xiong, and L. Mao, “Polymer-assisted synthesis of manganese dioxide/carbon nanotube nanocomposite with excellent electrocatalytic activity toward reduction of oxygen,” *J. Phys. Chem. C*, vol. 111, no. 5, pp. 1882–1887, 2007.
- [36] Y. Ye, Y. Jiang, T. Wang, J. Yu, and Z. Wu, “Preparation and characterization of polymeric PVDF films byultrasonic atomization,” *Integr. Ferroelectr.*, vol. 88, no. 1, pp. 27–32, 2007.
- [37] W. Haiss, N. T. K. Thanh, J. Aveyard, and D. G. Fernig, “Determination of size and concentration of gold nanoparticles from UV-Vis spectra,” *Anal. Chem.*, vol. 79, no. 11, pp. 4215–4221, 2007.
- [38] J.R. Miller, P. Simon, Materials science: electrochemical capacitors for energy management.*Science*321,651–652(2008)
- [39] Y. Kobayashi, T. Tanase, T. Tabata, T. Miwa, and M. Konno, “Fabrication and dielectric properties of the BaTiO₃ polymer nanocomposite thin films,” *J. Eur. Ceram. Soc.*, vol. 28, no. 1, pp. 117–122, 2008.

[40] P.Thakur,A.Kool,B.Bagchi,S.Das,P.Nandy, “Crystallization and dielectric properties of poly(vinylidene fluoride) thin films”.Phys.Chem.Chem.Phys.17,1368–1378(2014).

Chapter 2

Enhancement of dielectric properties and conductivity of materials doped with different nanoparticles

2.1. Chapter overview

In this study we have the objective to enhance the dielectric properties and conductivity of materials by doping it with different nanoparticles and to use these materials as promising candidates in electronic industry to mitigate the global crunch of energy harvesting and storage devices.

Here, we have synthesized metal nanoparticles and incorporated them in the polymer matrix (PVDF-HFP) by simple solution casting method to form nanocomposites. Then these composites are passed through a series of characterization techniques, such as Fourier transform infrared spectroscopy (FTIR), Scanning electron micrographs (SEM), Field emission scanning electron microscopy (FESEM) followed by several measurement of electrical properties such as Dielectric Constant measurement, Tangent loss measurements and AC conductivity measurements.

Through the results of various analysis and measurements, it has been shown that these nanocomposites have effective dielectric properties over a broadband frequency range with higher dielectric permittivity with significantly low dissipation factor ($\tan\delta$). Hence, these nanocomposite materials might have significant electrical importance in the field of modern electronic industry.

2.2. Introduction

Due to their intrinsic, adaptable and other exceptional properties such as high flexibility, low preparation temperature, moderate dielectric constant, high tolerance in dielectric field, and many others, Poly(vinylidene fluoride (PVDF) and its copolymers such as poly vinylidene fluoride Hexafluoropropylene (PVDF-HFP) have a great importance and have been used as a

potential candidate in the diverse fields of research including electronic industry[1,3]. For enhancing the capacitive performance of the polymer material, various metal nanoparticles have been widely used as doping materials to form the polymer matrix which are in great demand for research. Metal nanoparticles are distributed uniformly and homogeneously in the matrix that enabled them to have better interaction with the material of polymer matrix which is the basis of enhancement of the electrical properties of the polymer material [4,7]. In this study, PVDF-HFP composites have been developed with incorporation of nanomaterials for doping in the matrix with a great effort and high degree of precision. With the doping of metal nanoparticle the effective dielectric permittivity has been enhanced than that of the initial polymer matrix. These nanomaterial doped composites have enhanced conductivity and low tangent loss that allows them to use as potential candidates for modifies capacitors with high capacitance and for developing devices for electric energy storage [8-15]. In our study, copper (CuM) and cobalt (CoM) nanoparticles have been prepared by trituration method [16]. This method has a great advantage because the metal nanoparticles that are developed through this trituration method are soluble in the polar solvent and can be directly mixed with the polymer solution and the homogeneous film are formed by simply drying it. In the film the nanoparticles are dispersed in the polymer matrix in a homogeneous manner. There is an another advantage of the trituration method i.e., by rigorous shaking the particle size of the nanomaterialss can be controlled before mixing them with the solution of the polymer. These novel and exclusive metallic nanocomposites are nontoxic, less expensive and accessible easily. They are also extensively used as medicines that affect the permeability of the membrane [17] where the nanoparticle characteristics have been experimentally evidenced [18-20].

The metal nanoparticles developed through the method of trituration are incorporated in the s PVDF-HFP and dimethyl sulphoxide film, by using the simple technique of solution-casting in various concentrations of nanoparticle. Now for characterizations of these PVDF-HFP/CuM (CuPC) and PVDF/CoM (CoPC) nanocomposites, various characterization techniques have been employed such as FESEM, FTIR and dielectric property analysis. Through the analysis of the results of various characterizations techniques, several characteristics are observed i.e., presence of α and β -phases of metal doped nanocomposites, spherulites formation, enhancement of dielectric constant, decrement in tangent loss and conductivity improvement. The effect of various concentrations of CoM and CuM have been explored and the results obtained were compared with the pure film of PVDF-HFP. Employment of these environmental friendly, less expensive metallic nanocomposites for enhancing the electrical properties of polymer has a great impact in the worldwide electronic industry where modified and better electro active polymer films are extensively used.

2.3. Materials and methods

The metal-doped polymers are synthesized with the materials PVDF-HFP (Sigma Aldrich, USA) and dimethyl sulphoxide (DMSO) (Merck, India). Copper (CuM) and Cobalt (CoM) metals were collected from Hahnemann Publishing Company, India and nanoparticles were prepared from them by trituration method. The nanocomposites with metal-doping, CuPC and CoPC, were prepared by solution-casting method. 2 ml of DMSO was taken and 100 mg of PVDF-HFP was added to it and a mixture was prepared with rigorous stirring at a temperature of 60 °C for duration of 3 hours in a typical synthesis of metal doped nanocomposite. Specific amounts of CuM and CoM were added to the solution. Now the whole mixture was kept in the dry and clean

Petri dishes and CuPC and CoPC were obtained by evaporating the solvent by keeping it for 12 hours at a temperature of 60 °C in the incubated oven. DMSO was not totally removed in this process and hence the residual DMSO was present during taking further measurements. Then the thin film coatings of silver paste were done on both the sides of nanometal doped composites to create conducting surface for further electrical measurements. The thickness of the film was measured with digital screw gauge and the range of the thickness was ranges from 40 μm to 60 μm [11, 15, 21]. A flowchart for the method of sample preparation is shown in figure 2.1.

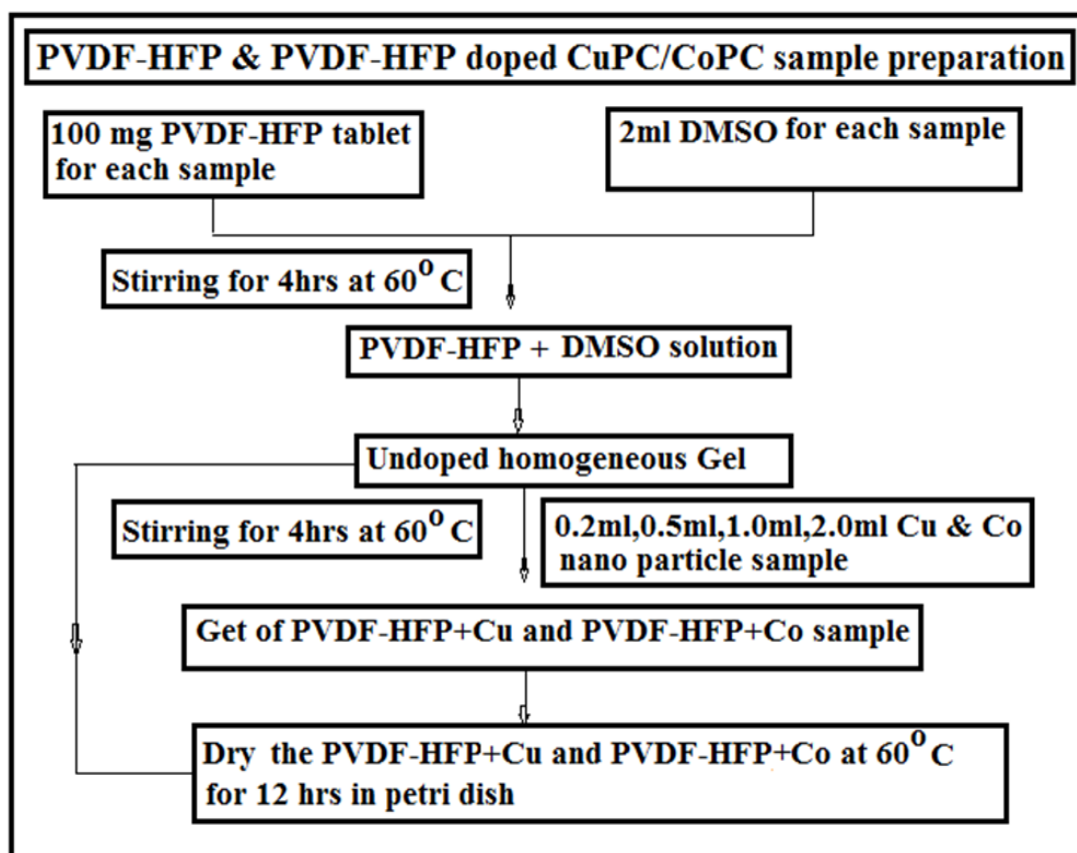


Figure 2.1 Flow chart of the sample preparation

The experiments were performed with various combinations of samples and their concentrations as the following:

In case of CuPC:

- i. PVDF-HFP (100 mg) + DMSO (2 ml)
- ii. PVDF-HFP (100 mg) + DMSO (2 ml) + CuM (0.2 ml) [0.2 CuPC].
- iii. PVDF-HFP (100 mg) + DMSO (2 ml) + CuM (0.5 ml) [0.5 CuPC].
- iv. PVDF-HFP (100 mg) + DMSO (2 ml) + CuM (1.0 ml) [1.0 CuPC].
- v. PVDF-HFP (100 mg) + DMSO (2 ml) + CuM (2.0 ml) [2.0 CuPC].

In case of CoPC:

- i. PVDF-HFP (100 mg) + DMSO (2 ml)
- ii. PVDF-HFP (100 mg) + DMSO (2 ml) + CoM (0.2 ml) [0.2 CoPC].
- iii. PVDF-HFP (100 mg) + DMSO (2 ml) + CoM (0.5 ml) [0.5 CoPC].
- iv. PVDF-HFP (100 mg) + DMSO (2 ml) + CoM (1.0 ml) [1.0 CoPC].
- v. PVDF-HFP (100 mg) + DMSO (2 ml) + CoM (2.0 ml) [2.0 CoPC]

2.4. Instrumentation for characterization of samples

Fourier transform infrared spectroscopy (Model : [FTIR]-8400S, Shimadzu) was employed to find out the characteristic stretching and bending modes of vibration of various chemical bonds of the samples. A LCR meter (Model HP- 4274 A, Hewlett-Packard, USA) was extensively used to measure the dielectric properties of the films. Dielectric permittivity (ϵ_r), tangent loss i.e., dissipation factor ($\tan \delta$) and AC conductivity (σ_{ac}) and other electrical properties of all samples were carried out in the frequency band of 20 Hz to 2 MHz.

Field-emission scanning electron microscopy (FESEM) was performed using the instrument model : INSPECT F50 SEM, FEI Europe BV in various operating conditions such as HV 20kV, mag 5000 \times , WD 10.9mm, and HFW 59.7 μ m. Sample was prepared by using turbo-pumped sputter coater model:EMS 150TS and the sample was further used for conducting metal coating.

2.5. Results and discussion

2.5.1. Fourier Transform Infrared Spectroscopy (FTIR) Analysis

FTIR spectra of both of the samples CuPC and CoPC at various concentrations are shown in the Figure 2.2a and 2.2b respectively. It is seen from the FTIR spectra that both the samples of nanocomposite films have characteristic absorbance bands at around 490 cm^{-1} , 530 cm^{-1} , 613 cm^{-1} , 763 cm^{-1} , 795 cm^{-1} and 975 cm^{-1} of wavenumber which corresponds to the α -phase and also at around 480 cm^{-1} , 510 cm^{-1} , 600 cm^{-1} and 839 cm^{-1} of wavenumber which corresponds to the β -phase [11, 15, 20]. From the spectra it is shown that there is no phase shift which reveals that there is no chemical interaction between the polymer film and the metal nanoparticles. It is also

seen from the spectra that the intensity in both the α - and β -phases changes with the concentration of CuM and CoM as doping material (Figure 2.2a and 2.2b).

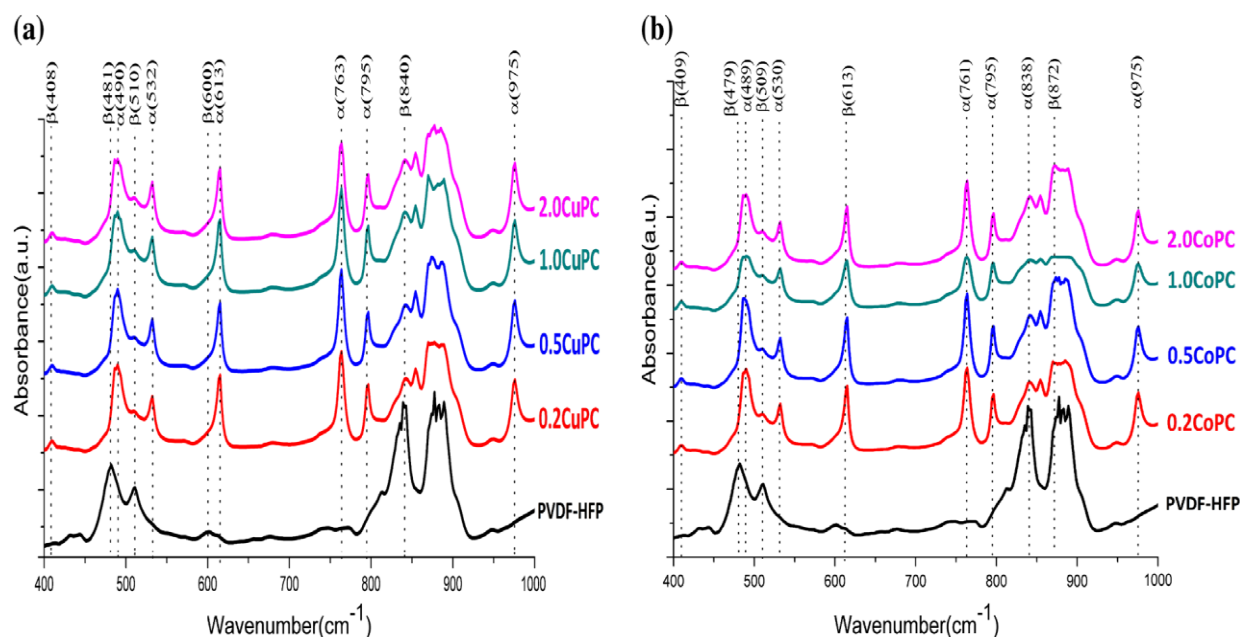


Figure 2.2(a) and 2.2(b) Fourier transform infrared spectra of CuPC and CoPC for all concentrations.

2.5.2. Field emission scanning electron microscopy

To explore the morphology of nanocomposite material samples, Field-Emission Scanning Electron Microscopy (FESEM) has been conducted on both the samples of CuPC and CoPC at various concentrations.

Microstructures of the sample CuPc with nanoparticles of CuM at three different concentrations are shown in Figure 2.3(a–c). It is seen from the figure 2.3(a) and 2.3(b) that the particles are more scattered, but in case of the figure 2.3(c) the particles are less scattered and it is revealed

from figure 2.3(c) that there are large number of agglomeration of particles. These agglomerated particles are embedded in the matrix of the polymer.

Micrographs of the sample CoPc with nanoparticles of CoM at three different concentrations are shown in figure 2.3(d–f). It is seen from the figures that the microstructures CoPc are changing with the different concentrations in similar fashion as in CuPC. Here also the particles are more scattered in case of figure 2.3(d) and 2.3(e), wherein figure 2.3(f) signatures the presence of large number of agglomerated particles embedded in the matrix [11,15,21,23].

In both the cases for CuPC and CoPC, presence of of Cu and Co in the polymer matrix are not very conclusive when they are present in very low concentration but with the increment of the concentrations of Cu and Co particles micrographs confirms the presence of the particles in agglomerated forms.

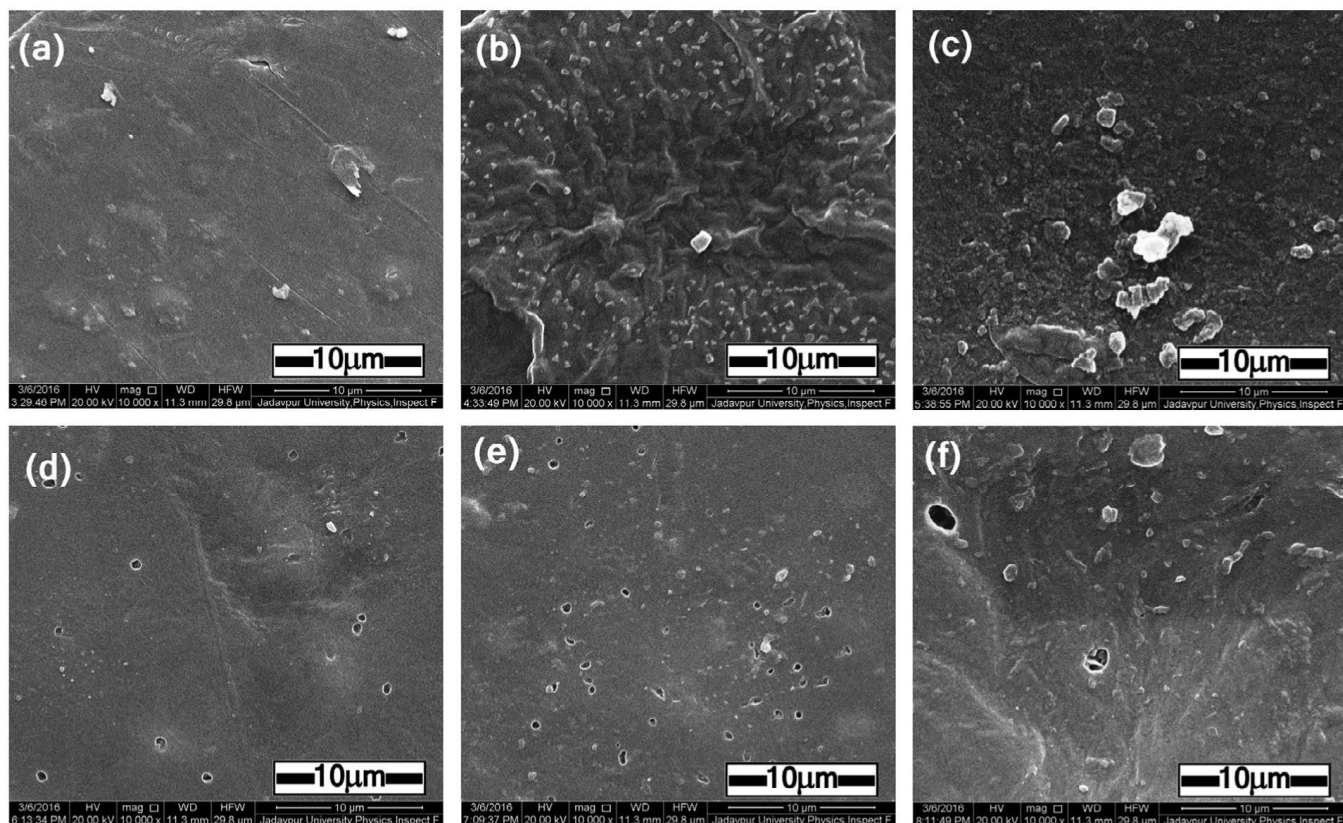


Figure 2.3. Field-Emission Scanning Electron Micrograph of (a) 0.2CuPC, (b) 0.5CuPC, (c) 2CuPC, (d) 0.2CoPC, (e) 0.5CoPC and (f) 2.0CoPC films.

2.6. Electrical properties measurement

To understand the improvement of electrical properties after doping with nano materials, dielectric constant, tangent loss and ac conductivity of both CuPC and CoPC in different doping concentrations are measured in a wide range of frequencies and then frequency vs dielectric constant graph, frequency vs tangent loss graph and frequency vs ac conductivity graph are plotted for all the samples..

2.6.1 Dielectric constant measurements

The dielectric constant (ϵ_r) of all samples with different concentration was measure using the formula -

$$\epsilon_r = \frac{dC_p}{A\epsilon_0}$$

here ϵ_r , C_p , d , A and ϵ_0 represent respectively the dielectric constant, capacitance of the material, width of the film, cross sectional area under study and permittivity of free space.

2.6.2 Effect of frequency on dielectric constant of the nanocomposite films

Frequency versus dielectric constant graphs through a wide range of frequencies (20Hz to 2MHz) of both of the samples CuPC and CoPC at various concentrations are shown in the figure 2.4a and 2.4b respectively. It is seen from figure 2.4a and 2.4b that for all concentrations of the samples, the dielectric constants of the films decrease continuously with increasing frequency at a higher rate up to 200 Hz

and this rate becomes slower above the frequency 200 Hz. At low frequency range the enhancement of dielectric constant occurs due to polarization in the interfaces between insulating matrix of PVDF-HFP and the thin film of good conducting dopind materials i.e., CuM/CoM. The enhancement of dielectric constant claims the dipolar orientations in the low frequency range. For further increment of the frequency, the response of the orientation of the dipoles is constrained and the rate if decrease of dielectric constant becomes slow tends towards a saturation [21, 22, 23] where the dielectric constant are the effect of the individual contribution of internal dipoles and confirms the phenomenon of electronic polarization [11, 15, 23–26].

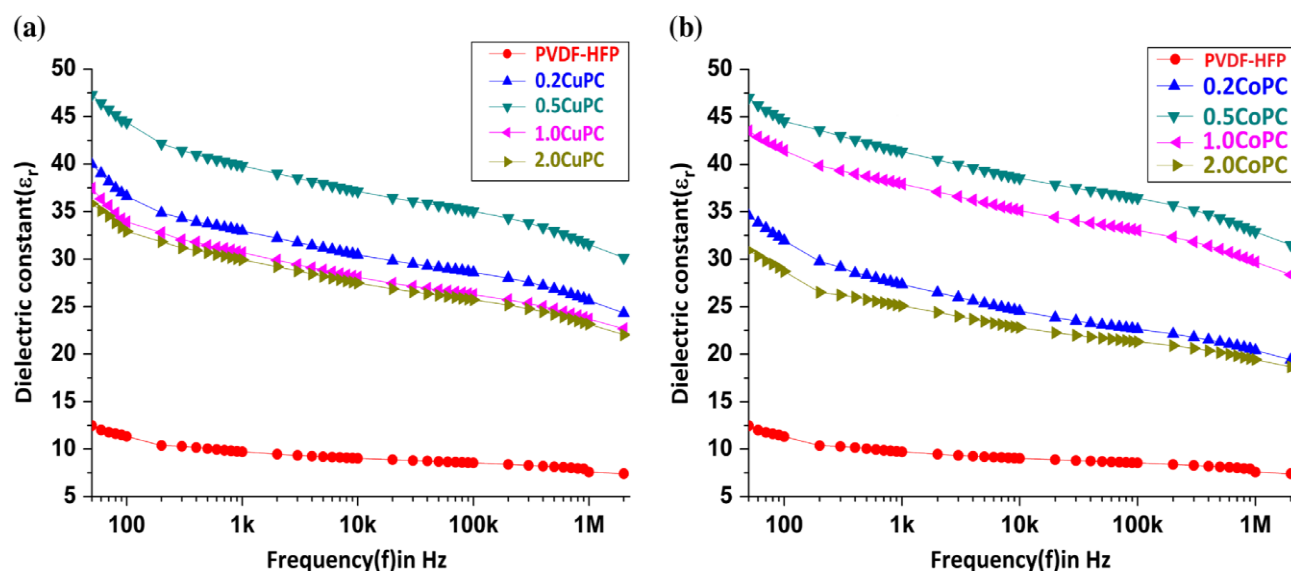


Figure 2.4(a) and 2.4(b) Frequency dependent dielectric constant (ϵ_r) of CuPC and CoPC for all concentrations

2.6.3 Effect of nanoparticle concentration on dielectric constant of the nanocomposite films

In figure 2.5a and 2.5b, the variation of dielectric constant with various concentrations of all nanocomposite films of the metal for both of the samples CuPC and CoPC is shown. Figure 2.5a and 2.5b shows that dielectric constant becomes significantly high when nanometal-doped composites are used in comparison to pure polymer matrix. The value of dielectric constant

increases with the concentration up to certain value (0.5 ml of CuM/CoM) above which the value of dielectric constant decreases. This phenomena of modification of dielectric properties of the nanocomposite with change in concentration of nanoparticle can be described by the effect of Maxwell–Wagner–Sillars interfacial polarization, where the charges are accumulated at the interfaces between insulating matrix of PVDF-HFP and the thin film of good conducting dopant materials i.e., CuM/CoM [27]. Initially, when the concentration of nanomaterial increases, the number of nanoparticle and also the area of interface in unit volume increase and consequently there is a decrease in the distance between two particles. This enhances the net polarization and the coupling between the neighboring sub-phases which is manifested by the increase in the value of dielectric constant.

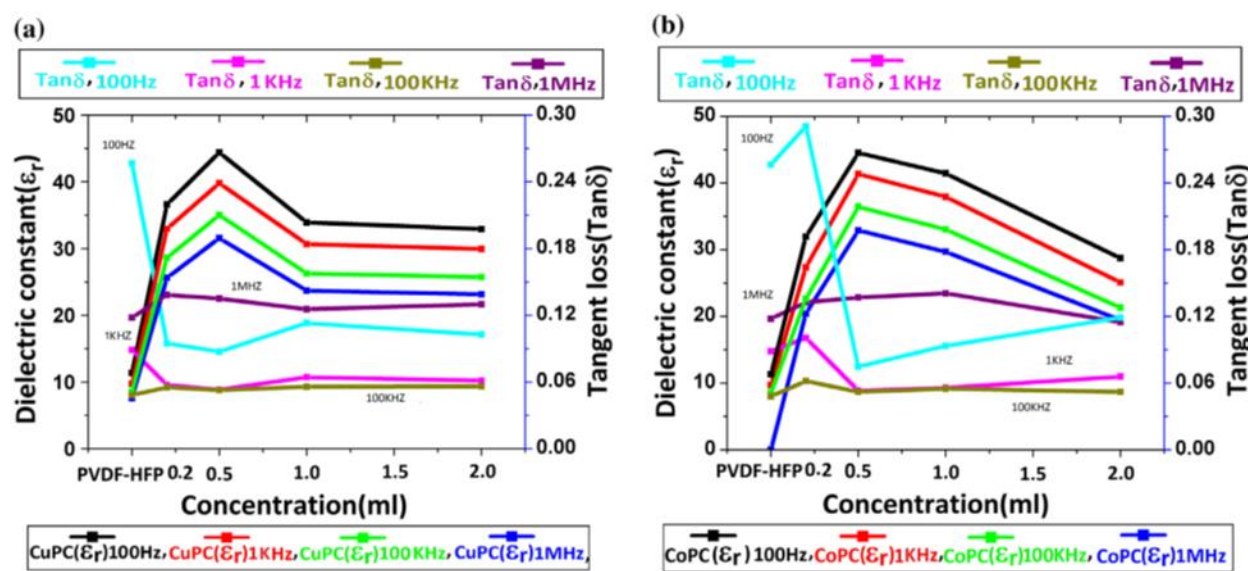


Figure 2.5(a) and 2.5(b) Concentration dependence of dielectric constant (ϵ_r) and tangent loss ($\tan\delta$) of CuPC and CoPC at various constant frequencies

However, when the dopant concentration further increases the nano particles becomes agglomerated (Figure 2.3a and 2.3b, FESEM image) subsequently area of interface per unit volume decreases and hence the dielectric constant decreases.

2.6.4 Tangent loss measurement

The tangent loss ($\tan \delta$) is a property of a material which measures the loss due to energy dissipation and defined as the ratio of conduction current through a material with its displacement current. it is calculated by the formula-

$$\tan \delta = \frac{\sigma_{ac}}{(2\pi f \epsilon_r \epsilon_0)}$$

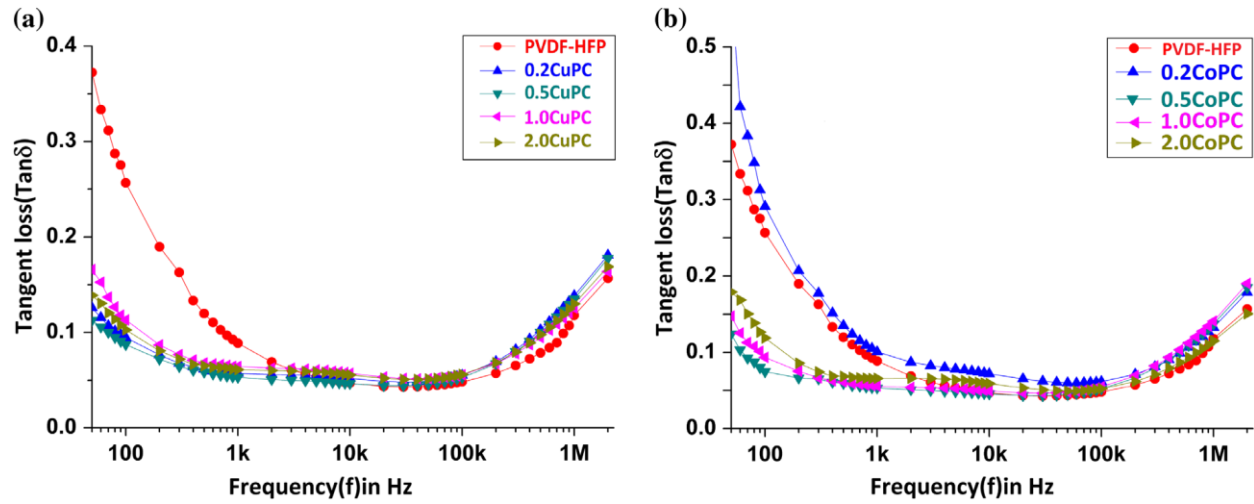


Figure 2.6(a) and 2.6(b): Frequency dependence of tangent loss ($\tan \delta$) of CuPC and CoPC at various concentrations.

In figure 2.6(a) and 2.6(b), the variation of tangent loss ($\tan \delta$) of CuPC and CoPC at various concentrations with frequency is shown. Figure 2.5(a) and 2.5(b) show that

Tangent loss decreases exponentially with increasing frequency for all nanocomposite samples till 10 kHz above which the tangent loss increases with frequency. In the lower range of frequency, the dipoles can easily orient themselves when an electric field is externally applied. Intermolecular vibration and frictions are the basis of this phenomenon. As dipoles orient themselves easily, there is less intermolecular vibration and less dissipation which is manifested as the decrease in the tangent loss. For further increase in frequency, polarization effect becomes less as the dipoles cannot be coherent with the rapid change of applied electric field and the

tangent loss suddenly increases above 10 kHz frequency. The increase in tangent loss above 100 kHz frequency is also contributed by the conduction of metal NPs he through the polymer.[4,7–15, 22–25]

2.6.5 AC conductivity measurement

AC conductivity (σ_{ac}) is calculated by the formula

$$\sigma_{ac} = 2\pi f \varepsilon_r \varepsilon_0 \tan \delta,$$

Where f , $\tan \delta$, ε_r and ε_0 are respectively the frequency, tangent loss, dielectric constant and vacuum permittivity.

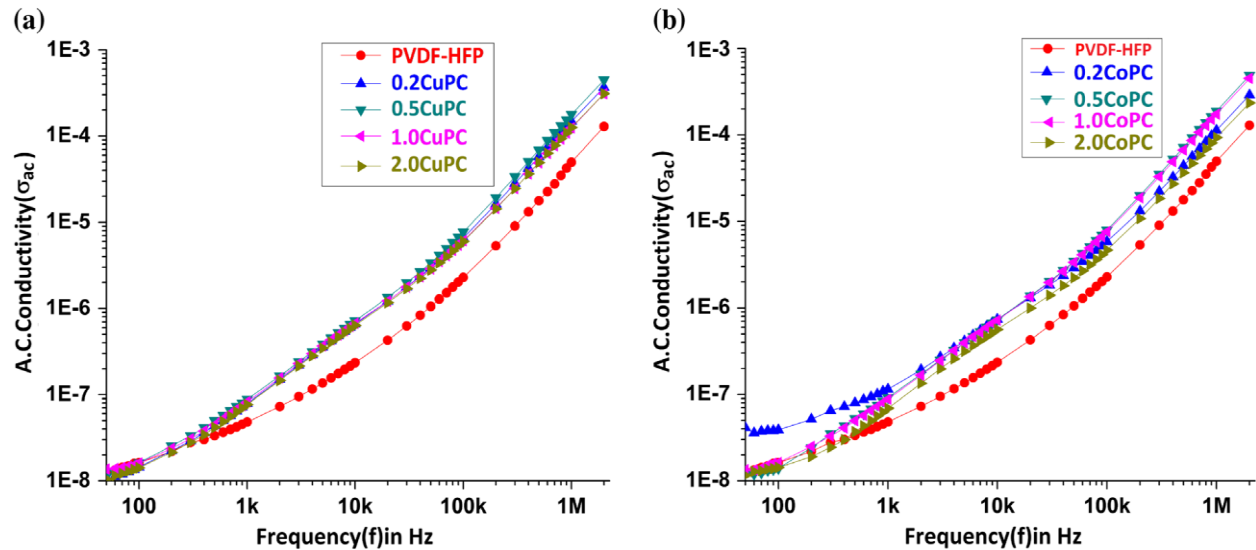


Figure 2.7(a) and 2.7(b): Frequency dependence of AC conductivity (σ_{ac}) of CuPC and CoPC at various concentrations

In figure 2.7(a) and 2.7(b) the variation of AC conductivity (σ_{ac}) with frequency of CuPC and CoPC at various concentrations is shown. It is seen from the figure that

the AC conductivity increases with frequencies in the full range of frequencies. The exponential growth of conductivity with frequency arises as metal nanoparticles in the matrix increase their mobility [11, 15, 21–26] and generating more conducting pathways. Furthermore when the concentration of the dopants is increased, the conducting pathways becomes less. As a result conductivity becomes low which is shown in figure 2.7(a) and 2.7(b).

In comparison of this result using triturated metal nanoparticles with our previous study of electrical properties for materials prepared by homogenous dispersion of Fe_2O_3 nanoparticles in the polymer matrix [11] it may inferred that in both the cases, the incorporation of NPs leads to strong interaction between the NPs and the polymer interface which in turn enhances dielectric constant of the material. The deviation in the observed values of the dielectric properties of these two cases is due to difference of surface charge, size, structure and degree of agglomeration of the NPs in the polymer matrix.

2.7 Conclusions

The stepwise increase of concentration of metal-nanoparticles in polymer matrix leads to gradual increment in both α -phase and β -phase (Figure 2.2a and 2.2b). That indicates the conglomeration nanoparticles at higher concentration which is further confirmed by the microstructures (Figure 2.2(a) and 2.2(b) of metal nanoparticle doped composites, The dielectric constant of nanomaterial doped composites decrease with increase in frequency for various concentrations of metal nanoparticles (Figure 2.4(a) and 2.4(b)). For metal nanocomposites the dielectric constant is enhanced than that of pure polymer throughout the frequency range from 20 Hz to 2 M Hz. It is also concluded that among the various concentrations of nanoparticles, the dielectric constant becomes highest for nanoparticles of 0.5 concentration. The composite perhaps attains the optimum conformation of α and β phases at this concentration. The tangent loss of nanomaterial

doped composites is less than that of pure polymer in the frequency range from 20 Hz to 10kHz (Figure 2.6(a) and 2.6(b)). It is also depicted that among the various concentrations of nanoparticles, the tangent loss becomes lowest for nanoparticles of 0.5 concentration in the frequency range from 20 Hz to 10kHz.

The AC conductivity of nanocomposites is also higher than that of pure matrix and for all nanoparticle doped and pure materials as a result of the presence of mobile metal ions in the polymer matrix. AC conductivity also increases with frequency throughout the frequency range.

Hence, pure polymer with comparatively low dielectric constant can be improved into materials doped with metal nanoparticles with greater dielectric constant and low tangent loss. These materials are nontoxic, environment friendly and easily available. So, by doping a specific concentration of metal nanoparticles, these nanocomposite films would have been a potential candidate for the fabrication of devices with high ability of energy harvesting and storage capacity and may be a promising material in electronic industry.

References

- [1] P. Martins, C. M. Costa, M. Benelmekki, G. Botelho and S. Lanceros-Mendez: ‘On the origin of the electroactive poly (vinylidene fluoride) β -phase nucleation by ferrite nanoparticles via surface electrostatic interactions’, *Cryst. Eng. Comm.*, 2012, **14**, 2807–2811.
- [2] P. Martins, A. C. Lopes and S. Lanceros-Mendez: ‘Electroactive phases of poly (vinylidene fluoride): determination, processing and applications’, *Prog. Polym. Sci.*, 2013, **39**, 683–706.
- [3] H.S.Nalwa: ‘Ferroelectric polymers: chemistry, physics, and applications’;1995, New York, Marcel Dekker.

- [4] Y. Li, X. Huang, Z. Hu, P. Jiang, S. Li and T. Tanaka: ‘Large dielectric constant and high thermal conductivity in poly(vinylidene fluoride)/barium titanate/silicon carbide three-phase nanocomposites’, *Appl. Mater.Interfaces*, 2011, **3**, 4396–4403.
- [5] Z. M. Dang, Y. H. Lin and C. W. Nan: ‘Novel ferroelectric polymer composites with high dielectric constants’, *Adv. Mater.*, 2003, **15**, 1625–1629.
- [6] Q. Chen, P. Y. Du, L. Jin, W. J. Weng and G. R. Han: ‘Percolative conductor/polymer composite films with significant dielectric properties’, *Appl. Phys. Lett.*, 2007, **91**, 022912-1–022912-3.
- [7] M. Panda, V. Srinivas and A. K. Thakur: ‘On the question of percolation threshold in poly vinylidene fluoride/nanocrystalline nickel composites’, *Appl. Phys. Lett.*, 2008, **92**, 132905-1–132905-3.
- [8] X. Y. Huang, P. K. Jiang and L. Y. Xie: ‘Ferroelectric polymer/silver nanocomposites with high dielectric constant and high thermal conductivity’, *Appl. Phys. Lett.*, 2009, **95**, 24290-1–24290-3.
- [9] Z. M. Dang, J. P. Wu, H. P. Xu, S. H. Yao, M. J. Jiang and J. B. Bai: ‘Dielectric properties of upright carbon fiber filled poly(vinylidene fluoride) composite with low percolation threshold and weak temperature dependence’, *Appl. Phys. Lett.*, 2007, **91**, 072912-1–072912-3.
- [10] S. H. Yao, Z. M. Dang, M. J. Jiang, H. P. Xu and J. B. Bai: ‘Influence of aspect ratio of carbon nanotube on percolation threshold in ferroelectric polymer nanocomposite’, *Appl. Phys. Lett.*, 2007, **91**, 212901-1–212901-3.
- [11] P. Thakur, A. Kool, B. Bagchi, S. Das and P. Nandy: ‘Effect of *in situ* synthesized Fe₂O₃ and Co₃O₄ nanoparticles on electroactive β phase crystallization and dielectric properties of poly(vinylidene fluoride) thin films’, *Phys. Chem. Chem. Phys.*, 2015, **17**, 1368–1378.

- [12] Z. M. Dang, L. Wang and Y. Yin: ‘Giant dielectric permittivities in functionalized carbon-nanotube/electroactive-polymer nanocomposites’, *Adv. Mater.*, 2007, **19**, 852–857.
- [13] Q. Li, Q. Z. Xue, L. Z. Hao, X. L. Gao and Q. B. Zheng: ‘Large dielectric constant of the chemically functionalized carbon nanotube/polymer composites’, *Compos. Sci. Technol.*, 2008, **68**, 2290–2296.
- [14] F. He, S. Lau, H. L. Chan and J. Fan: ‘High dielectric permittivity and low percolation threshold in nanocomposites based on poly(vinylidene fluoride) and exfoliated graphite nanoplates’, *Adv. Mater.*, 2009, **21**, 710–715.
- [15] P. Thakur, A. Kool, B. Bagchi, S. Das and P. Nandy: ‘Enhancement of β phase crystallization and dielectric behavior of kaolinite/halloysite modified poly (vinylidene fluoride) thin films’, *Appl. Clay. Sci.*, 2014, **99**, 149–159.
- [16] Homoeopathic Pharmacopoeia of India, 1971, Published by the Ministry of Health, Govt. of India.
- [17] P. Nandy, S. Bhandary, S. Das, R. Basu and S. Bhattacharya: ‘Nanoparticles and membrane anisotropy’, *Homeopathy*, 2011, **100**, 194.
- [18] P. Nandy: ‘A review of basic research on homoeopathy from a physicists point of view’, *Indian J. Res. Homeopath.*, 2015, **9**, 141–151.
- [19] P. S. Chikramane, A. K. Suresh, J. R. Bellare and S. G. Kane: ‘Extreme homeopathic dilutions retain starting materials: a nanoparticulate perspective’, *Homeopathy*, 2010, **99**, 231–242.
- [20] P. S. Chikramane, D. Kalita, A. K. Suresh, S. G. Kane and J. R. Bellare: ‘Why extreme dilutions reach non-zero asymptotes: a nanoparticulate hypothesis based on froth flotation’, *Langmuir*, 2012, **28**, 15864–15875.

- [21] K. Halder, B. K. Paul, B. Bagchi, A. Bhattacharya and S. Das: ‘Copperion doped mullite composite in poly(vinylidene fluoride) matrix: effect on microstructure, phase behavior and electrical properties’, *J. Res. Updat. Polym. Sci.*, 2014, **3**, 157–169.
- [22] B. K. Paul, K. Halder, D. Roy, B. Bagchi, A. Bhattacharya and S. Das: ‘Dielectric switching above a critical frequency occurred in iron mullite composites used as an electronic substrate’, *J. Mater. Sci. Mater. Electron*, 2014, **25**, 5218–5225.
- [23] P. Thakur, A. Kool, B. Bagchi, N. A. Hoque, S. Das and P. Nandy: ‘*In situ* synthesis of Ni(OH)₂ nanobelt modified electroactive poly(vinylidene fluoride) thin films: remarkable improvement in dielectric properties’, *Phys. Chem. Chem. Phys.*, 2015, **17**, 13082–13091.
- [24] P. Thakur, A. Kool, B. Bagchi, N. A. Hoque, S. Das and P. Nandy: ‘Improvement of electroactive β phase nucleation and dielectric properties of WO₃·H₂O nanoparticle loaded poly(vinylidene fluoride) thin films’, *RSC Adv.*, 2015, **5**, 62819–62827.
- [25] B. K. Paul, S. Kar, P. Bandyopadhyay, R. Basu, S. Das, D. S. Bhar, R. K. Manchanda, A. K. Khurana, D. Nayak and P. Nandy: ‘Significant enhancement of dielectric and conducting properties of electroactive polymer polyvinylidene fluoride films: an innovative use of *Ferrum metallicum* at different concentrations’, *Indian J. Res. Homeopath.*, 2016, **10**, (1), 52–57.
- [26] B. K. Paul, S. Das, R. Basu, D. S. Bhar, R. K. Manchanda, A. K. Khurana, D. Nayak, P. Nandy: ‘Effect of dilution of *Ferrum metallicum* and zincum oxidatum, homeopathic nanomedicines on the dielectric properties of poly(PVDF-HFP) film’, *Int. J. High Dilution Res.*, 2016, **15**, (1), 10–17
- [27] F. Rogti, M. Ferhat ‘Maxwell–Wagner polarization and interfacial charge at the multi-layers of thermoplastic polymers’, *J. Electrostat.*, 2014, **72**, 1, 91–97.

Chapter 3

Further improvisation of electrical properties:

Investigation of various materials doped with nanoparticles of different sizes

3.1 Chapter overview

In this chapter the electrical properties like dielectric constant, tangent loss and ac conductivity of poly (vinylidene fluoride Hexafluoropropylene) (PVDF-HFP) and its composites films has been improved by impregnating a novel material, the triturated copper (TCu) and cobalt (TCo) nanoparticles by applying synthesis technique like simple solution casting. Succession with serial dilution of the concentrated solution of these triturated nanoparticles in alcohol has been studied. The effect of this Very Low Molarity Repeatedly Shaken Diluted Liquid (VLMRSDL) the so called potentized liquid to enhance the electrical properties of the polymer based nanocomposite film has been studied. Dielectric constant (ϵ_r) is measured based on room temperature and depending on frequency ranges from 20 Hz to 2 MHz of the pure PVDF-HFP composites increases with increase in potentization (6C,30,200C) and dielectric constant(ϵ_r) reaches a maximum almost 4 times the value of dielectric constant of the pure PVDF-HFP. The different polymorphs like α and β phases and spherulitic crystal structure of PVDF-HFP and nanocomposite films have been detected by DTA, Fourier Transform Infrared Spectroscopy (FTIR), XRD and field emission scanning electron micrograph (FESEM) study. The alteration of phase between α to β is activated by nucleation of the metallic nanoparticles in the polymer matrix by interfacial polarization. This interfacial Polarization provides the nanocomposites to move higher mobile charge carriers. These films with potentization have higher dielectric polarization and significantly lower dissipation factor ($\tan\delta$) and ac conductivity at room temperature compared to the pure PVDF-HFP. These metallic fillers are low negative zeta potential, nontoxic, inexpensive, easy to fabricate and environment friendly also. The nucleation of these novel nanoparticles in polymer matrix to get enhanced improved electrical properties will have a significant contribution in the present

day research in electrical and electronic industry.

3.2 Introduction

Poly (vinylidene fluoride) (PVDF) and its copolymers like poly (vinylidene fluoride Hexafluoropropylene) (PVDF-HFP) are great promising candidate for their versatile and unique properties like low processing temperature, flexibility, high polarizability, low dielectric constant, high dielectric breakdown field etc., making them potential candidate for a broad range of applications in electronic industry [1–3].

In this respect to improve the capacitive performance of the polymer material, incorporation by polarization of metal nanoparticles in the polymer matrix has received great focus in recent years. Here the homogeneous and uniform distribution of the nanoparticles promises good interaction between them and the polymer matrix material which enhances the electrical properties of the host material [4–7].

In this respect, very much effort had been devoted to develop PVDF-HFP composites by impregnating different metallic nanoparticles within the host polymer matrix. The modified dielectric permittivity of these promising metal nanoparticle doped polymer composite are higher than that of the host polymer matrix. They also show enhancement of dielectric constant, conductivity and decrement of tangent loss making them effective candidates as good capacitors and electric energy storage devices [8–15]. These functionalized polymer composites with promising properties like dielectric constant, conductivity and tangent loss have been synthesized through different characterization [16–22] technique. Here, we have chosen triturated copper (TCu) and cobalt (TCO) nanoparticles, both are very novel and unique effective metallic fillers, which are inexpensive, nontoxic, with low processing temperature and are easily available. Experimentally it is proved that the nanoparticle aspect

of these potencies like 6C, 30C and 200C has been proved and it is established their medicinal efficacy [23–27]. In dimethyl sulfoxide (DMSO) solution these novel nanoparticles were incorporated in the polymer matrix PVDF-HFP and the series of films with different thickness were prepared by simple solution casting technique. Then serial characterization technique like DTA, FTIR, XRD and FESEM is applied to study several electrical properties of these nanocomposites of PVDF-HFP/TCu (CuPC) and PVDF/TCo (CoPC). By changing the potency of TCo and TCu and the presence of α and β phases, formation of spherulites, enhancement of conductivity, dielectric constant and decrease of tangent loss of the nanocomposite films were observed and it is compared with the pure PVDF-HFP film.

By the method of trituration, the NPs we selected for our work are prepared making these truly novel materials. By method of trituration the advantage is that in this way the shape and size of the NPs can be tuned by the continuous vigorous shaking. These NPs are now unique by this method compared to chemically synthesized ones. Besides that, these NPs are inexpensive, easily available, eco-friendly and nontoxic, metallic nano fillers that can improve the conductivity, membrane permeability, and decreases the dissipation factor of polymer films by several times of pure one. The enhanced electrical properties of polymer films by utilizing these unique metallic nano fillers focused great importance when electro active polymer films are gaining worldwide attention for their use in electronic industry.

3.3 Materials and methods

From Hahnemann Publishing Company, India, freshly prepared triturated metal nanoparticles like Copper (TCu) and Cobalt (TCo) of different potencies were obtained. The materials used in the synthesis of the nanocomposite films are TCu, TCo, PVDF-HFP (Sigma Aldrich, USA) and dimethyl sulfoxide (DMSO) (Merck, India).

In a typical synthesis technique, the amount of PVDF-HFP is 100 mg was added to 2 ml DMSO at 60 °C for 3h and mixed together under vigorous stirring. Now 0.6 ml, the measured amount of TCu and TCo of different potencies as 6C, 30C and 200C were added to the solution. The volume wt% of all triturated nanoparticles (NPs) of different potencies is 23.08%. CuPC and CoPC were obtained by casting the whole mixture in clean dry petri dishes and evaporating the solvent in an incubated oven at 60 °C for 12 h [28–32]. The films were then coated by silver paste on both sides for electrical measurements. The synthesized films had the thickness in the range of 48–54 μm as measured by using a digital screw gauge. The average density value of the fabricated films is 0.81 gm cm^{-3} .

3.4 Sample Details

For pure PVDF-HFP

100 mg PVDF-HFP + 2 ml DMSO (PVDF-HFP)

For CuPC

100 mg PVDF-HFP + 2 ml DMSO + 0.6 ml TCu of potency 6 C (CuPC-6)

100 mg PVDF-HFP + 2 ml DMSO + 0.6 ml TCu of potency 30 C (CuPC-30)

100 mg PVDF-HFP + 2 ml DMSO + 0.6 ml TCu of potency 200 C (CuPC-200)

For CoPC

100 mg PVDF-HFP + 2 ml DMSO + 0.6 ml TCo of potency 6 C (CoPC-6)

100 mg PVDF-HFP + 2 ml DMSO + 0.6 ml TCo of potency 30 C (CoPC-30)

100 mg PVDF-HFP + 2 ml DMSO + 0.6 ml TCo of potency 200 C (CoPC-200)

3.5 Instrumentation

The developed crystalline phases were analyzed in the samples by X-ray diffractometer (model-D8, Bruker AXS, Wisconsin, USA) using operating voltage at 40 KV and Cu K_{α} radiation of 1.5418 Å with a scan speed of 0.3s/step. The characteristic stretching and bending modes of vibration of chemical bonds like of the CuPC and CoPC samples were effectively evaluated by FTIR spectroscopy (FTIR-8400S, Shimadzu). Using INSPECT F50 SEM, FEI Europe BV, Field-emission scanning electron microscopy (FESEM) was done. In the FESEM images the operating conditions are mentioned as follows: HV 20.00 kV, WD 10.9 mm, magnification $\times 5000$, and HFW 59.7 μm . Turbo pumped sputter coater EMS 150TS was used for sample preparation and was used for gold coating. Electrometer (HP Model 4274 A, Hewlett Packard, USA) was used for electrical properties of these films were carried out by using such as dielectric permittivity (ϵ_r), dissipation factor ($\tan \delta$), and ac conductivity (σ_{ac}) of all CuPC films and CoPC film were measured in the frequency range 20 Hz to 2.0 MHz using LCR meter.

3.5.1 Characterization**3.5.2 XRD Analysis**

By doping TCu and TCo NPs the crystallization behavior of the films have been investigated by using an X-ray diffractometer. Figure 3.1, shows these X-ray diffraction (XRD) patterns of the TCu and TCo NPs modified PVDF films. The diffraction pattern of pure PVDF having the α -phase shows peaks at 2θ values of 17.5 (100), 18.1 (020), 19.9 (021) and 26.4 [(201), (310)] and for the γ -phase the peaks are at 38.91 (211). But the TCu and TCo NPs doped nanocomposite films showed all peaks corresponding to α or γ phases disappear and at 20.5 [(110), (200)] only one characteristic peak of PVDF appeared which confirmed the nucleation of the electro active

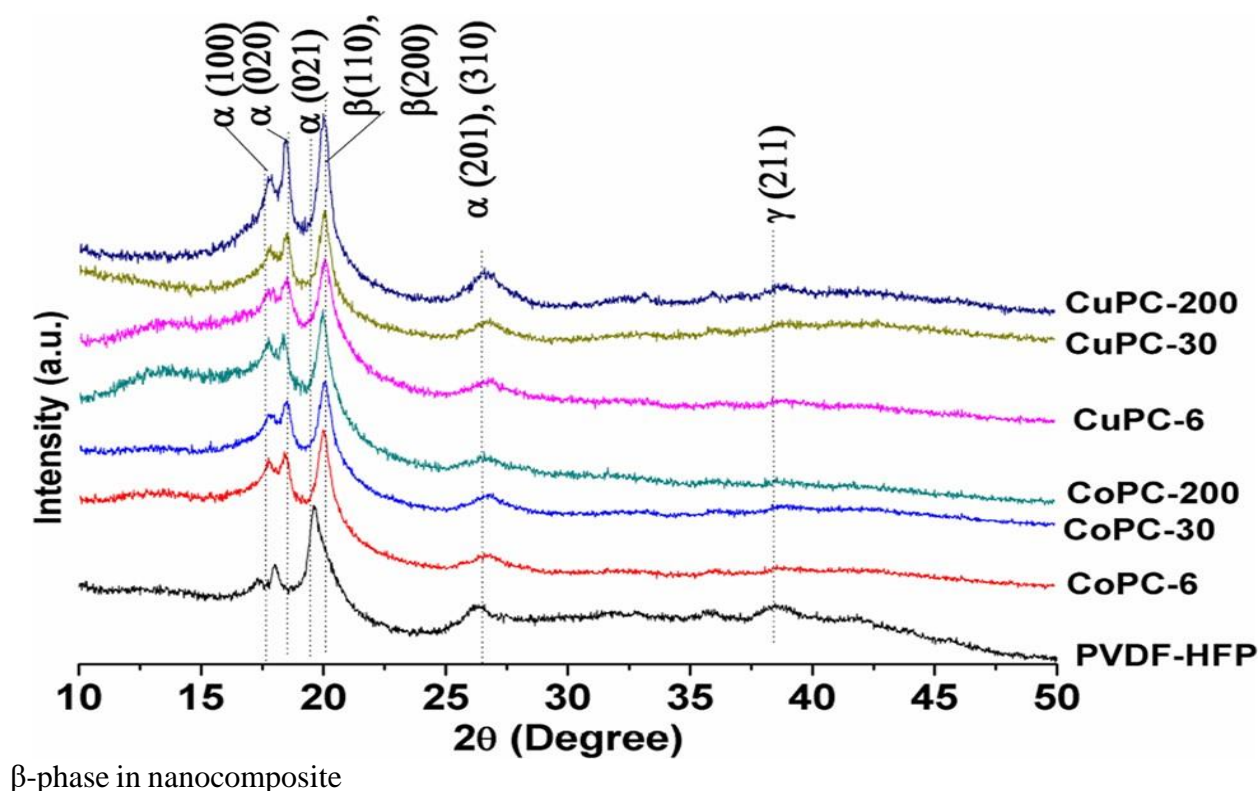


Figure 3.1 XRD patterns of pure and all composite films doped with TCu and TCo of 6C, 30C and 200C potencies

films [1, 14, 15, 30, 31]. Thus the nucleation of the electro active β -phase is significantly

accelerated for both the TCu and TCo NPs. The characteristic peaks of the metal nanoparticles are not evident in the pattern due to the very high dilution of these NPs in the PVDF matrix.

3.5.3 FTIR

For chemical bonds identification and to check the purity of the sample, Fourier Transform Infrared Spectroscopy (FTIR) study of these nanocomposite films in the selected range of 400–1100 cm^{-1} detected and the presence of α and β phases has observed given in Fig.3.2a. The FTIR spectra of CuPC and CoPC nanocomposite film show characteristic absorbance bands at 510 and 840 cm^{-1} corresponding to the β -phase and around 484, 606 and 878 cm^{-1} corresponding to the α phase. The spectra indicate that there good interaction in between polymer matrix and nanoparticles by intensifying the α and β phases with the change of concentration of doping material and no phase shift or chemical interaction between the metal nanoparticles and the polymer film[28–30].

We observe in Fig.3.2b that with the increase in potency, the β phase peaks have grown significantly compared to those of PVDF-HFP. The enhancement of β phase has been measured by using Beer–Lambert law, which relates absorbance with concentration of the absorbing species, the fraction of β phase, F_β , present in the (crystalline regions of) films was calculated using the formula,

$$F(\beta)\% = \frac{A_\beta}{1.26A_\alpha + A_\beta}$$

where A_α and A_β are the absorption fractions of α and β phases respectively. The maximum absorbance at 484 cm^{-1} was chosen as A_α and the maximum absorbance around 840 cm^{-1} as A_β .

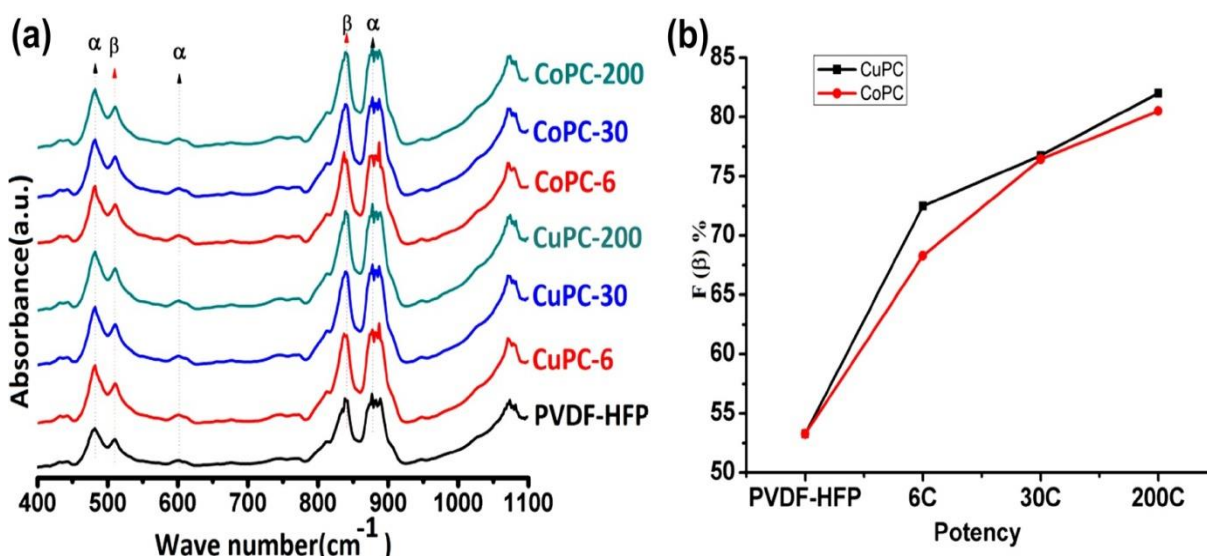


Figure 3.2(a) Fourier transform infrared spectra of CuPC and CoPC for all potency and 3.2(b) shows increase of $F(\beta)\%$ with increase in potency.

Using the above formula calculation has performed led to results which are presented graphically in Fig. 3.2b indicating undoped PVDF had 53% β phase that increased with the addition of the different potency of the nanoparticles. The enhancement in β phase was maximum (82.04%) for TCu nanoparticles of 200C potency among all the composites. All composite film showed a constant increasing trend with increase in potency [28–30].

3.5.4 DTA

Differential thermo gravimetric (DTA) has been used for the identification of the crystalline phase of PVDF-HFP as a supporting data of XRD and FTIR. Fig. 3.3 shows the DTA thermographs of pure PVDF and the NPs incorporated PVDF films. The DTA thermograph of pure

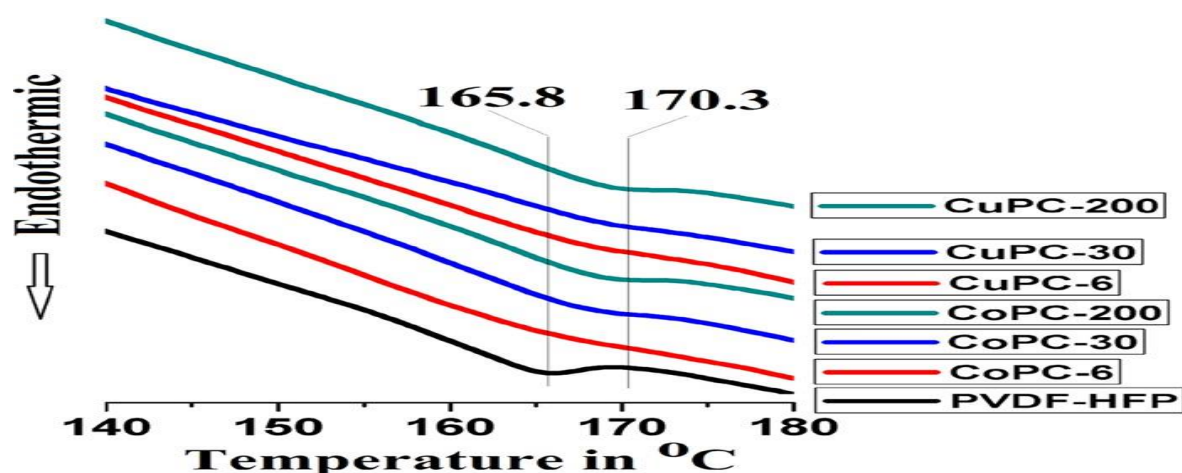


Figure 3.3 DTA patterns of pure and of composite films doped with TCu and TCo of 6C, 30C and 200C potencies

PVDF shows a strong endothermic peak position at 165.8 °C suggesting phase crystallization with some presence of electro active β phase content in pure PVDF that was also observed in FTIR. But for PVDF-HFP films doped with CuPC-200 NPs, this point shifted to 170.3 °C [1, 11, 15, 30, 31]. The endothermic peak position of all the other PVDF-HFP films doped with NPs at different potencies lie in between these two temperatures. The shifted endothermic peaks confirm the existence of strong β phase. Thus DTA results suggest more electro active β phase crystallization for all NPs doped PVDF films, which are consistent with the XRD and FTIR data.

3.5.5 Zeta potential

Our current study based on TCu/TCo-PVDF-HFP nanocomposites proposes a strong interaction between the positively CH_2 dipoles of PVDF and the negatively charged nanoparticles leading to the alignment of stabilized chains in longer all trans conformation on the

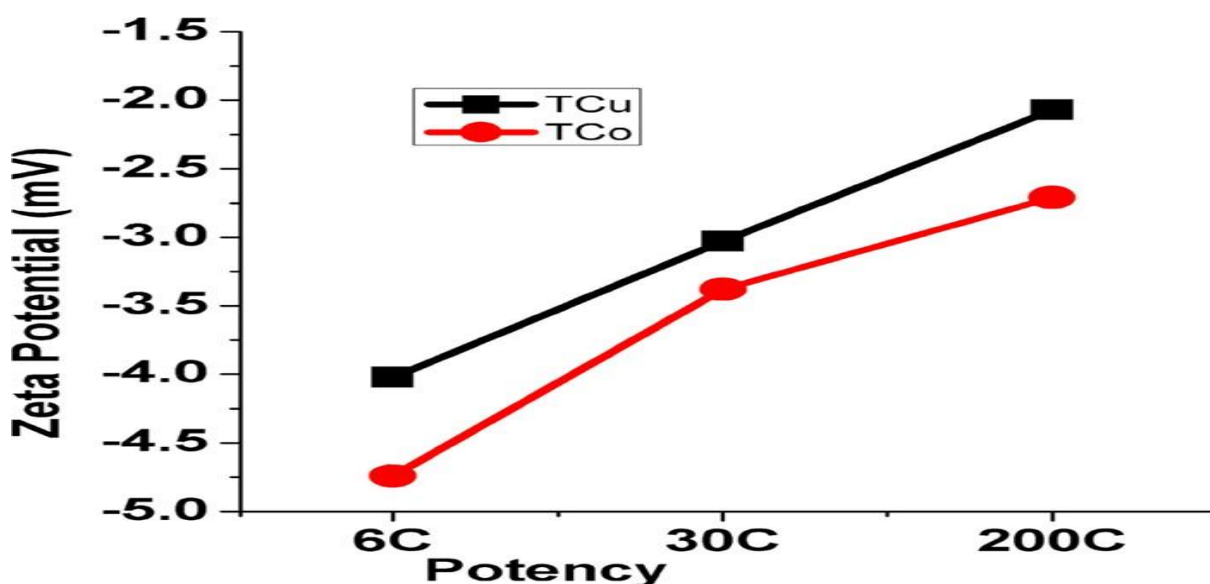


Figure 3.4 Zeta potential of pristine TCu and TCo of 6C, 30C and 200C potencies

TCu and TCo nanoparticle surface. Thus, to explain the origin of β phase crystallization in our present work, the surface charges of the TCu and TCo NPs have been investigated. Without adding PVDF-HFP the possible electrostatic charge on the surface of the TCu and TCo NPs has been investigated by zeta potential analysis. The obtained results of Zeta potential distribution has been shown in Fig.3.4. Both NPs show negative zeta Potentials. Thus it confirms, the nucleation of the electro active β phase taking place on the negatively charged surfaces of TCu and TCo NPs. The positive CH_2 dipoles of PVDF chains undergo strong electrostatic interaction

with the negatively charged surface of the NPs resulting in stabilized longer TTTT or all Trans conformation on the NP surfaces. Figure 3.5. Shows the ion–dipole or electrostatic interaction mechanism between the NPs and polymer chains during the formation of the electro active β -phase [1,11]. Enhanced electro active β -phases of PVDF have been obtained by doping TCu and TCo NPs on PVDF matrix using solvent casting method. Similar studies were made earlier in our laboratory, where the formation of β -phase was reported with the addition of fillers by solvent-casting method. The growth mechanism for the formation of TCu or TCo/PVDFHFP composites has been explained based on the chemistry concept by the schematic diagram which shows the formation of β phase as given in Fig. 5. This formation of electro active β phase may be explained by the theory of β phase nucleation, which is based upon dipole surface charge interaction model. According to this

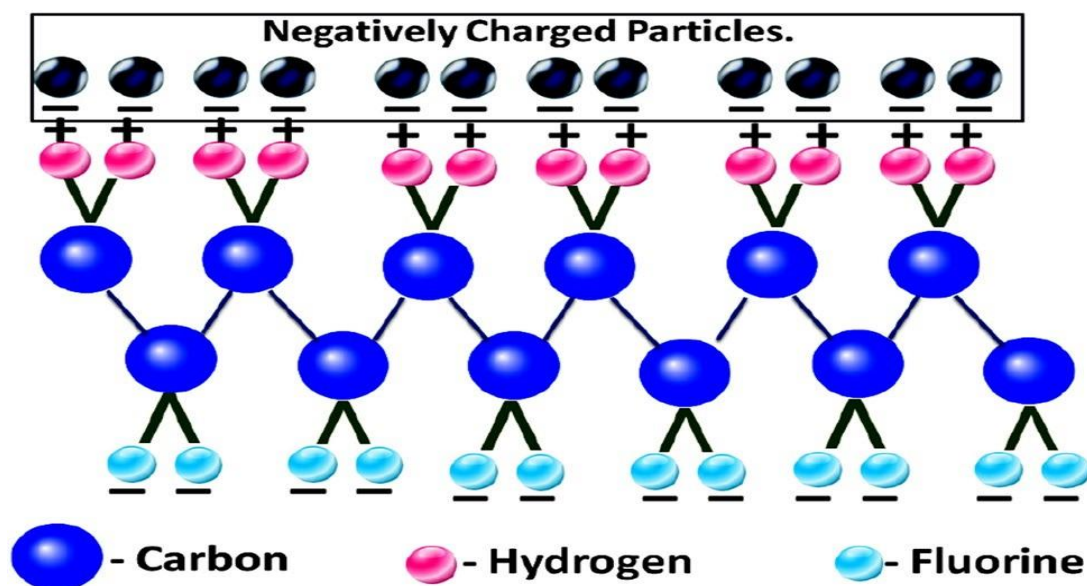


Figure 3.5 Schematic diagram showing the growth mechanism for the formation of TCu or TCo/PVDF-HFP composites

model, when fillers were added to the PVDF solution, the negatively charged surface of filler, which acted as substrates for β phase nucleation, got attracted to the partially positive CH_2 dipoles, thus leading to the alignment of stabilized PVDF chains in longer all trans-conformation, resulting in electro active β phase [1,11,15]. From this analysis, it is evident that CuPC-200 sample got maximum enhancement of β phase.

3.5.6 Microstructure and elemental composition analysis

3.5.6.1 FESEM Analysis Pristine TCu and TCo

Figure 3.6 show the morphology and microstructures of pristine TCu and TCo NPs that was directly doped in PVDF matrix. The dispersed nanoparticles were drop casted on silica substrate and all TCu and TCo NPs of 200C potency confirms good and homogeneous distribution on the surface with not much agglomeration have been found for both triturated NPs.

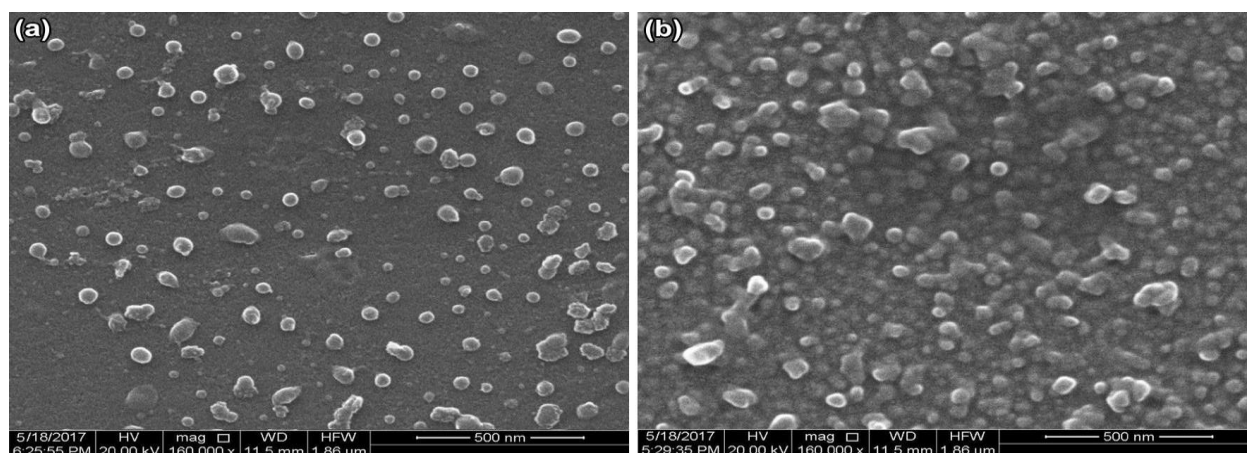


Figure 3.6 Field-Emission Scanning Electron Micrograph (FESEM) of Pristine, (a) TCu and (b) TCo of 200C.

TCu and TCo doped PVDF

Fig.3.7(a–f) show the morphology and microstructure of all composite films doped with TCu and TCo nanoparticles of 6C, 30C and 200C potencies respectively. Fig. 7(a),(d) is the evidence of large number of densely packed agglomerated particles embedded in the polymer matrix whereas Fig.7(c),(f) show that the particles are more scattered, well separated and also homogeneously distributed maintaining an intermolecular distance [29–32]. The polymer matrix is also well crystallized Fig.7(c),(f) with the increasing potencies and got maximum enhancement at 200C potency.

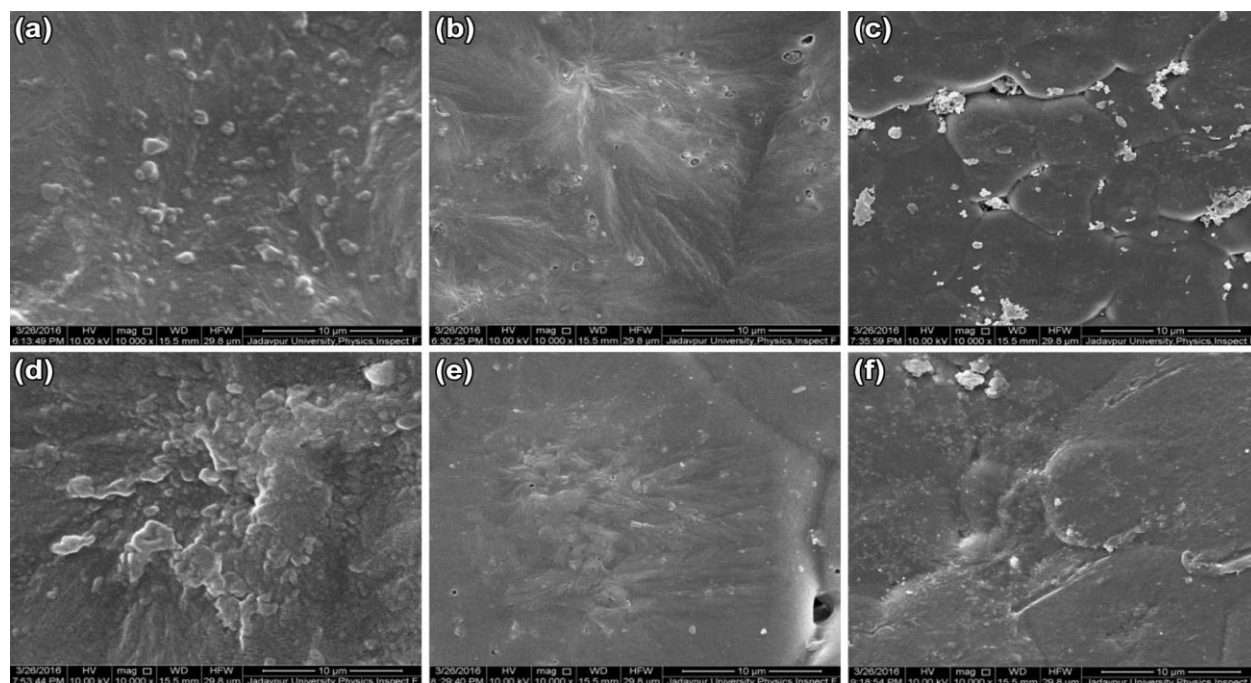


Figure 3.7 Field emission scanning electron micrograph (FESEM) of (a) CuPC-6, (b) CuPC-30, (c) CuPC-200, (d) CoPC-6, (e) CoPC-30 and (f) CoPC-200 films.

The evidence for the incorporation of TCu and TCo in the polymer was not very conclusive as the samples were of extreme dilution and the presence of the particles was difficult to detect.

3.5.6.2 EDX Analysis

Elemental mapping and EDX spectra of TCu and TCo doped PVDF

Fig.3.8 shows the elemental mapping image of (a) CuPC- 200, (b) CoPC-200 and their EDX spectra respectively. The figure confirms the presence of all the elements of PVDF and NPs.

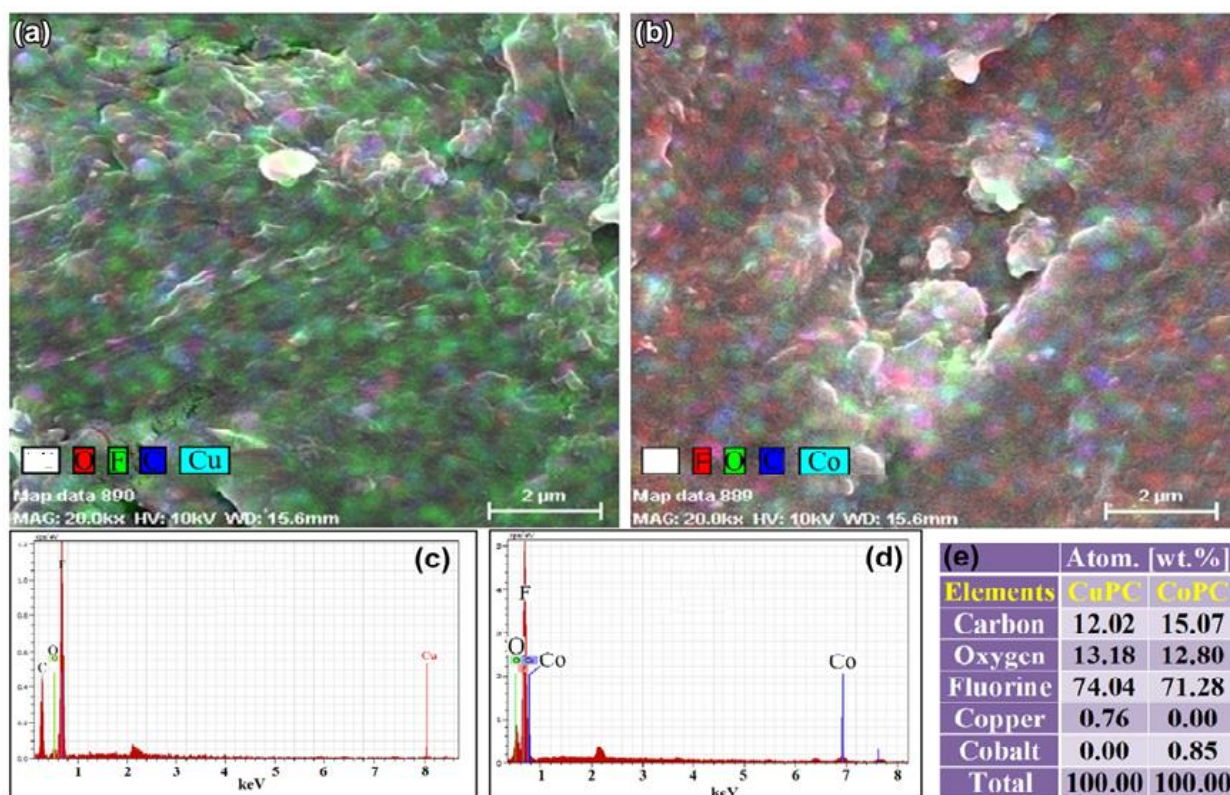


Figure 3.8 High resolution elemental mapping images of (a) CuPC-200, (b) CoPC-200 and EDX spectra of (c) CuPC-200, (d) CoPC-200. (e) Elements obtained from EDX study with their normality weight percentages are shown in the inserted table.

These also show high resolution FESEM micro graph of optimized CuPC-200 and CoPC-200. The EDX images (c) and (d) confirm the presence of copper or cobalt along with polymeric elements into the composite system. Elements obtained from EDX study with their normality weight percentages are shown in Tables Fig.3.8(e).

3.6. Electrical properties measurement

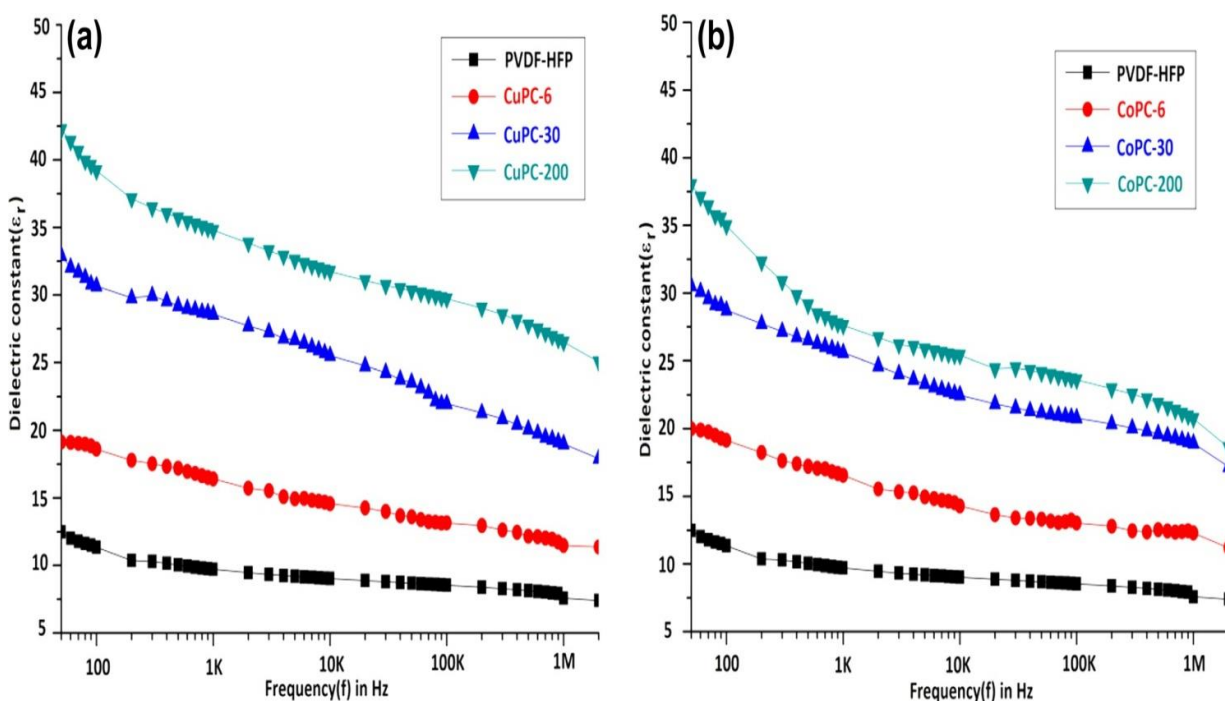
3.6.1 Frequency vs Dielectric Constant Measurement

The capacitance of the capacitor increases by the factor of permittivity of dielectric material or insulator increases compared to air is known as the Dielectric Constant (ϵ_r), and high dielectric permittivity of a material is better in comparison to an insulator with low dielectric constant. Dielectric constant is the ratio of permittivity of two medium which is a dimensionless quantity since it is relative to free space. The dielectric constant (k) or relative permittivity (ϵ_r) of each sample was calculated from the capacitance using the formula,

$$\epsilon_r = \frac{dC_p}{A\epsilon_0}$$

where ϵ_r , C , d , A and ϵ_0 are the dielectric constant of the material, capacitance, thickness of the film, area of the cross-section and permittivity of the free space respectively. The enhancement of dielectric constant of all composite films, CuPC and CoPC with frequency are shown in Fig. 9 (a),(b) respectively. It is clearly observed that within the frequency range 20 Hz to 2 MHz, dielectric constant for composite films like CuPC and CoPC films decrease continuously with increase in frequency for all concentration of CuPC and CoPC film at about upto 200Hz and after that it seems to remain constant at about upto 100kHz. It is also seen that throughout the whole frequency range, dielectric constant has substantially higher value in case of all CuPC and CoPC films

Figure 3. 9 Frequency dependent dielectric constant (ϵ_r) of (a) CuPC and (b) CoPC for all potency.



With respect to the pure polymer film. Due to the presence of two different conducting media (e.g. PVDF-HFP and TCu or TCo), this increment of dielectric constant and capacitance also may be explained by MWS (Maxwell–Wagner–Sillars) interfacial polarization. The interfacial polarization is related with the entrapment or accumulation of free charges generated in polymer matrix termed as core at the interfaces between the polymer matrix and surface charge of nano particles. It can be explained from FESEM micrographs that, as the separation, dispersion and distribution of poles of polymer matrix and the nanoparticles is homogeneous the dielectric constant increased because of the enhancement of effective interaction area between the polymer matrix and the nanoparticles. Easy orientation of dipoles as well as MWS interfacial polarization is possible at lower frequency which contribute this ~four times

enhancement of dielectric constant. Due to further increase of frequency, relaxation time decreases as a result dipole response is restricted and the dielectric constant has a saturation tendency. So the internal individual dipoles contribute to the dielectric constant which is ideally the electronic polarization effect [29–34].

3.6.2 Frequency vs Tangent loss analysis

Another factor which surprisingly affects the operation of a capacitor is heat generation or dielectric Leakage. Dielectric leakage occurs in a capacitor as the result of an unwanted movement of poles in the matrix and the metal nanoparticles. This effect is termed as dielectric loss or conduction loss or damping loss or leakage current which is the ratio of conduction current and displacement current is called tangent loss of the dielectric material. In figure 3.10 (a), (b) show the variation of tangent loss with frequency for pure polymer and the composite polymer termed as CuPC and CoPC films in the frequency range 20Hz to 2MHz.

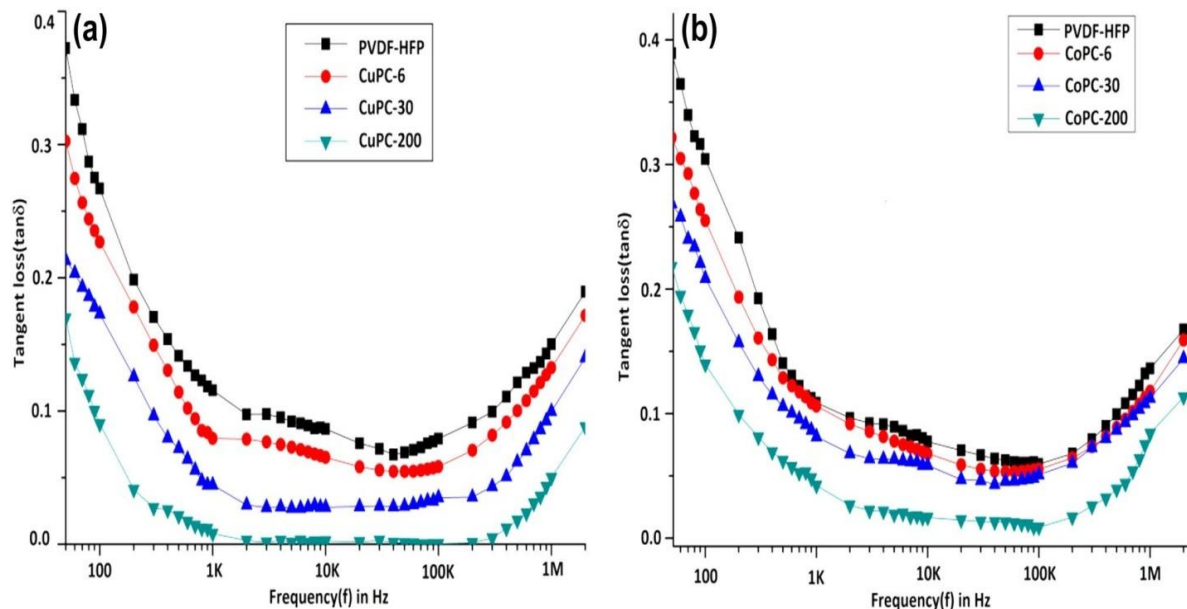


Figure 3.10 Frequency dependent Tangent loss ($\tan\delta$) of (a) CuPC and (b) CoPC for all potency.

It is clearly observed from the figure that throughout the frequency range dielectric loss or tangent loss continuously decreases with increasing frequency for pure polymer and composite polymer termed as CuPC and CoPC film upto 2kHz. This fast destruction of dielectric loss may be for poles of polymer and individual poles of metal nanoparticles. Which generates inter molecular friction or vibration. At lower frequency range the easy orientation is possible of the dipoles for higher relaxation time which contributes to higher tangent loss. As frequency increases, due to less relaxation time, less polarization effect continues. So intermolecular friction or vibration diminishes which is responsible for saturated tangent loss. Beside that after 100kHz the tangent loss increases due to the motion of individual poles for all films may that is the leakage current [29–34].

3.6.3 Frequency vs ac conductivity analysis

Specific conductance or electrical conductivity is the reciprocal of electrical resistivity, and measured as the material's ability to conduct an electric current. It is commonly represented by the Greek letter σ (sigma). Its SI unit is Siemens per metre (S/m). A.C. conductivity (σ_{ac}) is calculated using the formula,

$$\sigma_{ac} = 2\pi f \tan\delta \epsilon_r \epsilon_0$$

where σ_{ac} , f , $\tan\delta$, ϵ_r and ϵ_0 , are the AC conductivity, frequency in Hz, tangent loss factor, dielectric constant of the material and vacuum permittivity respectively. During the conductivity measurements 1.0V was applied. The variation of ac conductivity with frequency for pure polymer and all polymers composite like CuPC and CoPC film is shown in Figure.3.11(a) & (b) respectively. It shows ac conductivity increases exponentially with frequency for both pure polymer and the nanocomposite films. At higher frequency range, rapid increase of conductivity due to motion of individual poles of polymer and the poles of

the metal nanoparticles with increasing frequency is referred to electronic polarization effect in which a easy path of movement of poles is generated. It is also seen from Figure 3.11(a) & (b) that the value of ac conductivity is higher for all nanocomposite films than the pure polymer film. The increase of $\sigma_{a.c}$ is due to the increased incorporation of metal ions [29–34].

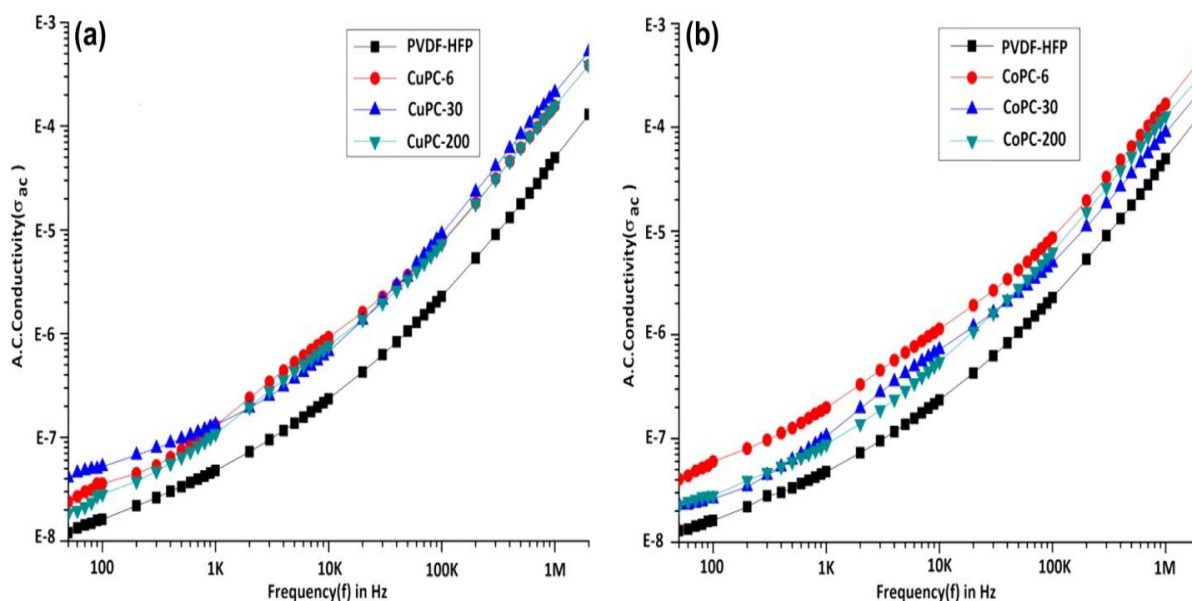


Figure 3.11 Frequency dependent ac conductivity ($\sigma_{a.c}$) of (a) CuPC and (b) CoPC for all potency.

3.6.4 Concentration vs dielectric constant

It is clearly seen from the figure.3.12 that dielectric constant has maximum value at

200C potency at a specific frequency (500 Hz).

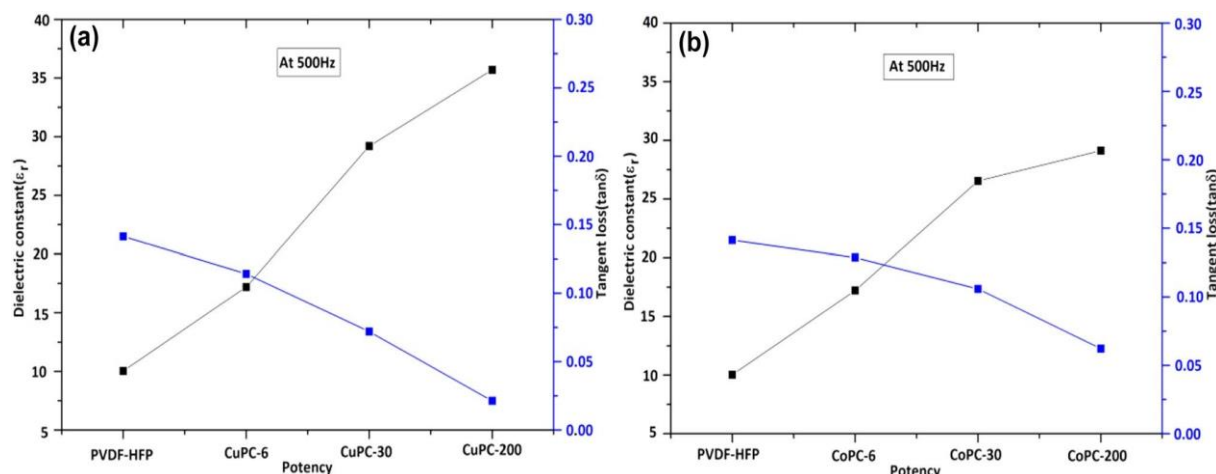


Figure 3.12 Potency dependent dielectric constant and tangent loss of a CuPC and b CoPC for all

substantially higher value in case of all polymer composite films termed as CuPC and CoPC than pure polymer film and it is also observed that the dielectric constant of these films at 200C respond the highest. This electrical phenomenon can be explained by Maxwell–Wagner–Sillars (MWS) interfacial polarization effect which appears in heterogeneous medium like poles of polymer matrix and the poles of metal nanoparticles consisting of different phases with different permittivity and ac conductivity due to accumulation of the charges at the interfaces. For these films, the well crystalline metal nanoparticles and polymer ions are well separated from each other with no such effective interaction between them. So the number of homogeneously distributed nanoparticles and their interfacial area per unit volume increases. This improves the average polarization associated with the particles and the coupling between neighboring grains, resulting in the significant enhancement of dielectric constant as well as significant decrement of tangent loss [29–32]. For lower potencies like 6C and 30C of these films, the particles are in bulk form and agglomerated which is embedded in the polymer matrix.

So the interfacial area per unit volume decreases while the inter particle distance decreases. This decreases the average polarization associated with the particles resulting in the further decrement of dielectric constant and ac conductivity as well as increment of tangent loss. This phenomenon is also clearly observed from their microstructures (FESEM).

3.7 Conclusions

From the above experiment we found that the addition of NPs in PVDF-HFP leads to

- (a) As the potency of NPs increased, better interaction observed on polymer matrix and thereby found homogeneously distributed particles.
- (b) Gradual increase in electro active β phase compared to PVDF-HFP.
- (c) The dielectric constant of all nanocomposites (1) increases with potency at any particular frequency and (2) decreases with increase in frequency for all potencies of metal nanoparticles. The dielectric constant got highest enhancement for CuPC-200 HNPs concentration.
- (d) AC conductivity increases with frequency for all nanocomposite films due to the presence of mobile metal ions in the polymer composites.
- (e) Tangent loss decreases with increasing frequency upto 10kHz and effect is more at higher potency.

Figure 3.12 summarizes the dielectric constant and tangent loss with change in potency for pure and composite of both CuPC and CoPC. We have shown that the incorporation leads to strong interfacial interaction between the NPs and the polymer resulting in enhanced dielectric constant of the thin films. The observed variation of the dielectric properties of the thin films depends on the surface, size and extent of agglomeration of the NPs in the polymer matrix.

Thus, pure polymer film which has comparatively low dielectric constant can be modified into materials with enhanced dielectric constant and comparatively low tangent loss by making a composite with triturated metal nanoparticles, which are nontoxic, eco-friendly and easily available in the nano form. As a dielectric material, these nanocomposite films can then be a promising candidate for the fabrication of high charge- storing multilayer capacitors and can be of great use in electronic industry.

References

- [1] P.Martins, C.M. Costa, M. Benelmekki, G. Botelho, S. Lanceros-Mendez, “On the origin of the electroactive poly(vinylidene fluoride) β -phase nucleation by ferrite nanoparticles via surface electrostatic interactions”. *Cryst. Eng. Comm.* **14**, 2807–2811 (2012)
- [2] P. Martins, A.C. Lopes, S. Lanceros-Mendez, “Electroactive phases of poly (vinylidene fluoride): determination, processing and applications”. *Prog. Polym. Sci.* **39**, 683–706 (2013)
- [3] H.S. Nalwa, “Ferroelectric polymers: chemistry, physics, and applications” (Marcel Dekker, New York, 1995)
- [4] Y. Li, X. Huang, Z. Hu, P. Jiang, S. Li, T. Tanaka, “Large dielectric constant and high thermal conductivity in poly(vinylidene fluoride)/barium titanate/silicon carbide three-phase nanocomposites”. *Appl. Mater. Interfaces* **3**, 4396–4403 (2011)
- [5] Z.M.Dang, Y.H. Lin, C.W.Nan, “Novel ferroelectric polymer composites with high dielectric constants”. *Adv. Mater.* **15**, 1625–1629 (2003)
- [6] Q. Chen, P.Y. Du, L. Jin, W.J. Weng, G.R. Han, “Percolative conductor/polymer composite films with significant dielectric properties”. *Appl. Phys. Lett.* **91**, 022912-1-022912-3 (2007)

- [7] M. Panda, V. Srinivas, A. K. Thakur, "On the question of percolation threshold in polyvinylidene fluoride/nanocrystalline nickel composites". *Appl. Phys. Lett.* **92**, 132905-1-132905-3 (2008)
- [8] X. Y. Huang, P. K. Jiang, L. Y. Xie, "Ferroelectric polymer/silver nanocomposites with high dielectric constant and high thermal conductivity". *Appl. Phys. Lett.* **95**, 24290-1-24290-3 (2009)
- [9] Z. M. Dang, J. P. Wu, H. P. Xu, S. H. Yao, M. J. Jiang, J. B. Bai, "Dielectric properties of upright carbon fiber filled poly(vinylidene fluoride) composite with low percolation threshold and weak temperature dependence". *Appl. Phys. Lett.* **91**, 072912-1-072912-3 (2007)
- [10] S. H. Yao, Z. M. Dang, M. J. Jiang, H. P. Xu, J. B. Bai, "Influence of aspect ratio of carbon nanotube on percolation threshold in ferroelectric polymer nanocomposite". *Appl. Phys. Lett.* **91**, 212901-1-212901-3 (2007)
- [11] P. Thakur, A. Kool, B. Bagchi, S. Das, P. Nandy, "Effect of in situ synthesized Fe_2O_3 and Co_3O_4 nanoparticles on electroactive β phase crystallization and dielectric properties of poly(vinylidene fluoride) thin films". *Phys. Chem. Chem. Phys.* **17**, 1368–1378 (2015)
- [12] Z. M. Dang, L. Wang, Y. Yin, "Giant dielectric permittivities in functionalized carbon nanotube/electroactive polymer nanocomposites". *Adv. Mater.* **19**, 852–857 (2007)
- [13] Q. Li, Q. Z. Xue, L. Z. Hao, X. L. Gao, Q. B. Zheng, "Large dielectric constant of the chemically functionalized carbon nanotube/ polymer composites". *Compos. Sci. Technol.* **68**, 2290–2296 (2008)
- [14] B. K. Paul, D. Roy, S. Bal, A. Bhattacharya, S. Das, P. Nandy, "A comparative study of strontium and titanium doped mullite in PVDF matrix and their phase behavior, microstructure and electrical properties". *Mater. Chem. Phys.* **187**, 119–132 (2017)

- [15] P. Thakur, A. Kool, B. Bagchi, S. Das, P. Nandy, “Enhancement of β phase crystallization and dielectric behavior of kaolinite/halloysite modified poly(vinylidene fluoride) thin films”. *Appl. Clay.Sci.* **99**, 149–159 (2014)
- [16] Y.P. Zhang, S.H. Lee, K.R. Reddy, A.I. Gopalan, K.P. Lee, “Synthesis and characterization of core–shell SiO₂ nanoparticles/ poly(3-aminophenylboronic acid) composites”. *J. Appl. Polym. Sci.* **104**, 2743–2750 (2007)
- [17] D.R.Son,A.V.Raghu,K.R.Reddy, H.M. Jeong, “Compatibility of thermally reduced graphene with polyesters”. *J. Macro mol. Sci.Part B Phys* **55**, 1099–1110 (2016)
- [18] K.R. Reddy, B.C. Sin, K.S. Ryu, J.C. Kim, H. Chung, Y. Lee, “Conducting polymer functionalized multi walled carbon nano tubes with noble metal nanoparticles: synthesis, morphological characteristics and electrical properties”. *Synth. Met.* **159**, 595– 603 (2009)
- [19] M. Hassan, K.R. Reddy, E. Haque, S.N. Faisal, S. Ghasemi, A. Minett, V.G. Gomes, “Hierarchical assembly of graphene/poly- aniline nanostructures to synthesize free-standing supercapacitorelectrode”. *Compos. Sci. Technol.* **98**, 1–8 (2014)
- [20] K.R. Reddy, W. Park, B.C. Sin, J. Noh, Y. Lee, “Synthesis of electrically conductive and super paramagnetic mono dispersed iron oxide-conjugated polymer composite nanoparticles by in situ chemical oxidative polymerization”. *J. Colloid Interface Sci.* **335**,34–39 (2009)
- [21] M. Hassan, K.R. Reddy, E. Haque, A.I. Minett, V.G. Gomes, “High-yield aqueous phase exfoliation of graphene for facile nanocomposite synthesis via emulsion polymerization”. *J. ColloidInterface Sci.* **410**, 43–51 (2013)
- [22] K.R. Reddy, K.P. Lee, A.I. Gopalan, “Self assembly directed synthesis of poly(ortho-toluidine)-metal (gold and palladium) composite nanospheres”. *J. Nanosci. Nanotechnol.* **7**, 3117–3125 (2007)

- [23] A.L. Gayen, B.K. Paul, D. Roy, S. Kar, P. Bandyopadhyay, R. Basu, S. Das, D.S. Bhar, R.K. Manchanda, A.K. Khurana, D. Nayak, P. Nandy, "Enhanced dielectric properties and conductivity of triturated copper and cobalt nanoparticles doped PVDF-HFP film and their possible use in electronic industry". *Mater. Res. Innovations* (2016). doi:[10.1080/14328917.2016.1196563](https://doi.org/10.1080/14328917.2016.1196563)
- [24] P. Nandy, S. Bhandary, S. Das, R. Basu, S. Bhattacharya, "Nanoparticles and membrane anisotropy". *Homeopathy* **100**, 194 (2011)
- [25] P. Nandy, "A review of basic research on homoeopathy from a physicist's point of view". *Indian J. Res. Homeopath.* **9**, 141–151 (2015)
- [26] P.S. Chikramane, A.K. Suresh, J.R. Bellare, S.G. Kane, 'Extreme homeopathic dilutions retain starting materials: a nanoparticulate perspective'. *Homeopathy* **99**, 231–242 (2010)
- [27] P.S. Chikramane, D. Kalita, A.K. Suresh, S.G. Kane, J.R. Bellare, 'Why extreme dilutions reach non-zero asymptotes: a nanoparticulate hypothesis based on froth flotation'. *Langmuir* **28**, 15864–15875 (2012)
- [28] K. Halder, B.K. Paul, B. Bagchi, A. Bhattacharya, S. Das, "Copper ion doped mullite composite in poly(vinylidene fluoride) matrix: effect on microstructure, phase behavior and electrical properties". *J. Res. Updat. Polym. Sci.* **3**, 157–169 (2014)
- [29] B.K. Paul, K. Halder, D. Roy, B. Bagchi, A. Bhattacharya, S. Das, "Dielectric switching above a critical frequency occurred in iron mullite composites used as an electronic substrate". *J. Mater. Sci. Mater. Electron.* **25**, 5218–5225 (2014)
- [30] P. Thakur, A. Kool, B. Bagchi, N.A. Hoque, S. Das, P. Nandy, 'In situ synthesis of Ni(OH)₂ nanobelt modified electroactive poly(vinylidene fluoride) thin films: remarkable improvement in dielectric properties. *Phys. Chem. Chem. Phys.* **17**, 13082–13091 (2015)

- [31] P. Thakur, A. Kool, B. Bagchi, N.A. Hoque, S. Das, P. Nandy, “Improvement of electroactive β phase nucleation and dielectric properties of $\text{WO}_3 \cdot \text{H}_2\text{O}$ nanoparticle loaded poly(vinylidene fluoride) thin films”. RSC Adv. **5**, 62819–62827 (2015)
- [32] B.K. Paul, S. Kar, P. Bandyopadhyay, R. Basu, S. Das, D.S. Bhar, R.K. Manchanda, A.K. Khurana, D. Nayak, P. Nandy, “Significant enhancement of dielectric and conducting properties of electro active polymer polyvinylidene fluoride films: an innovative use of Ferrum metallicum at different concentrations”. Indian J. Res. Homeopath. **10**(1), 52–57 (2016)
- [33] B.K. Paul, S. Das, R. Basu, D.S. Bhar, R.K. Manchanda, A.K. Khurana, D. Nayak, P. Nandy, “Effect of dilution of Ferrum metallicum and zincum oxidatum, homeopathic nano medicines on the dielectric properties of poly(PVDF-HFP) film”. Int. J. High Dilution Res **15**(1), 10–17 (2016)
- [34] F.Rogti, M.Ferhat, “Maxwell–Wagner polarization and interfacial charge at the multi-layers of thermoplastic polymers”. J. Electrostat. **72**(1), 91–97 (201).

Chapter 4

**Effect of Dilutions of Cuprum Arsenicosum on the Electrical
Properties of PolyVinylidene Fluoride Cohexafluoro propylene**

4.1 Overview

Cuprum Arsenicosum is a Cu and As based salt and it has medicinal values. With the degree of dilution of the salt and proper shaking nanoparticles of different sizes are formed. Due to formation of nanoparticles, Cuprum Arsenicosum in different dilution or concentrations might have ability to improve the electrical properties of polymer film. So the objective of this study is to investigate the effect of various dilution of Cuprum Arsenicosum to enhance the electric properties of polymer material.

An electro active polymer film is frequently used as a capacitor in the electronic sector and it has been shown to have its dielectric constant and alternating current (AC) conductivity increased by the addition of metal-derived salt like Cuprum Arsenicosum. Here, we discuss the impact of diluting Cuprum arsenicosum (CuAs) to a potency of 200C on the electrical characteristics of the polymer film made of poly (vinylidene fluoride co-hexafluoropropylene).

The salt ,CuAs with dilution 200C, is incorporated in the polymer matrix by the solution casting method to form a composite. An inductance, capacitance, and resistance meter is used to measure the electrical properties at various frequencies. Fourier transform infrared spectroscopy (FTIR) is employed to find the CuAs-induced phase changes in the polymer film. Energy dispersive X-ray (EDX) spectroscopy and field emission scanning electron microscopy (FESEM) were used to examine the morphology and particle size of the metal in the composite. When 2 ml CuAs with dilution 200C is added to the polymer film both the dielectric constant and AC conductivity is enhanced by around 18 times at 10 kHz frequency. While spherical

CuAs particles were confirmed by FESEM and EDX, FTIR suggested an increase in the conducting phase. The conductivity and dielectric properties of the electro active polymer film is improved by the addition of CuAs. Hence CuAs doped polymer matrix with enhanced dielectric properties would also be promising candidate in electronic industry.

4.2 Introduction

Some salts such as Cuprum Arsenicosum are widely used as alternative medicine for complementary therapies. However, the mainstream scientific community is still baffled by the mechanism of action of these medications at very high dilution. Many hypotheses have been put forth, but none have been exactly confirmed.

In the process of preparation of these alternative medicines, a process known as succession is followed where mechanical energy is transferred to the solution [1]. In this process, the original aggregated drug particles are fragmented into nanoparticles [2]. In our previous study, we have demonstrated that how the drugs are permeable through the membrane in its nano dimension and how it is dependent on the potency [3-5]. Studies by our team and other teams have shown that nanoparticle production occurs at high dilutions [6-10] and this nanoparticle production is a key indicator for comprehending how these medicines behave at ultra molecular dilution.

The nanoparticle aspects and their relations with the dilution of these medicines are further investigated to explore its utility in several technological applications. In one instance, we have demonstrated that the chemical Zincum oxydatum (ZnO) (used as another alternative medicine) can increase the generation of thermo voltage and photo

voltage [11-14]. This discovery might have significant effects on solar energy harvesting.

We have then delved deeper into the nanoparticle component of various dilutions and employed them in several technical applications. In a different instance, we have investigated a novel method of utilizing the nanoparticle aspect of these alternative medicines to enhance the electrical properties of electro active polymer films, which have recently been commercially used as an alternative to traditional electro-active ceramics for technological applications. To enhance electrical properties in terms of the high dielectric constant and alternating current (AC) conductivity, and low tangent loss of the electro active polymer films, several chemicals with medicinal importance such as ferrum metallicum (FeM), cuprum metallicum (CuM), cobaltum metallicum (CoM), and zinc oxide (ZnO) are incorporated to the polymer matrix of polyvinylidene fluoride cohexafluoropropylene (PVDF-HFP)[15-22] in appropriate dilutions. Here, we describe how adding Cuprum arsenicosum (CuAs) nanoparticles to various proportions of the polymer matrix can further enhance the electrical characteristics of the polymer film. For instance, compared to the undoped film, polymer film integrated with 2 ml of CuAs at 200 C potency enhanced dielectric constant and AC conductivity by almost 18 times.

4.3 Method

4.3.1 Solution Casting Method

Firstly, CuAs at 200C dilution was taken from the Hahnemann Publishing Company, India. Pellets of PVDF-HFP were brought from Sigma Aldrich, United States, and dimethyl sulfoxide (DMSO) was obtained from Merck, Germany.

The solution casting method was employed to synthesize CuAs doped nanocomposites. The flowchart of the method of preparation of CuAs doped nanocomposite films is shown in Figure 4.1. In a typical synthesis, 2 ml of DMSO and 100 mg of PVDF-HFP were combined while being vigorously stirred at 60°C for three hours. The solution received additions of CuAs in precise proportions. All of the composite films were created by pouring the entire mixture into dry, clean Petri dishes and letting the solvent evaporate for 12 hours at 60°C in an oven. We conducted all of our measurements using the remaining DMSO because it cannot be completely eliminated. After that, silver paste was applied on both sides of the films to coat them on both sides of the films electrical measurements.

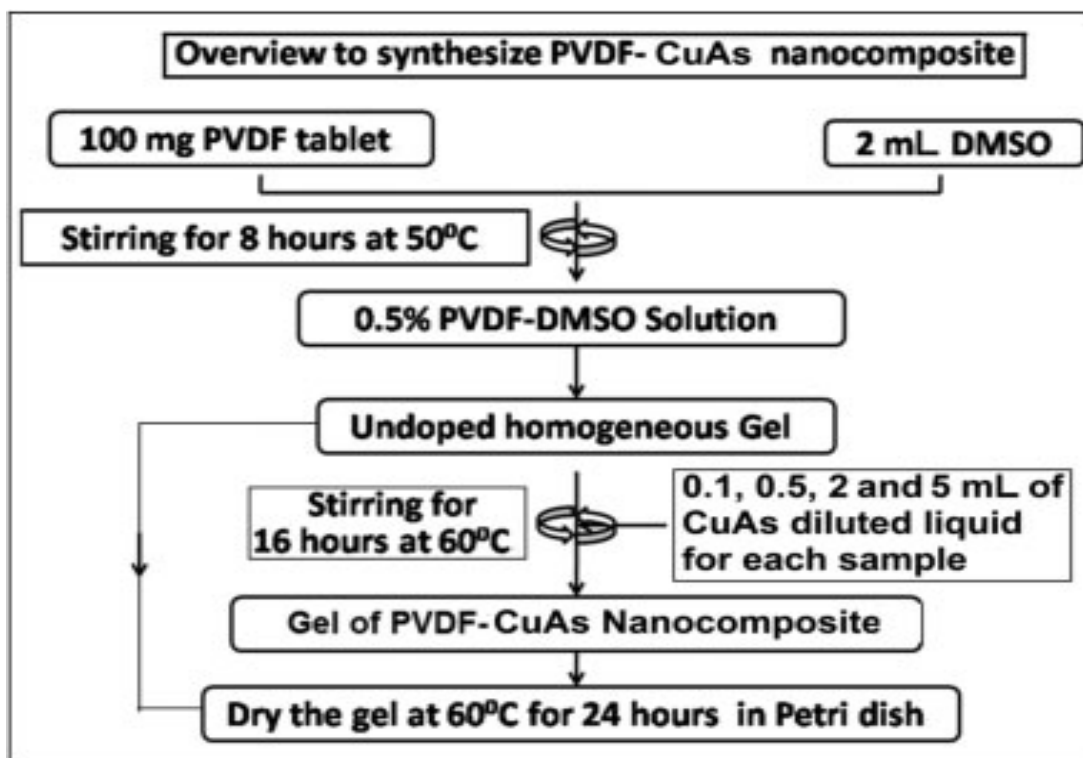


Figure 4.1 Flowchart to synthesize PVDF-CuAs nanocomposite films.

Using a digital screw gauge, the thickness of the synthesized films was found to be between 50-55 μm [19-22].

4.3.2 Electrical Characteristics, Phase Change, Morphology, and Particle Size

An inductance, capacitance, and resistance (LCR) metre (Hewlett-Packard (HP) Model 4274) was used to measure the electrical properties at various frequencies [23]. The incorporation of CuAs caused a phase change in the polymer film, which was detected by Fourier transform infrared spectroscopy (FTIR) (FTIR-8400S, Shimadzu) [15,19-22]. Field emission scanning electron microscopy (FESEM) (ZEISS Sigma 300) was used to investigate morphology, particle size, and energy dispersive X-ray (EDX) spectroscopy. Below are the summarized sample details. The samples in Figures 4.2, 4.3, 4.4, and 4.5 were designated by specific sample codes.

4.3.3 Sample details

Sample code 0: 100 mg PVDF + 2 ml DMSO + 0 ml CuAs

Sample code 0.1: 100 mg PVDF + 2 ml DMSO + 0.1 ml CuAs

Sample code 0.5: 100 mg PVDF + 2 ml DMSO + 0.5 ml CuAs

Sample code 2: 100 mg PVDF + 2 ml DMSO + 2 ml CuAs

Sample code 5: 100 mg PVDF + 2 ml DMSO + 5 ml CuAs

4.4 Result & discussion

4.4.1 FTIR Analysis

FTIR was employed to study the identification and confirmation of Phases. FTIR spectra in the wavenumber range between 400 cm^{-1} to 1100 cm^{-1} of CuAs doped PVDF-HFP nanocomposite films at various concentrations are shown in Figure 4.2. The spectra shows the characteristic absorbance bands at wavenumbers 487, 530, 615, 763, 795, and 875 cm^{-1} that corresponds to the α -phase and at around 512 and 842 cm^{-1} that refers to the β phase. From FTIR spectra, it is seen that there is a variation in intensity of both α and β -phases. This increment in phase intensity confirms the chemical interaction between the polymer matrix and the CuAs nanoparticles [15,19-22].

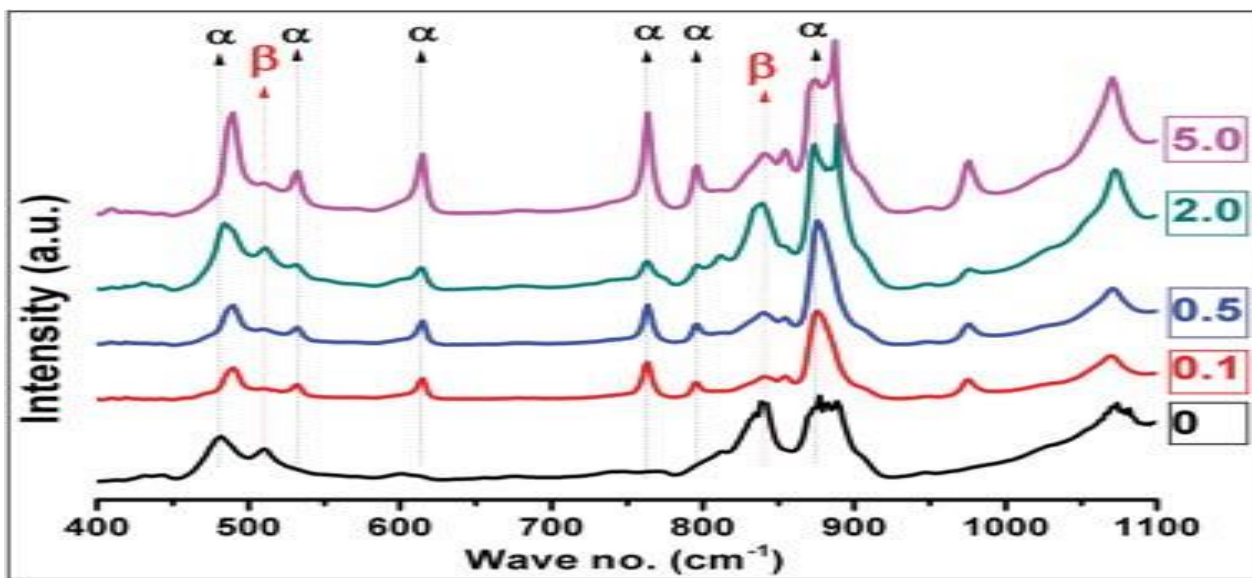


Figure 4.2 Phase identification and confirmation study by FTIR of all the samples.

Figure 4.2 shows that, as the concentration of CuAs increases, there is a significant growth of β phase as compared to the pure PVDF-HFP and reached at maximum for the sample of 2 ml insertion. It indicates that the most effective interaction takes place between the PVDF matrix and CuAs nanoparticle at this concentration. If more CuAs nanoparticles are inserted, the phase intensity decreases as a result of the network destruction. This is further supported by FESEM in Figure 4.3.

4.4.2 FESEM Analysis

The morphology, particle size of CuAs incorporated PVDF films are analyzed through micrographs, as shown in Figure 4.3, captured by Field Emission Scanning Electron Microscopy FESEM.

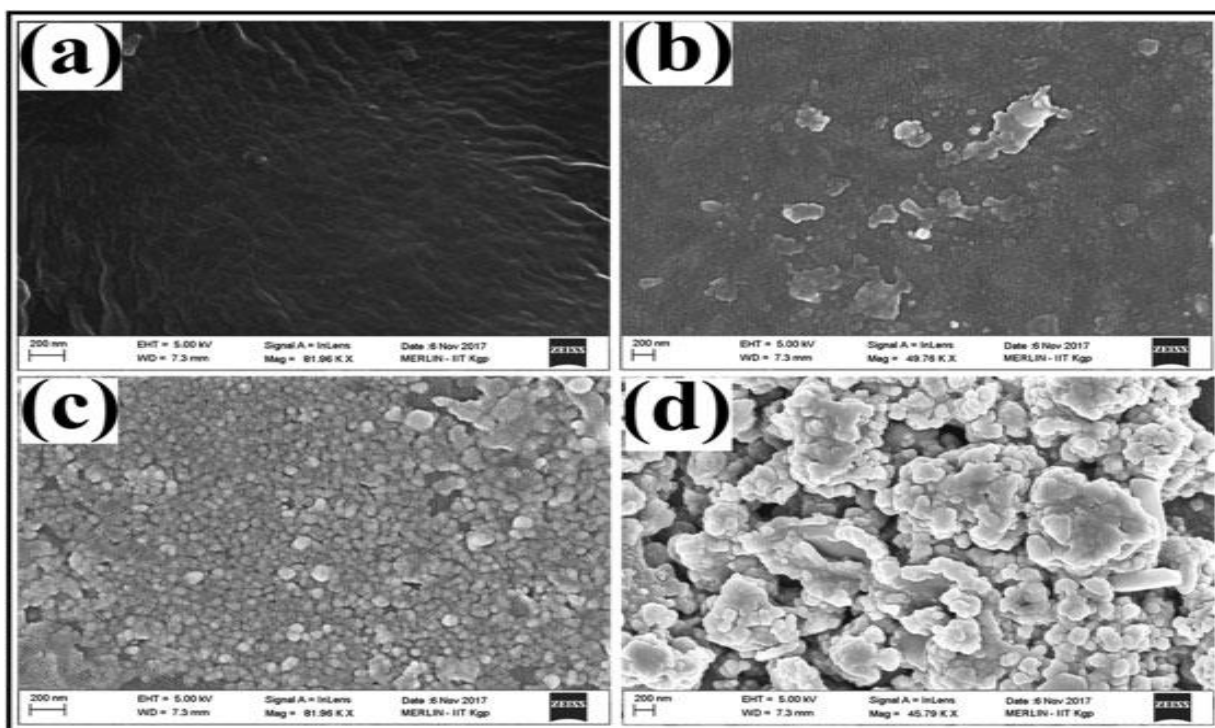


Figure 4.3 Morphology and microstructural analysis of CuAs incorporated PVDF-HFP films by FESEM (a) 0(PVDF-HFP), (b) 0.5(CuAsPC), (c) 2.0(CuAsPC) and (d) 5.0(CuAs PC)

The figure 4.3 illustrates that the microstructures of the 5 samples of the polymer film with different concentration of doped CuAs : (a) pure PVDF-HFP (b) 0.5 ml (c) 2 ml and (d) 5 ml. The micrographs show the presence of several morphology and micro structures of CuAs incorporated in the polymer samples in different concentrations.

A few spherical-shaped nanoparticles are seen to be incorporated in the PVDF-HFP matrix at lower insertion concentrations (0.5 ml). For the doping concentration of 2 ml, many spherical CuAs nanoparticles are seen that are uniformly distributed and tightly packed within the polymer matrix. Evidence of a significant number of agglomerated nanoparticles embedded in the polymer matrix is seen for further increase in doping concentration. So these chemicals of medical importance are clearly present in the polymer matrix, which suggests the presence of nanoparticles of such low dimension [15,19-22].

4.4.3 EDX Analysis

Elemental mapping images of CuAs nanoparticle incorporated in PVDF-HFP composite were obtained through EDX measurements. The EDX spectra of 2 ml PVDF-HFP (incorporated composite films) is shown in Figure 4.4. The presence of arsenic, copper and polymeric elements into the composite system is confirmed through EDX images. Elements found from EDX study, along with their normality and weight percentages, are illustrated in Figure 4.4.

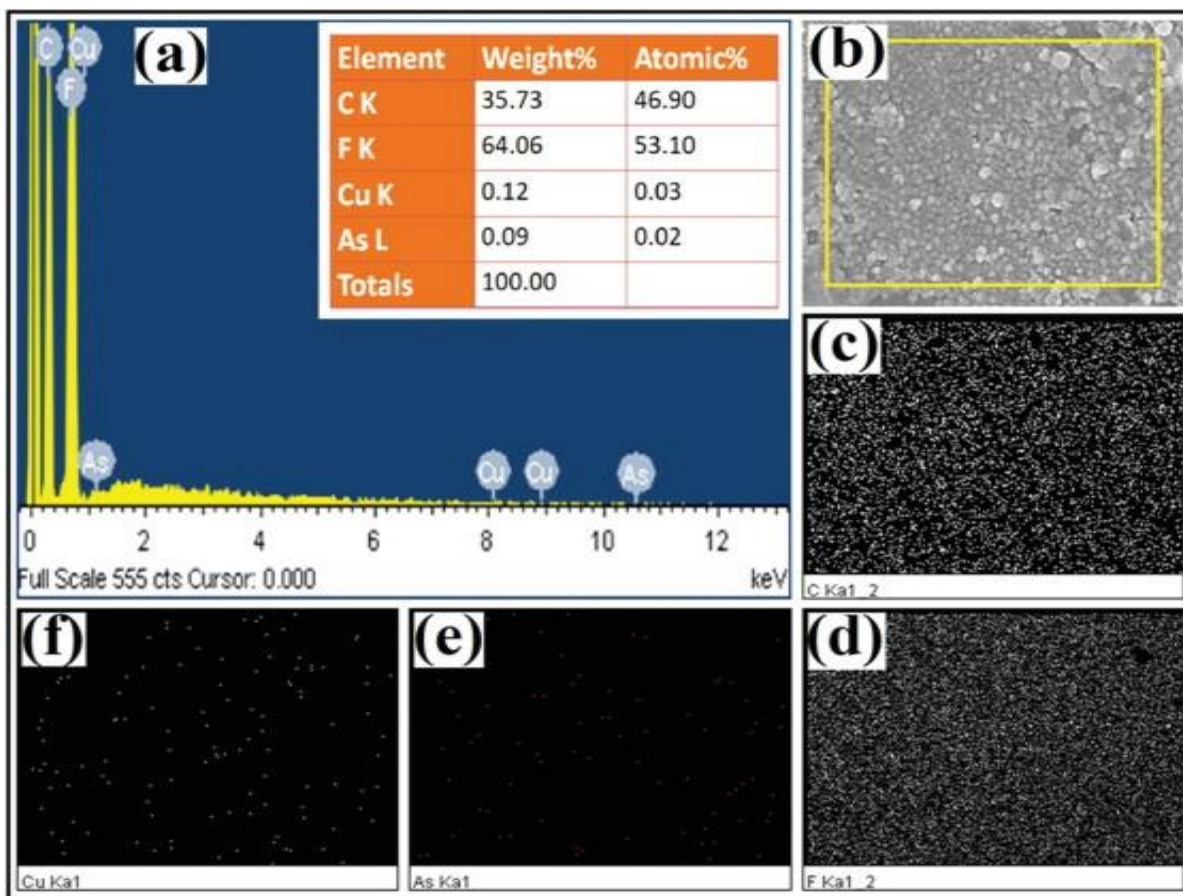


Figure 4.4. (a) Elemental confirmation of all elements present in the 2 ml CuAs incorporated PVDF film by EDX spectra (C, Carbon; Cu, Copper; F, Fluorine; As, Arsenic); (b) selected area for measurement; and (c–f) elemental mapping image (c) Carbon, (d) Fluorine, (e) Arsenic, and (f) Copper of 2 ml CuAs-doped PVDF-HFP film. K, L, and Ka 1 refer respectively to the K-band, L-band, and K_{α} -band of the X-ray beam used for the EDX spectroscopy. CuAs, Cuprum arsenicosum, EDX, energy dispersive X-ray; PVDF-HFP, poly(vinylidene fluoride Co hexafluoropropylene).

Ultra-high dilution is verified by low atomic percentage of copper and arsenic in the CuAs-PVDF matrix. In figure 4.4 b the selected region of the composite films is shown and Figure 4.4.c–f verifies that all the elements are homogeneously distributed in the composite.

4.5 Study of electrical properties of PVDF-HFP Composites

4.5.1 Frequency versus Dielectric Constant

The electrical properties of CuAs doped PVDF-HFP are analyzed by using an LCR meter and the parameters are compared with that of the pure PVDF film. Dielectric constant (ϵ_r) of the material is calculated by the formula-

$$\epsilon_r = \frac{dC_p}{A\epsilon_0}$$

where, C_p is the capacitance of the material, d is the thickness of the film, A is the area of the sample, and ϵ_0 is the permittivity of free space. The dielectric constant vs frequency graphs are plotted in frequency range 20 Hz to 2 MHz in figure 4.5. Figure shows that the dielectric constant continuously decreases with increasing frequency. Dielectric constant is substantially higher in the whole frequency range for all CuAs doped compared to the pure polymer film. The value of dielectric constant increases with the increment of concentration of CuAs and at a specific value of concentration i.e., 2 ml, it becomes maximum which is approximately 18-fold larger in compared to the 0 ml sample (Table- 1); this effect may be due to Maxwell–Wagner-Sillars polarization [15] at the interface and maximum interfacing area per unit volume.

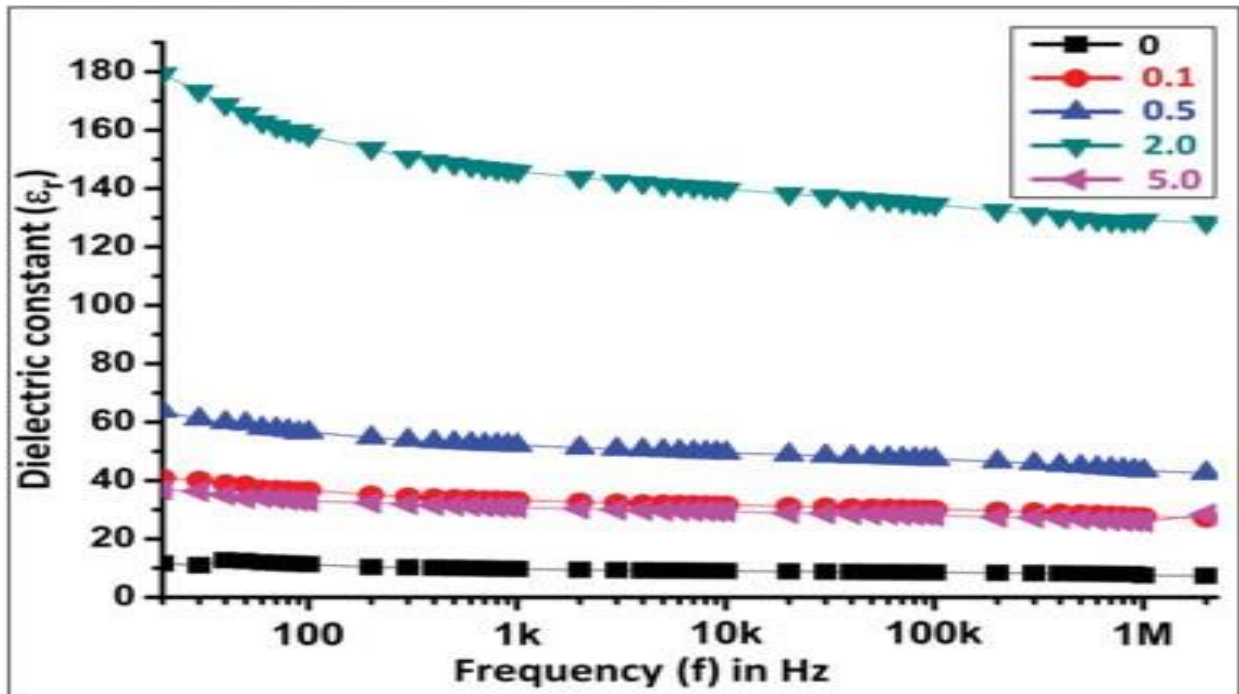


Figure 4.5 Variation of dielectric constant with frequency for all samples including CuAs incorporated PVDF films.

If the doping concentration is increased further, the value of dielectric constant is decreased due to agglomeration or reducing the inter particle distance. If the frequency is increased, the dipole response becomes limited and the dielectric constant tends towards saturation [19-22].

4.5.2 Tangent loss analysis

The ratio of conduction current to displacement current is known as the tangent loss of a medium. The variation of tangent loss with frequency for all the samples clearly indicated that tangent loss decreases with increasing frequency for all samples up to 10 kHz (Figure 4.6).

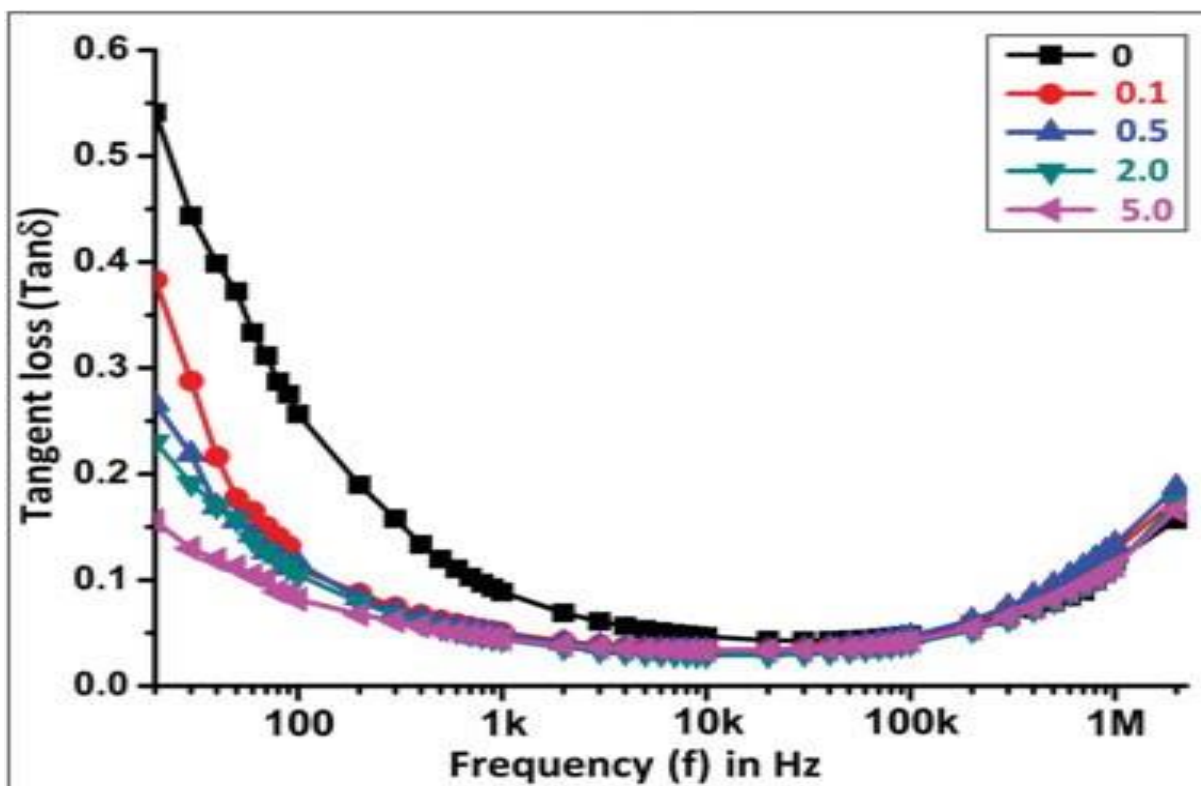


Fig. 4.6 Variation of tangent loss with frequency for all CuAs incorporated PVDF films. CuAs, Cuprum arsenicosum; PVDF, poly(vinylidene fluoride).

At lower frequency range, greater tangent loss is seen and that is due to higher polarization effect followed by more relaxation time. Within 10 kHz polarization effect is reduced as frequency is increased, and relaxation time is less here and inter-molecular vibration is reduced, as a result there is a decrease in tangent loss. However, above 10 kHz, due to the heat generation and hence more inter molecular vibration [15, 19-22] the tangent loss is increased.

4.5.3 Frequency vs Electrical Conductivity

Electrical AC conductivity ($\sigma_{a.c.}$) is calculated by the formula

$$\sigma_{ac} = 2\pi f T \tan \delta \epsilon_r \epsilon_0$$

where $\sigma_{a.c.}$, f , $\tan \delta$, ϵ_r , and ϵ_0 are respectively the AC conductivity, frequency in Hz, tangent loss factor, dielectric constant of the material, and vacuum permittivity.

AC conductivity is measured to investigate the nature of ionic motion in conducting materials. Figure 4.7 shows that the AC conductivity exponentially increases with increasing frequency for all the sample polymer films.

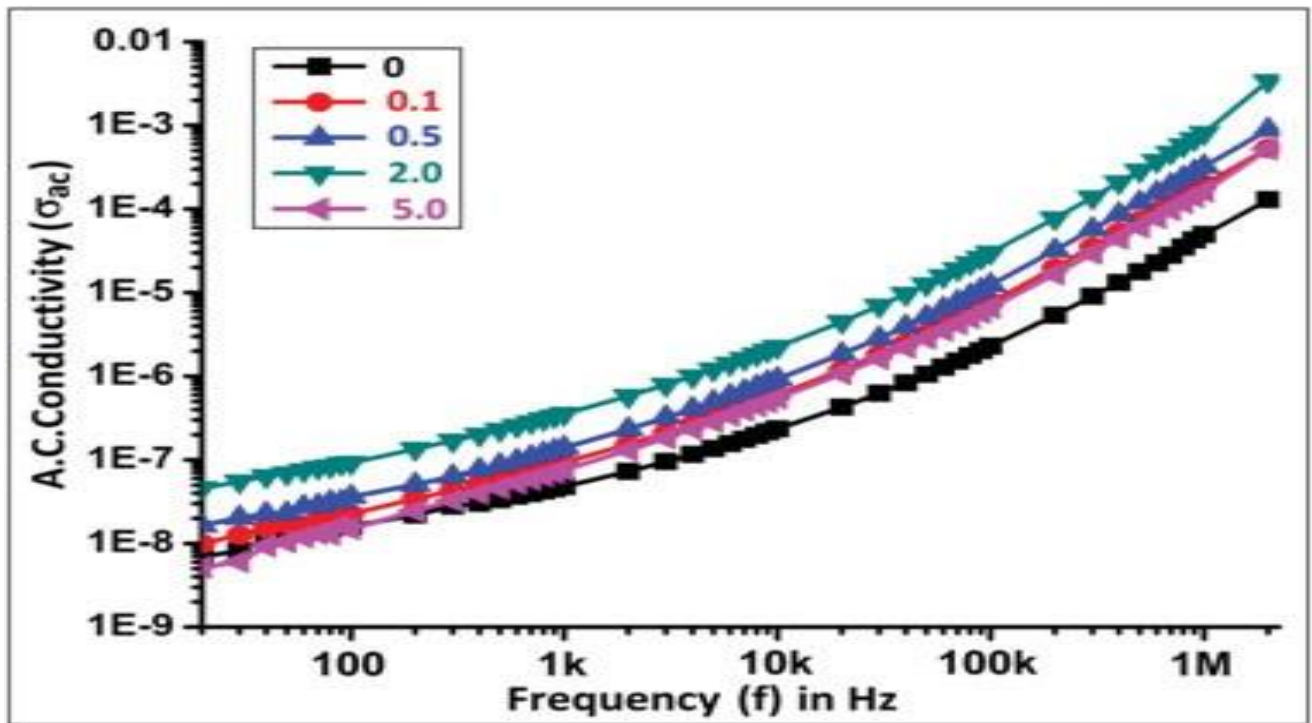


Figure 4.7 Variation of AC conductivity (Siemens/meter) with frequency for all samples including CuAs incorporated PVDF films.

This happens as the number of hopping of conducting electrons is increased in these polymer films [23]. At a given frequency, AC conductance is enhanced in films with

higher concentrations and becomes maximum at 2 ml. AC conductivity is approximately 18-fold greater in 2 ml sample than that of 0 ml sample (Table 4.1).

Dielectric constant (Figure 4.5)		
For Sample 0	For sample 2.0	Increase by factor
8.3	146	17.6–18.0
AC conductivity (Figure 4.7)		
For Sample 0	For sample 2.0	Increase by factor
1.8×10^{-7}	3.2×10^{-6}	17.8–18.0
Siemens/meter	Siemens/meter	

Table 4.1 Variation in dielectric constant and AC conductivity of polymer film due to incorporation of CuAs at 10 kHz frequency

4.6. Conclusion

With the incorporation of CuAs in the film of polymer PVDF-HFP, the electrical properties, such as dielectric constant and electrical AC conductivity are enhanced significantly in comparison with those of the pure polymer film. The dielectric constant enhancement is due to the presence of two different metallic nanoparticles in the composite film. Also, the incorporation of CuAs induces a phase change in the polymer film which is also verified by the FTIR spectrum, which is physical basis of the enhancement of AC conductivity.

These findings lead logically to the conclusion that this chemical, which has also great importance in alternative medicines, have their innate electrical property which gives them their effects on various physical processes and they can be used as promising candidates in electronic technologies.

Reference

- [1] Shah R. “Standardization of the potentizing machine and quantification of impact of potentisation”. *Ind J Res Homoeopathy* 2016; 10:126–132
- [2] Upadhyay RP, Nayak C. “Homeopathy emerging as nanomedicine”. *Int J High Dilution Res.* 2011; 10:299–310
- [3] Nandy P, Bhandary S, Das S, Basu R, Bhattacharya S. Nanoparticles and membrane anisotropy. *Homeopathy* 2011; 100:194
- [4] Ghosh S, Chakraborty M, Das S, Basu R, Nandy P. “Effect of different potencies of nanomedicine *Cuprum metallicum* on membrane fluidity a biophysical study”. *Am J Homeopathic Medicine* 2014; 107:161–169
- [5] Bhandary S, Das S, Basu R, Bhattacharyya S, Nandy P. “Effect of *Aconitum napellus* on liposomal micro viscosity”. *Int J Emerg Technol Sci Eng* 2011; 3:1–5
- [6] Kar S, Bandyopadhyay P, Chakraborty S, et al. “Derivation of an empirical relation between the size of the nanoparticle and the potency of homeopathic medicines”. *Int J High Dilution Res* 2015; 14:2–7
- [7] Nandy P. “A review of basic research on homeopathy from a physicist’s point of view”. *Ind J Res Homoeopathy* 2015; 9:141–151

- [8] Chikramane PS, Kalita D, Suresh AK, Kane SG, Bellare JR. “Why extreme dilutions reach non-zero asymptotes: a nanoparticulate hypothesis based on froth flotation”. *Langmuir* 2012;28:15864–15875
- [9] Chikramane PS, Suresh AK, Bellare JR, Kane SG. “Extreme homeopathic dilutions retain starting materials: a nanoparticulate perspective”. *Homeopathy* 2010; 99:231–242
- [10] Rajendran ES. “Field emission scanning electron microscopic (FESEM) and energy dispersive spectroscopic (EDS) studies of centesimal scale potencies of the homeopathic drug *Lycopodium clavatum*”. *Am J Homeopath Med* 2015;108:9–18
- [11] Bandyopadhyay P, Nandy P, Basu R, Bhar DS, Das S. “Effect of dilution on thermo voltage generation using homeopathic nanomedicine *Zincum oxydatum*”. *Int J Innov Res Sci Eng* 2015;3:225–230
- [12] Bandyopadhyay P, Nandy P, Basu R, Bhar DS, Das S. “Thermo voltage generation using homeopathic medicine”. *Ind Photo biol News Lett* 2016;53:13–16
- [13] Bandyopadhyay P, Chakraborty S, Basu R, et al. “Efficiency of a dye sensitized photo-electrochemical device using thionine and triturated zinc oxide at different potency”. *Energy Source A, Recovery Util Environ Effects* 2016. In press
- [14] Mondal A, Basu R, Das S, Nandy P. “Increased quantum efficiency in hybrid photo electrochemical cell consisting of thionine and zinc oxide nanoparticles”. *J Photo chem. Photo boil Chem* 2010;211: 143–146
- [15] Martins P, Lopes AC, Lanceros-Mendez S. “Electro active phases of poly (vinylidene fluoride): determination, processing and applications”. *Prog Polym Sci* 2013;39:683–706

- [16] Nalwa HS. “Hand book of Low and High Dielectric Constant Materials and Their Applications, Volume 1”: Materials and Processing. 1st ed. San Diego, CA: Academic Press; 1999
- [17] Kingon AI, Maria JP, Streiffer SK. “Alternative dielectrics to silicon dioxide for memory and logic devices”. *Nature* 2000;406:1032–1038
- [18] Singh R, Ulrich RK. “High and low dielectric constant materials”. *Electro chem Soc Interface* 1999;8:26–30
- [19] Chatterjee A, Paul BK, Kar S, et al. “Effect of ultrahigh diluted homeopathic medicines on the electrical properties of PVDF-HFP”. *Int J High Dilution Res* 2016;15:10–17
- [20] Paul BK, Kar S, Bandyopadhyay P, et al. “Significant enhancement of dielectric and conducting properties of electro active polymer poly vinylidene fluoride films : an innovative use of Ferrum metallicum at different concentrations”. *Ind J Res Homoeopathy* 2016;10:52–58
- [21] Gayen AL, Paul BK, Roy D, et al. “Enhanced dielectric properties and conductivity of triturated copper and cobalt nanoparticles doped PVDF-HFP film and their possible use in electronic industry”. *J Material Res Innovations* 2017;21:166–171
- [22] Gayen AL, Mondal D, Roy D, et al. “Improvisation of electrical properties of PVDF-HFP: use of novel metallic nanoparticles”. *J Mater Sci Mater Electron* 2017; 28:14798–14808
- 23 Jonscher AK. Dielectric relaxation in solids. *J Phys D Appl Phys* 1999;32:R57–R70

Chapter 05

**Effect of both serial dilution and succession of potentised
Cuprum metallicum in comparison to succussion alone on
Escherichia coli bacterial system and Capacitive performance
of poly(vinylidene fluoride cohexafluoropropylene) polymer**

5.1 Over view

Nanoparticles are prepared by traditional method like potentization by serial dilution followed by succussion or trituration. The respective roles of these two components need to be assessed and explored in our present study. To study and compare the effect of the nanoparticles Cuprum metallicum (Cup. met.) which is potentized through both serial dilution with succussion and only succussion alone on selected biological and capacitive performance of a physical systems. Beginning with the potensized nanoparticles, Cup. met. at potency 6C, we potentized it further to 30C and 200 C by serial dilution, followed by succussion. It is termed as sample Set A having all three potency like 6C, 30C and 200C with small particle size respectively. The same nanoparticle are prepared at 6C was also potentized to 30C and 200C by using succussion alone termed as another sample Set B. Then two set of sample with different potency was applied to study antibacterial property on *E. coli*, a biological system and electrical properties on polymer matrix PVDF-HFP (widely used as charge separator) a physical system. Field Emission Scanning Electron Microscopy (FESEM) shows that the particles get more agglomerated decreasing its surface to volume ratio at higher potency in Set B. So anti bacterial effect like growth of bacterial system on set B at higher potency is high. Anti bacterial effect of Cup. met. in Set A at 30C and 200C was observed to be more significant as compared to Set B. Effect of Cup. met. on a physical system like PVDF-HFP a polymer matrix in Set A varied significantly with increase in the potency as compared to Set B. In set B less beta phase crystallization was produced due to agglomeration of particle as only succussion was there which served as no significant change in electrical properties with less formation of β phase. From these two results we assure that the nanoparticle preparation of Cup. met. in two experimental set ups shows that serial dilution with succussion makes an important difference between the two sets.

5.2 Introduction

Nanoparticle preparation by potentization of Hahnemannian era constituted of serial dilution followed by either succession or trituration or both depending on the type of bulk substances. When we prepared potencies from solid bulk substances, decimal and centesimal scales are used. From the preparation of liquid solution with nanoparticle substances, manufacturing of liquid metal particle is from the mother solution (tincture) by serial dilution and succession or trituration (mechanical agitations) in one of the three potency ranges, decimal (1:9), centesimal (1:99), or fifty millesimal. Solid insoluble materials (e.g., Cuprum metallicum [Cup. met.]) are triturated with lactose in the ratio of 1:10 till the 6X potency, and then the liquid dilutions are carried out. The liquid dilutions or potentization are prepared by the Hahnemannian method [1] till the 200C potency and the Korsakovian method is followed for potencies beyond 200C. The most vital part of preparation of nanoparticles is the potentization which transforms the starting material to a therapeutically active one. It can be classified in two components: (a) Serial dilution and (b) Vigorous vertical jerking, known as succussion. The paradox created debate between practicing rationalists and other homeopaths as they felt that there is no medicine present at very high dilution.[2] However, as the effectiveness of high potencies is experienced by the practicing homoeopaths and countless patients, more positive opinions started accumulating, backed by different models, in favour of the therapeutic effect of these nanoparticles at high potency. The question naturally arises, why do, in the preparation of nanoparticle, we dilute instead of concentrating.[3] due to increase in surface to volume ratio. We have, for the first time, shown that there is a difference between the effects of two kinds of potentisation: serial dilution, followed by succussion, and only succussion. Recently, it has been experimentally proved that it is not only the dilution, but the succussion followed after each dilution is necessary, which is

responsible for these effects at high potency by increasing more interaction area with the other substance. In vigorous shaking, a large amount of external force or mechanical energy is transferred, this energy breaks the drug associates and reduces its size or dimension to nanodimension.[4-6] This reduction in size or dimension increases more interaction faces i.e membrane permeability.[7] The empirical relation between potency (X) and the size of the drug aggregates (Y) is given by the following equation:[8] $Y = ax^{-n}$

Where a and n are characteristic constants of different nanoparticles. From experiment it is proved that extreme dilutions retain starting materials.[9] From a biological perspective to understand the extreme dilutions, it has been shown that metal concentration as low as fg/ml which increases the intracellular protein synthesis.[10] It has also been shown that the nanoparticles develop in a coat of silica, and a hypothesis has been proposed that all types of metal and inorganic salt based nanoparticles consist of silicate coated nanostructures dispersed in the solvent.[11] So the term potentisation proves the qualitative and quantitative increase in interactive power as compared to mere dilution. And thus, dilution is seen as nanomedicine.[12] The activity increases of the drug with potentisation arises as the surface area increases manifold and the number of points of contact with the living fibre increases. At the same time, the process of succussion is responsible decreasing the dimension of particles for inducing electrical nature due to domain formation as predicted by quantum electrodynamics (QED). Due to this, the physicochemical properties and aspects of the vehicle medium change severely, as the effect of QED starts playing a major role.[13-18] According to scientist Hahnemann, a small dose of nanoparticles, when potentized, is also very powerful due to the decrease of its size with increase in more contact area. This not only reduces the toxic effect of overdose but also forms intimate mixture of the medicine with the vehicle due to vigorous shaking. This is intended to avoid

aggravation of the disease and increase the activity of the nanoparticles as the medicine acts ‘not atomically but dynamically’. Dilution is necessary for getting the decrease of dimensional effect by succussion and that ‘all the shaking in the world will not dynamize an undiluted substance’. Thus, potentisation (dilution, followed by succussion) affects both the nanoparticles material of a medicine and the medium as follows: from classical point of view, due to succussion, the drug material achieves nanodimension and nanoparticles are formed. This reduces the toxic effect and increases the activity due to the increase in aspect ratio [4-8]. From quantum mechanical point of view, it changes the electrical nature of the polar medium through the formation of coherent domains of the solvent molecules, which provides quasi-free electrons and increases the stored electrical energy of the medium.[13-18] This establishes the electrical nature and the mode of action of medicinal value of the nanoparticles. Perhaps, this electrical energy which is stored in the system is the so called dynamic power of the nanoparticle medicine as envisaged by Dr. Hahnemann. The question then naturally arises is, as to how to compare the role of dilution and succussion in potentizing a medicine. In the present study, the experiment is conducted to observe and compare the effect of serial dilution and succussion to succussion alone using nanoparticle medicine, Cup. met. on the biological and physical systems, whereas in our earlier study,[7] the standard potentised Cup. met. has been used. This medicine is used because of its good dispersion in different polymers and good antibacterial and conductive properties which can be utilized as a dielectric charge separator in high charge storage system. In addition, the formation of the film using this polymer is an easy, low-cost and simple solution casting technique.

5.3 Methods

For both the biological and physical systems, we have used Cup. met. That the presence of the drug is responsible for the observed medicinal effect is justified as the vehicle medium of 91% ethanol had been evaporated in both cases within a very short span of time. Hence, the responsible particle is the drug only for the observed effects.

5.3.1 Preparation of the two sets of nanoparticle

The preparation of potencies with lactose in porcelain mortar and pestle of the two triturated samples as set A and set B a mechanical device manufactured by F. Kurt Retsch KG from Germany was used. When potentization is done in centesimal scale with ethyl alcohol each step was done manually using a new glass, termed as neutral (USP III) glass bottles. The whole operation was done following the Good Manufacturing Practice. To prepared potencies of Cup. met. pure copper powder was used, first by trituration with lactose up to 6X potency, converting the same into liquid 8X (=4C) potency and potentiating the 4C potency by dilution (with 91% ethanol) followed by succussion up to 6C potency. Here 6C potency was taken as the starting material for our study.[19] Set A: The potencies of Cup. met. were prepared in the method described in the medicinal Pharmacopoeia of India (HPI). The method tells us as one part of copper metal powder (99.6% pure) was triturated mechanically with 9 parts of 80 mesh lactose powder of pharmacopoeial (HPI, British Homeo Pharmacopeia [BHP] and United States Homoeopathic Pharmacopeia [HPUS]) quality for 1 h to produce 1X potency. The same 1X potency of Cup. met. was further triturated with lactose followed by same way and proportion to yield 2X potency. This following method of trituration was continued until we got 6X potency of Cup. met. having Single part by weight of this Cup. met. 6X was dissolved in 50 parts by

volume of purified water of HPI/BHP/HPUS standard to which 50 parts by volume of ethyl alcohol (91%) was added, and the solution mixture was given ten succussions to get 8X (=4C) potency. So potentisation was done by diluting one part of the previous potency with 99 parts of ethyl alcohol and giving the mixture ten succussions (shaking strongly with downwards stroke) always in a new glass bottle, one third volume of which was kept empty for proper shaking, to reach the next potency in centesimal scale. This process of serial dilution and succussion was carried out till 6C initially, as 6C is taken as the starting material in both the groups (Set A and Set B). In Set A: Serial dilution and succussion was carried out as stated above till 200C as per the standard method of potentisation. In Set B: Here starting from 6C potency, further potentisation was done without further dilution by succussing the 6C potency, making it equivalent to 30C and then further succussion to make it equivalent to 200C potency. Effects of these two sets of potentised medicines were compared for the antibacterial property on Gram-negative bacteria *Escherichia coli*[20] and on the electrical properties of a polymer matrix poly(vinylidene fluoride Cohexafluoropropylene) (PVDF-HFP).[21-24] The schematic diagram for the preparation of these two sets of medicine is shown in Fig.5.1.

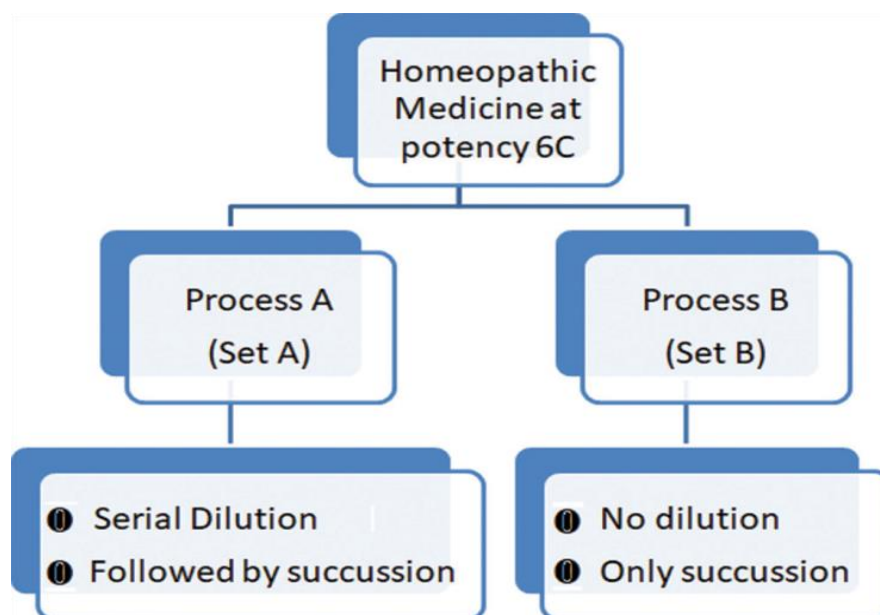


Figure 5.1. The two sets of potentisation: Set A and Set B.

5.3.2 Antibacterial effect of *Cuprum metallicum*

Set A and Set B of nanoparticles *Cup. met.* at required potency, prepared as in 91% alcohol was applied in freshly culture of *E. coli* in nutrient broth was treated and left overnight.[20] The alcohol was allowed to evaporate gradually. There was a chance of the bacteria being affected by the alcohol present in the medicine. However, this effect should be same for all the potencies of the medicine used. And hence, it was inferred that the final outcome was the effect of the potency of the medicine. The vehicle control was 91% alcohol. In order to make sure about the reproducibility, all the experiments with Set A and Set B at the potencies 6C, 30C and 200C were repeated at least 3–4 times.

5.3.3 Cuprum metallicum poly(vinylidene fluoride Cohexafluoropropylene) Composite film preparation technique

Polymer based nanocomposite was prepared by doping Cuprum metallicum were synthesized by simple solution casting fabrication technique. In a typical synthesis process, 100 mg of PVDF-HFP (Sigma Aldrich, USA, 3050 Spruce St., St. Louis, MO 63103, 400 Summit Drive, Burlington, MA 01803) was dissolved into 2 ml of dimethyl sulfoxide (Merck, India, 8th Floor, Godrej One, Pirojshanagar, Eastern Express Highway, Vikhroli (E) Mumbai-400079, India) and mixed together under vigorous stirring at 50°C for 4 h. Selected amount of freshly prepared Cup.met. at a specific potency was obtained from Hahnemann Publishing Company, India (Near Sealdah Fly over & Koley Market, Kolkata, West Bengal 700012), and was added to the above solution and stirred for another 2 h at 50°C. To complete removal of the air bubbles from the solutions whole mixture was sonicated three times for 10 min each at 50°C with 30 min of time interval.

Finally, composite films were obtained in clean dry Petri dishes by casting the whole mixture and solvent was evaporated in an oven at 80⁰ C for 24h. Then silver paste is coated in both sides of the composite films for electrical measurements.[21-24] The synthesised films had the thickness in the range 40-50µmeter

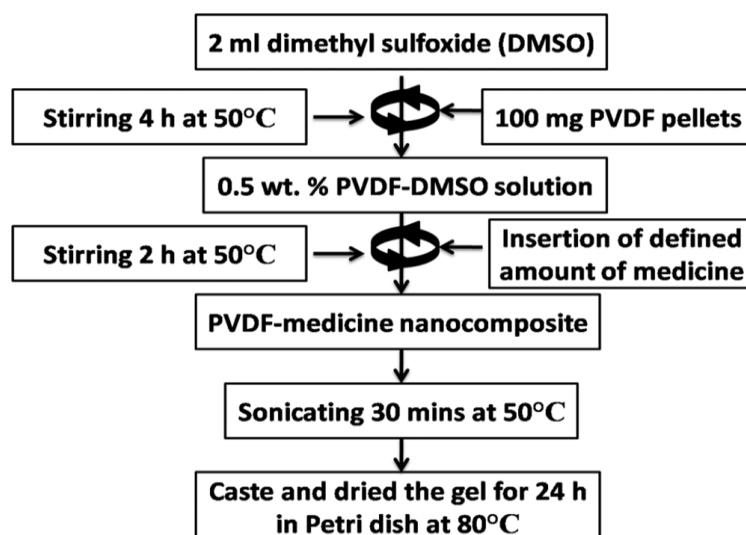


Figure 5.2 The schematic diagram for the preparation of Cup. met. poly (vinylidene fluoride co hexafluoropropylene) composite films.

5.4 Result

5.4.1 FESEM of SET A and SET B

Micro structural overview of pure Cup. met. at 200C as obtained from two different preparation

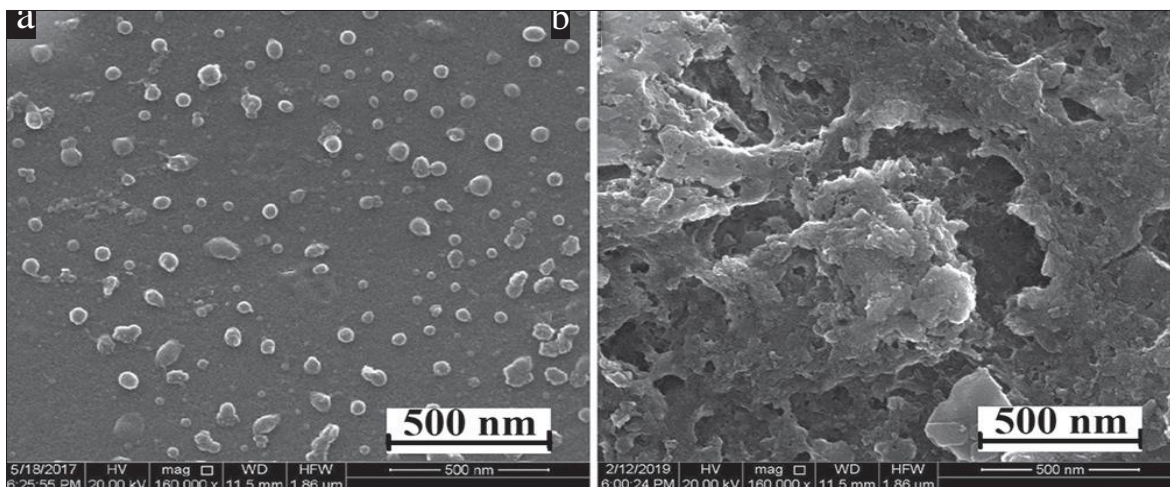


Figure 5.3 FESEM of Prestine Set-A and Set B

processes of Set A and Set B by field emission scanning electron microscope (FESEM) is shown in Figure 5.3. (a) and (b) respectively. Pristine 200C Cup. met. of Set A.[22] Figure 3a shows the microstructure and morphology of A very good and homogeneous distribution of the nanoparticles on the surface of the glass cover slip was confirmed by FESEM and the particles are more scattered, are well separated and also homogeneously distributed, maintaining an intermolecular distance. This is due to the very high dilution at 200C for the set A. In the dilute medium, particles are scattered in figure 3(a).

On the other hand, Figure 5.3(b) shows the microstructure and morphology, where only succussion is done without dilution. The morphology and microstructure of the sample confirmed an evidence of large number of densely packed agglomerated particles having high dimension embedded in the surface of the glass cover slip of the pristine 200C Cup. met. of Set B. However, in the absence of dilution, nanoparticles created due to succussion get agglomerated figure 5.3(b).

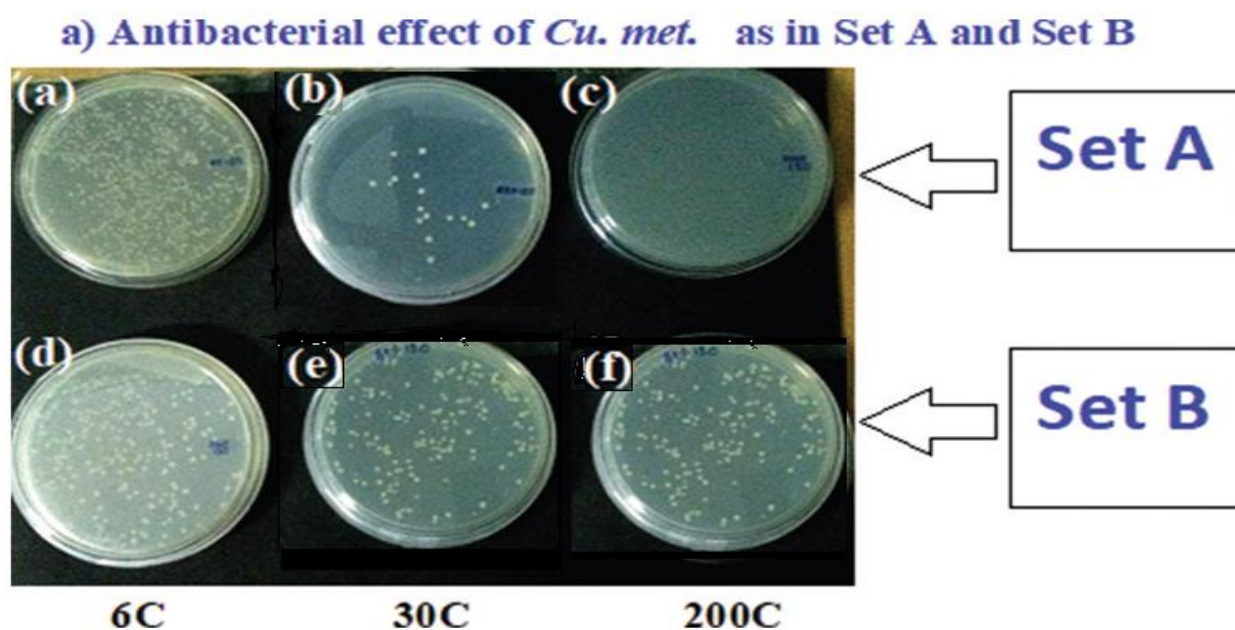


Figure 5.4 Antibacterial effect of Cup. met. for Set A (a) 6C, (b) 30C and (c) 200C and Set B (d)

6C, (e) 30C and (f) 200C

Here Set A shown in Figure 5.4a (6C), figure 5.4b (30C) and figure 5.4c (200C), the antibacterial effect is for the potentised medicine Cup. met. [20] Whereas figure 5.4d (6C), figure 5.4e (30C) and Figure 5.4f (200C) are for Set B of Cup. met. It is observed from the figure, that for Set A, the antibacterial effect is more for drug at 200C, compared to that for 30C and 6C.[20] The effect becomes more for drug at 200C for set A. In Set A of potency 200C there is no growth of bacteria. The reason is that smaller particle size with more interaction area perhaps as at higher potency and high dilution [8] and the penetration power through membrane barrier is more, that rise to higher antibacterial effect.[20] In Set B, as there is no dilution, the amount of drug available is same for all potencies from 6C to 200C, a larger number of agglomerated nanoparticles are produced which is observed in FESEM due to succussion and the antibacterial effect is less here for 30C and 200C compared to that in Set A. For Set B, at 200C, the figure 5.4(e) and (f) indicates that in the presence of significant number of drug molecules, which produced less membrane permeability or less contact area due to large number of nanoparticles are created through succussion, which agglomerate, which creates growth of bacteria as is evident from the FESEM, and are incapable to penetrate the bacterial membrane.

5.4.2 FESEM analysis of Antibacterial effect of Cuprum metallicum

Figure 5.5 FESEM images in (a-c) shows the evidence of densely packed and good homogenous dispersion of nanoparticles embedded in the polymer matrix. From the critical observation, it is observed that with higher potentisation, the polymer matrix had an increasing crystallization and reached maximum enhancement of electro active β -polymorph at 200C potency for the medicine of Set A. Figure 5.6(a) and (b) shows the evidence of significant

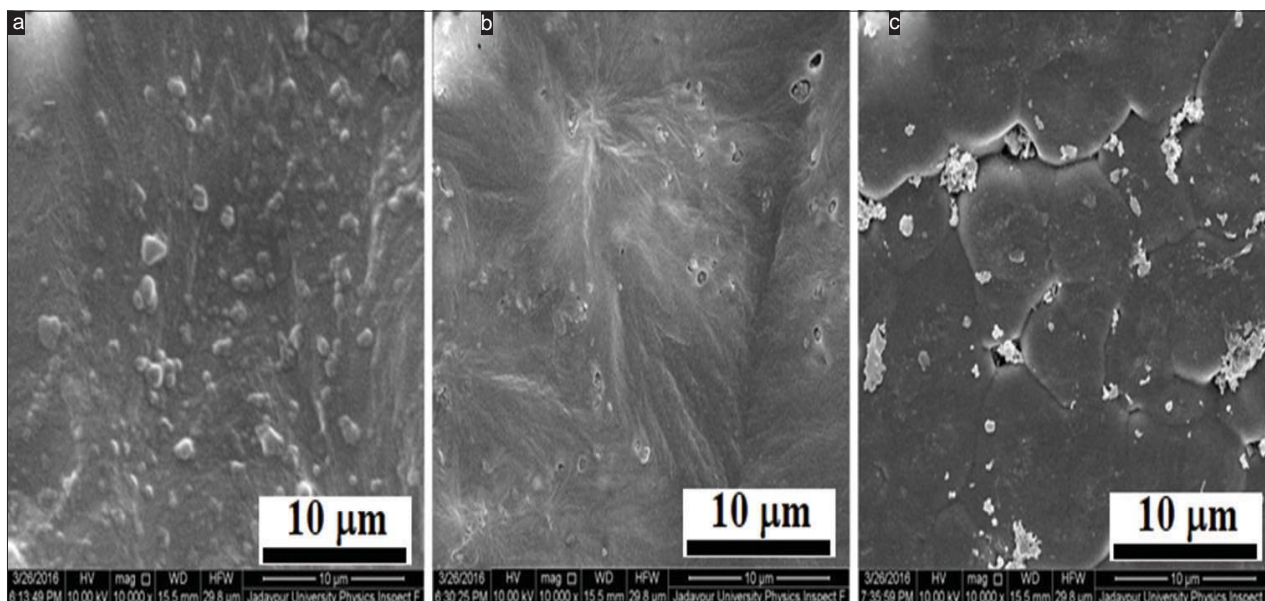


figure 5.5 Field emission scanning electron microscope micro structural overview for Set A of poly (vinylidene fluoride cohexafluoro propylene) doped Cuprum metallicum (a) 6C, (b) 30C and (c) 200C

number got agglomerated nanoparticles at higher potency of Set B and embedded in the PVDF-HFP matrix. This is due to the large number of succussions at 30C and 200C. Thus, from investigation through FESEM, it can be clearly concluded that, for the Set A medicine [dilution followed by succussion figure 5.5(a-c), there is no significant agglomeration perhaps very good dispersion and distribution due to high dilution of the medicine with high β phase formation, whereas for the Set B medicine without dilution, only succussion Figure 5.6 (a and b), there is agglomeration of embedded nanoparticles in the PVDF-HFP matrix, which results in less β -phase crystallisation.

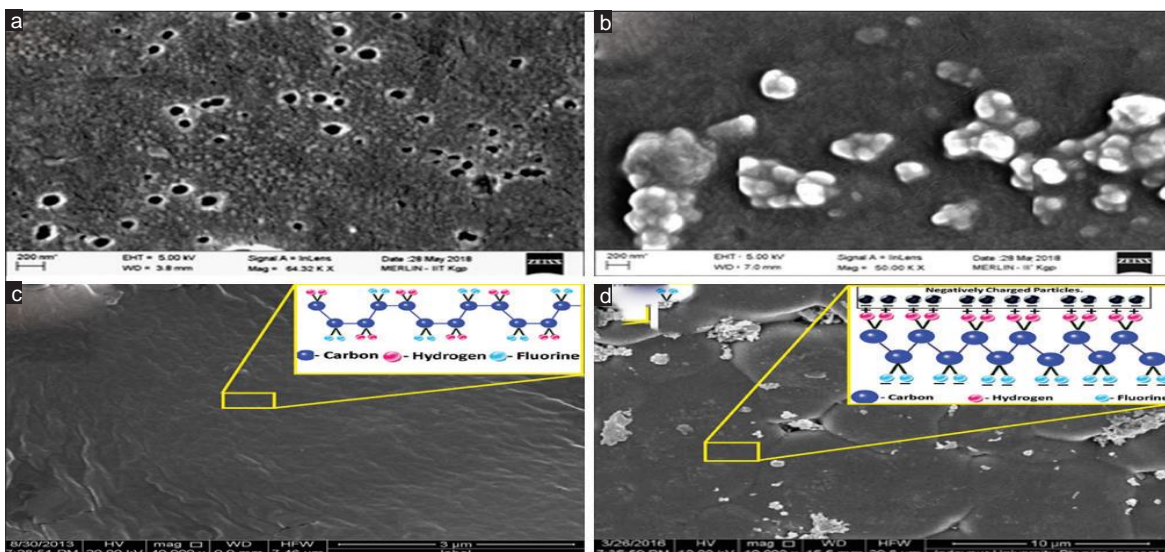


Figure 5.6 Field emission scanning electron microscope micro structural overview for Set B of PVDF-HFP doped Cup. met. (a) 30C, (b) 200C and (c) microstructure of PVDF-HFP doped Cup. met. of 200C and the crystal structure of β -polymorph (inset graph) and (d) microstructure of Cup. met. of 200C embedded PVDF-HFP and the crystal structure of β -polymorph (inset graph).[22]

The inset graph of Figure 5.6c shows the crystalline β polymorph where the oppositely charged hydrogen and fluorine dipoles are packed in anti parallel way with the carbon atoms, whereas the inset graph of Figure 5.6(d) shows the positively charged CH_2 dipoles of PVDF-HFP interacted with the negatively charged nanoparticles Cup.met, leading to the alignment of stabilized β chains which have been shown in the inset graph of Fig. 6(d) and Figure 5.(7).

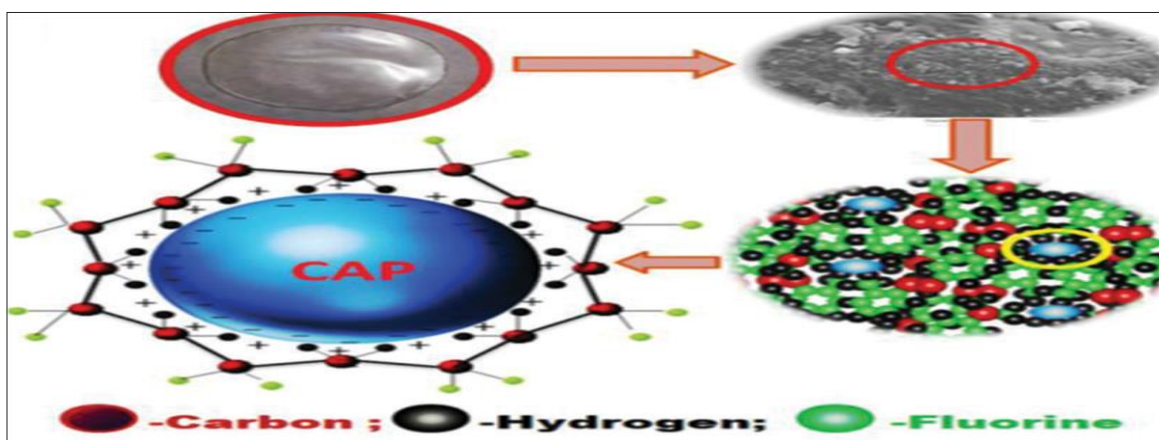


Figure 5.7 The schematic representation for nucleation of β polymorph in poly (vinylidene fluoride Cohexafluoropropylene).

Which was also explained by the theory of β phase nucleation in our previous publications.[22-24] Based on this theory, when the positively or negatively charged nanoparticles are added to the host solution, the opposite (partially negative CF_2 or positive CH_2) dipoles are oriented towards the surface of the nanoparticles, which perform as substrates for β phase nucleation. This mechanism leading to the alignment of stabilised PVDF-HFP chains in longer all trans conformation, results in electro active β phase.[23,24]

5.4.3 Measurement of electrical properties of polymer matrix: effect of potentized Cuprum metallicum in Set A and Set B

For Set A, Cup. met. enhances the more electro active β phase of the polymer matrix, at higher potency enhancing the conductivity and dielectric constant and decreasing the tangent loss of the medium.[21-25] In set B for the polymer matrix, when many more agglomerated nanoparticles are available for the presence of same number of particles for all potency the arrangement of the β polymorph in the matrix gets destroyed, which becomes less electro active and reaches a stable nature. Hence, the electrical properties like dielectric constant, ac conductivity and tangent loss cannot be further enhanced.

5.4.4 Frequency vs Dielectric Constant

Figure 5.8 (a) and (b) shows the variation of the dielectric constant of pure and the composite material as a function of frequency(Hz).[21-26] In Set A, the number of nanoparticles decreases with dilution and the size decreases with succussion.[8] Hence, the surface to volume ratio increases followed by particles are more scattered and well separated and also homogeneously distributed, maintaining an homogeneous intermolecular distance between the particles, which enhances the nucleation of β polymorph, resulting in very good dielectric performance.[21-25] shown in figure 5.8 (a)

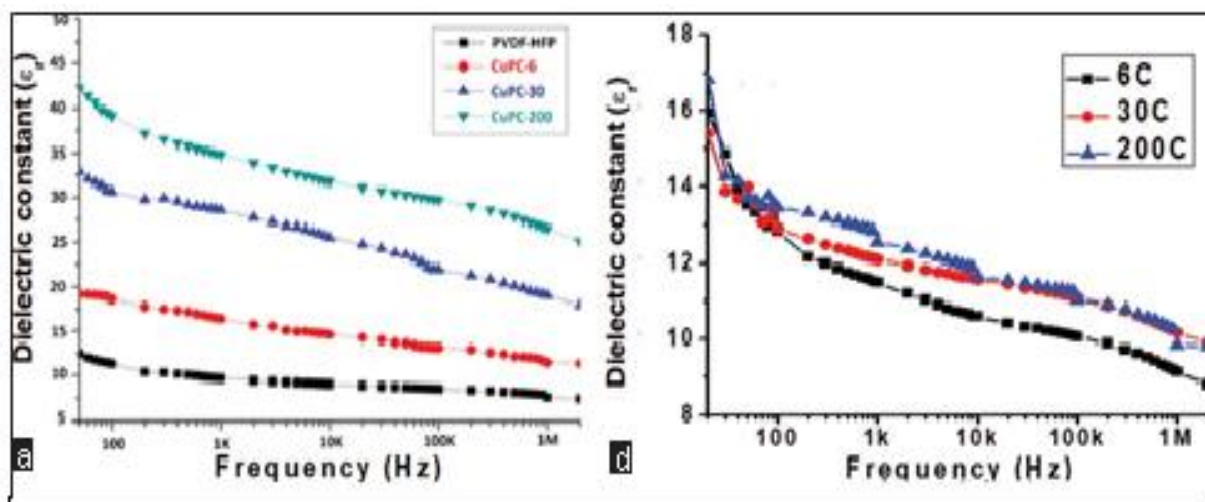


Figure 5.8. Frequency vs Dielectric Constant (a) of Set-A and (b) set-B.

In Set B, there is only succussion so the number of nanoparticles associates remains constant, but the size decreases with succussion but enhancing the agglomeration in the polymer matrix. Thus, the increasing encapsulation and agglomeration of the material will increase and the mobility of the particles will be inhibited, keeping the electrical properties unaltered.

Hence, the observed phenomena of these two set experiments using Set A and Set B on *E. coli* and polymer matrix have been quite interesting. The generation of larger number of

nanoparticles in Set B plays a major role and changes the usual pattern obtained with Set A. As in both the cases the solvent had been evaporated to dryness to make films, we can rule out the effect of vehicle medium on the observed phenomena. The presence of copper in the film had been verified earlier.[24,26] shown in figure 5.8.(b)

5.4.5 Frequency vs Tangent loss analysis

Figure 5.9 (a) shows as set-A, there are three potency 6C, 30C and 200C, all are succession with dilution and another set of same potency with only succession as set-B. In set A, 300C has the decreased size of the nanoparticle. At low frequency relaxation time is large, so there is a good interaction of nanoparticle with polymer matrix. So real dielectric constant is high and imaginary dielectric constant which is

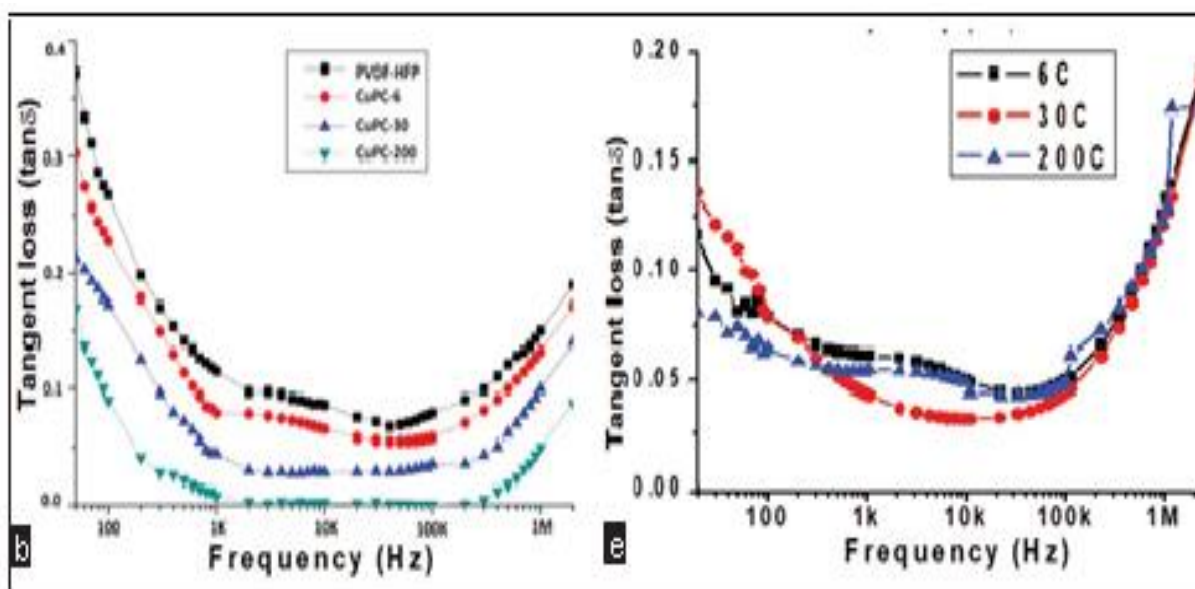


Figure 5.9. Frequency vs Tangent loss of (a) Set-A and (b) set-B.

Tangent loss is also high up to 1K Hz. After that tangent loss is constant from 1K to 100K Hz. due to small relaxation time. The nano particle cannot orient towards the polymer matrix so constant tangent loss. At this high frequency above 100K to 2 M Hz dipoles are in habitat to orient with the electric field as the relaxation time is small so poor interaction with polymer matrix but friction in individual poles and vibrations of poles produce high tangent loss. Figure 5.9.(b) the Set-B in the low frequency range relaxation time is high, so dipole orient towards the polymer matrix. So, large polarization is there and large tangent loss. In 1K to 100K frequency relaxation time is small, so real dielectric const is small and constant and tangent loss also small and constant. Above 100K Hz frequency will produce a high temperature due to destruction of percolative network individual poles of atoms start vibrate and friction among them will produce high tangent loss.

5.4.6 Frequency vs Electrical Conductivity

Due to the nature of particle size of higher potential in set A at low frequency due to space charge polarization and large relaxation time low ac conductivity observed, as frequency increases destruction of network and polarity of individual atoms will produce a conducting path which increases increase of ac conductivity.

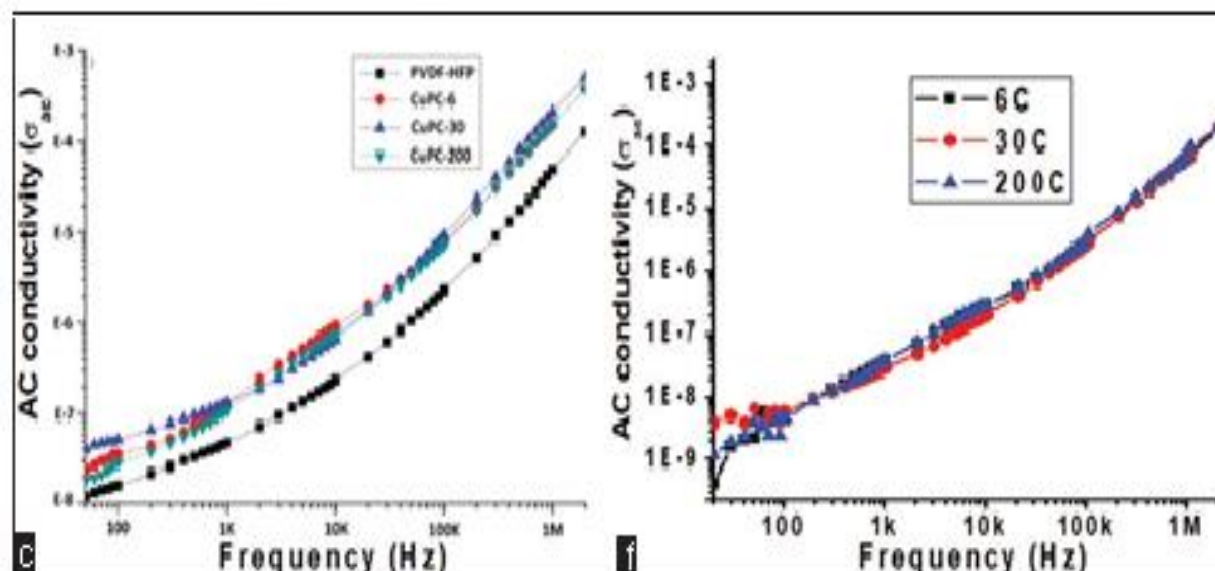


Figure 5.10. Frequency vs ac conductivity (a) of Set-A and (b) set-B.

Similarly, in set B low frequency shows low ac conductivity as high relaxation time. As frequency increases individual pole of the atom will produce a conducting path which enhance the ac conductivity.

5.5 Conclusions

The interesting difference between the two results of two set of samples gives an indication about the role of dilution and succussion in the process of potentisation of nanoparticle medicines and their effect on the biological and physical systems. Our experimental observed results show that the nanoparticles drug Cup. met., potentized by serial dilution, followed by succussion, can produce significant effect on both bacterial system to decrease the growth of bacterial system and enhancement of electrical properties polymer matrix. However, by increasing the potency by succussion only, a large number of homogeneously distributed, well dispersed nanoparticles are created which produce significant change in higher potencies, monitoring the effect of the medicine in both biological and physical systems. Due to proximity,

these nanoparticles may agglomerate again to make bigger particles. Thus, while succussions are necessary for the potentisation, the role of dilution seems equally important. Further experimentations are required using different drugs to identify the appropriate and most effective way of the degree of dilutions i.e., the critical level of dilution. We would like to mention here that to the best of our knowledge, this experiment is the first of its kind to find out the role of succussion and dilution to potencies the starting material to a therapeutically active one.

Reference

- [1] Hahnemann S. Organon of Medicine. Boericke and Tafel: Philadelphia; 1901.
- [2] Available from: <https://www.hindustantimes.com/india/homeopathy-astrology-are-bogus-says-nobel-laureate-venkatraman-ramakrishna/story-on-NzWBnosMFiLnrnmfkdxI.html>. [Last accessed on 2016 Jan 07].
- [3] Adams G. "Potentisation and the peripheral forces of nature". Br Homoeopath J 1989; 78:69-79.
- [4] Shah R. "Standardization of the potentizing machine and quantification of impact of potentization". Indian J Res Homoeopathy 2016; 10:126-32.
- [5] Nandy P, Bhandary S, Das S, Basu R, Bhattacharya S. "Nanoparticles and membrane anisotropy". Homeopathy 2011; 100:194.
- [6] Nandy P. "A review article of basic research on homoeopathy from a physicist's point of view". Indian J Res Homoeopathy 2015; 9:141-51.
- [7] Ghosh S, Chakraborty M, Das S, Basu R, Nandy P. "Effect of different potencies of nano medicine Cuprum metallicum on membrane fluidity: A biophysical study". Am J Homeopathic Med 2014; 107:161-9.

- [8] Kar S, Bandyopadhyay P, Chakraborty S, Chakrabarty M, Ghosh S, Basu R, et al. “Derivation of an empirical relation between the size of the nanoparticle and the potency of homeopathic medicines”. *Int J High Dilution Res* 2015;4:2-7.
- [9] Chikramane PS, Suresh AK, Bellare JR, Kane SG. “Extreme homeopathic dilutions retain starting materials: A nanoparticulate perspective”. *Homeopathy* 2010; 99:231-42.
- [10] Chikramane PS, Suresh AK, Kane SG, Bellare JR. “Metal nanoparticle induced hormetic activation: A novel mechanism of homeopathic medicines”. *Homeopathy* 2017; 106:135-44.
- [11] Temgire MK, Suresh AK, Kane SG, Bellare JR. “Establishing the interfacial nanostructure and elemental composition of homeopathic medicines based on inorganic salts: A scientific approach”. *Homeopathy* 2016; 105:160-72.
- [12] Rajendran ES. “Homeopathy seen as personalized nanomedicine. *Homeopathy*” 2019; 108:66-70.
- [13] Bandyopadhyay P, Bera D, Das K, Paul BK, Das S, Bhar DS, et al. “Vigorous shaking enhances voltage and power generation in polar liquids due to domain formation, as predicted by QED”. *Water* 2017; 8:172-82.
- [14] Nandy P, Das K, Bandyopadhyay P, Paul BK, Bhar DS, Das S, et al. “Extraction of electrical energy from alcohol and bi-distilled water separated by a platinum foil – AQED Effect”. *Energ Educ Sci Tech Part A Energ Sci Res* 2017;35:285-90.
- [15] Yinnon TA, Liu ZQ. “Domains formation mediated by electromagnetic fields in very dilute aqueous solutions: Quantum electrodynamic aspects”. *Water* 2015; 7:33-47.
- [16] Yinnon TA, Elia V. “Dynamics perturbed very diluted aqueous solutions: Theory and experimental evidence”. *Int J Mod Phys* 2013; 27:1350005-40.
- [17] Ho MW. Large Supra molecular water cluster caught in camera – A review. *Water* 2014;

6:1-12.

[18] Bhattacharya TS, Maitra P, Bera D, Das K, Bandyopadhyay P, Das S, et al. “Investigation of the origin of voltage generation in poetized homeopathic medicine through Raman spectroscopy”. Homeopathy 2019; 108:121-7.

[19] Homeopathic Pharmacopoeia of India. Ministry of Health. Govt of India. Available from: <https://www.nhp.gov.in/HomeopathicPharacopeia> of India (HPL).mtl. [Last accessed on 2017 Dec 10].

[20] Chakraborty M, Das S, Manchanda RK, Basu R, Nandy P. “Application of nanomedicine cuprum metallicum as an agent for remediation of an azo dye methyl orange and study its associated antimicrobial activity environment”. sci 2015;6:345-351

[21] Chatterjee A, Paul BK, Kar S, Das S, Basu R, Bhar DS, et al. “Effect of ultrahigh diluted homeopathic nanomedicines on the electrical properties of PVDF-HFP”. Int High Dilution Research 2016; 15:10-7.

[22] Gayen AL, Mondal D, Paul BK, Roy D, Bandyopadhyay P, Manna S, et al. “Improvisation of electrical properties of PVDF-HFP: use of novel metallic nanoparticles”. J Mater Sci 2017; 28:14798-808.

[23] Gayen A, Mondal D, Bandyopadhyay P, Bera D, Bhar DS, Das S, et al. “Effect of homeopathic dilutions of Cuprum arsenicosum on the electrical properties of poly (vinylidene fluoride co hexa fluoro propylene)”. Homeopathy 2018; 107:130-6.

[24] Mondal D, Gayen AL, Paul BK, Bandyopadhyay P, Bera D, Bhar DS, et al. “Enhancement of β -phase crystallization and electrical properties of PVDF by impregnating ultra high diluted novel metal derived nanoparticles: prospect of use as a charge storing devices”. J Mater Sci 2018; 28:14535-45.

- [25] Paul BK, Kar S, Bandyopadhyay P, Basu R, Das S, Bhar DS, et al. “Significant enhancement of dielectric and conducting properties of electro active polymer poly vinylidene fluoride films: An innovative use of Ferrum metallicum at different concentrations”. Indian J Res Homoeopathy 2016; 10:52-7.
- [26] Mondal D, Gayen AL, Paul BK, Bhar DS, Das K, Nandy P, et al. “Colossal dielectric response of PVDF-HFP amalgamated ultra low dense metal derived nanoparticles: Frontier of an excellent charge separator”. J Electron Mater 2019; 48:5570-80

Chapter 06

Summery

6.1 General Conclusions

In my research work, I have emphasized the research avenues to explore various materials with enhanced electrical properties and their wide range application in diverse fields of science and technology to mitigate the global needs in terms of energy harvesting and its storage. Therefore, our aim of this work is to find out a family of materials which can allow the sufficient doping of necessary elements inside the host material with proper regulation for manipulation of its characteristics, engineering the defects and tuning the morphology along with the particles size for achieving promising material candidates with advance properties.

For proposing new materials with enhanced properties with diverse applications, the priority has been given on several properties of the materials, like - high dielectric constant, easy ion diffusion ability, high specific capacitance, low tangent loss factor, high porosity as well as bio-compatibility. Based on availability, moderate conductivity, toxicity, cost and applicability in industry. Among the transitional metal nanoparticle, Copper (Cu), Arsenicosum (As) and Cobalt (Co) and other materials are of special interest among the scientific community. All crystallographic polymorphs of Cu, As and Co have been used as multifunctional materials as the β phase with different concentration of all those metal nanoparticles has established the potentiality in diverse fields due to its structural advantages as well as biocompatibility in nature. Also, the dilution effect and mechanical impulses through succession facilitate for formation of electro active composite materials. The host polymer matrix and its dipole structure are supportive for sufficient doping inside the structure by the interactions between matrix and metal nanoparticles. In our work, the efficiency of the metal nanoparticles doped polymer composite has been improved by using several techniques like reduction of particle's dimension, impregnating transitional polymer matrix by tuning its structure. Based on our applications, the

surface to volume ratio has been enhanced dramatically by transiting the dimension of the particles from bulk to nano regime. Here, we have adopted a novel approach to synthesize the high temperature sustainable β phase of Cu, Co and As nanoparticle which enabled them as the most promising doping candidates to make nano dimensional advanced materials for electronic, electrical and optoelectronic industrial applications.

The metal nanocomposites with stepwise increase of concentration of metal-nanoparticles in polymer matrix leads showed increment in both α -phase and β -phase and conglomeration nanoparticles was occurred at higher concentration that was confirmed by the microstructure analysis of metal nanoparticle doped composites. The dielectric constant of metal nanocomposites was enhanced than that of pure polymer throughout a wide band of frequency and it became highest value at a specific concentration (0.5) of nanoparticles. The optimum conformation of α and β phases were attained at this concentration. The tangent loss of nanomaterial doped composites was less in comparable to that of pure polymer in the frequency band 20 Hz to 10kHz and this loss also became its lowest value for nanoparticles of 0.5 concentration. The AC conductivity of nanocomposites was also higher than that of pure matrix.

Hence, pure polymer with comparatively low dielectric constant were improved by doping with metal nanoparticles in various concentrations where tangent loss was less. So, by doping a specific concentration of metal nanoparticles, these nanocomposites films have shown a notable enhancements in their electrical properties and the nanometal doped composites may be used as potential candidates for designing devices with higher efficiency for energy harvesting and storage storage.

6.2 Future Prospect

In recent time, sources of emitting radiation are increasing day by day. These radiations are so much dangerous that they can cause severe damage to our lives and also to nature. My intention is to fabricate a device which can entirely shield the external radiation. Some electronic devices work on specific frequency range. If we are able to fabricate such device which can pass the selective frequency range, then it will be more beneficial to active the device as well as protect us from the radiation emitted by the devices. Also, the modification in supercapacitor, parallel plate capacitor performance will be progressively revised by optimizing the influencing several parameters. This type of supercapacitor needs a power source to charge up it but if it has the ability to harvest the energy from environment by itself then the self charging power cell (SCPC) will be more promising non conventional energy device. Present time, solar cell based non conventional energy harvesters are the most useful energy sources. The hybrid solar cell based self charging power cell will have a combination of two completely different technologies like energy harvester and energy storage in a single device. Some environment related issues like sensitivity to humidity, long term light soaking, sunshine irradiation and induced temperature rise also will be taken into consideration in our fabrication of new devices.

Enhanced dielectric properties and conductivity of triturated copper and cobalt nanoparticles-doped PVDF-HFP film and their possible use in electronic industry

A. L. Gayen, B. K. Paul, D. Roy, S. Kar, P. Bandyopadhyay, R. Basu, S. Das, D. S. Bhar, R. K. Manchanda, A. K. Khurana, D. Nayak & P. Nandy

To cite this article: A. L. Gayen, B. K. Paul, D. Roy, S. Kar, P. Bandyopadhyay, R. Basu, S. Das, D. S. Bhar, R. K. Manchanda, A. K. Khurana, D. Nayak & P. Nandy (2016): Enhanced dielectric properties and conductivity of triturated copper and cobalt nanoparticles-doped PVDF-HFP film and their possible use in electronic industry, Materials Research Innovations, DOI: [10.1080/14328917.2016.1196563](https://doi.org/10.1080/14328917.2016.1196563)

To link to this article: <http://dx.doi.org/10.1080/14328917.2016.1196563>



Published online: 17 Jun 2016.



Submit your article to this journal [↗](#)



Article views: 4



View related articles [↗](#)



View Crossmark data [↗](#)

Enhanced dielectric properties and conductivity of triturated copper and cobalt nanoparticles-doped PVDF-HFP film and their possible use in electronic industry

A. L. Gayen¹, B. K. Paul^{1,2}, D. Roy², S. Kar^{1,2}, P. Bandyopadhyay^{1,2}, R. Basu^{2,3}, S. Das^{1,2,4}, D. S. Bhar², R. K. Manchanda⁵, A. K. Khurana⁵, D. Nayak⁵ and P. Nandy^{*2}

We have synthesised a novel nanocomposite film by incorporating copper and cobalt nanoparticles, prepared by the method of trituration, in the poly(vinylidene fluoride-co-hexafluoropropylene) (PVDF-HFP) films by simple solution-casting technique. Fourier transform infrared spectroscopy (FTIR) study of these nanocomposite films detected presence of α - and β -phases. Scanning electron micrographs showed spherulitic crystal structure of PVDF-HFP in the nanocomposite film and study of dielectric properties over broadband frequency of these doped nanocomposite film showed that these films have higher dielectric permittivity and significantly lower dissipation factor ($\tan\delta$) at room temperature compared to the pure PVDF-HFP. The incorporation of metallic nanoparticles in the polymer matrix activates the transition of phase between α and β and provides the nanocomposites higher mobile charge carriers which participate in the interfacial polarisation. The room temperature dielectric constant of the pure PVDF-HFP at 20 Hz frequency increases with increase in concentration of the metal nanoparticles and reaches a maximum almost four times the value of the pure one. At higher concentrations, the effect reduces, perhaps due to agglomeration of the nanoparticles. The metal nanoparticles, obtained by the method of trituration, are inexpensive, easy to fabricate and environment friendly. Thus, their incorporation in polymer matrix to get enhanced electrical properties will have a significant contribution to the present day research.

Keywords: PVDF-HFP, Triturated nanoparticles, Dielectric constant, Tangent loss, AC conductivity, Capacitor

Introduction

Poly(vinylidene fluoride) P(VDF) and its copolymers like poly(vinylidene fluoride-hexa-fluoropropylene P(VDF-HFP) are in great demand for their versatile and unique properties like flexibility, low processing temperature, low dielectric constant, high dielectric breakdown field, etc. making them potential candidate for a broad range of applications in electronic industry.^{1–3}

In order to improve the capacitive performance of the polymer material, incorporation of metal nanoparticles in the polymer matrix has received great attention. Here, the uniform and homogeneous distribution of the nanoparticles allows good interaction between them and the polymer matrix material and enhances the electrical properties of the host material.^{4–7}

In this endeavour, a great deal of effort had been devoted to develop PVDF-HFP composites by incorporating different metallic nanoparticles within the matrix. The effective dielectric permittivity of these metal nanoparticle-doped polymer composites are higher than that of the host polymer matrix. They also show enhancement of conductivity and decrement of tangent loss making them potential candidates as good capacitors and electric energy storage devices.^{8–15}

In this work, we have prepared copper (CuM) and cobalt (CoM) nanoparticles by the method of trituration.¹⁶ The great advantage of this method is that as the metal nanoparticles, prepared by the method of trituration, can be dissolved in a polar solvent, it can be mixed directly with the dissolved polymer and dried to form the film of homogeneous dispersion of NP in the polymer matrix. Another benefit of the method of trituration is that the size of the particles can be regulated by vigorous shaking prior to mixing with the polymer solution. These are very novel and unique metallic fillers, which are nontoxic, inexpensive and are easily available. They are used as homeopathic medicines, which affect the membrane permeability¹⁷ and their nanoparticle aspect has been proved experimentally.^{18–20}

¹Department of Physics, Jadavpur University, Kolkata 700032, India

²Centre for Interdisciplinary Research and Education, Kolkata 700 068, India

³Department of Physics, Jogamaya Devi College, Kolkata 700026, India

⁴Department of Physics, Indian Institute of Engineering Science and Technology, Shibpur, India

⁵Central Council for Research in Homeopathy, New Delhi, India

*Corresponding author, email ciresedu@yahoo.in

The metal nanoparticles were incorporated in the films PVDF-HFP and dimethyl sulphoxide, by simple solution-casting technique for different nanoparticle concentrations. These nanocomposites of PVDF-HFP/CuM (CuPC) and PVDF/CoM (CoPC) were studied by FTIR, FESEM and dielectric analysis. The presence of α - and β - phases, formation of spherulites, enhancement of dielectric constant and conductivity and decrease in tangent loss of the nanocomposite films were observed by changing the concentration of CoM and CuM and the observed values were compared with the pure PVDF-HFP film.

Utilising these eco-friendly, inexpensive metallic fillers to enhance the electrical properties of polymer film is of great importance when electroactive polymer films are gaining worldwide attention for their use in electronic industry.

Materials and methods

The materials used in the synthesis of metal-doped polymers are PVDF-HFP (Sigma Aldrich, USA.) and dimethyl sulphoxide (DMSO) (Merck, India). Freshly prepared trituated metal nanoparticles, Copper (CuM) and Cobalt (CoM) were obtained from Hahnemann Publishing Company, India.

The metal-doped nanocomposites, CuPC and CoPC, were synthesised by solution-casting method. In a typical synthesis, 100 mg of PVDF-HFP was added to 2 ml of DMSO and mixed together under vigorous stirring at 60 °C for 3 h. Measured amounts of CuM and CoM were added to the solution. CuPC and CoPC were obtained by casting the whole mixture in clean dry Petri dishes and evaporating the solvent in an incubated oven at 60 °C for 12 h. As DMSO cannot be totally removed, we did all our measurements with the residual DMSO. The films were then coated by silver paste on both sides for electrical measurements. The synthesised films had the thickness in the range of 40–60 μ m as measured using a digital screw gauge.^{11,15,21}

Sample details

For CuPC

- 100 mg PVDF-HFP + 2 ml DMSO + No metal nanoparticle (PVDF-HFP).
- 100 mg PVDF-HFP + 2 ml DMSO + 0.2 ml CuM (0.2 CuPC).
- 100 mg PVDF-HFP + 2 ml DMSO + 0.5 ml CuM (0.5 CuPC).
- 100 mg PVDF-HFP + 2 ml DMSO + 1.0 ml CuM (1.0 CuPC).
- 100 mg PVDF-HFP + 2 ml DMSO + 2.0 ml CuM (2.0 CuPC).

For CoPC

- 100 mg PVDF-HFP + 2 ml DMSO + No metal nanoparticle (PVDF-HFP).
- 100 mg PVDF-HFP + 2 ml DMSO + 0.2 ml CoM (0.2 CoPC).
- 100 mg PVDF-HFP + 2 ml DMSO + 0.5 ml CoM (0.5 CoPC).
- 100 mg PVDF-HFP + 2 ml DMSO + 1.0 ml CoM (1.0 CoPC).
- 100 mg PVDF-HFP + 2 ml DMSO + 2.0 ml CoM (2.0 CoPC).

Instrumentation

The characteristic stretching and bending modes of vibration of chemical bonds of these samples were effectively evaluated

by Fourier transform infrared spectroscopy ([FTIR]-8400S, Shimadzu). Dielectric measurements of these films were carried out by an electrometer (HP Model 4274 A, Hewlett-Packard, USA). Electrical properties such as dielectric permittivity (ϵ_r), dissipation factor ($\tan \delta$) and AC conductivity (σ_{AC}) of all samples were measured in the frequency range of 20 Hz to 2.0 MHz using LCR meter (HP Model 4274 A, Hewlett-Packard, USA). Field-emission scanning electron microscopy (FESEM) was done using INSPECT F50 SEM, FEI Europe BV. The operating conditions are mentioned in the FESEM images as follows: HV 20.00 kV, mag 5000 \times , WD 10.9 mm, and HFW 59.7 μ m. Sample preparation was done using turbo-pumped sputter coater EMS 150TS and was used for gold coating.

Results and discussion

Fourier transform infrared spectroscopy analysis

The FTIR spectra of all nanocomposite films show characteristic absorbance bands ~490, ~530, ~613, ~763, ~795 and ~975 cm^{-1} corresponding to the α -phase and around 480, 510, 600 and 839 cm^{-1} corresponding to the β -phase.^{11,15,20} The spectra indicate that there is no phase shift or chemical interaction between the metal nanoparticles and the polymer film, but the intensity of α - and β -phases changes with the concentration of doping material (Fig. 1(a) and (b)).

Field-emission scanning electron microscopy

Figure 2(a–c) shows the morphology and microstructures of nanocomposite samples loaded with CuM nanoparticles at different concentrations. In Fig. 2(a) and (b), the particles are more scattered, whereas Fig. 2(c) shows the evidence of large number of agglomerated particles embedded in the polymer matrix.

Similarly, Fig. 2(d–f) shows the morphology and microstructures of nanocomposite samples loaded with CoM nanoparticles at different concentrations. In Fig. 2(d) and (e), the particles are more scattered, whereas Fig. 2(f) shows the evidence of large number of agglomerated particles embedded in the polymer matrix.^{11–15,21,23–25}

Evidence for the inclusion of Cu and Co in the polymer was not very conclusive as the samples were of extreme dilution and the presence of the particles was difficult to detect.

However, the presence of particles (Cu or Co) in growing numbers is evident from the fact that their number density increased with higher concentration (Fig. 2).

Dielectric constant measurements

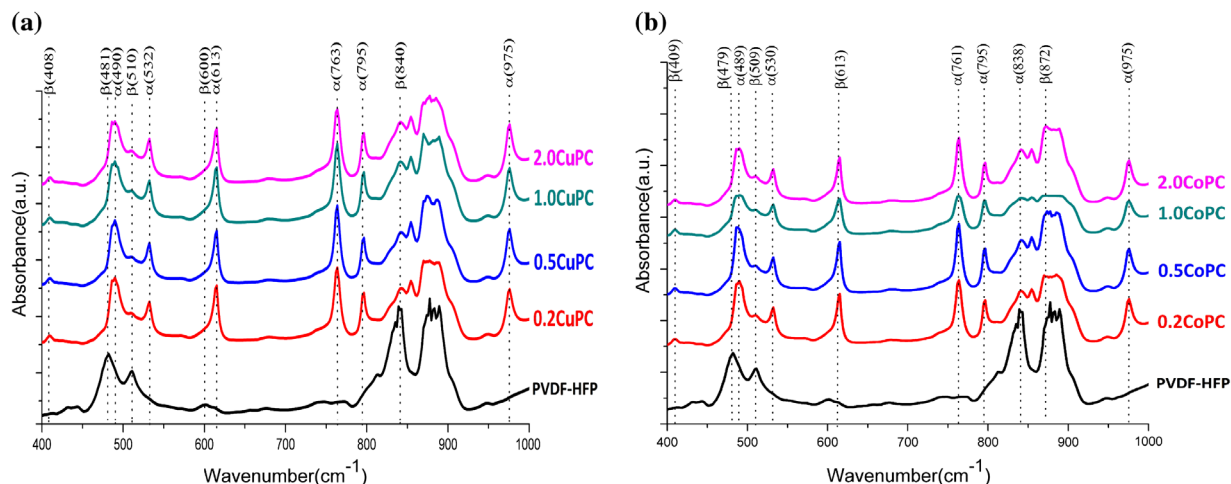
The dielectric constant (ϵ_r) of each sample was calculated using the formula,

$$\epsilon_r = (Cp \times d)/A\epsilon_0,$$

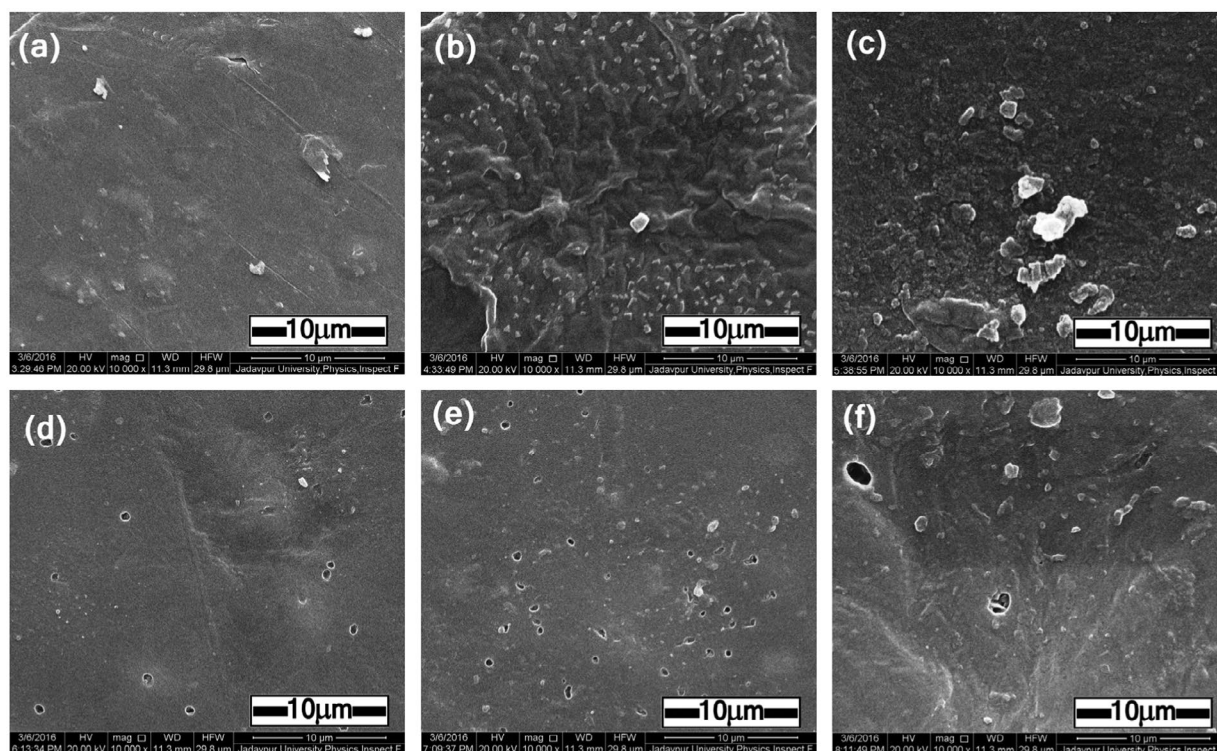
where ϵ_r , Cp, d, A and ϵ_0 are the dielectric constant of the material, capacitance, thickness of the film, area of cross section and permittivity of free space, respectively.

Effect of frequency on dielectric constant of the nanocomposite films

From Fig. 3, it is seen that within the frequency range 20 Hz to 2 MHz, dielectric constants of the films decrease continuously



1 a and b Fourier transform infrared spectra of CuPC and CoPC for all concentrations



2 Field-emission scanning electron micrograph of a 0.2CuPC, b 0.5CuPC, c 2CuPC, d 0.2CoPC, e 0.5CoPC and f 2CoPC films

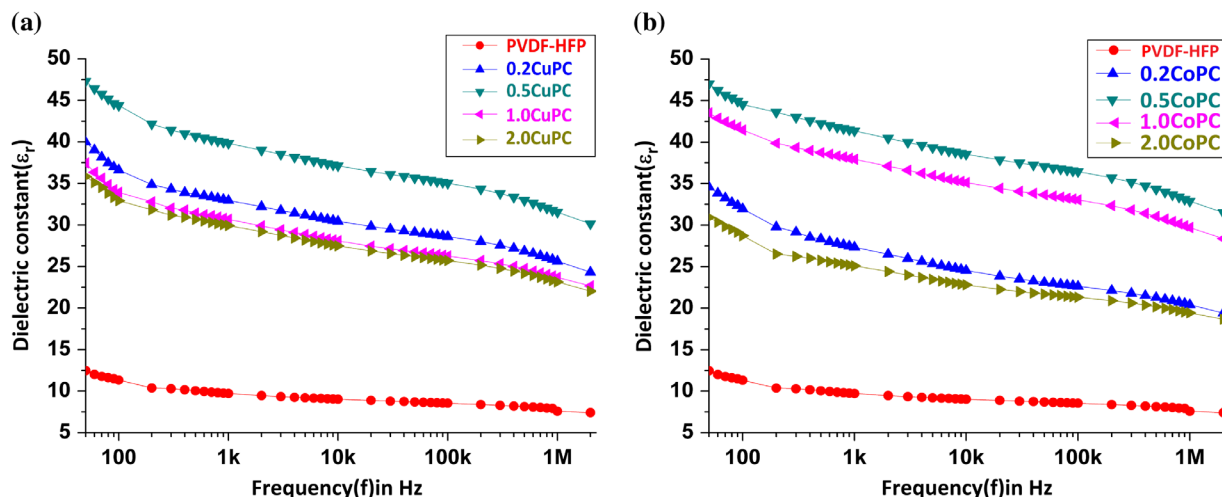
with increasing frequency for all concentrations of the metal nanoparticles up to 200 Hz and after that the rate of decrease slows down.

Enhancement of dielectric constant at lower frequency may be explained from interfacial polarisation which occurred in the interfaces between insulators (e.g. PVDF-HFP) and the conducting materials (e.g. CuM/CoM). This effect overrules the effect of orientation of dipoles at lower frequency. As the frequency is increased further, dipole response is restricted and the dielectric constant has a saturation tendency.^{21,22} In this case, the internal individual dipoles contribute to the dielectric constant which is ideally the electronic polarisation effect.^{11,15,23–26}

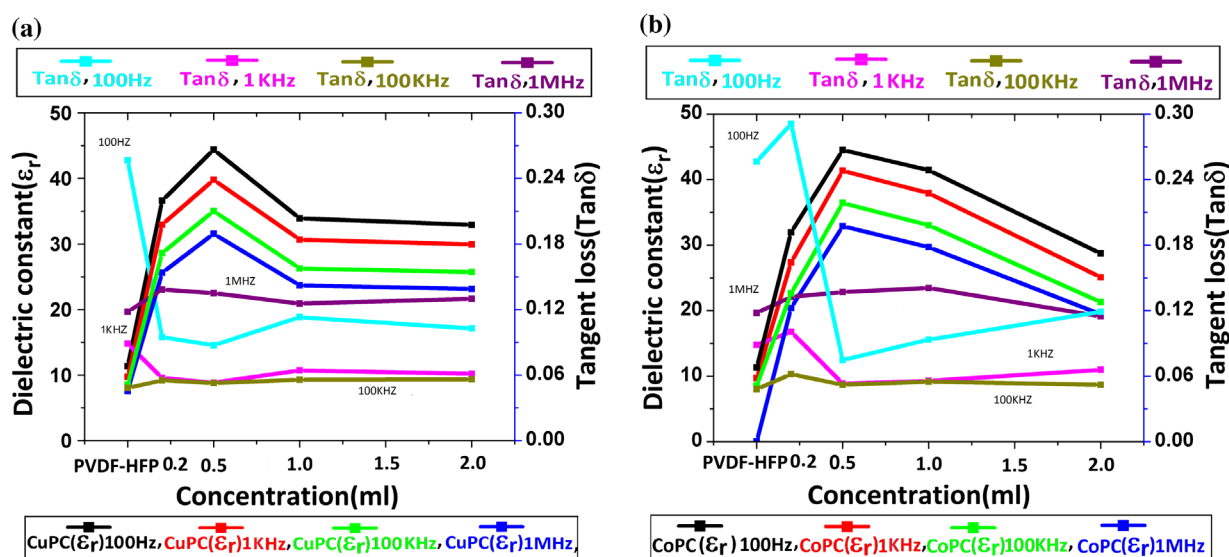
Effect of NP concentration on dielectric constant of the nanocomposite films

The variation of dielectric constant of all nanocomposite films for different concentrations of the metal NPs is shown in Fig. 4. It is clearly seen that dielectric constant has substantially higher values in case of all nanocomposite films compared to the pure polymer film. The value increases with concentration up to a critical value of 0.5 ml of CuM/CoM added in the polymer film, after which the value decreases.

The observed modification of dielectric properties of the composite with change in concentration of the dopant NPs can be explained from Maxwell–Wagner–Sillars interfacial



3 a and b Frequency-dependent dielectric constant (ϵ_r) of CuPC and CoPC for all concentrations



4 a and b Concentration-dependent dielectric constant (ϵ_r) and tangent loss ($\tan\delta$) of CuPC and CoPC for constant frequencies

polarisation effect, which occurs due to accumulation of charges at the interfaces in the inhomogeneous medium consisting of different phases with different permittivity and conductivity which in this case is PVDF-HFP, an insulator and CuM/CoM, a conducting material.²⁷

Initially with increase in NP concentration, the number, as well as the interfacial area per unit volume, increased with a consequent decrease in the interparticle distance. This improved the average polarisation and the coupling between the neighbouring sub-phases and is then reflected in the increase in the value of dielectric constant.

However, with further increase in doping concentration, the interfacing area per unit volume decreased owing to agglomeration of the NPs (Fig. 2 FESEM image), as a result of which the dielectric constant decreased.

Tangent loss measurement

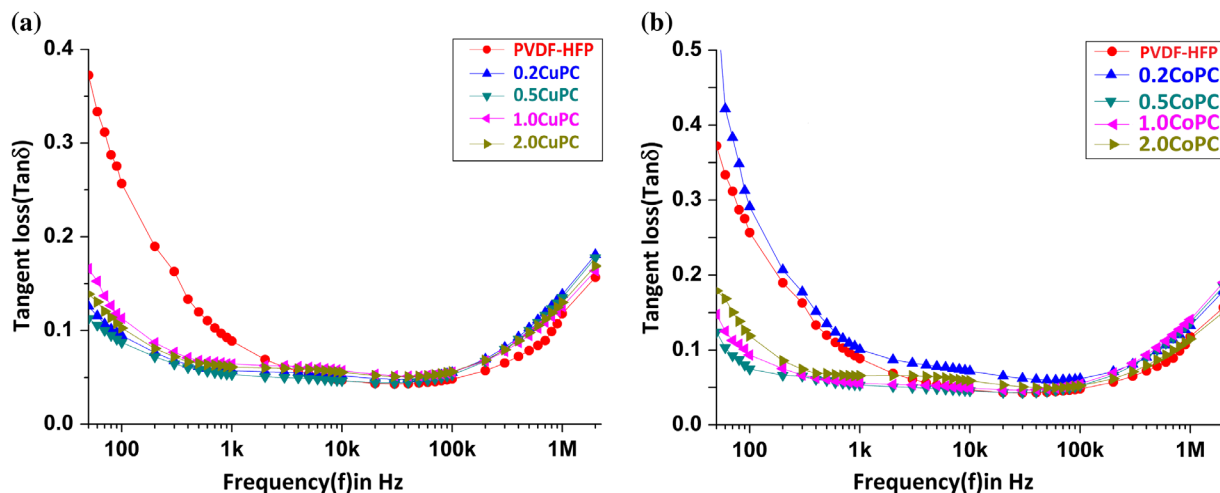
The tangent loss ($\tan\delta$) of a medium includes dielectric damping loss and conductivity loss of the material and is the ratio of conduction current and displacement current.

$$\tan\delta = \sigma_{ac} / (2\pi f \epsilon_r \epsilon_o)$$

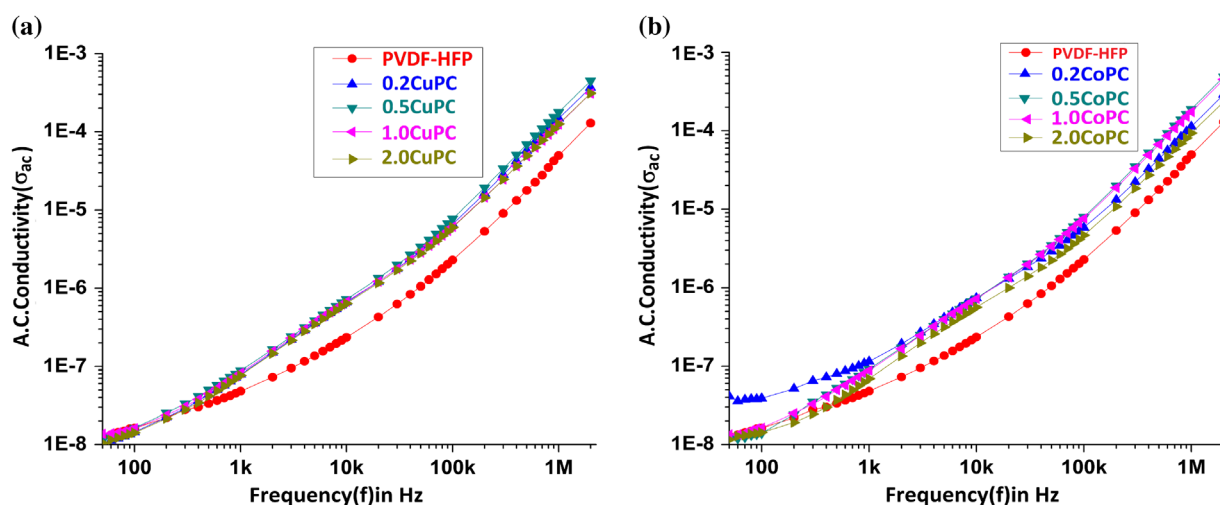
From Fig. 5, it is clearly seen that throughout the frequency range, tangent loss continuously decreases exponentially with increasing frequency for all nanocomposite films up to 10 kHz. At comparatively lower frequency range, the dipoles can orient easily with external electric field. This phenomenon is mainly responsible for intermolecular friction or vibration, which contributes to the exponential decrease in tangent loss. As the frequency increases further, polarisation effect is less as the dipoles cannot follow the rapidly changing applied electric field and there is no further tangent loss.^{20,21} For lower frequencies, the value of tangent loss decreases slowly for all concentrations. Their value suddenly increases for 1 MHz frequency. The increase in tangent loss above 100 kHz frequency arises due to the contribution from the conduction of metal NPs through the polymer.^{4,7-15,22-25}

AC conductivity measurement

AC conductivity (σ_{ac}) is given by,



5 a and b Frequency-dependent tangent loss ($\tan \delta$) of CuPC and CoPC for all concentrations



6 a and b Frequency-dependent AC conductivity (σ_{ac}) of CuPC and CoPC for all concentrations

$$\sigma_{ac} = 2\pi f \tan \delta \epsilon_r \epsilon_0$$

where f , $\tan \delta$, ϵ_r and ϵ_0 are the frequency in Hz, tangent loss factor, dielectric constant of the material and vacuum permittivity, respectively.

The AC conductivity increases with all frequencies as shown in Fig. 6 due to the formation of more conducting pathway, i.e. leakage current. Further increase in doping element may inhibit the conducting pathways resulting in low conductivity.

The exponential increase in conductivity with frequency arises due to the increase in mobility of metal nanoparticles present in the polymer matrix.^{11,15,21–26}

Conclusion

Gradual addition of metal nanoparticles in PVDF-HFP leads to

- gradual increase in α -phase at the cost of electroactive β -phase (Fig. 1).
- the nanoparticles conglomerate at higher concentration (Fig. 2).

- the dielectric constant of all nanocomposites decrease with increase in frequency for all concentrations of metal nanoparticles (Fig. 3).
- the dielectric constant of all nanocomposites at all concentrations of metal nanoparticles is higher than the pure polymer throughout the frequency range of 20 Hz to 2 MHz. The dielectric constant is highest for 0.5 nanoparticle concentration. Perhaps, the composite reaches the optimum conformation of α - and β -phases at this concentration (Fig. 4).
- the tangent loss of these nanocomposites is also considerable in that frequency range. At higher frequency, the value of $\tan \delta$, which is a measure of the ratio of conduction current and displacement current, increases with increase in conductivity (Fig. 5).
- the AC conductivity increases with frequency for all nanocomposite films due to the presence of mobile metal ions in the polymer composites (Fig. 6).

We can compare this result using trituated metal nanoparticle with our earlier study of homogenous dispersion of Fe_2O_3 NPs in the polymer matrix.¹¹ We have shown that the incorporation leads to strong interfacial interaction between

the NPs and the polymer resulting in enhanced dielectric constant of the thin films. The observed variation of the dielectric properties of the thin films depends on the surface charge, size, geometrical shape and extent of agglomeration of the NPs in the polymer matrix. The AC conductivity and dielectric constant of the nanocomposite films increased with frequency, and were found to depend on the concentration of mobile ions present in the composites.

Thus, pure polymer film which has comparatively low dielectric constant can be modified into materials with enhanced dielectric constant and comparatively low tangent loss by making a composite with triturated metal nanoparticles, which are nontoxic, eco-friendly and easily available in the nano form. Our similar work using other metal NPs and different triturated metal nanoparticles also gives promising result and compares well with this result.^{11,21–25}

As a dielectric material, these nanocomposite films can then be a promising candidate for the fabrication of high-charge-storing multilayer capacitors and can be of great use in electronic industry.

Financial Support and Sponsorship

This work was supported by Central Council for Research in Homeopathy, New Delhi, India [grant number 17-209/2013-14/CCRH/Tech/Coll/CIRE49]. The authors are thankful to the Central Council for Research in Homeopathy (CCRH), the Ministry of AYUSH, Govt. of India, for providing the financial assistance. The study was undertaken in joint collaboration between CIRE, Kolkata and CCRH, New Delhi.

Conflicts of Interest

There is no conflict of interest.

References

1. P. Martins, C. M. Costa, M. Benelmekki, G. Botelho and S. Lanceros-Mendez: 'On the origin of the electroactive poly(vinylidene fluoride) β -phase nucleation by ferrite nanoparticles via surface electrostatic interactions', *Cryst. Eng. Comm.*, **2012**, *14*, 2807–2811.
2. P. Martins, A. C. Lopes and S. Lanceros-Mendez: 'Electroactive phases of poly (vinylidene fluoride): determination, processing and applications', *Prog. Polym. Sci.*, **2013**, *39*, 683–706.
3. H. S. Nalwa: 'Ferroelectric polymers: chemistry, physics, and applications'; **1995**, New York, Marcel Dekker.
4. Y. Li, X. Huang, Z. Hu, P. Jiang, S. Li and T. Tanaka: 'Large dielectric constant and high thermal conductivity in poly(vinylidene fluoride)/barium titanate/silicon carbide three-phase nanocomposites', *Appl. Mater. Interfaces*, **2011**, *3*, 4396–4403.
5. Z. M. Dang, Y. H. Lin and C. W. Nan: 'Novel ferroelectric polymer composites with high dielectric constants', *Adv. Mater.*, **2003**, *15*, 1625–1629.
6. Q. Chen, P. Y. Du, L. Jin, W. J. Weng and G. R. Han: 'Percolative conductor/polymer composite films with significant dielectric properties', *Appl. Phys. Lett.*, **2007**, *91*, 022912-1–022912-3.
7. M. Panda, V. Srinivas and A. K. Thakur: 'On the question of percolation threshold in polyvinylidene fluoride/nanocrystalline nickel composites', *Appl. Phys. Lett.*, **2008**, *92*, 132905-1–132905-3.

8. X. Y. Huang, P. K. Jiang and L. Y. Xie: 'Ferroelectric polymer/silver nanocomposites with high dielectric constant and high thermal conductivity', *Appl. Phys. Lett.*, **2009**, *95*, 24290-1–24290-3.
9. Z. M. Dang, J. P. Wu, H. P. Xu, S. H. Yao, M. J. Jiang and J. B. Bai: 'Dielectric properties of upright carbon fiber filled poly(vinylidene fluoride) composite with low percolation threshold and weak temperature dependence', *Appl. Phys. Lett.*, **2007**, *91*, 072912-1–072912-3.
10. S. H. Yao, Z. M. Dang, M. J. Jiang, H. P. Xu and J. B. Bai: 'Influence of aspect ratio of carbon nanotube on percolation threshold in ferroelectric polymer nanocomposite', *Appl. Phys. Lett.*, **2007**, *91*, 212901-1–212901-3.
11. P. Thakur, A. Kool, B. Bagchi, S. Das and P. Nandy: 'Effect of *in situ* synthesized Fe_2O_3 and Co_3O_4 nanoparticles on electroactive β phase crystallization and dielectric properties of poly(vinylidene fluoride) thin films', *Phys. Chem. Chem. Phys.*, **2015**, *17*, 1368–1378.
12. Z. M. Dang, L. Wang and Y. Yin: 'Giant dielectric permittivities in functionalized carbon-nanotube/electroactive-polymer nanocomposites', *Adv. Mater.*, **2007**, *19*, 852–857.
13. Q. Li, Q. Z. Xue, L. Z. Hao, X. L. Gao and Q. B. Zheng: 'Large dielectric constant of the chemically functionalized carbon nanotube/polymer composites', *Compos. Sci. Technol.*, **2008**, *68*, 2290–2296.
14. F. He, S. Lau, H. L. Chan and J. Fan: 'High dielectric permittivity and low percolation threshold in nanocomposites based on poly(vinylidene fluoride) and exfoliated graphite nanoplates', *Adv. Mater.*, **2009**, *21*, 710–715.
15. P. Thakur, A. Kool, B. Bagchi, S. Das and P. Nandy: 'Enhancement of β phase crystallization and dielectric behavior of kaolinite/halloysite modified poly(vinylidene fluoride) thin films', *Appl. Clay Sci.*, **2014**, *99*, 149–159.
16. Homeopathic Pharmacopoeia of India, **1971**, Published by the Ministry of Health, Govt. of India.
17. P. Nandy, S. Bhandary, S. Das, R. Basu and S. Bhattacharya: 'Nanoparticles and membrane anisotropy', *Homeopathy*, **2011**, *100*, 194.
18. P. Nandy: 'A review of basic research on homeopathy from a physicist's point of view', *Indian J. Res. Homeopath.*, **2015**, *9*, 141–151.
19. P. S. Chikramane, A. K. Suresh, J. R. Bellare and S. G. Kane: 'Extreme homeopathic dilutions retain starting materials: a nanoparticulate perspective', *Homeopathy*, **2010**, *99*, 231–242.
20. P. S. Chikramane, D. Kalita, A. K. Suresh, S. G. Kane and J. R. Bellare: 'Why extreme dilutions reach non-zero asymptotes: a nanoparticulate hypothesis based on froth flotation', *Langmuir*, **2012**, *28*, 15864–15875.
21. K. Halder, B. K. Paul, B. Bagchi, A. Bhattacharya and S. Das: 'Copper ion doped mullite composite in poly(vinylidene fluoride) matrix: effect on microstructure, phase behavior and electrical properties', *J. Res. Updat. Polym. Sci.*, **2014**, *3*, 157–169.
22. B. K. Paul, K. Halder, D. Roy, B. Bagchi, A. Bhattacharya and S. Das: 'Dielectric switching above a critical frequency occurred in iron mullite composites used as an electronic substrate', *J. Mater. Sci. Mater. Electron.*, **2014**, *25*, 5218–5225.
23. P. Thakur, A. Kool, B. Bagchi, N. A. Hoque, S. Das and P. Nandy: '*In situ* synthesis of $\text{Ni}(\text{OH})_2$ nanobelt modified electroactive poly(vinylidene fluoride) thin films: remarkable improvement in dielectric properties', *Phys. Chem. Chem. Phys.*, **2015**, *17*, 13082–13091.
24. P. Thakur, A. Kool, B. Bagchi, N. A. Hoque, S. Das and P. Nandy: 'Improvement of electroactive β phase nucleation and dielectric properties of $\text{WO}_3 \cdot \text{H}_2\text{O}$ nanoparticle loaded poly(vinylidene fluoride) thin films', *RSC Adv.*, **2015**, *5*, 62819–62827.
25. B. K. Paul, S. Kar, P. Bandyopadhyay, R. Basu, S. Das, D. S. Bhar, R. K. Manchanda, A. K. Khurana, D. Nayak and P. Nandy: 'Significant enhancement of dielectric and conducting properties of electroactive polymer polyvinylidene fluoride films: an innovative use of *Ferrum metallicum* at different concentrations', *Indian J. Res. Homeopath.*, **2016**, *10*, (1), 52–57.
26. B. K. Paul, S. Das, R. Basu, D. S. Bhar, R. K. Manchanda, A. K. Khurana, D. Nayak, P. Nandy: 'Effect of dilution of *Ferrum metallicum* and zincum oxidatum, homeopathic nanomedicines on the dielectric properties of poly(PVDF-HFP) film', *Int. J. High Dilution Res.*, **2016**, *15*, (1), 10–17.
27. F. Rogti, M. Ferhat: 'Maxwell–Wagner polarization and interfacial charge at the multi-layers of thermoplastic polymers', *J. Electrostat.*, **2014**, *72*, 1, 91–97.

Improvisation of electrical properties of PVDF-HFP: use of novel metallic nanoparticles

A. L. Gayen^{1,2} · D. Mondal^{1,2} · D. Roy¹ · P. Bandyopadhyay^{1,2} · S. Manna^{1,4} ·
R. Basu^{1,3} · S. Das^{1,2} · D. S. Bhar¹ · B. K. Paul^{1,2} · P. Nandy¹

Received: 20 February 2017 / Accepted: 12 June 2017
© Springer Science+Business Media, LLC 2017

Abstract The electrical properties of poly (vinylidene fluoride-co-hexafluoropropylene) (PVDF-HFP) films has been improved by incorporating a novel material, the triturated copper (TCu) and cobalt (TCo) nanoparticles by simple solution casting technique. Serial dilutions of the solution of these triturated nanoparticles in alcohol have been shaken vigorously and we studied the effect of these VLMRSDL (Very Low Molarity Repeatedly Shaken Diluted Liquid—the so called potentised liquid) on the improvement of electrical properties of the nanocomposite film. The room temperature dielectric constant of the pure PVDF-HFP at 20 Hz frequency increases with increase in potentisation of the solvent containing the triturated metal nano particles and reaches a maximum almost 4 times the value of the pure one. The presence of α - and β -phases and spherulitic crystal structure of PVDF-HFP of these nanocomposite films have been detected by XRD, Fourier Transform Infrared Spectroscopy (FTIR), DTA and by field emission scanning electron micrograph (FESEM) study. The transition of phase between α and β is activated by the incorporation of metallic nanoparticles in the polymer

matrix. This provides the nanocomposites higher mobile charge carriers which participate in the interfacial polarization. These films have higher dielectric permittivity and significantly lower dissipation factor ($\tan\delta$) at room temperature compared to the pure PVDF-HFP. The triturated metal nanoparticles are inexpensive, easy to fabricate and environment friendly. The incorporation of these novel nanoparticles in polymer matrix to get enhanced improved electrical properties will have a significant contribution in the present day research in electronics.

1 Introduction

Poly(vinylidene fluoride) (PVDF) and its copolymers like poly(vinylidene fluoride-hexa-fluoropropylene) (PVDF-HFP) are in great demand for their versatile and unique properties like flexibility, low processing temperature, low dielectric constant, high dielectric breakdown field etc., making them potential candidate for a broad range of applications in electronic industry [1–3].

In order to improve the capacitive performance of the polymer material, incorporation of metal nanoparticles in the polymer matrix has received great attention in recent years. Here the uniform and homogeneous distribution of the nanoparticles allows good interaction between them and the polymer matrix material which enhances the electrical properties of the host material [4–7].

In this endeavour, a great deal of effort had been devoted to develop PVDF-HFP composites by incorporating different metallic nanoparticles within the matrix. The effective dielectric permittivity of these metal nanoparticle doped polymer composite are higher than that of the host polymer matrix. They also show enhancement of conductivity and decrement of tangent loss making them potential

✉ P. Nandy
pnandy00@gmail.com

B. K. Paul
destinationbiplab@gmail.com

¹ Centre for Interdisciplinary Research and Education,
Kolkata 700 068, India

² Department of Physics, Jadavpur University, Kolkata 700032,
India

³ Department of Physics, Jogamaya Devi College,
Kolkata 700026, India

⁴ Jagadish Bose National Science Talent Search,
Kolkata 700 107, India

candidates as good capacitors and electric energy storage devices [8–15]. On the other hand various filler functionalized polymer composites with enhanced properties have been synthesized through different methodologies [16–22].

In this work, we have chosen trituated copper (TCu) and cobalt (TCo) nanoparticles, two very novel and unique metallic fillers, which are nontoxic, inexpensive and are easily available. The nanoparticle aspect of these potencies has been proved experimentally and their medicinal efficacy has been established [23–27]. These novel nanoparticles were incorporated in the polymer PVDF-HFP in dimethyl-sulfoxide solution and films were prepared by simple solution casting technique. These nanocomposites of PVDF-HFP/TCu (CuPC) and PVDF/TCo (CoPC) were studied by XRD, FTIR, DTA, FESEM, EDX, Mapping and dielectric analysis. The presence of α and β phases, formation of spherulites, enhancement of dielectric constant and conductivity and decrease of tangent loss of the nanocomposite films were observed by changing the potency of TCo and TCu and the observed values were compared with the pure PVDF-HFP film.

The NPs we selected for our work are prepared by the method of trituration making these truly novel materials. The advantage of this method is that in this way the shape and size of the NPs can be regulated by the amount of vigorous shaking. Thus this method makes these NPs unique compared to the chemically synthesized ones. Moreover, these NPs are eco-friendly, inexpensive, nontoxic, easily available metallic nano fillers which can enhance the membrane permeability, conductivity and decreases the dissipation factor of polymer films by many folds. Utilising these unique metallic nanofillers to enhance the electrical properties of polymer film is of great importance when electroactive polymer films are gaining worldwide attention for their use in electronic industry.

2 Materials and methods

Freshly prepared trituated metal nanoparticles, Copper (TCu) and Cobalt (TCo) of different potencies were obtained from Hahnemann Publishing Company, India. The materials used in the synthesis of the nano composite films are TCu, TCo, PVDF-HFP (Sigma Aldrich, USA) and dimethyl sulfoxide (DMSO) (Merck, India).

In a typical synthesis, 100 mg of PVDF-HFP was added to 2 ml DMSO and mixed together under vigorous stirring at 60 °C for 3 h. Measured amount (0.6 ml) of TCu and TCo of different potencies were added to the solution. The volume wt% of all trituated nanoparticles (NPs) of different potencies are 23.08%. CuPC and CoPC were obtained by casting the whole mixture in clean dry petri dishes and evaporating the solvent in an incubated oven at 60 °C for

12 h [28–32]. The films were then coated by silver paste on both sides for electrical measurements. The synthesized films had the thickness in the range of 48–54 μm as measured by using a digital screw gauge. The average density value of the fabricated films is 0.81 gm cm^{-3} .

3 Sample details

3.1 For pure PVDF-HFP

- 100 mg PVDF-HFP + 2 ml DMSO (PVDF-HFP)

3.2 For CuPC

- 100 mg PVDF-HFP + 2 ml DMSO + 0.6 ml TCu of potency 6 C (CuPC-6)
- 100 mg PVDF-HFP + 2 ml DMSO + 0.6 ml TCu of potency 30 C (CuPC-30)
- 100 mg PVDF-HFP + 2 ml DMSO + 0.6 ml TCu of potency 200 C (CuPC-200)

3.3 For CoPC

- 100 mg PVDF-HFP + 2 ml DMSO + 0.6 ml TCo of potency 6 C (CoPC-6)
- 100 mg PVDF-HFP + 2 ml DMSO + 0.6 ml TCo of potency 30 C (CoPC-30)
- 100 mg PVDF-HFP + 2 ml DMSO + 0.6 ml TCo of potency 200 C (CoPC-200)

4 Instrumentation

The crystalline phases developed in the samples were analyzed by X-ray diffractometer (model-D8, Bruker AXS, Wisconsin, USA) using Cu K α radiation- 1.5418 \AA and operating at 40 KV with a scan speed of 0.3 s/step. The characteristic stretching and bending modes of vibration of chemical bonds of the CuPC and CoPC samples were effectively evaluated by FTIR spectroscopy (FTIR-8400S, Shimadzu). Field-emission scanning electron microscopy (FESEM) was done using INSPECT F50 SEM, FEI Europe BV. The operating conditions are mentioned in the FESEM images as follows: HV 20.00 kV, magnification $\times 5000$, WD 10.9 mm, and HFW 59.7 μm . Sample preparation was done using turbo-pumped sputter coater EMS 150TS and was used for gold coating. Dielectric measurements of

these films were carried out by using an electrometer (HP Model 4274 A, Hewlett–Packard, USA). Electrical properties such as dielectric permittivity (ϵ_r), dissipation factor ($\tan \delta$), and a.c. conductivity ($\sigma_{a.c.}$) of all CuPC films and CoPC film were measured in the frequency range 20 Hz to 2.0 MHz using LCR meter.

5 Characterization

5.1 XRD analysis

The crystallization behaviour of the films by doping TCu and TCo NPs have been investigated by using an X-ray diffractometer. Figure 1, shows these X-ray diffraction (XRD) patterns of the TCu and TCo NPs modified PVDF films. The diffraction pattern of pure PVDF shows peaks at 2θ values of 17.5 (100), 18.1 (020), 19.9 (021) and 26.4 [(201), (310)]

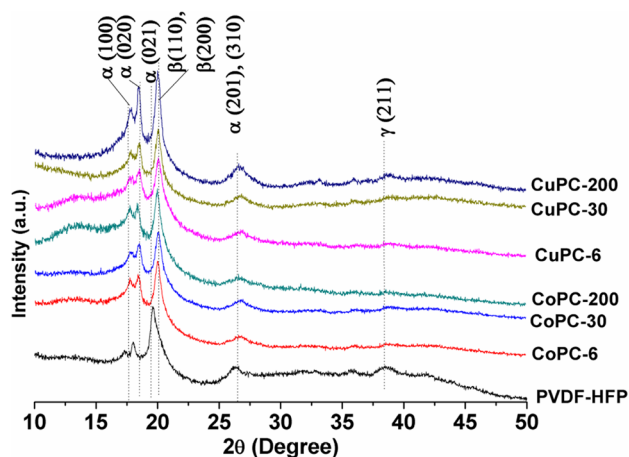


Fig. 1 XRD patterns of pure and all composite films doped with TCu and TCo of 6C, 30C and 200C potencies

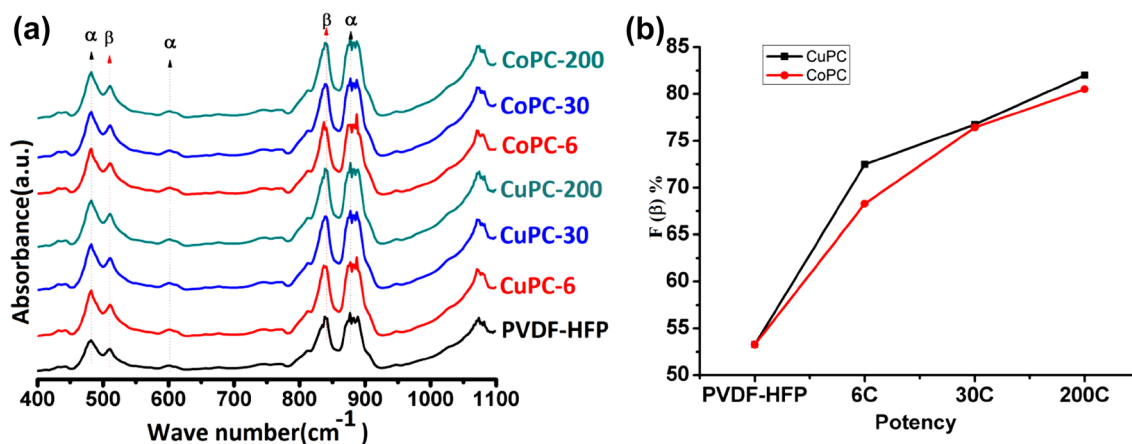


Fig. 2 **a** Fourier transform infrared spectra of CuPC and CoPC for all potency. **b** Increase of F(β)% with increase in potency

corresponding to the α -phase and 38.91 (211) for the γ -phase. But the nanocomposite films doped with TCu and TCo NPs showed all peaks corresponding to α or γ phases disappear and only one characteristic peak of PVDF at 20.5 [(110), (200)] appeared which confirmed the nucleation of the electroactive β -phase in nanocomposite films [1, 14, 15, 30, 31]. Thus the nucleation of the electroactive β -phase is significantly accelerated for both the TCu and TCo NPs. The characteristic peaks of the metal nanoparticles are not evident in the pattern due to the very high dilution of these NPs in the PVDF matrix.

5.2 FTIR analysis

Fourier Transform Infrared Spectroscopy (FTIR) study of these nanocomposite films in the selected range of 400–1100 cm^{-1} detected presence of α - and β -phases Fig. 2a. The FTIR spectra of CuPC and CoPC nanocomposite film show characteristic absorbance bands at 484, 606 and 878 cm^{-1} corresponding to the α -phase and around 510 and 840 cm^{-1} corresponding to the β -phase. The spectra indicate that there is no phase shift or chemical interaction between the metal nanoparticles and the polymer film, but the intensity of α - and β -phases change with the concentration of doping material [28–30].

We observe in Fig. 2b that with increase in potency, the β -phase peaks have grown significantly compared to those of PVDF-HFP. Using Beer–Lambert law, which relates absorbance with concentration of the absorbing species, the fraction of β -phase, F_β , present in the (crystalline regions of) films was calculated using the formula,

$$F(\beta) = \frac{A\beta}{1.26A\alpha + A\beta}$$

where, A_α and A_β are the absorption fractions of α and β -phases respectively. The maximum absorbance at 484 cm^{-1} was chosen as A_α and the maximum absorbance around 840 cm^{-1} as A_β . The calculations based on the above formula led to results which are presented graphically in Fig. 2b. Undoped PVDF had 53% β -phase that increased with the addition of the different potency of the nanoparticles. The enhancement in β -phase was maximum (82.04%) for TCu nanoparticles of 200 C potency among all the composites. All composite film showed a constant increasing trend with increase in potency [28–30].

5.3 DTA analysis

Differential thermo gravimetric (DTA) has been used for the identification of the crystalline phase of PVDF as a supporting data of XRD and FTIR. Figure 3 shows the DTA thermographs of pure PVDF and the NPs incorporated PVDF films. The DTA thermograph of pure PVDF shows a strong endothermic peak position at 165.8°C suggesting a phase crystallization with some presence of electroactive β -phase content in pure PVDF that was also observed in FTIR. But for PVDF films doped with CuPC-200 NPs, this point shifted to 170.3°C [1, 11, 15, 30, 31]. The endothermic peak position of all the other PVDF films doped with NPs at different potencies lie in between these two temperature. The shifted endothermic peaks confirm the existence of strong β -phase. Thus DTA results suggest more electroactive β -phase crystallization for all NPs doped PVDF films, which are consistent with the XRD and FTIR data.

5.4 Zeta potential analysis and schematic diagram

Our current study based on TCu/TCo-PVDF nanocomposites proposes a strong interaction between the positively CH_2 dipoles of PVDF and the negatively charged

nanoparticles leading to the alignment of stabilized chains in longer all trans conformation on the TCu and TCo nanoparticle surface. Thus, to explain the origin of β -phase crystallization in our present work, the surface charges of the TCu and TCo NPs have been investigated. Without adding PVDF the possible electrostatic charge on the surface of the TCu and TCo NPs has been investigated by zeta potential analysis. The obtained results of zeta potential distribution have been shown in Fig. 4. Both NPs show negative zeta Potentials. Thus it confirms, the nucleation of the electroactive β phase taking place on the negatively charged surfaces of TCu and TCo NPs. The positive CH_2 dipoles of PVDF chains undergo strong electrostatic interaction with the negatively charged surface of the NPs resulting in stabilized longer TTTT or all trans conformation on the NP surfaces. Figure 5. shows the ion–dipole or electrostatic interaction mechanism between the NPs and

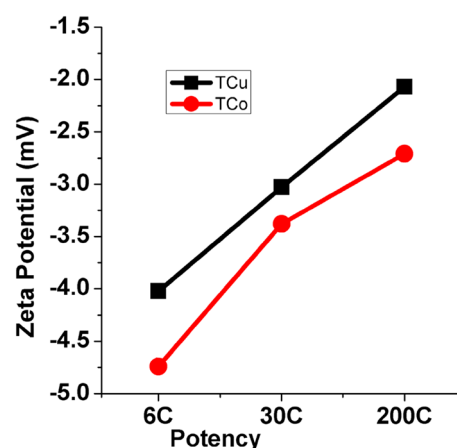


Fig. 4 Zeta potential of pristine TCu and TCo of 6C, 30C and 200C potencies

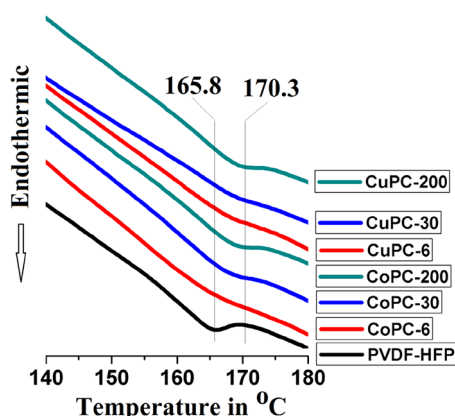


Fig. 3 DTA patterns of pure and of composite films doped with TCu and TCo of 6C, 30C and 200C potencies

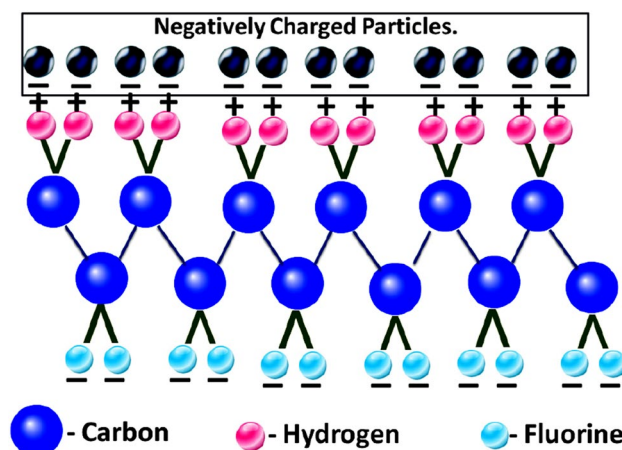


Fig. 5 Schematic diagram showing the growth mechanism for the formation of TCu or TCo/PVDF-HFP composites

polymer chains during the formation of the electroactive β -phase [1, 11].

Enhanced electroactive β -phases of PVDF have been obtained by doping TCu and TCo NPs on PVDF matrix using solvent-casting method. Similar studies were made earlier in our laboratory, where the formation of β -phase was reported with the addition of fillers by solvent-casting method. The growth mechanism for the formation of TCu or TCo/PVDFHFP composites has been explained based on the chemistry concept by the schematic diagram which shows the formation of β -phase as given in Fig. 5. This formation of electroactive β -phase may be explained by the theory of β -phase nucleation, which is based upon dipole-surface charge interaction model. According to this model, when fillers were added to the PVDF solution, the negatively charged surface of filler, which acted as substrates for β -phase nucleation, got attracted to the partially positive CH_2 dipoles, thus leading to the alignment of stabilized PVDF chains in longer all trans-conformation, resulting in electroactive β -phase [1, 11, 15]. From this analysis, it is evident that CuPC-200 sample got maximum enhancement of β -phase.

5.5 FESEM analysis

5.5.1 Pristine TCu and TCo

Figure 6 shows the morphology and microstructures of pristine TCu and TCo NPs that was directly doped in PVDF matrix. The dispersed nanoparticles were drop casted on silica substrate and all TCu and TCo NPs of 200C potency confirms good and homogenous distribution on the surface

with not much agglomeration have been found for both triturated NPs.

5.5.2 TCu and TCo doped PVDF

Figure 7a–f show the morphology and microstructure of all composite films doped with TCu and TCo nanoparticles of 6C, 30C and 200C potencies respectively. Figure 7a, d is the evidence of large number of densely packed agglomerated particles embedded in the polymer matrix whereas Fig. 7c, f show that the particles are more scattered, well separated and also homogeneously distributed maintaining an intermolecular distance [29–32]. The polymer matrix is also well crystallized (Fig. 7c, f) with the increasing potencies and got maximum enhancement at 200C potency.

The evidence for the incorporation of TCu and TCo in the polymer was not very conclusive as the samples were of extreme dilution and the presence of the particles was difficult to detect.

5.5.3 Elemental mapping and EDX spectra of TCu and TCo doped PVDF

Figure 8 shows the elemental mapping image of (a) CuPC-200, (b) CoPC-200 and their EDX spectra respectively. The figure confirms the presence of all the elements of PVDF and NPs. These also show high resolution FESEM micrograph of optimised CuPC-200 and CoPC-200. The EDX images (c and d) confirm the presence of copper or cobalt along with polymeric elements into the composite system. Elements obtained from EDX study with their normality weight percentages are shown in Tables (Fig. 8e).

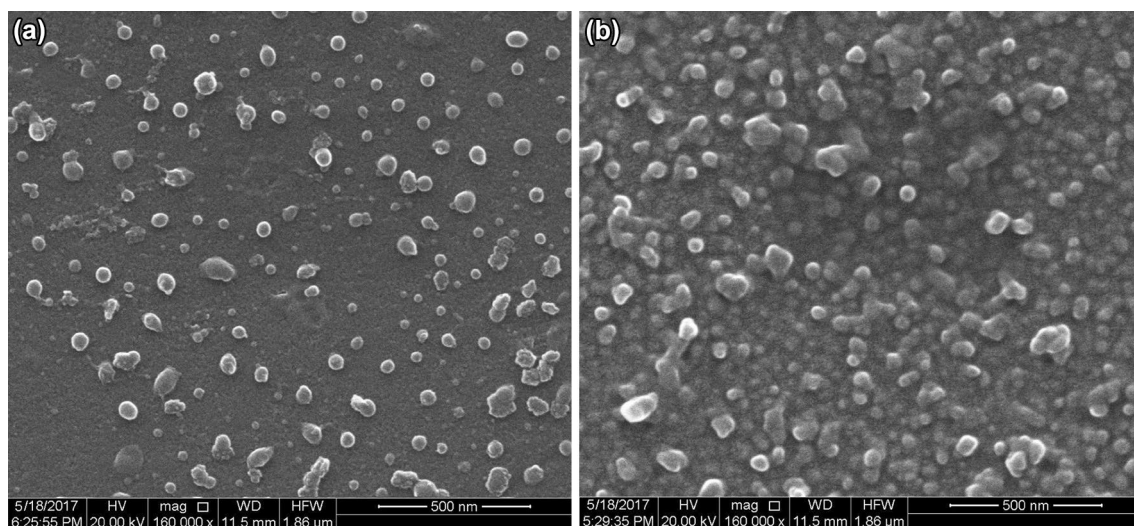


Fig. 6 Field-emission scanning electron micrograph (FESEM) of pristine, **a** TCu and **b** TCo of 200C

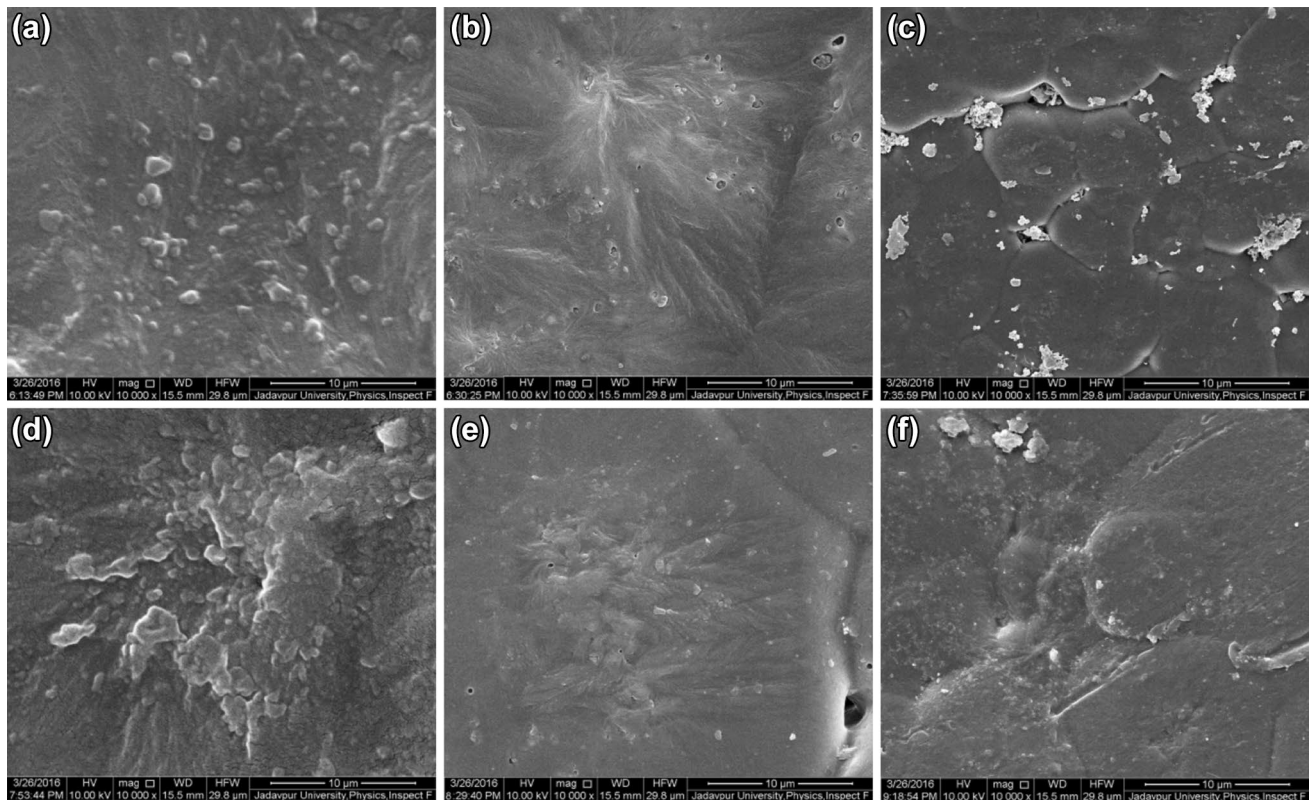


Fig. 7 Field-emission scanning electron micrograph (FESEM) of **a** CuPC-6, **b** CuPC-30, **c** CuPC-200, **d** CoPC-6, **e** CoPC-30 and **f** CoPC-200 films

6 Dielectric measurements and discussions

6.1 Frequency dependent dielectric measurements

6.1.1 Dielectric constant

The factor by which the dielectric material, or insulator, increases the capacitance of the capacitor compared to air is known as the Dielectric Constant (ϵ_r), and a dielectric material with high dielectric constant is a better insulator than one with low dielectric constant. Dielectric constant is a dimensionless quantity since it is relative to free space. The dielectric constant (k) or relative permittivity (ϵ_r) of each sample was calculated from the capacitance using the formula,

$$C = \epsilon_r \epsilon_0 \frac{A}{d},$$

where ϵ_r , C , d , A and ϵ_0 are the dielectric constant of the material, capacitance, thickness of the film, area of the cross-section and permittivity of the free space respectively.

The variations of dielectric constant of all CuPC and CoPC film with frequency are shown in Fig. 9a, b respectively. From the figure it is clearly seen that within the

frequency range 20 Hz to 2 MHz, dielectric constant for all CuPC and CoPC films continuously decrease with increase in frequency for all concentration of CuPC and CoPC film at about upto 200 Hz and after that it seems to remains constant at about upto 100 KHz. It is also seen that throughout the whole frequency range, dielectric constant has substantially higher value in case of all CuPC and CoPC films compared to the pure polymer film. As there are two different conducting media present here (e.g. PVDF-HFP and TCu or TCo), this enhancement may be explained by MWS (Maxwell–Wagner–Sillars) interfacial polarisation. The interfacial polarization is associated with the entrapment or accumulation of free charges generated in the cores at the interfaces between the cores and the matrix. FESEM micrographs strongly support that, as the dispersion, separation and distribution is well the dielectric constant increased because of the enhancement of effective interaction area between the polymer matrix and the nanoparticles.

At lower frequency the easy orientation of dipoles as well as MWS interfacial polarization contribute this ~four times enhancement. As the frequency is increased further, dipole response is restricted and the dielectric constant has a saturation tendency. In this case, the internal individual

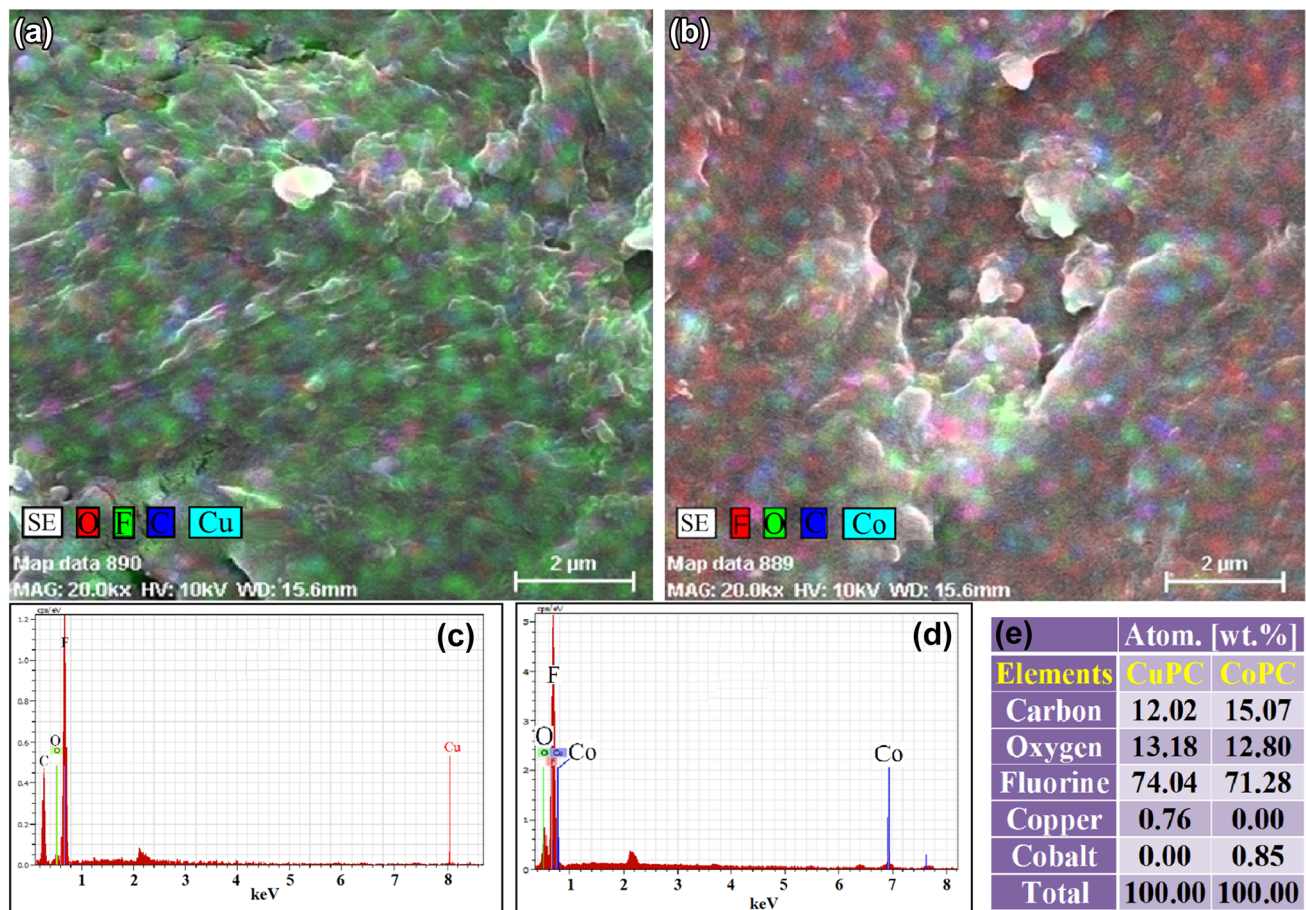


Fig. 8 High resolution elemental mapping images of **a** CuPC-200, **b** CoPC-200 and EDX spectra of **c** CuPC-200, **d** CoPC-200. **e** Elements obtained from EDX study with their normality weight percentages are shown in the inserted table

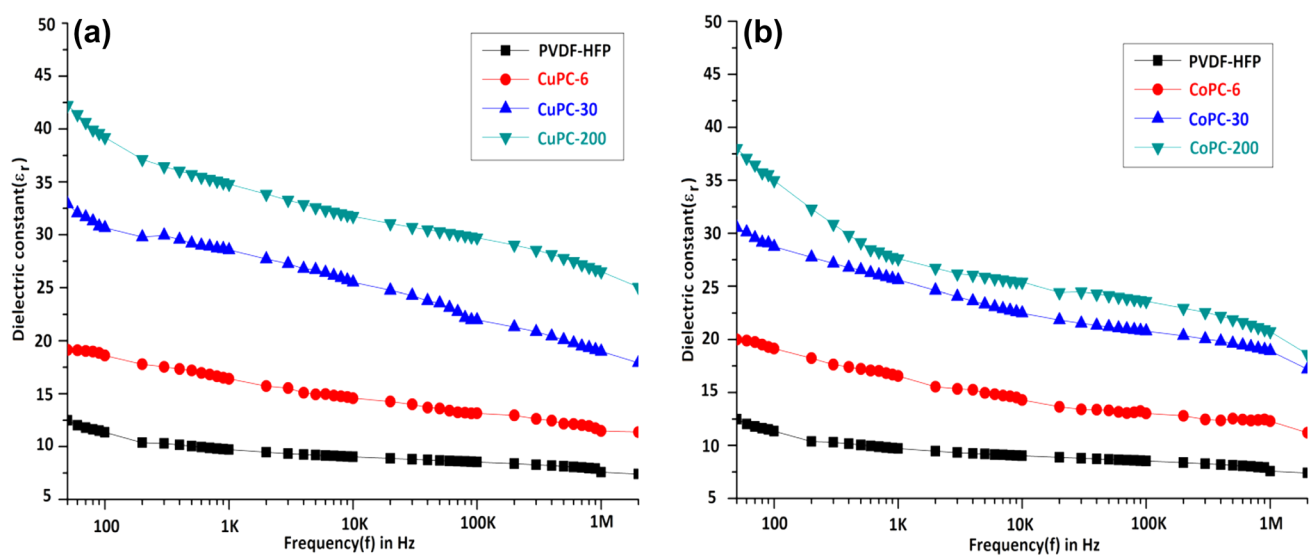


Fig. 9 Frequency dependent dielectric constant (ϵ_r) of **a** CuPC and **b** CoPC for all potency

dipoles contribute to the dielectric constant which is ideally the electronic polarisation effect [29–34].

6.1.2 Tangent loss

Another factor which affects the operation of a capacitor is Dielectric Leakage. Dielectric leakage occurs in a capacitor as the result of an unwanted leakage current which flows through the dielectric material. The ratio of conduction current and displacement current is called dielectric loss or conduction loss or damping loss.

Figure 10a, b show the variation of tangent loss with frequency for all CuPC and CoPC films in the frequency range 20 Hz to 2 MHz. From the figure it is clearly seen that throughout the frequency range tangent loss continuously decreases with increasing frequency for all CuPC and CoPC film upto 2 KHz. This rapid destruction decrease may be for intermolecular friction or vibration. At lower frequency range the easy orientation of dipoles for higher relaxation time contributes to higher tangent loss. As frequency increases, less polarization effect continues due to less relaxation time. So intermolecular friction or vibration diminishes which is responsible for saturated tangent loss. On the other hand after 100 KHz the tangent loss increases for all films may be due to leakage current [29–34].

6.1.3 A.C. conductivity

Electrical conductivity or specific conductance is the reciprocal of electrical resistivity, and measures a material's ability to conduct an electric current. It is commonly represented by the Greek letter σ (sigma). Its SI unit is Siemens

per metre (S/m). A.C. conductivity ($\sigma_{a.c}$) is calculated using the formula,

$$\sigma_{a.c.} = 2\pi f \tan \delta \epsilon_r \epsilon_0,$$

where $\sigma_{a.c}$, f , $\tan \delta$, ϵ_r and ϵ_0 , are the AC conductivity, frequency in Hz, tangent loss factor, dielectric constant of the material and vacuum permittivity respectively. During the conductivity measurements 1.0 V was applied.

The variation of ac conductivity with frequency for all CuPC and CoPC film is shown in Fig. 11a, b respectively. It shows ac conductivity increases exponentially with frequency for both the nanocomposite films. At higher frequency range, rapid increase of conductivity with increasing frequency is referred to electronic polarization effect. This increase in conductivity with frequency also arises due to the presence of free ions in the polymer matrix that may increase the mobility of the ions which finds an easy path to move and hence increase the electrical conductivity. It is also seen from Fig. 11a, b that the value of ac conductivity is higher for all nanocomposite films than the pure polymer film. The increase of $\sigma_{a.c}$ is due to the increased incorporation of metal ions [29–34].

6.2 Potency dependent dielectric measurements

From Fig. 12 it is clearly seen that at 500 Hz, dielectric constant has substantially higher value in case of all CuPC and CoPC films than pure polymer film and it is also seen that the dielectric constant of these films at 200 C respond the best. This phenomenon can be explained by Maxwell–Wagner–Sillars (MWS) interfacial polarization effect which appears in heterogeneous medium consisting of different phases with different permittivity and conductivity

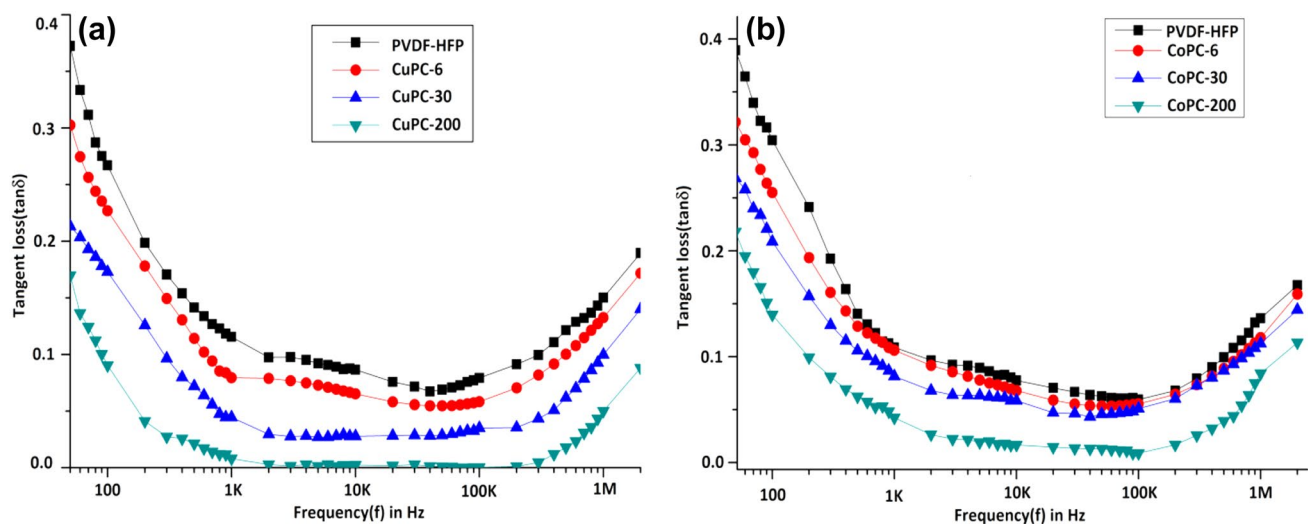


Fig. 10 Frequency dependent Tangent loss ($\tan \delta$) of **a** CuPC and **b** CoPC for all potency

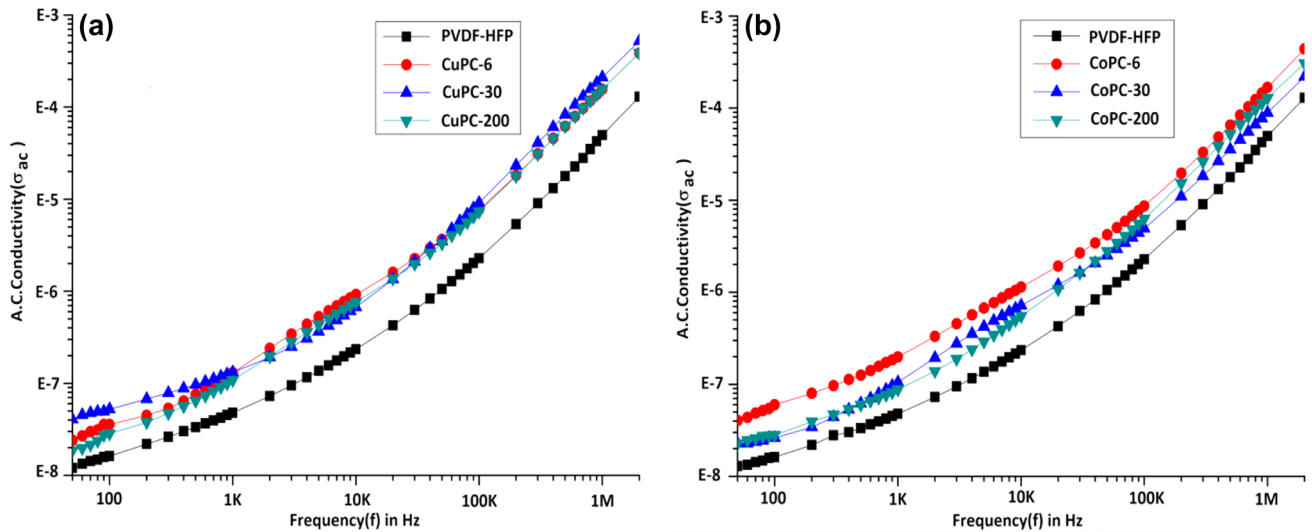


Fig. 11 Frequency dependent ac conductivity (σ_{ac}) of **a** CuPC and **b** CoPC for all potency

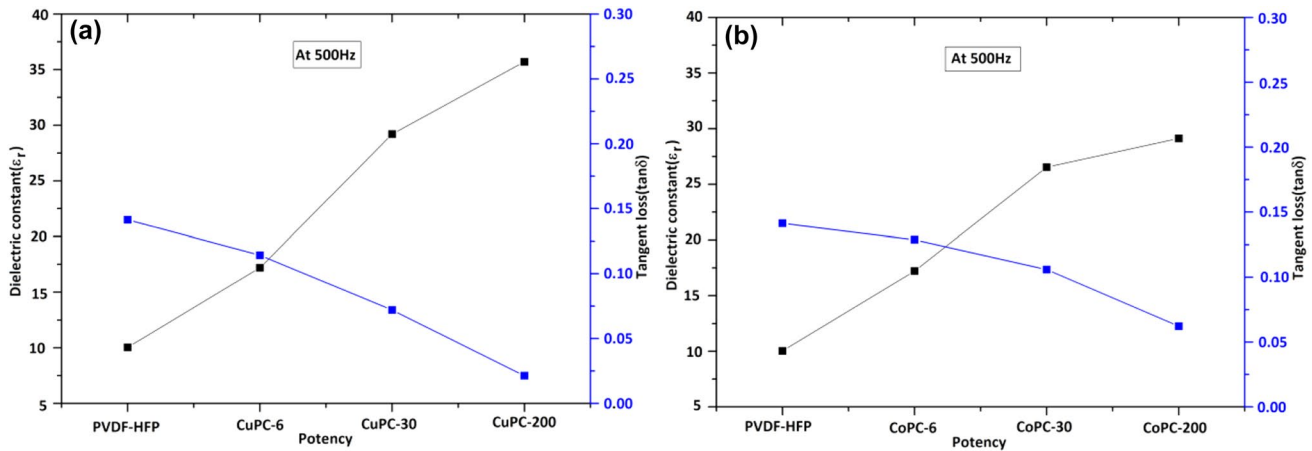


Fig. 12 Potency dependent dielectric constant and tangent loss of **a** CuPC and **b** CoPC for all potency at a specific frequency (500 Hz)

due to accumulation of the charges at the interfaces. For these films, the well crystalline nano particles are well separated from each other with no such effective interaction between them. So the number of homogeneously distributed nanoparticles and their interfacial area per unit volume increases. This improves the average polarization associated with the particles and the coupling between neighboring grains, resulting in the significant enhancement of dielectric constant as well as significant decrement of tangent loss [29–32].

For lower potencies of these films, the particles are in bulk form and agglomerated which is embedded in the polymer matrix. So the interfacial area per unit volume decreases while the interparticle distance decreases. This decreases the average polarization associated with the particles resulting in the further decrement of dielectric

constant and ac conductivity as well as increment of tangent loss. This phenomenon is also clearly observed from their microstructures (FESEM).

7 Conclusion

From the above experiment we found that the addition of HNPs in PVDF-HFP leads to

- Gradual increase in electroactive β -phase compared to PVDF-HFP.
- As the potency of HNPs increased, better interaction observed on polymer matrix and thereby found homogeneously distributed particles.

- (c) The dielectric constant of all nanocomposites (1) increases with potency at any particular frequency and (2) decreases with increase in frequency for all potencies of metal nanoparticles. The dielectric constant got highest enhancement for CuPC-200 HNPs concentration.
- (d) Tangent loss decreases with increasing frequency upto 10 KHz and effect is more at higher potency.
- (e) AC conductivity increases with frequency for all nanocomposite films due to the presence of mobile metal ions in the polymer composites.
- (f) Figure 12 summarizes the dielectric constant and tangent loss with change in potency for both CuPC and CoPC.

We have shown that the incorporation leads to strong interfacial interaction between the HNPs and the polymer resulting in enhanced dielectric constant of the thin films. The observed variation of the dielectric properties of the thin films depends on the surface, size and extent of agglomeration of the HNPs in the polymer matrix. Thus, pure polymer film which has comparatively low dielectric constant can be modified into materials with enhanced dielectric constant and comparatively low tangent loss by making a composite with triturated metal nanoparticles, which are nontoxic, eco-friendly and easily available in the nano form. As a dielectric material, these nanocomposite films can then be a promising candidate for the fabrication of high charge- storing multilayer capacitors and can be of great use in electronic industry.

Acknowledgements The authors are thankful to the Central Council for Research in Homeopathy (CCRH), the Ministry of AYUSH, Govt. of India, for providing the financial assistance. (Grant Number 17-209/2013-14/CCRH/Tech/Coll/CIRE49). The study was undertaken in joint collaboration between CIRE, Kolkata and CCRH, New Delhi.

Compliance with ethical standards

Conflict of interest There is no conflict of interest.

References

1. P. Martins, C.M. Costa, M. Benelmekki, G. Botelho, S. Lanceros-Mendez, On the origin of the electroactive poly(vinylidene fluoride) β -phase nucleation by ferrite nanoparticles via surface electrostatic interactions. *Cryst. Eng. Comm.* **14**, 2807–2811 (2012)
2. P. Martins, A.C. Lopes, S. Lanceros-Mendez, Electroactive phases of poly(vinylidene fluoride): determination, processing and applications. *Prog. Polym. Sci.* **39**, 683–706 (2013)
3. H.S. Nalwa, *Ferroelectric polymers: chemistry, physics, and applications* (Marcel Dekker, New York, 1995)
4. Y. Li, X. Huang, Z. Hu, P. Jiang, S. Li, T. Tanaka, Large dielectric constant and high thermal conductivity in poly(vinylidene fluoride)/barium titanate/silicon carbide three-phase nanocomposites. *Appl. Mater. Interfaces* **3**, 4396–4403 (2011)
5. Z.M. Dang, Y.H. Lin, C.W. Nan, Novel ferroelectric polymer composites with high dielectric constants. *Adv. Mater.* **15**, 1625–1629 (2003)
6. Q. Chen, P.Y. Du, L. Jin, W.J. Weng, G.R. Han, Percolative conductor/polymer composite films with significant dielectric properties. *Appl. Phys. Lett.* **91**, 022912-1-022912-3 (2007)
7. M. Panda, V. Srinivas, A.K. Thakur, On the question of percolation threshold in polyvinylidene fluoride/nanocrystalline nickel composites. *Appl. Phys. Lett.* **92**, 132905-1-132905-3 (2008)
8. X.Y. Huang, P.K. Jiang, L.Y. Xie, Ferroelectric polymer/silver nanocomposites with high dielectric constant and high thermal conductivity. *Appl. Phys. Lett.* **95**, 24290-1-24290-3 (2009)
9. Z.M. Dang, J.P. Wu, H.P. Xu, S.H. Yao, M.J. Jiang, J.B. Bai, Dielectric properties of upright carbon fiber filled poly(vinylidene fluoride) composite with low percolation threshold and weak temperature dependence. *Appl. Phys. Lett.* **91**, 072912-1-072912-3 (2007)
10. S.H. Yao, Z.M. Dang, M.J. Jiang, H.P. Xu, J.B. Bai, Influence of aspect ratio of carbon nanotube on percolation threshold in ferroelectric polymer nanocomposite. *Appl. Phys. Lett.* **91**, 212901-1-212901-3 (2007)
11. P. Thakur, A. Kool, B. Bagchi, S. Das, P. Nandy, Effect of in situ synthesized Fe_2O_3 and Co_3O_4 nanoparticles on electroactive β phase crystallization and dielectric properties of poly(vinylidene fluoride) thin films. *Phys. Chem. Chem. Phys.* **17**, 1368–1378 (2015)
12. Z.M. Dang, L. Wang, Y. Yin, Giant dielectric permittivities in functionalized carbon-nanotube/electroactive-polymer nanocomposites. *Adv. Mater.* **19**, 852–857 (2007)
13. Q. Li, Q.Z. Xue, L.Z. Hao, X.L. Gao, Q.B. Zheng, Large dielectric constant of the chemically functionalized carbon nanotube/polymer composites. *Compos. Sci. Technol.* **68**, 2290–2296 (2008)
14. B.K. Paul, D. Roy, S. Bal, A. Bhattacharya, S. Das, P. Nandy, A comparative study of strontium and titanium doped mullite in PVDF matrix and their phase behavior, microstructure and electrical properties. *Mater. Chem. Phys.* **187**, 119–132 (2017)
15. P. Thakur, A. Kool, B. Bagchi, S. Das, P. Nandy, Enhancement of β phase crystallization and dielectric behavior of kaolinite/halloysite modified poly(vinylidene fluoride) thin films. *Appl. Clay Sci.* **99**, 149–159 (2014)
16. Y.P. Zhang, S.H. Lee, K.R. Reddy, A.I. Gopalan, K.P. Lee, Synthesis and characterization of core-shell SiO_2 nanoparticles/poly(3-aminophenylboronic acid) composites. *J. Appl. Polym. Sci.* **104**, 2743–2750 (2007)
17. D.R. Son, A.V. Raghu, K.R. Reddy, H.M. Jeong, Compatibility of thermally reduced graphene with polyesters. *J. Macromol. Sci. Part B Phys* **55**, 1099–1110 (2016)
18. K.R. Reddy, B.C. Sin, K.S. Ryu, J.C. Kim, H. Chung, Y. Lee, Conducting polymer functionalized multi-walled carbon nanotubes with noble metal nanoparticles: synthesis, morphological characteristics and electrical properties. *Synth. Met.* **159**, 595–603 (2009)
19. M. Hassan, K.R. Reddy, E. Haque, S.N. Faisal, S. Ghasemi, A. Minett, V.G. Gomes, Hierarchical assembly of graphene/polyaniline nanostructures to synthesize free-standing supercapacitor electrode. *Compos. Sci. Technol.* **98**, 1–8 (2014)
20. K.R. Reddy, W. Park, B.C. Sin, J. Noh, Y. Lee, Synthesis of electrically conductive and superparamagnetic monodispersed iron oxide-conjugated polymer composite nanoparticles by in situ chemical oxidative polymerization. *J. Colloid Interface Sci.* **335**, 34–39 (2009)
21. M. Hassan, K.R. Reddy, E. Haque, A.I. Minett, V.G. Gomes, High-yield aqueous phase exfoliation of graphene for facile

- nanocomposite synthesis via emulsion polymerization. *J. Colloid Interface Sci.* **410**, 43–51 (2013)
22. K.R. Reddy, K.P. Lee, A.I. Gopalan, Self-assembly directed synthesis of poly(ortho-toluidine)-metal (gold and palladium) composite nanospheres. *J. Nanosci. Nanotechnol.* **7**, 3117–3125 (2007)
 23. A.L. Gayen, B.K. Paul, D. Roy, S. Kar, P. Bandyopadhyay, R. Basu, S. Das, D.S. Bhar, R.K. Manchanda, A.K. Khurana, D. Nayak, P. Nandy, Enhanced dielectric properties and conductivity of trituated copper and cobalt nanoparticles-doped PVD-FHFP film and their possible use in electronic industry. *Mater. Res. Innovations* (2016). doi:[10.1080/14328917.2016.1196563](https://doi.org/10.1080/14328917.2016.1196563)
 24. P. Nandy, S. Bhandary, S. Das, R. Basu, S. Bhattacharya, Nanoparticles and membrane anisotropy. *Homeopathy* **100**, 194 (2011)
 25. P. Nandy, A review of basic research on homeopathy from a physicist's point of view. *Indian J. Res. Homeopath.* **9**, 141–151 (2015)
 26. P.S. Chikramane, A.K. Suresh, J.R. Bellare, S.G. Kane, 'Extreme homeopathic dilutions retain starting materials: a nanoparticulate perspective'. *Homeopathy* **99**, 231–242 (2010)
 27. P.S. Chikramane, D. Kalita, A.K. Suresh, S.G. Kane, J.R. Bellare, 'Why extreme dilutions reach non-zero asymptotes: a nanoparticulate hypothesis based on froth flotation'. *Langmuir* **28**, 15864–15875 (2012)
 28. K. Halder, B.K. Paul, B. Bagchi, A. Bhattacharya, S. Das, Copper ion doped mullite composite in poly(vinylidene fluoride) matrix: effect on microstructure, phase behavior and electrical properties. *J. Res. Updat. Polym. Sci.* **3**, 157–169 (2014)
 29. B.K. Paul, K. Halder, D. Roy, B. Bagchi, A. Bhattacharya, S. Das, Dielectric switching above a critical frequency occurred in iron mullite composites used as an electronic substrate. *J. Mater. Sci. Mater. Electron.* **25**, 5218–5225 (2014)
 30. P. Thakur, A. Kool, B. Bagchi, N.A. Hoque, S. Das, P. Nandy, 'In situ synthesis of Ni(OH)₂ nanobelt modified electroactive poly(vinylidene fluoride) thin films: remarkable improvement in dielectric properties. *Phys. Chem. Chem. Phys.* **17**, 13082–13091 (2015)
 31. P. Thakur, A. Kool, B. Bagchi, N.A. Hoque, S. Das, P. Nandy, 'Improvement of electroactive β phase nucleation and dielectric properties of WO₃·H₂O nanoparticle loaded poly(vinylidene fluoride) thin films'. *RSC Adv.* **5**, 62819–62827 (2015)
 32. B.K. Paul, S. Kar, P. Bandyopadhyay, R. Basu, S. Das, D.S. Bhar, R.K. Manchanda, A.K. Khurana, D. Nayak, P. Nandy, Significant enhancement of dielectric and conducting properties of electroactive polymer polyvinylidene fluoride films: an innovative use of Ferrum metallicum at different concentrations. *Indian J. Res. Homeopath.* **10**(1), 52–57 (2016)
 33. B.K. Paul, S. Das, R. Basu, D.S. Bhar, R.K. Manchanda, A.K. Khurana, D. Nayak, P. Nandy, Effect of dilution of Ferrum metallicum and zincum oxidatum, homeopathic nanomedicines on the dielectric properties of poly(PVDF-HFP) film. *Int. J. High Dilution Res* **15**(1), 10–17 (2016)
 34. F. Rogti, M. Ferhat, Maxwell–Wagner polarization and interfacial charge at the multi-layers of thermoplastic polymers. *J. Electrostat.* **72**(1), 91–97 (2014)

Effect of Homeopathic Dilutions of *Cuprum Arsenicosum* on the Electrical Properties of Poly(Vinylidene Fluoride-Co-Hexafluoropropylene)

Anandalal Gayen^{1,2} Dheeraj Mondal² Poonam Bandyopadhyay^{1,2} Debbethi Bera¹
 Durga Sankar Bhar¹ Sukhen Das^{1,2} Raj Kumar Manchanda³ Anil Kumar Khurana³ Debadatta Nayak³
 Biplab Kumar Paul⁴ Papiya Nandy¹

¹ Centre for Interdisciplinary Research and Education, Kolkata, West Bengal, India

² Department of Physics, Jadavpur University, Kolkata, West Bengal, India

³ Central Council for Research in Homeopathy, New Delhi, India

⁴ CSIR-Central Glass and Ceramic Research Institute, Non-Oxide Ceramics and Composites Division (NOCCD), Kolkata, West Bengal, India

Address for correspondence Papiya Nandy, PhD, Centre for Interdisciplinary Research and Education, Kolkata 700 068, West Bengal, India (e-mail: pnandy00@gmail.com).

Homeopathy

Abstract

Background We report the effects of nanoparticles in homeopathic preparations of copper salts on the electrical properties of polymer film. Previous work showed that the incorporation of metal-derived homeopathic medicines increases the dielectric constant and alternating current (AC) conductivity of an electroactive polymer film that is commonly used as a capacitor in the electronic industry.

We report here the effect of dilution of one homeopathic medicine, *Cuprum arsenicosum* (*CuAs*), at 200C potency on the electrical properties of the polymer film of poly (vinylidene fluoride-co-hexafluoropropylene).

Methods *CuAs* 200c was incorporated in the film by the solution casting method. The electrical characteristics were measured at different frequencies using an inductance, capacitance, and resistance meter. Fourier transform infrared spectroscopy (FTIR) was performed to detect phase change in the polymer film due to the incorporation of *CuAs*. Morphology and particle size were studied using field emission scanning electron microscopy (FESEM) and energy dispersive X-ray (EDX) spectroscopy.

Results At 10 kHz frequency, both dielectric constant and AC conductivity increased approximately 18 times for the polymer film when incorporated with 2 mL *CuAs* at 200C potency. FTIR indicated the increase in conducting phase, while FESEM and EDX confirmed the presence of spherical *CuAs* particles.

Conclusion The incorporation of *CuAs* in the electroactive polymer film enhances the conductivity and dielectric constant. We conclude that these changes arise from the change in phase of the polymer film, and because of the presence of two different metals that affects the interfacial polarization.

Keywords

- homeopathic medicine
- nanoparticles
- electrical properties
- polymer film

received
 September 26, 2016
 accepted
 December 30, 2017

Copyright © The Faculty of Homeopathy DOI <https://doi.org/10.1055/s-0038-1626733>.
 ISSN 1475-4916.

Introduction

Homoeopathic medicine is one of the world's most widely practiced complementary therapies. However, the mechanism of action of these medicines at very high dilution remains a puzzle to the conventional scientific community. Several theories have been advanced, but are yet to be confirmed.

Succession, an integral part of preparing homeopathic medicines, transfers mechanical energy to the solution,¹ causing the size reduction of the original aggregated drug particles to the nano-dimension.² We have previously shown that the permeability of drugs of nano-dimension through the membrane is a function of the potency.^{3–5} Our research and those of other groups have demonstrated the formation of nanoparticles at high homeopathic dilutions.^{6–10} We believe that this nanoparticle formation is a major clue to understanding the behavior of the homeopathic medicine at ultramolecular dilution.

We have investigated the nanoparticle aspect of homeopathic dilutions further, using them in several technological applications. In one case, we have shown that thermovoltage and photo-voltage generation are enhanced with the homeopathic medicine *Zincum oxydatum* (ZnO).^{11–14} This finding may have important implications in solar energy conversion.

In another case, to improve the electrical properties of electroactive polymer films, which have been commercially used in recent times as an alternative for traditional electroactive ceramics for technological applications, we have explored a novel method of exploiting the nanoparticle aspect of homeopathic medicines. By incorporating homeopathic dilutions including *Ferrum metallicum* (FeM), *Cuprum metallicum* (CuM), *Cobaltum metallicum* (CoM), and ZnO in the polymer matrix of poly(vinylidene fluoride-co-hexafluoropropylene) (PVDF-HFP), we were able to improve the electrical properties of these polymers, enhancing the dielectric constant and alternating current (AC) conductivity, followed by decrease in tangent loss of these electroactive polymer films.^{15–22}

We report here how these enhanced electrical properties of the polymer film can be further improved by incorporating *Cuprum arsenicosum* (CuAs) nanoparticles at different proportions in the polymer matrix. At 10 kHz frequency, for example, both dielectric constant and AC conductivity increased approximately 18 times for polymer film incorporated with 2 mL of CuAs at 200 C potency compared with the undoped film.

Methods

Solution Casting Method

To synthesize CuAs nanoparticles incorporated PVDF-HFP films, freshly prepared CuAs at 200C potency was obtained from the Hahnemann Publishing Company, India. PVDF-HFP pellets were supplied by Sigma Aldrich, United States, and dimethyl sulfoxide (DMSO) from Merck, Germany.

The CuAs-doped nanocomposites were synthesized by the solution-casting method (see ►Fig. 1). In a typical synthesis, 100 mg of PVDF-HFP was added to 2 mL of DMSO and mixed together with vigorous stirring at 60°C for 3 hours. Measured amounts of CuAs were added to the solution. All the composite films were obtained by casting the whole mixture in clean dry Petri dishes and evaporating the solvent in an oven at 60°C for 12 hours. As DMSO cannot be totally removed, we did all our measurements with the residual DMSO. The films were then coated by silver paste on both sides for electrical measurements. The synthesized films had a thickness in the range of 50 to 55 µm as measured using a digital screw gauge.^{19–22}

Electrical Characteristics, Phase Change, Morphology, and Particle Size

The electrical characteristics were measured at different frequencies using an inductance, capacitance and resistance (LCR) meter (HP Model 4274 A, Hewlett-Packard, United States).²³ Fourier transform infrared spectroscopy (FTIR) (FTIR-8400S, Shimadzu) was performed to detect phase change in the polymer film due to the incorporation of CuAs.^{15,19–22} Morphology, particle size, and energy dispersive X-ray (EDX) spectroscopy were studied using field emission scanning electron microscopy (FESEM) (ZEISS Sigma 300).

Synthesized sample details and codes are given below. Particular colors and numbers in ►Figs. 2, 3, 4, and 5 were used to identify the samples.

Sample code 0: 100 mg PVDF + 2 mL DMSO + 0 mL CuAs

Sample code 0.1: 100 mg PVDF + 2 mL DMSO + 0.1 mL CuAs

Sample code 0.5: 100 mg PVDF + 2 mL DMSO + 0.5 mL CuAs

Sample code 2.0: 100 mg PVDF + 2 mL DMSO + 2.0 mL CuAs

Sample code 5.0: 100 mg PVDF + 2 mL DMSO + 5.0 mL CuAs

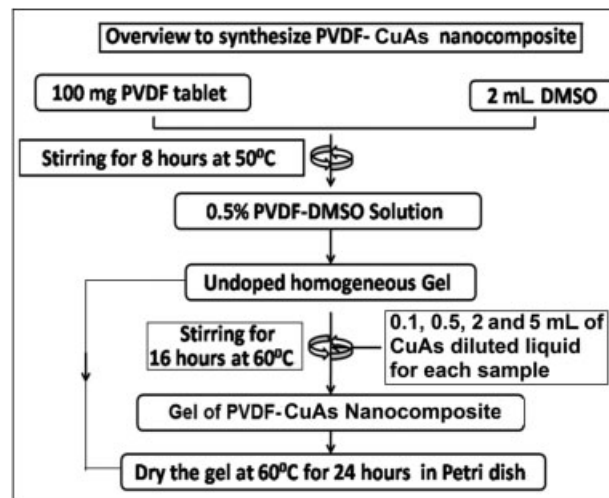


Fig. 1 Flowchart to synthesize PVDF-CuAs homeopathic medicine nanocomposite films. DMSO, dimethyl sulfoxide. PVDF-CuAs, poly(vinylidene fluoride-Cuprum arsenicosum).

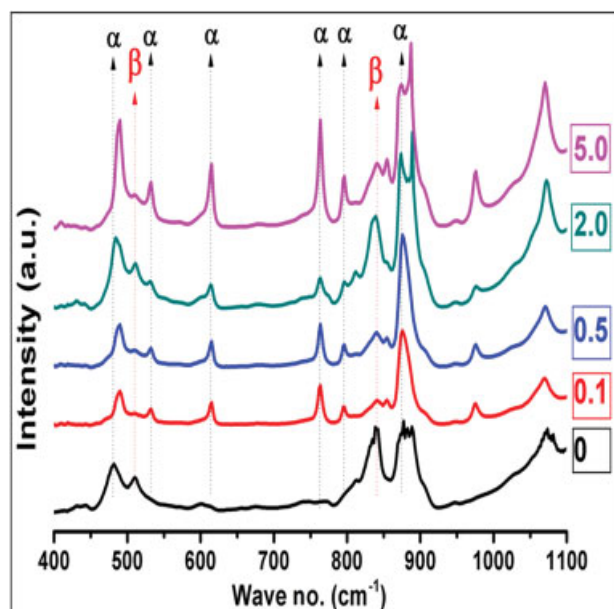


Fig. 2 Phase identification and confirmation study by FTIR of all the samples. FTIR, Fourier transform infrared spectroscopy.

Results and Discussion

FTIR Analysis

Phase identification and confirmation studies were performed by FTIR. ➤ **Fig. 2** shows the FTIR spectroscopic pattern in the range of 400 to 1,100 cm^{-1} of all CuAs doped PVDF-HFP nanocomposite films. The FTIR spectra show the characteristic absorbance bands at 487, 530, 615, 763, 795, and 875 cm^{-1} corresponding to the α -phase and around 512 and 842 cm^{-1} corresponding to the β -phase. From FTIR spectra, we observe a variation in phase intensity of α -

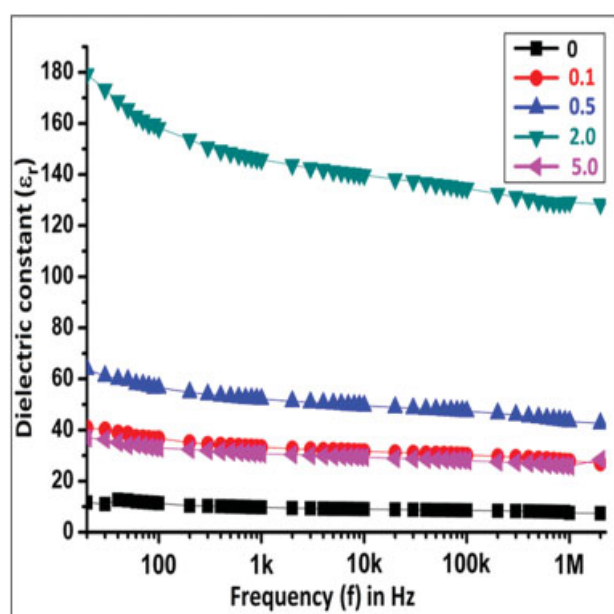


Fig. 3 Variation of dielectric constant with frequency for all CuAs incorporated PVDF films. See also ➤ **Table 1**. CuAs, *Cuprum arsenicosum*, PVDF, poly(vinylidene fluoride).

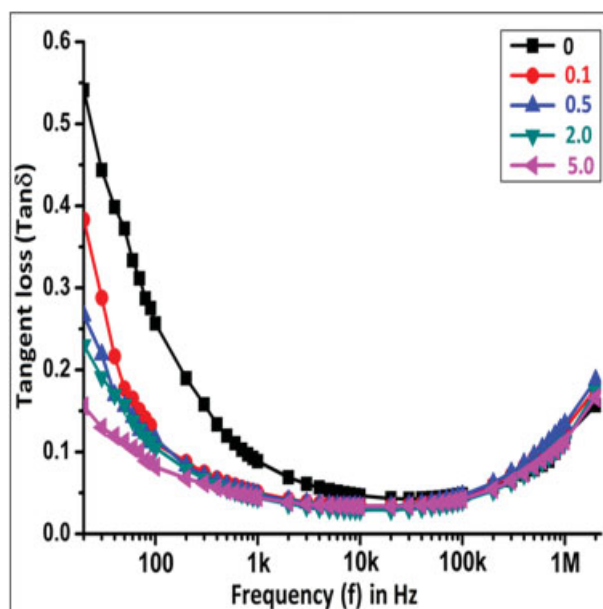


Fig. 4 Variation of tangent loss with frequency for all CuAs incorporated PVDF films. CuAs, *Cuprum arsenicosum*; PVDF, poly(vinylidene fluoride).

and β -phases which confirms chemical interaction between the CuAs nanoparticles with the polymer film.^{15,19–22} From ➤ **Fig. 2** it is also confirmed that, with increase in concentration of CuAs, the β -phase peaks have grown significantly compared with the pure PVDF-HFP and reached maximum for 2 mL insertion, which signifies that the best effective interaction occurred between the CuAs nanoparticle and PVDF matrix at this concentration. With further insertion of CuAs nanoparticles, the phase intensity decreased because of the network destruction. This was confirmed by FESEM (➤ **Fig. 6**).

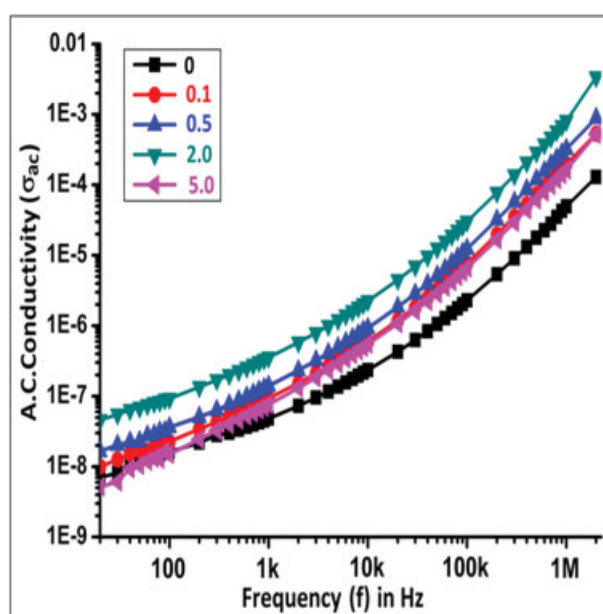


Fig. 5 Variation of AC conductivity (Siemens/meter) with frequency for all CuAs incorporated PVDF films. See also ➤ **Table 1**. CuAs, *Cuprum arsenicosum*, PVDF, poly(vinylidene fluoride).

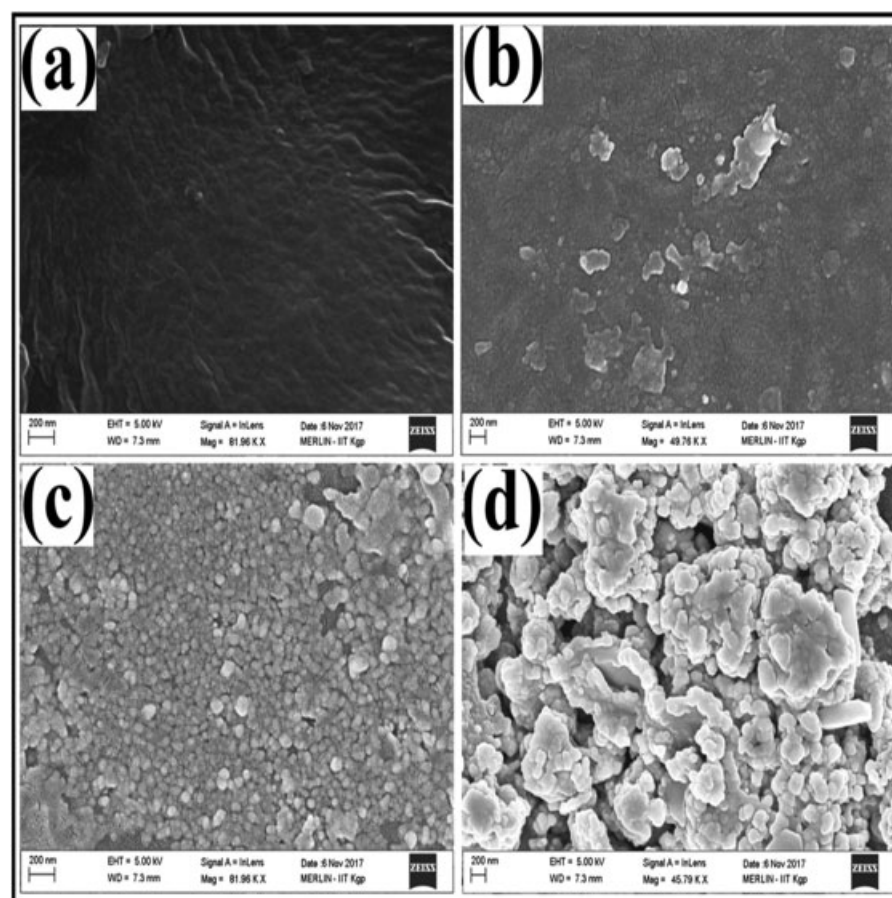


Fig. 6 Morphology and microstructural analysis of (a) 0, (b) 0.5, (c) 2.0, and (d) 5.0 CuAs incorporated PVDF films by FESEM. CuAs, *Cuprum arsenicosum*, FESEM, field emission scanning electron microscopy; PVDF, poly(vinylidene fluoride).

Field Emission Scanning Electron Microscopy Analysis

We examined the particle size and morphology of CuAs-incorporated PVDF films with FESEM (►Fig. 6). The figure depicts the microstructures in the polymer film of the five samples of (a) pure PVDF-HFP, (b) 0.5 mL, (c) 2 mL, and (d) 5 mL doping concentration of CuAs incorporated in the polymer films. The result shows the presence of several morphology and microstructures of CuAs incorporated in the polymer samples. For lower insertion concentration (0.5 mL), a small number of spherical shaped nanoparticles are seen to be embedded in the PVDF-HFP matrix. A large number of spherical shaped CuAs nanoparticles, homogenously distributed and densely packed in the polymer matrix, are observed for the doping concentration of 2 mL. For further increase in doping concentration, evidence of a large number of agglomerated nanoparticles embedded in the polymer matrix is observed. The clear presence of homeopathic medicines of such low dimension in the polymer matrix indicates existence of nanoparticles.^{15,19–22}

Energy Dispersive X-ray Spectroscopy and Elemental Analysis

Elemental mapping images of CuAs compound nanoparticle-incorporated PVDF-HFP composite film were performed from EDX measurements.

►Fig. 7A shows the EDX spectrum of 0.5 mL incorporated PVDF-HFP composite films. The EDX images confirm the presence of copper and arsenic along with polymeric elements into the composite system. Elements obtained from EDX study, with their normality as well as weight percentages, are shown in ►Fig. 7 (tabulated insert). Presence of low atomic percentage of copper and arsenic is the evidence of ultra-high dilution of metallic element present in the CuAs-PVDF matrix. ►Fig. 7B shows the selected region of the composite films and ►Fig. 7C–F confirmed that all the elements present in the composite films are homogenously distributed in the sample.

Study of Electrical Properties of Polyvinyl Film PVDF-HFP

We studied the following electrical properties of CuAs-doped PVDF-HFP with the help of an LCR instrument and compared with that of the pure PVDF film.

Dielectric Constant

Dielectric property (ϵ_r) of a material is its ability to be polarized by an applied electric field and can be calculated as,

$$\epsilon_r = c_p d / (A \epsilon_0)$$

where, c_p is the charge stored in the material, d is the thickness of the plate or film, A is the area of the sample, and ϵ_0 is the permittivity in free space.

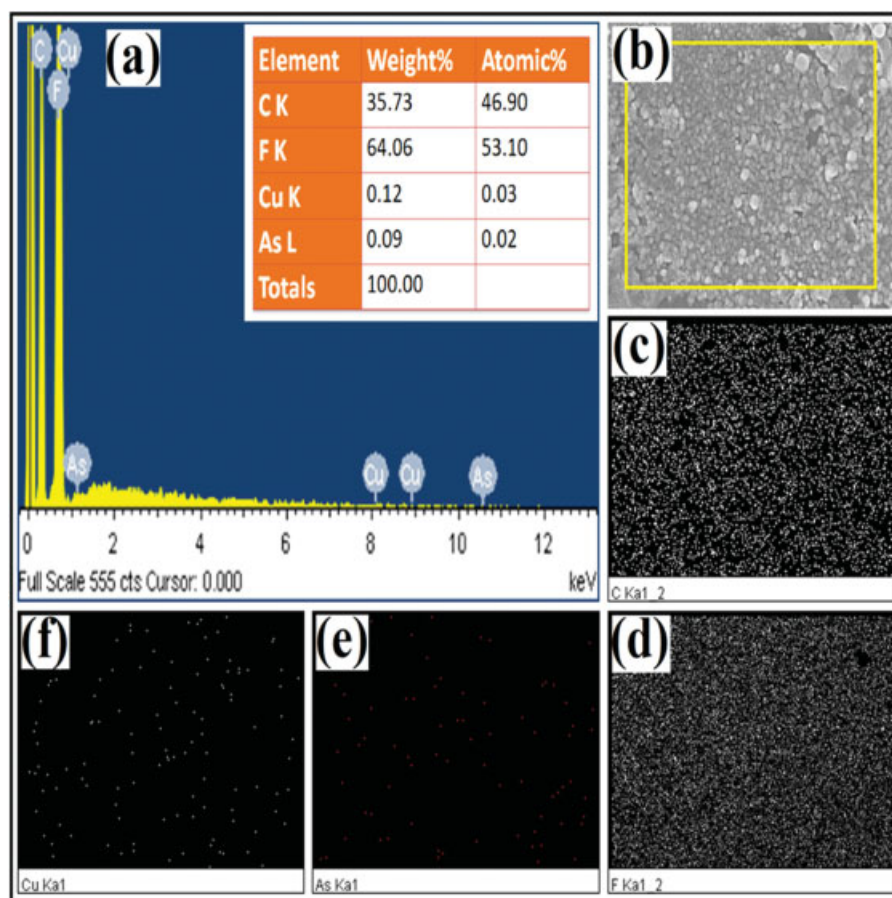


Fig. 7 (a) Elemental confirmation of all elements present in the 2 mL CuAs incorporated PVDF film by EDX spectra (C, Carbon; Cu, Copper; F, Fluorine; As, Arsenic); (b) selected area for measurement; and (c–f) elemental mapping image (c) Carbon, (d) Fluorine, (e) Arsenic, and (f) Copper of 2 mL CuAs-doped PVDF-HFP film. K, L, and Ka 1 refer respectively to the K-band, L-band, and K α -band of the X-ray beam used for the EDX spectroscopy. CuAs, *Cuprum arsenicosum*, EDX, energy dispersive X-ray; PVDF-HFP, poly(vinylidene fluoride-co-hexafluoropropylene).

The variation in dielectric constant with frequency for all films clearly shows that within the frequency range 20 Hz to 2 MHz, the dielectric constant continuously decreases with increasing frequency (►Fig. 3). It has substantially higher values throughout the whole frequency range for all films doped with CuAs, compared with the pure polymer film. The value increases with increasing concentration of CuAs and at a certain concentration (2 mL) it becomes maximum at approximately 18-fold compared with the 0-mL sample (►Table 1); this effect is due to Maxwell–Wagner–Sillars interfacial polarization¹⁵ followed by maximum interfacing area per unit volume. Upon further increasing the doping concentration, the value of dielectric constant decreases due to the decreasing of their inter-particle distance or agglomeration. As the frequency is increased further, dipole response is limited and the dielectric constant has a saturation tendency.^{19–22}

Tangent Loss

The tangent loss ($\tan \delta$) of a medium includes dielectric damping loss and conductivity loss of the material and is the ratio of conduction current and displacement current. This loss quantifies a dielectric material's inherent dissipa-

tion of electromagnetic energy (e.g., heat) and can be calculated as

$$\tan \delta = \epsilon''/\epsilon'$$

where, ϵ'' is the imaginary part of permittivity and ϵ' is the real part of permittivity.

Table 1 Variation in dielectric constant and AC conductivity of polymer film due to incorporation of CuAs at 10 kHz frequency

Dielectric constant (►Fig. 3)		
For Sample 0	For sample 2.0	Increase by factor
8.3	146	17.6–18.0
AC conductivity (►Fig. 5)		
For Sample 0	For sample 2.0	Increase by factor
1.8×10^{-7} Siemens/meter	3.2×10^{-6} Siemens/meter	17.8–18.0

Abbreviations: AC, alternating current; CuAs, *Cuprum arsenicosum*.

Note: The LCR meter records data in a continuous way: the data are not taken individually at each point. From the graphs (►Figs. 3 and 5), an approximate value was therefore taken.

The variation in tangent loss with frequency for all homeo-polymer films clearly shows that, throughout the frequency range, tangent loss continuously decreases with increasing frequency for all films up to 10 kHz (►Fig. 4). At comparatively lower frequency, more tangent loss is observed due to higher polarization effect followed by more relaxation time. As frequency increases within 10 kHz, polarization effect reduces further due to less relaxation time and inter-molecular friction or vibration diminishes, which is responsible for the decrease in tangent loss. However, after 10 kHz the tangent loss increases, perhaps due to the heat generation followed by more inter-molecular vibration or leakage current.^{15,19–22}

Electrical Conductivity

Electrical conductivity ($\sigma_{a.c.}$) is an intrinsic property of a material that indicates how strongly a given material allows the flow of electric current. It is commonly represented by the Greek letter σ (sigma) and is calculated using the formula,

$$\sigma_{a.c.} = 2\pi f \tan\delta \epsilon_r \epsilon_0,$$

where $\sigma_{a.c.}$, f , $\tan\delta$, ϵ_r , and ϵ_0 are the AC conductivity, frequency in Hz, tangent loss factor, dielectric constant of the material, and vacuum permittivity, respectively.

Measurements of AC conductivity have been widely used to investigate the nature of ionic motion in ionically conducting materials since it is assumed that they are responsible for this type of conduction. Our results (►Fig. 5) show that the AC conductivity increases exponentially with frequency for all homeo-polymer films. This arises due to increase in hopping of conducting electrons present in the homeo-polymer films.²³ For a given frequency, enhanced AC conductance is evident in films with higher concentrations of CuAs: at 10 kHz, for example, there is approximately 18-fold greater AC conductance for the 2 mL sample than for the 0 mL sample (►Table 1). At higher frequency ranges, the rapid increase in conductivity with increasing frequency is referred to as the electronic polarization effect. The increase in conductivity with frequency also arises due to the presence of free metallic ions in the polymer matrix.^{15,19–22}

Conclusion

Here we have shown that by the incorporation of CuAs at 200C potency in the film of polymer PVDF-HFP, the electrical properties, namely dielectric constant and electrical conductivity measured at 10 kHz frequency, increase by approximately 18 times compared with those of the pure polymer film.

The enhancement of dielectric constant results from the presence of two different metallic nanoparticles in the composite film. Also, the incorporation of CuAs induces a phase change in the polymer film, as is evident from the FTIR spectrum, which is responsible for the enhancement of AC conductivity.

A logical conclusion from these observations is that these homeopathic medicines are more than just alcohol or water: their inherent electrical property is responsible for their effect on different physical processes. And through our experiments, we have shown that the important and unquantifiable effects of homeopathic medicines can be connected with the latest quantifiable technology, potentially opening up a whole new era of research in homeopathy.

Acknowledgment

The authors are thankful to the Central Council for Research in Homeopathy (CCRH), the Ministry of AYUSH, Government of India, for providing the financial assistance. The study was undertaken in joint collaboration between the Centre for Interdisciplinary Research and Education (CIRE), Kolkata, and CCRH, New Delhi.

References

- Shah R. Standardization of the potentizing machine and quantification of impact of potentisation. *Ind J Res Homoeopathy* 2016; 10:126–132
- Upadhyay RP, Nayak C. Homoeopathy emerging as nanomedicine. *Int J High Dilution Res*. 2011;10:299–310
- Nandy P, Bhandary S, Das S, Basu R, Bhattacharya S. Nanoparticles and membrane anisotropy. *Homeopathy* 2011;100:194
- Ghosh S, Chakraborty M, Das S, Basu R, Nandy P. Effect of different potencies of nanomedicine *Cuprum metallicum* on membrane fluidity – a biophysical study. *Am J Homeopathic Medicine* 2014; 107:161–169
- Bhandary S, Das S, Basu R, Bhattacharyya S, Nandy P. Effect of *Aconitum napellus* on liposomal microviscosity. *Int J Emerg Technol Sci Eng* 2011;3:1–5
- Kar S, Bandyopadhyay P, Chakraborty S, et al. Derivation of an empirical relation between the size of the nanoparticle and the potency of homeopathic medicines. *Int J High Dilution Res* 2015; 14:2–7
- Nandy P. A review of basic research on homeopathy from a physicist's point of view. *Ind J Res Homoeopathy* 2015;9:141–151
- Chikramane PS, Kalita D, Suresh AK, Kane SG, Bellare JR. Why extreme dilutions reach non-zero asymptotes: a nanoparticulate hypothesis based on froth flotation. *Langmuir* 2012;28:15864–15875
- Chikramane PS, Suresh AK, Bellare JR, Kane SG. Extreme homeopathic dilutions retain starting materials: a nanoparticulate perspective. *Homeopathy* 2010;99:231–242
- Rajendran ES. Field emission scanning electron microscopic (FESEM) and energy dispersive spectroscopic (EDS) studies of centesimal scale potencies of the homeopathic drug *Lycopodium clavatum*. *Am J Homeopath Med* 2015;108:9–18
- Bandyopadhyay P, Nandy P, Basu R, Bhar DS, Das S. Effect of dilution on thermovoltage generation using homeopathic nanomedicine *Zincum oxydatum*. *Int J Innov Res Sci Eng* 2015;3:225–230
- Bandyopadhyay P, Nandy P, Basu R, Bhar DS, Das S. Thermovoltage generation using homeopathic medicine. *Ind Photobiol News Lett* 2016;53:13–16
- Bandyopadhyay P, Chakraborty S, Basu R, et al. Efficiency of a dye-sensitized photo-electrochemical device using thionine and trituated zinc oxide at different potency. *Energy Sourc A, Recovery Util Environ Effects* 2016. In press
- Mondal A, Basu R, Das S, Nandy P. Increased quantum efficiency in hybrid photoelectrochemical cell consisting of thionine and zinc oxide nanoparticles. *J Photochem Photobiol Chem* 2010;211: 143–146

- 15 Martins P, Lopes AC, Lanceros-Mendez S. Electroactive phases of poly(vinylidene fluoride): determination, processing and applications. *Prog Polym Sci* 2013;39:683–706
- 16 Nalwa HS. *Handbook of Low and High Dielectric Constant Materials and Their Applications*, Volume 1: Materials and Processing. 1st ed. San Diego, CA: Academic Press; 1999
- 17 Kingon AI, Maria JP, Streiffer SK. Alternative dielectrics to silicon dioxide for memory and logic devices. *Nature* 2000;406:1032–1038
- 18 Singh R, Ulrich RK. High and low dielectric constant materials. *Electrochem Soc Interface* 1999;8:26–30
- 19 Chatterjee A, Paul BK, Kar S, et al. Effect of ultrahigh diluted homeopathic medicines on the electrical properties of PVDF-HFP. *Int J High Dilution Res* 2016;15:10–17
- 20 Paul BK, Kar S, Bandyopadhyay P, et al. Significant enhancement of dielectric and conducting properties of electroactive polymer polyvinylidene fluoride films: an innovative use of *Ferrum metallicum* at different concentrations. *Ind J Res Homoeopathy* 2016;10:52–58
- 21 Gayen AL, Paul BK, Roy D, et al. Enhanced dielectric properties and conductivity of triturated copper and cobalt nanoparticles-doped PVDF-HFP film and their possible use in electronic industry. *J Material Res Innovations* 2017;21:166–171
- 22 Gayen AL, Mondal D, Roy D, et al. Improvisation of electrical properties of PVDF-HFP: use of novel metallic nanoparticles. *J Mater Sci Mater Electron* 2017;28:14798–14808
- 23 Jonscher AK. Dielectric relaxation in solids. *J Phys D Appl Phys* 1999;32:R57–R70

Effect of *Cuprum metallicum* potentised through both serial dilution and succussion in comparison to succussion alone on *Escherichia coli* bacterial system and electrical properties of poly (vinylidene fluoride-co-hexafluoropropylene) polymer

A. L. Gayen¹, D. Mondal², D. Bera¹, P. Biswas², B. K. Paul², D. S. Bhar¹, S. Das^{1,2}, R. Narula³, A. K. Khurana³, R. K. Manchanda³, P. Nandy^{1*}

¹Centre for Interdisciplinary Research and Education, Kolkata, West Bengal, ²Physics Department, Jadavpur University, Kolkata, West Bengal,

³Central Council for Research in Homeopathy, New Delhi, India

Abstract

Background: Homoeopathic medicines are traditionally potentized by serial dilution followed by succussion. Respective roles of these two components need to be assessed and explored for which the present study was undertaken. **Objective:** To compare the effect of the medicine *Cuprum metallicum* (*Cup. met.*) potentised through both serial dilution and succussion with succussion alone on selected biological and physical systems. **Method:** Starting with the medicine *Cup. met.* at 6C, we potentized it further to 30C and 200C by serial dilution, followed by succussion (Set A). The same medicine at 6C was also potentized to 30C and 200C by using succussion alone (Set B). The antibacterial property of these two sets was compared on *E. coli*, a biological system and electrical properties on polymer matrix PVDF-HFP (widely used as charge separator) a physical system. **Results:** Field Emission Scanning Electron Microscopy shows that the particles get more agglomerated at higher potency in Set B. Antibacterial effect of *Cup. met.* in Set B at 30C and 200C was observed to be more significant as compared to Set A. Effect of *Cup. met.* on polymer matrix in Set A varied significantly with the potency as compared to Set B wherein less beta phase crystallization was produced followed by no significant change in electrical properties. **Conclusion:** Comparison of results using the medicine *Cup. met.* in two experimental set ups shows that serial dilution with succussion makes an important difference between the two sets.

Keywords: *Cuprum metallicum*, *Escherichia coli*, Polymer film, Potentisation, Serial dilution, Succussion

INTRODUCTION

Homoeopathic potentisation of Hahnemannian era constituted of serial dilution followed by either trituration or succussion or both depending on the type of drug substances. In the preparation of potencies from solid drug substances, decimal and centesimal scales are used. In the preparation of liquid drug substances, manufacturing of homoeopathic medicines is from the mother solution (tincture) by serial dilution and succussion (mechanical agitations) in one of the three potency ranges, decimal (1:9), centesimal (1:99), or fifty-millesimal. Solid insoluble materials (e.g., *Cuprum metallicum* [*Cup. met.*]) are triturated with lactose in the ratio of 1:10 till the 6X potency, after which, the liquid dilutions are carried out. The liquid dilutions are prepared by the Hahnemannian method^[1] till the 200C potency and the Korsakovian method for potencies beyond 200C.

Potentisation, the most vital part of preparation of homoeopathic medicine, transforms the starting material to a therapeutically active one. It has got two components: (a) Serial dilution and (b) vigorous vertical jerking, known as succussion.

The paradox created debate between practicing homoeopaths and rationalists, as they felt that there is no medicine present

***Address for correspondence:** Dr. P. Nandy,
Centre for Interdisciplinary Research and Education,
Kolkata - 700 068, West Bengal, India.
E-mail: pnandy00@gmail.com

Received: 02.08.2019; **Accepted:** 28.11.2019; **Published:** 27.12.2019.

This is an open access journal, and articles are distributed under the terms of the Creative Commons Attribution-NonCommercial-ShareAlike 4.0 License, which allows others to remix, tweak, and build upon the work non-commercially, as long as appropriate credit is given and the new creations are licensed under the identical terms.

For reprints contact: reprints@medknow.com

How to cite this article: Gayen AL, Mondal D, Bera D, Biswas P, Paul BK, Bhar DS, et al. Effect of *Cuprum metallicum* potentised through both serial dilution and succussion in comparison to succussion alone on *Escherichia coli* bacterial system and electrical properties of poly (vinylidene fluoride-co-hexafluoropropylene) polymer. Indian J Res Homoeopathy 2019;13:209-18.

Access this article online

Quick Response Code:



Website:
www.ijrh.org

DOI:
10.4103/ijrh.ijrh_60_19

at very high dilution.^[2] However, as the effectiveness of high potencies is experienced by the practicing homoeopaths and countless patients, more positive opinions started accumulating, backed by different models, in favour of the therapeutic effect of these medicines at high potency.

The question naturally arises, why do, in the preparation of homoeopathic medicine, we dilute instead of concentrating.^[3] We have, for the first time, shown that there is a difference between the effects of two kinds of potentisation: serial dilution, followed by succussion, and only succussion.

Recently, it has been realised that it is not only the dilution, but the succussion followed after each dilution, which is responsible for these effects at high potency. By means of vigorous shaking, a large amount of mechanical energy is transferred, This energy breaks the drug associates and reduces the size to nanodimension.^[4-6] This reduction in size increases membrane permeability.^[7]

The empirical relation between potency (X) and the size of the drug aggregates (Y) is given by the following equation:^[8]

$$Y = aX^{-n}$$

Where *a* and *n* are characteristic constants of different medicine.

It has been experimentally proven that extreme homoeopathic dilutions retain starting materials.^[9] To understand the extreme dilutions from a biological perspective, it has been shown that metal concentration as low as fg/ml increases the intracellular protein synthesis.^[10] It has also been shown that the particles develop a coat of silica, and a hypothesis has been proposed that all types of metal and inorganic salt-based homoeopathic medicines consist of silicate-coated nanostructures dispersed in the solvent.^[11]

Hence, the term potentisation indicates the qualitative and quantitative increase in medicinal power as compared to mere dilution. And thus, Homoeopathy is seen as nanomedicine.^[12] The increase of the activity of the drug with potentisation arises as the surface area increases manifold and the number of points of contact with the living fibre increases. At the same time, the process of succussion is responsible for inducing electrical nature due to domain formation as predicted by quantum electrodynamics (QED). Due to this, the physicochemical properties of the vehicle medium change drastically, as the effect of QED starts playing a major role.^[13-18]

According to Hahnemann, a small dose of medicine, when potentised, is also very powerful. This not only reduces the toxic effect of overdose but also forms intimate mixture of the medicine with the vehicle due to vigorous shaking. This is intended to avoid aggravation of the disease and increase the activity of the medicine as the medicine acts '*not atomically but dynamically*'. Dilution is essential for getting the dynamising effect of succussion and that '*all the shaking in the world will not dynamize an undiluted substance*'.

Thus, potentisation (dilution, followed by succussion) affects both the drug material of a homoeopathic medicine and the medium as follows:

- From *classical point of view*, due to succussion, the drug material achieves nanodimension and nanoparticles are formed. This reduces the toxic effect and increases the activity due to the increase in aspect ratio^[4-8]
- From *quantum mechanical point of view*, it changes the electrical nature of the polar medium through the formation of coherent domains of the solvent molecules, which provides quasi-free electrons and increases the stored electrical energy of the medium.^[13-18]

This establishes the electrical nature and the mode of action of homoeopathic medicine. Perhaps, this electrical energy which is stored in the system is the so-called dynamic power of the homoeopathic medicine as envisaged by Dr. Hahnemann.

The question then naturally arises is, as to how to compare the role of dilution and succussion in potentiating a medicine. In the present study, the experiment is conducted to observe and compare the effect of serial dilution and succussion to succussion alone using homoeopathic medicine, *Cup. met.* on the biological and physical systems, whereas in our earlier study,^[7] the standard potentised *Cup. met.* has been used. This medicine is used because of its good dispersion in different polymers and good antibacterial and conductive properties which can be utilised as a dielectric charge separator in high charge storage system. In addition, the formation of the film using this polymer is an easy, low-cost and simple solution casting technique.

METHODS

For both the biological and physical systems, we have used control, where *Cup. met.* was not used. That the presence of the drug is responsible for the observed effect is justified as the vehicle medium of 91% ethanol had been evaporated in both cases within a very short span of time. Hence, the presence of drug only is responsible for the observed effects.

Preparation of the two sets of homoeopathic medicine

For making potencies by trituration with lactose in porcelain mortar and pestle, a mechanical device manufactured by F. Kurt Retsch KG from Germany was used. During potentisation in centesimal scale with ethyl alcohol, each step of potentisation was done manually in neutral (USP III) glass bottles using new bottle in each step. The whole operation was done following the Good Manufacturing Practice.

Potencies of *Cup. met.* were prepared from pure copper powder, first by trituration with lactose up to 6X potency, converting the same into liquid 8X (=4C) potency and potentiating the 4C potency by dilution (with 91% ethanol) followed by succussion up to 6C potency. This 6C potency was taken as the starting material for our study.^[19]

Set A: The potencies of *Cup. met.* were prepared in the method described in the Homoeopathic Pharmacopoeia of India

(HPI). The method may be elaborated as one part of copper metal powder (99.6% pure) was triturated mechanically with 9 parts of 80 mesh lactose powder of pharmacopoeial (HPI, British Homoeopathic Pharmacopoeia [BHP] and United States Homoeopathic Pharmacopoeia [HPUS]) quality for 1 h to produce 1X potency. The same 1X potency of *Cup. met.* was again triturated with lactose in the same way and proportion to yield 2X potency. This method of trituration was continued till we got 6X potency of *Cup. met.*

One part by weight of this *Cup. met.* 6X was dissolved in 50 parts by volume of distilled water (purified water of HPI/BHP/HPUS standard) to which 50 parts by volume of ethyl alcohol (91%) was added, and the mixture was given ten succussions to get 8X (=4C) potency. Henceforth, potentisation was done by diluting one part of the previous potency with 99 parts of ethyl alcohol and giving the mixture ten succussions (shaking strongly with downwards stroke) always in a new glass bottle, one-third volume of which was kept empty for proper shaking, to get the next potency in centesimal scale. This process of serial dilution and succussion was carried out till 6C initially, as 6C is taken as the starting material in both the groups (Set A and Set B).

- Set A: Serial dilution and succussion was carried out as stated above till 200C as per the standard method of potentisation
- Set B: Here starting from 6C potency, further potentisation was done without further dilution by succussing the 6C potency, making it equivalent to 30 and then further succussion to make it equivalent to 200C potency.

The schematic diagram for the preparation of these two sets of medicine is shown in Figure 1.

Effects of these two sets of potentised medicines were compared for the antibacterial property on Gram-negative bacteria *Escherichia coli*^[20] and on the electrical properties of a polymer matrix poly (vinylidene fluoride-co-hexafluoropropylene) (PVDF-HFP).^[21-24]

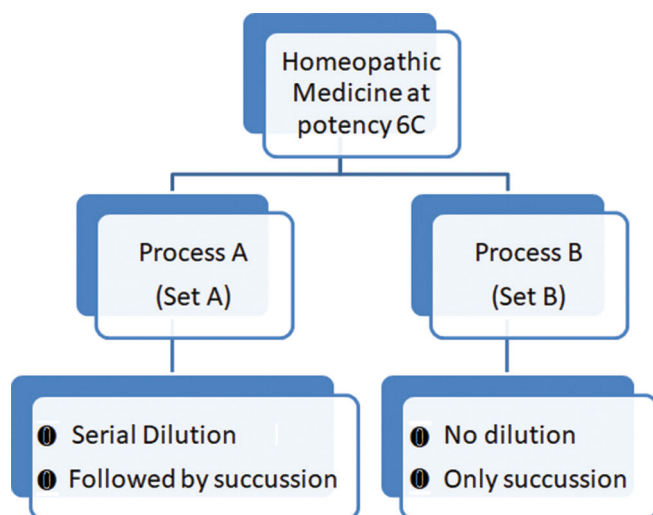


Figure 1: The two sets of potentisation: Set A and Set B

Antibacterial effect of *Cuprum metallicum*

Fresh culture of *E. coli* in nutrient broth was treated with *Cup. met.* at required potency, prepared as in Set A and Set B in 91% alcohol and left overnight.^[20] The alcohol was allowed to evaporate gradually. There was a possibility of the bacteria being affected by the alcohol present in the medicine. However, this effect should be same for all the potencies of the medicine used. And hence, it was inferred that the final outcome was the effect of the potency of the medicine.

The vehicle control was 91% alcohol. In order to make sure about the reproducibility, all the experiments with Set A and Set B at the potencies 6C, 30C and 200C were repeated at least 3–4 times.

Cuprum metallicum–poly (vinylidene fluoride-co-hexafluoropropylene) composite film preparation technique

The *Cuprum metallicum*-doped composite films were synthesised by low-cost and simple solution-casting fabrication technique. In a typical synthesis process, 100 mg of PVDF-HFP (Sigma Aldrich, USA, 3050 Spruce St., St. Louis, MO 63103, 400 Summit Drive, Burlington, MA 01803) was dissolved into 2 ml of dimethyl sulfoxide (Merck, India, 8th Floor, Godrej One, Pirojshanagar, Eastern Express Highway, Vikhroli (E) Mumbai - 400 079, India) and mixed together under vigorous stirring at 50°C for 4 h. Measured amount of freshly prepared *Cup. met.* at a specific potency was obtained from Hahnemann Publishing Company, India (Near Sealdah Fly-Over & Koley Mrkt, Kolkata, West Bengal 700012), and was added to the solution and stirred for another 2 h at 50°C. Afterwards, the whole solution was sonicated three times for 10 min each at 50°C with 30 min of time interval for the complete removal of the air bubbles from the solutions. Finally, films were obtained by casting the whole mixture in clean dry Petri dishes and solvent was evaporated in an oven at 80°C for 24 h. The films were then coated by silver paste on both sides for electrical measurements.^[21-24] The synthesised films had the thickness in the range of 50–55 µm as measured using a digital micrometer. The schematic diagram for the preparation of *Cup. met.* PVDF composite films is shown in Figure 2.

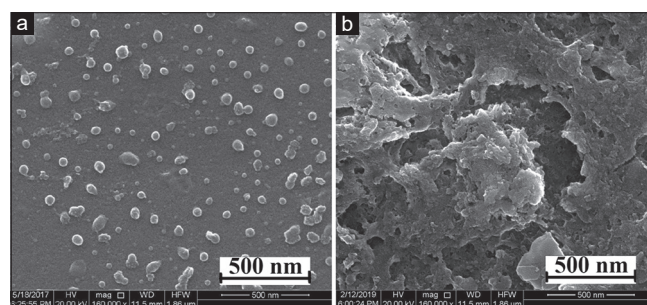


Figure 2: Field emission scanning electron microscope images of poly (vinylidene fluoride-co-hexafluoropropylene) doped 200C *Cup. met.* medicine of (a) Set A^[22] and (b) Set B

Field emission scanning electron microscope analysis of pure *Cuprum metallicum* medicine of Set A and Set B potentisation

To examine the microstructure, 20 drops of each medicine was dried in a cover slip and finally made to pass through the experiment under the microscope namely FEI-F50 (Netherlands).

Measurement of electrical properties

The dielectric properties were investigated using a LCR meter (HP model 4274A, Hewlett Packard, USA, 99 Washington Street, Melrose, MA 02176-6024). The dielectric constant (ϵ_r), tangent loss ($\tan\delta$) and AC conductivity (σ_{ac}) were recorded in the frequency range of 20 Hz–2 MHz at room temperature.

RESULTS

Field emission scanning electron microscope analysis of pure *Cuprum metallicum* medicine of Set A and Set B potentisation

The field emission scanning electron microscope (FESEM) microstructural overview of pure *Cup. met.* at 200C as obtained from two different potentisation processes of Set A and Set B is shown in Figure 3a and b, respectively. Figure 3a shows the morphology and microstructure of pristine 200C *Cup. met.* of Set A.^[22] The microstructure of the sample confirmed a very good and homogeneous distribution of the nanoparticles on the surface of the glass cover slip. The particles are more scattered, are well separated and also homogeneously distributed, maintaining an intermolecular distance. This is due to the very high dilution at 200C.

On the other hand, Figure 3b shows the microstructure and morphology of the pristine 200C *Cup. met.* of Set B, where only succussion is done without dilution. The microstructure of the sample confirmed an evidence of large number of densely packed agglomerated particles having very low dimension embedded in the surface of the glass cover slip.

In the dilute medium, particles are scattered [Figure 3a]. However, in the absence of dilution, nanoparticles created due to succussion get agglomerated [Figure 3b].

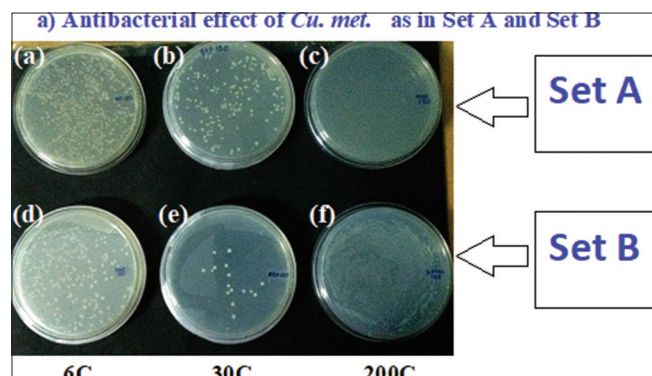


Figure 3: Antimicrobial effect of *Cup. met.* for Set A (a) 6C, (b) 30C and (c) 200C^[20] and Set B (d) 6C, (e) 30C and (f) 200C

Antibacterial effect of *Cuprum metallicum*

The antibacterial effect shown in Figure 4a (6C), Figure 4b (30C) and Figure 4c (200C) is for the potentised medicine *Cup. met.* namely as in Set A,^[20] whereas Figure 4d (6C), Figure 4e (30C) and Figure 4f (200C) are for Set B of *Cup. met.* From the figure, we realise that for Set A, the antibacterial effect is more for drug at 30C, compared to that for 6C.^[20] The effect becomes more for drug at 200C. The reason for this is perhaps as at higher potency, the size of the drug particles becomes smaller^[8] and the penetration through membrane barrier is more, giving rise to higher antibacterial effect.^[20]

In Set B, as there is no dilution, the amount of drug available is same for all potencies from 6C to 200C, a larger number of nanoparticles are produced by succussion and the antibacterial effect is more here for 30C and 200C compared to that in Set A.

For Set B, at 200C, the figure indicates that in the presence of significant number of drug molecules, a large number of nanoparticles are created through succussion, which agglomerate, as is evident from the FESEM, and are incapable to penetrate the bacterial membrane.

Field emission scanning electron microscope morphological investigation of poly (vinylidene fluoride-co-hexafluoropropylene)-*Cuprum metallicum* nanocomposite films

Figure 5a-c shows the evidence of densely packed and good dispersion of nanoparticles embedded in the polymer matrix. From the critical observation, it can be seen that with increasing potentisation, the polymer matrix had an increasing crystallisation and reached maximum enhancement of electroactive β -polymorph at 200C potency for the medicine of Set A.

Figure 6a and b shows the evidence of significant number of nanoparticles which got agglomerated at higher potency of Set B and embedded in the PVDF-HFP matrix. This is due to the high number of succussions at 30C and 200C.

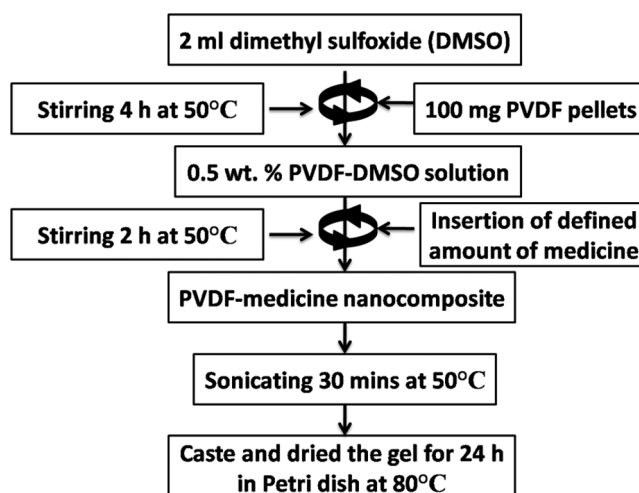


Figure 4: The schematic diagram for the preparation of *Cup. met.*-poly (vinylidene fluoride-co-hexafluoropropylene) composite films

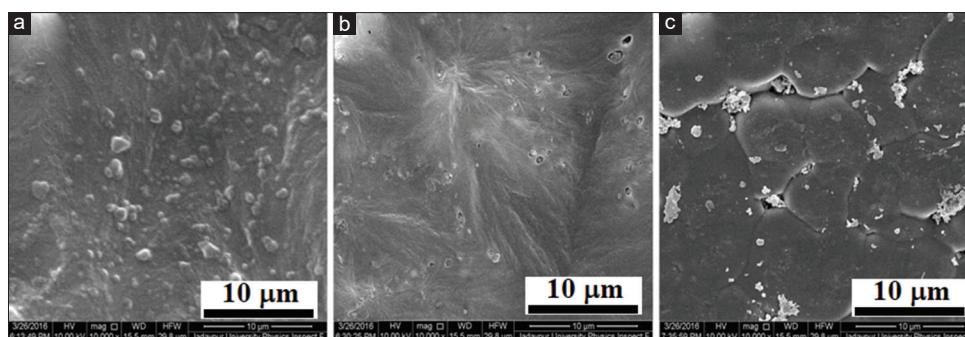


Figure 5: Field emission scanning electron microscope microstructural overview for Set A of poly (vinylidene fluoride-co-hexafluoropropylene) doped *Cuprum metallicum* (a) 6C, (b) 30C and (c) 200C^[22]

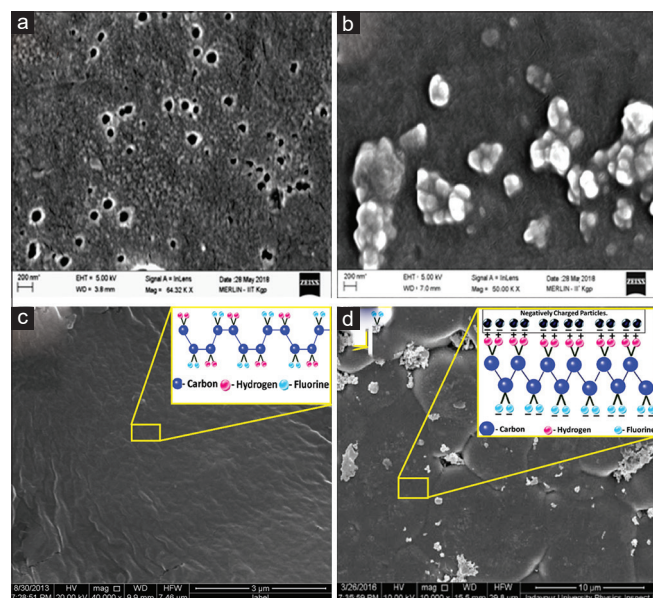


Figure 6: Field emission scanning electron microscope microstructural overview for Set B of poly (vinylidene fluoride-co-hexafluoropropylene) doped *Cup. met.* (a) 30C, (b) 200C and (c) microstructure of poly (vinylidene fluoride-co-hexafluoropropylene) doped *Cup. met.* of 200C and the crystal structure of α -polymorph (inset graph) and (d) microstructure of *Cup. met.* of 200C embedded poly (vinylidene fluoride-co-hexafluoropropylene) and the crystal structure of β -polymorph (inset graph).^[22] 6C is the starting material both for Set A and Set B and is not shown separately

Thus, from the FESEM investigation, it can be clearly concluded that, for the Set A medicine [dilution followed by succussion – Figure 5a-c], there is no significant agglomeration with very good dispersion and distribution due to high dilution of the medicine, whereas for the Set B medicine [without dilution, only succussion – Figure 6 (a and b)], there is agglomeration of embedded nanoparticles in the PVDF matrix, which results in less β -phase crystallisation. The inset graph of Figure 6c shows the crystalline α -polymorph where the hydrogen and fluorine dipoles are packed in antiparallel way with the carbon atoms, whereas the inset graph of Figure 6d shows the positively charged CH_2 dipoles of PVDF-HFP interacted with the negatively charged nanoparticles, leading to the alignment of stabilised β -chains which have been shown in

the inset graph of Figure 6d and Figure 7. From chemistry point of view, a clear electrostatic interaction mechanism was also explained by the theory of β -phase nucleation in our previous publications.^[22-24] Based on this theory, when the positively or negatively charged nanoparticles are added to the host solution, the opposite (partially negative CF_2 or positive CH_2) dipoles are oriented towards the surface of the nanoparticles, which perform as substrates for β -phase nucleation. This mechanism leading to the alignment of stabilised PVDF-HFP chains in longer all trans-conformation, results in electroactive β -phase.^[23-24]

Measurement of electrical properties of polymer matrix: effect of potentised *Cuprum metallicum* in Set A and Set B

For Set A, *Cup. met.* enhances the more electroactive β -phase of the polymer matrix, enhancing the conductivity and dielectric constant and reducing the tangent loss of the medium.^[21-25]

For the polymer matrix, when many more agglomerated nanoparticles are available as in the case of Set B, the arrangement of the β -polymorph in the matrix gets destroyed, which becomes less electroactive and reaches a stable nature. Hence, the electrical properties cannot be further enhanced.

Figure 8 shows the variation of the dielectric constant, tangent loss and electrical conductivity of the composite material as a function of frequency. All the details regarding measurement procedure have been reported by us earlier in various reputed journals.^[21-26] In Set A, the number of drug particles decreases with dilution and the size decreases with succussion.^[8] Hence, the particles are more scattered and well separated and also homogeneously distributed, maintaining an intermolecular distance between the particles, which enhances the nucleation of β -polymorph, resulting in very good dielectric performance.^[21-25] In Set B, the number of drug associates remains constant, but the size decreases with succussion, enhancing the agglomeration in the polymer matrix. Thus, the increasing agglomeration and the encapsulation of drug material by silicates will increase and the mobility of the particles will be inhibited, keeping the electrical properties unaltered.

Hence, the outcome of these two experiments using Set A and Set B on *E. coli* and polymer matrix has been quite interesting. The generation of larger number of nanoparticles in Set B

plays a major role and changes the usual pattern obtained with Set A. As in both the cases the solvent had been evaporated to dryness to make films, we can rule out the effect of vehicle medium on the observed phenomena. The presence of copper in the film had been verified earlier.^[24,26]

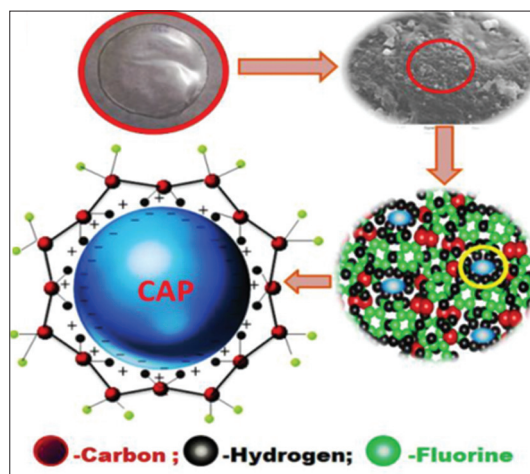


Figure 7: The schematic representation for nucleation of β -polymorph in poly(vinylidene fluoride-co-hexafluoropropylene)^[24]

DISCUSSION

The results using Set A and Set B have been summarised as follows:

Antibacterial effect of the medicine *Cuprum metallicum* on *Escherichia coli*

In Set A, the number of drug particles decreases with dilution and the size decreases with succussion, enhancing the membrane permeability, and the growth is inhibited, as expected. However, for Set B, when there is no dilution, the amount of drug available is same for all potencies from 6C to 200C and a larger number of nanoparticles are produced by succussion and the antibacterial effect is more here for 30C and 200C compared to that in Set A.

Effect of *Cuprum metallicum* on the electrical properties of poly(vinylidene fluoride-co-hexafluoropropylene) matrix

- For Set A, the effect varied significantly with potency (i.e., with dilution). Here, the number of drug associates decreased with dilution and the size decreased with succussion, enhancing the mobility of the particles, which enhances the electroactive beta phase of the polymer matrix, enhancing the conductivity and good dielectric performance

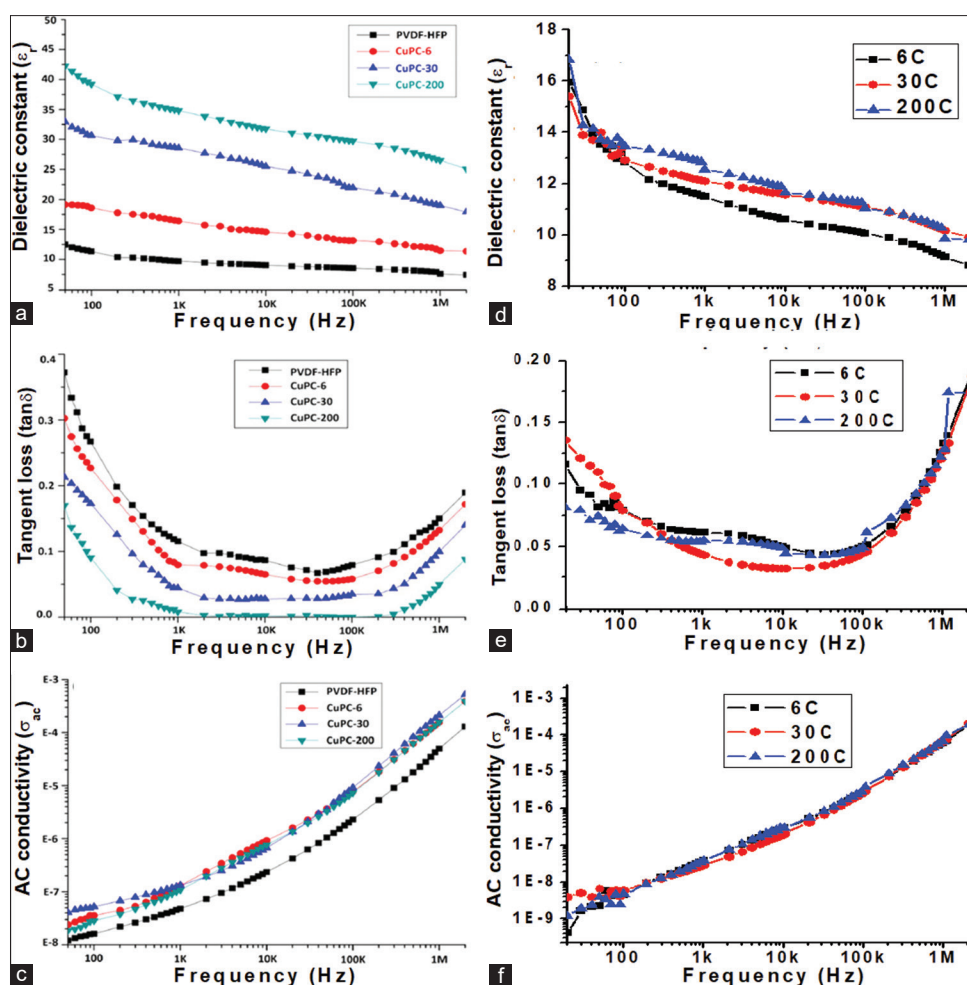


Figure 8: Effect of *Cup. met.* on the electrical properties of polymer matrix (a), (b), (c) for Set A^[22] and (d), (e), (f) for Set B

- For Set B, no significant change in electrical properties with change in potency is observed. Here, the number of drug associates remains constant, but the size decreases with succussion, enhancing the surface area. Thus, the effect will be twofold: the number of nanoparticles will increase, increasing the possibility of agglomeration and restricting the movement of charged particles, and also due to the encapsulation of drug material by silicates, the mobility of the particles will be inhibited. Both these factors will keep the electrical properties unaltered.

The difference between the two results gives an indication about the role of dilution and succussion in the process of potentisation of homeopathic medicines and their impact on the biological and physical systems.

From the conducted experiments, it is observed that in case of Set B, when there is no serial dilution and only succussion, the total number of drug associates remains the same at all potencies, and a large number of nanoparticles are created due to succussion, which produced more significant antibacterial effect in both 30C and 200C of Set B, as compared to Set A where the maximum antibacterial effect was exhibited only at 200C. In Set B, the electrical properties of the polymer matrix remained unaltered with potency of *Cup. met.* as compared to Set A, where serial dilution with succussion was carried out. Here, the particles were more scattered and well separated and also homogeneously distributed, maintaining an intermolecular distance between the particles. This enhanced the nucleation of β -polymorph results in very good dielectric performance, which signifies the role of dilution as in Set A.

We agree with the principle of Homeopathy, where it is always advocated to use the minimum dose, which means that the lower the concentration of the drug, better is the result. For higher concentration of the drug, the functioning of the medicine will be inhibited, which may be due to the re-agglomeration of nanoparticles of the drug material or due to saturation of the holding/absorption points in the system.

Higher number of succussions would ensure proper formation of the drug nanoparticles of different degree while bringing these remedies into the range of hormetic biological action.^[10]

CONCLUSION

Our experimental results show that the drug *Cup. met.*, potentised by serial dilution, followed by succussion, can produce significant effect on both bacterial system and polymer matrix. However, by increasing the potency by succussion only, a large number of nanoparticles are created which produce significant change in lower potencies, monitoring the effect of the medicine in both biological and physical systems chosen. Due to proximity, these nanoparticles may agglomerate again to make bigger particles. Thus, while succussions are necessary for the potentisation, the role of dilution seems equally important.

Further experimentations are required using different drugs to identify the appropriate and most effective way of the degree of dilutions i.e., the critical level of dilution.

We would like to mention here that to the best of our knowledge, this experiment is the first of its kind to find out the role of succussion and dilution to potentise the starting material to a therapeutically active one.

Acknowledgement

The study was undertaken as a joint collaboration between the Centre for Interdisciplinary Research and Education (CIRE), Kolkata, and the Central Council for Research in Homoeopathy (CCRH), the Ministry of AYUSH, Government of India, New Delhi, and was funded by the CCRH (till 31 March 2018).

The results from References 22 and 24 were quoted here for the sake of comparison, and the authors express their thanks for the permission received from *Springer Nature* as follows:

License number	4626030180723
License date	11 July 2019
Licensed content publisher	<i>Springer Nature</i>
Licensed content publication	<i>Journal of Materials Science: Materials in Electronics</i>

Financial support and sponsorship

Centre for Interdisciplinary Research and Education, Kolkata.

Conflicts of interest

None declared.

REFERENCES

- Hahnemann S. Organon of Medicine. Boericke and Tafel: Philadelphia; 1901.
- Available from: <https://www.hindustantimes.com/india/homeopathy-astrology-are-bogus-says-nobel-laureate-venkatraman-ramakrishna/story-oNNzWBnosMFILnrmfkdxI.html>. [Last accessed on 2016 Jan 07].
- Adams G. Potentisation and the peripheral forces of nature. *Br Homeopath J* 1989;78:69-79.
- Shah R. Standardization of the potentizing machine and quantification of impact of potentization. *Indian J Res Homoeopathy* 2016;10:126-32.
- Nandy P, Bhandary S, Das S, Basu R, Bhattacharya S. Nanoparticles and membrane anisotropy. *Homeopathy* 2011;100:194.
- Nandy P. A review article of basic research on homeopath from a physicist's point of view. *Indian J Res Homoeopathy* 2015;9:141-51.
- Ghosh S, Chakraborty M, Das S, Basu R, Nandy P. Effect of different potencies of nano medicine *Cuprum metallicum* on membrane fluidity: A biophysical study. *Am J Homeopathic Med* 2014;107:161-9.
- Kar S, Bandyopadhyay P, Chakraborty S, Chakraborty M, Ghosh S, Basu R, *et al.* Derivation of an empirical relation between the size of the nanoparticle and the potency of homeopathic medicines. *Int J High Dilution Res* 2015;4:2-7.
- Chikramane PS, Suresh AK, Bellare JR, Kane SG. Extreme homeopathic dilutions retain starting materials: A nanoparticulate perspective. *Homeopathy* 2010;99:231-42.
- Chikramane PS, Suresh AK, Kane SG, Bellare JR. Metal nanoparticle induced hormetic activation: A novel mechanism of homeopathic medicines. *Homeopathy* 2017;106:135-44.
- Temgire MK, Suresh AK, Kane SG, Bellare JR. Establishing the interfacial nano-structure and elemental composition of homeopathic medicines based on inorganic salts: A scientific approach. *Homeopathy* 2016;105:160-72.
- Rajendran ES. Homeopathy seen as personalised nanomedicine. *Homeopathy* 2019;108:66-70.

13. Bandyopadhyay P, Bera D, Das K, Paul BK, Das S, Bhar DS, *et al.* Vigorous shaking enhances voltage and power generation in polar liquids due to domain formation, as predicted by QED. *Water* 2017;8:172-82.
14. Nandy P, Das K, Bandyopadhyay P, Paul BK, Bhar DS, Das S, *et al.* Extraction of electrical energy from alcohol and bi-distilled water separated by a platinum foil – AQED Effect *Energ Educ Sci Tech Part A Energ Sci Res* 2017;35:285-90.
15. Yinnon TA, Liu ZQ. Domains formation mediated by electromagnetic fields in very dilute aqueous solutions: Quantum electrodynamic aspects. *Water* 2015;7:33-47.
16. Yinnon TA, Elia V. Dynamics perturbed very diluted aqueous solutions: Theory and experimental evidence. *Int J Mod Phys* 2013;27:1350005-40.
17. Ho MW. Large Supramolecular water cluster caught in camera – A review. *Water* 2014;6:1-12.
18. Bhattacharya TS, Maitra P, Bera D, Das K, Bandyopadhyay P, Das S, *et al.* Investigation of the origin of voltage generation in potentized homeopathic medicine through Raman spectroscopy. *Homeopathy* 2019;108:121-7.
19. Homeopathic Pharmacopoeia of India. Ministry of Health. Government of India. Available from: [https://www.nhp.gov.in/Homeopathic-Pharmacopoeia-of-India-\(HPL\).mtl](https://www.nhp.gov.in/Homeopathic-Pharmacopoeia-of-India-(HPL).mtl). [Last accessed on 2017 Dec 10].
20. Chakraborty M, Das S, Manchanda RK, Basu R, Nandy P. Application of nanomedicine cuprum metallicum as an agent for remediation of an azo dye methyl orange and study its associated antimicrobial activity *Environ Sci* 2015;6:345-51.
21. Chatterjee A, Paul BK, Kar S, Das S, Basu R, Bhar DS, *et al.* Effect of ultrahigh diluted homeopathic nanomedicines on the electrical properties of PVDF-HFP. *Int High Dilution Research* 2016;15:10-7.
22. Gayen AL, Mondal D, Paul BK, Roy D, Bandyopadhyay P, Manna S, *et al.* Improvisation of electrical properties of PVDF-HFP: use of novel metallic nanoparticles. *J Mater Sci* 2017;28:14798-808.
23. Gayen A, Mondal D, Bandyopadhyay P, Bera D, Bhar DS, Das S, *et al.* Effect of homeopathic dilutions of Cuprum arsenicosum on the electrical properties of poly (vinylidene fluoride-co-hexafluoropropylene). *Homeopathy* 2018;107:130-6.
24. Mondal D, Gayen AL, Paul BK, Bandyopadhyay P, Bera D, Bhar DS, *et al.* Enhancement of β -phase crystallization and electrical properties of PVDF by impregnating ultra high diluted novel metal derived nanoparticles: prospect of use as a charge storing devices. *J Mater Sci* 2018;28:14535-45.
25. Paul BK, Kar S, Bandyopadhyay P, Basu R, Das S, Bhar DS, *et al.* Significant enhancement of dielectric and conducting properties of electroactive polymer polyvinylidene fluoride films: An innovative use of Ferrum metallicum at different concentrations. *Indian J Res Homoeopathy* 2016;10:52-7.
26. Mondal D, Gayen AL, Paul BK, Bhar DS, Das K, Nandy P, *et al.* Colossal dielectric response of PVDF-HFP amalgamated ultra low dense metal derived nanoparticles: Frontier of an excellent charge separator. *J Electron Mater* 2019;48:5570-80.

ई-कोलाई बैकटीरिया प्रणाली और PVDF HFP बहुलक के विद्युत गुणों पर अकेले उत्तरावर्धन की तुलना में क्रमिक विलयन और उत्तरावर्धन दोनों के माध्यम से प्रबलित क्यूप्रम मेटालिकम का प्रभाव।

पृष्ठभूमि : होम्योपैथिक दवाओं को पारंपरिक रूप से क्रमिक विलयन के पश्चात उत्तरावर्धन प्रक्रियाओं द्वारा शक्तिकृत किया जाता है। इन दो घटकों की प्रतिक्रियात्मक भूमिकाओं के आंकलन और अन्वेषण की आवश्यकता हेतु अध्ययन किया गया।

उद्देश्य : अकेले उत्तरावर्धन की तुलना में क्रमिक विलयन और उत्तरावर्धन दोनों के माध्यम से प्रबलित क्यूप्रम मेटालिकम का चयनित जैविक और भौतिक प्रणालियों पर दवा के प्रभाव का तुलनात्मक अध्ययन।

विधि : शुरुआत में क्यूप्रम मेट 6C को लिया, क्रमिक विलयन के पश्चात उत्तरावर्धन द्वारा इसे 30C और 200C तक बढ़ा दिया गया (सेट ए)। इसी दवा को 6C से 30C और 200C तक अकेले उत्तरावर्धन प्रक्रिया द्वारा शक्तिकृत किया गया (सेट बी) ई कोलाई पर दवा के जीवाणुरोधी गुणों का प्रभाव एक जैविक प्रणाली और बहुलक मैट्रिक्स PVDF-HFP जो व्यापक रूप से चार्ज विभाजक के रूप में उपयोग किया जाता है, के प्रभाव की तुलना भौतिक प्रणाली से की गई।

परिणाम : फील्ड एमिशन स्कैनिंग इलेक्ट्रॉन माइक्रोस्कोपी से पता चलता है कि क्यूप्रम मेट के सेट बी एंटीबैक्टीरियल प्रभाव में कणों को उच्च क्षमता पर अधिक एग्लोमेरेट किया जाता है। सेट ए की तुलना में सेट बी में क्यूप्रम मेट, 30 सी और 200 सी की जीवाणु रोधी प्रभावोत्पादकता अधिक महत्वपूर्ण पाई गई। सेट ए में पॉलिमर मैट्रिक्स पर सेट बी की तुलना में क्यूप्रम मेट की पोर्टेसी के प्रभाव में महत्वपूर्ण परिवर्तन हुआ। जिसमें कम बीटा चरण क्रिस्टलीकरण का उत्पादन हुआ, विद्युत गुणों में कोई महत्वपूर्ण परिवर्तन नहीं हुआ।

निष्कर्ष : दवा क्यूप्रम मेट का उपयोग करके दो प्रयोगात्मक सेट अप के परिणामों की तुलना करने पर पता चलता है कि क्रमिक विलयन और उत्तरावर्धन के दो सेटों के बीच एक महत्वपूर्ण अंतर होता है।

Effet du *Cuprum metallicum* dilué à la fois par dilution en série et par succussion par rapport à uniquement la succussion sur le système bactérien *E. Coli* et les propriétés électriques du polymère PVDF-HFP

Contexte : Les médicaments homéopathiques sont traditionnellement dilués par une dilution en série suivie d'une succussion. Les rôles respectifs de ces deux composantes doivent être évalués et explorés et c'est la raison pour laquelle la présente étude a été entreprise. **Objectif :** Comparer l'effet du médicament *Cuprum metallicum* (*Cup. met.*) dilué à la fois par dilution en série et succussion avec succussion seule sur des systèmes biologiques et physiques sélectionnés. **Méthode :** Ayant démarré l'expérience avec le médicament *Cup. met.* à 6°C, nous l'avons davantage dilué à 30°C et à 200°C par dilution en série, suivie d'une succussion (Ensemble A). Le même médicament à 6°C a également été dilué à 30°C et à 200°C uniquement par succussion (Ensemble B). La propriété antibactérienne de ces deux ensembles a été comparée sur *E. coli*, un système biologique et les propriétés électriques ont été comparées sur la matrice polymère PVDF-HFP, un système physique, utilisée couramment comme séparateur de charges. **Résultats :** La microscopie électronique à balayage à émission de champ montre que les particules deviennent plus agglomérées à une dilution plus élevée dans l'ensemble B. L'effet antibactérien de *Cup. met.* dans l'ensemble B à 30°C et à 200°C s'est avéré être plus significatif par rapport à l'ensemble A. L'effet de *Cup. met.* sur la matrice polymère dans l'ensemble A variait considérablement selon la dilution alors que dans l'ensemble B, moins de cristallisation en phase bêta a été produite et aucun changement significatif dans les propriétés électriques n'a suivi. **Conclusion :** La comparaison des résultats lors de l'utilisation du médicament *Cup. met.* dans deux montages expérimentaux montre que la dilution en série avec succussion donne lieu à une différence sensible entre les deux ensembles.

Efecto de *Cuprum metallicum* potenciado a través de diluciones y sucusiones seriadas en comparación con la sucusión sola con un sistema bacteriano de *E. coli* y las propiedades eléctricas del polímero PVDF-HFP

Fundamento: Los medicamentos homeopáticos se potencian mediante diluciones seriadas seguidas de sucusión. Es necesario estudiar y examinar los respectivos roles, por lo que efectuó el presente estudio. **Objetivos:** Investigar el efecto del medicamento *Cuprum metallicum* (*Cup. met.*) potenciado mediante diluciones seriadas y sucusiones en comparación con la sucusión sola utilizando sistemas biológicos y físicos seleccionados. **Método:** El procedimiento se inició con el medicamento *Cup. met.* a la 6C. Se fue potenciando a la 30C y 200 C mediante diluciones seriadas seguidas de sucusión (set A). El mismo medicamento a la 6C también fue potenciado a 30C y 200C utilizando únicamente la sucusión (set B). Las propiedades antibacterianas de estos dos sets se compararon con un sistema biológico, *E. coli*, y un sistema físico, las propiedades eléctricas sobre una matriz de polímero PVDF-HFP (sistema ampliamente utilizado como separador de cargas). **Resultados:** La Microscopia de Barrido Electrónico de Emisión de Campos mostró que las partículas se aglomeran a una potencia superior en el Set B. Se constató que el efecto antibacteriano de *Cup. met.* en el set B a 30C y 200C era más significativo en comparación con el set A. En el Set A, el efecto de *Cup. met.* en la matriz de polímeros varió significativamente con la potencia, en comparación con el set B, en el que la cristalización de la fase beta fue inferior y no se siguió de un cambio significativo en las propiedades eléctricas. **Conclusiones** La comparación de los resultados utilizando el medicamento *Cup. met.* en dos preparaciones experimentales muestra que la dilución seriada con sucusión da lugar a una diferencia importante entre los dos sets.

Wirkung des potenzierten Arzneimittels *Cuprum metallicum* durch fortlaufende Verdünnungen und Schüttelschlägen im Vergleich zum alleinigen Schütteln überprüft an zwei verschiedenen Systemen mit *E. coli* und den elektrischen Eigenschaften des PVDF-HFP Polymers

Hintergründe: Der klassische Potenzierungsweg homöopathischer Arzneimittel verläuft mit verschiedenen Schritten der Verdünnung und nachfolgendem Schütteln. In dieser Arbeit sollen die entsprechenden Rollen beider Komponenten beurteilt und untersucht werden. **Zielsetzung:** Vergleich der Wirkung des Arzneimittels *Cuprum metallicum* (*Cup. met.*), welches durch fortlaufende Verdünnungen und entsprechenden Schüttelschlägen oder durch alleinigem Schütteln potenziert und an ausgewählten biologischen und physikalischen Systemen überprüft wurde. **Methode:** Als Ausgangssubstanz wurde das Arzneimittel *Cup. met.* C6 benutzt, welches auf C30 und C200 durch die entsprechenden Verdünnungen und Schüttelschlägen hochpotenziert wurde (Set A). Das gleiche Arzneimittel (C6) wurde auch auf C30 und C200 durch alleiniges Schütteln hochpotenziert (Set B). Die antibakteriellen Eigenschaften dieser beiden Sets wurden mittels einem biologischen System (*E. coli*) und einem physikalischen System (elektrische Eigenschaften der polymerischen Matrice PVDF-HFP, ein als Chragentrenner weitläufig benutztes System) untersucht. **Ergebnisse:** Durch Feldelektronenmikroskopie zeigte sich, daß die Partikel im Set B bei höheren Potenzen Agglomerate aufwiesen. Die antibakterielle Wirkung von *Cup. met.* (C30 und C200) im Set B war signifikanter im Vergleich zum Set A. Die Wirkung von *Cup. met.* auf die polymerische Matrice im Set A erwies signifikante Variationen je nach Potenz. Hingegen im Set B ergab sich eine geringere Krystallisation in der Beta-Phase, der keine signifikante Veränderung der elektrischen Eigenschaften folgte. **Fazit:** Der Vergleich der Ergebnisse dieser beiden Versuchsaufbaue mit dem Arzneimittel *Cup. met.* zeigt, daß die fortlaufenden Verdünnungen und entsprechenden Schüttelschlägen einen großen Unterschied zwischen beiden Sets darstellen.

透過連續稀釋和震盪，對比單獨進行震盪，加能的銅金屬（Cup. met.）對大腸桿菌系統及PVDF-HFP聚合物電性能的效果

背景：順勢療法藥物在傳統上是先透過連續稀釋，然後再進行震盪，來達至加能。這兩個組成過程的各自作用需要進行評估和探討，本研究就是針對這兩個過程部分進行。

目的：透過在選定的生物和物理系統上進行連續稀釋和震盪，以及單獨進行震盪，以比較順勢療法藥物銅金屬（Cup. met.）的效果。

方法：開始時使用6C層級的銅金屬（Cup. met.），我們透過連續稀釋進一步將其加能到30C和200C，然後進行震盪（A組）。同樣的藥物在6C時，只進行震盪將其加能至30C和200C（B組）。在大腸桿菌生物體系和聚合物基體PVDF-HFP（廣泛用作電荷分離器）物理體系上比較了這兩種抗菌劑的抗菌性能。

結果：場發射掃描式電子顯微鏡顯示，在B組中，粒子在較高的加能下更易凝聚。在B組中，當銅金屬（Cup. met.）處於30C和200C層級時，其抗細菌效果比A組更為顯著。與B組相比，A組銅金屬（Cup. met.）對聚合體基質的效果隨著加能而變得顯著，B組中產生的 β 相結晶較少，而電性則沒有顯著變化。

在兩組實驗設置中使用銅金屬（Cup. met.）的結果比較表明，連續稀釋伴震盪的加能法對於兩組設置有重要區別。

CIRE

CENTRE FOR INTERDISCIPLINARY RESEARCH AND EDUCATION

404B, Jodhpur Park, Kolkata – 700068

25th March, 2017

CERTIFICATE OF PARTICIPATION

This is to certify that

Anandalal Gayen

*has contributed through Lecture / Oral Presentation / Poster Presentation / Participation to the success
of the One Day National Symposium on Nanotechnology:*

*From Materials to Medicine and their Social Impact held on 25th March, 2017
at Birla Industrial and Technological Museum, Kolkata.*

Sanjib Sarkar

Prof Sanjib Sarkar
President, CIRE

International Conference on
EMERGING TRENDS IN CHEMICAL SCIENCES (ETCS-2018)

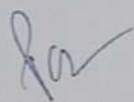



DEPARTMENT OF CHEMISTRY, DIBRUGARH UNIVERSITY
Dibrugarh, Assam, India.


Certificate

This is to certify that Prof./Dr./Mr./Ms..... **Anandalal Gayen**
of..... **Jadavpur university**.....attended/presented research paper

(Invited lecture/Oral/Poster) in the International Conference "Emerging Trends in
Chemical Sciences" held during 26 -28 February, 2018.


(P. Das)
Convener


(S. K. Sarker)
Co-Convener


(A. Baruah)
Co-Convener



**ONE DAY SEMINAR
ON
Recent Trend in Frontier Research in Physics**

Organised By :
Department of Physics, Jadavpur University, Kolkata

CERTIFICATE OF PARTICIPATION

This is to certify that Mr./Mrs/Dr./Prof. Anandalal Gayen
has participated/presented (oral/poster) a paper entitled
..... In the one day seminar
on "Recent trend in Frontier research in Physics" on 6th March, 2018 held at Department of Physics, Jadavpur
University, Kolkata-700 032.

Dr. Sanat Karmakar
Dr. Soumen Mondal
Dr. Abhijit Samanta
Dr. Subrata Sarkar
(Conveners)

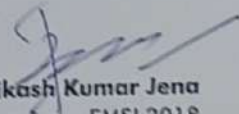
Debasish Lohar
Prof. Debasish Lohar
Head, Department of Physics
Jadavpur University



**International Conference on Microscope &
XXXIX Annual Meeting of Electron Microscope Society of India**
18 - 20 July, 2018 | Mayfair Convention Center, Bhubaneswar

Certificate of Participation

This is to certify that Mr. / Ms. / Dr. / Prof. Anandalal Gayen
has participated in "International Conference on Microscopy - EMSI 2018" organized by Electron Microscope
Society of India (EMSI) in collaboration with IOP, NISER, CSIR-IMMT, IIT BBSR, ILS and CSIR-CGCRI, held at Mayfair
Convention Center, Bhubaneswar, Odisha, India during 18th - 20th July, 2018.
He / She made ☒ Invited / ☒ Oral / ☒ Poster presentation in the conference.


Bikash Kumar Jena
Convener, EMSI 2018


Parlapalli V Satyam
Chairman, EMSI 2018